Table of contents

List of figures and illustrations

List of tables

Abbreviations and acronyms

#

ω

Angular frequency · 70

η_∞

The infinite shear rate viscosity · 70

η^*

Complex viscosity · 70

η_0

The zero shear rate viscosity · 70

ε_C

Composite's strain · 225

ε^e

Elastic conponent of the strain · 240

ρ_f

Fiber's density · 221

ε_F

Fiber's strain · 225

ρ_m

Matrix density · 221

ε_M

Matrix strain · 225

ε^p

Plastic component of the strain · 240

ε^{ve}

Visco-elastic component of the strain · 240

ε^{vp}

Visco-plastic component of the strain · 240

A

a

Index controlling transition from the Newtonian to the polwer-law behavior · 70

A

Pre-exponential factor · 64

ABS

Acrylonitrile butadiene styrene · 41

AFM

Atomic force microscopy · 229

ANN

Artificial neural network method · 244

ASTM

American Society for Testing and Materials · 48

C

C

Cauchy-Green's tensor components · 235

Cc

Cross model's constant · 70

C_i

Weight coefficient of i · 64

Cp

Heat capacity · 65

Specific heat capacity · 220

CRR

Cooperatively relaxing regions · 240

CTRI

Centre Technologique des Résidus Industriels · x

D

DMA

Dynamic mechanical analysis · 228

DSC

Differencial scanning calorimeter · 222

E

E_a

Activation energy · 64

F

FEA

Finite element analysis · 246

FQRNT

Fonds de recherche du Québec – Nature et technologies · x

G

G’

Storage modulus · 70

G’’

Loss modulus · 70

GMA

Glycidyl methacrylate · ii

Méthacrylate de glycidyle · vi

H

H_2SO_4

Sulfuric acid · 54

HDPE

High density polyethylene · 43

He

Helium · 45

I

ICTAC

International Confederation for Thermal Analysis and Calorimetry · 63

I_i

Invariants of the stress tensor · 235

ISO

International Organization for Standardization · 48

K

K

Consistency index · 70

Thermal conductivity · 220

K_f

Fiber's thermal conductivity · 220

K_m

Matrix thermal conductivity · 220

L

LiP

Lignin peroxidases · 45

LS

The least squares method · 242

M

MA-PP

Maleic anhydride grafted polypropylene · 30

N

n

Apparent reaction order · 64

The power law index · 70

N_2

Nitrogen · 45

NaOH

Sodium hydroxyde · 261

n_f

Flow index · 70

NSERC

The Natural Sciences and Engineering Research Council of Canada · x

O

O_2

Oxygen · 45

P

PA 6

Polyamide 6 · 43

PA 6, 6

Polyamide 6,6 · 43

P_c

Critical pressure · 151

PCL

Polycaprolactone · ii, vi

PET

Polyéthylène téréphtalate · v

Polyethylene terephthalate · i

PMDA

Dianhydride pyromellitique · vi

Pyromellitic dianhydride · ii

PMMA

Polymethyl methacrylate · 243

PP

Polypropylene · 30

PS

Polystyrene · 41

CHAPTER: 1

INTRODUCTION

This chapter discusses the background of the work covered in this thesis, the challenges it tackled, its targeted objectives and an overview of its resulting scientific contributions.

1.1 *Background*

A growing interest in the application of vegetal fiber-reinforced composites in various engineering sectors has been witnessed during the past decades. Moreover, numerous new avenues are still being explored through an intensive and effective Research and Development (R&D). The actual context indicates a significantly less utilization of high temperature melting thermoplastics ($T_m \geq 200°C$) reinforced with vegetal fibers compared to those of low temperature melting matrices ($T_m \leq 200°C$), despites all the measures taken to qualitatively and quantitatively improve on the applications of vegetal fiber-reinforced composites also known as ligno-cellulosic fiber-reinforced composites. In fact, the proportion of the applications with high temperature melting thermoplastics such as polyethylene terephthalate (PET) is still negligible owing to their melt processing challenges with vegetal fibers whose onset of thermal degradation is as low as 190°C. In this regard, high temperature melting thermoplastics reinforced with ligno-cellulosic fibers constitute a great industrial potential, whose under-exploitation is caused by the temperature gap between the onset of thermal degradation of vegetal fibers and the high temperature melting point of the matrices.

1.2 *Thesis motivation*

This thesis addresses some critical issues faced by both the scientific and the industrial communities with respect to the development and application of high temperature melting thermoplastic bio-composite materials. An elaboration and characterization of PET-hemp fiber composites for thermoforming applications is motivated by the development of profitable and environmental friendly vegetal fiber-reinforced composites with high temperature melting thermoplastics, with positive impacts in the following fields:

(i) Fundamental research
(ii) Applied research
(iii) Environment
(iv) Agriculture
(v) Economy

The formulation of a novel group of thermoplastic bio-composite materials is expected to significantly impact fundamental research through a better understanding of the raw materials, their modification as well as tackling other processing challenges and finding optimal thermoforming conditions. Such material development is also expected to have an impressive environmental impact as a catalyst for the plastic recycling. Moreover, it will lead to the development of environmental friendly agricultural products which will boast the economy of the forestry regions of Canada. A possible replacement of wood by hemp fibers may considerably contribute to forest regeneration. Finally, through the use of the new composite material in design, the scientific community would be able to explore a new field at the interface of material sciences, numerical simulation and engineering.

Although bio-composite materials have been making an appreciable impact in many industries, high temperature melting thermoplastics reinforced with vegetal fibers have mostly been inexistent due to their processing challenges.

1.3 *The problem Statement*

There are two levels of challenge associated with this work. The first is associated with the elaboration process which is restricted by the high temperature difference between the onset of thermo-degradation of hemp fibers which has been reported around 190°C and the high temperature melting of PET which is found around 250°C. Such high temperature difference results in a risk of natural fiber thermo-degradation which needs to be addressed prior to the melt processing. The second is associated with the thermoforming process for which natural fiber reinforced composites known as brittle materials are unfit. In fact, vegetal fiber-reinforced composite materials have generally been found in applications which require smaller deformations and which are inadequate for the thermoforming process. Besides the problems associated with both the elaboration and the thermoforming of PET-hemp fiber composites, there are also minor problems related to the handling the high fiber volume while taking advantage of their important length.

1.4 *Thesis objectives and scope*

This thesis aims at opening up vegetal fiber-reinforced composites to high temperature melting thermoplastic matrices and extending the applicability of the resulting material by the thermoforming process.

Table 1-1: Objectives of this study.

Objectives and rationale	Specificities guiding questions
Section 1: Elaboration of PET-hemp fiber composites	
Objective 1: Determine the method of elaboration of PET-hemp fiber composites without fibers' thermal degradation. Rationale**:** To find a general strategy to tackle the processing challenges of high temperature melting thermoplastic materials with vegetal fibers and find the needed additives.	1: Is it possible to simultaneously modify PET and hemp fibers to allow high temperature melting processing without the thermal degradation of hemp fibers? 2: Which processes would permit it? 3: Which additives can be used in future applications of PET-hemp fiber composite?
Section 2: Characterization of PET-hemp fiber composites	
Objective 2: Determine the variation of the mechanical, rheological, morphological and thermo-physical properties of PET-hemp fiber composites with respect to their compositions and their processing conditions. Rationale: Choosing the appropriate formulation and the optimal conditions for the thermoforming process.	1: Is it possible to understand the variation of the thermoforming properties with the composition of PET-hemp fiber composites? 2: Is it possible to determine the additives which are needed for the thermoforming of PET-hemp fiber composites? 3: What is the constitutional equation describing the behavior of PET-hemp fiber composites with the composition and other thermo-physical parameters?
Section 3: Thermoforming of the optimal formulation of PET-hemp fiber composites	
Objective 3: Determine the best PET-hemp fiber composite candidate for thermoforming and find the optimal processing conditions. Rationale: Optimization of the thermoforming process.	1: What are the variations of the thermoforming parameters of the different PET-hemp fiber composite formulations? 2: Which formulation exhibits the best behavior during the forming process? 3: What are the best processing conditions for the best PET-hemp fiber composite thermoforming candidates?

The objectives of this work are summarized in Table 1-1 based on previous sections which have shown the different levels of challenge associated with the formulation of PET reinforced with hemp fibers for thermoforming applications. In fact, two levels of challenge must be tackled in this work. The first concerns processing the high temperature melting PET resin with vegetal fibers while avoiding thermal degradation of the latter and the second concerns creating the large deformations required in thermoforming the brittle composite resulting from the reinforcement of PET with hemp fibers.

This work aims at determining and applying the appropriate strategies to tackle the processing challenges presented in the previous section. Attaining such objectives would result in filling the applications gap of high temperature melting thermoplastic matrices reinforced with vegetal fibers and the thermoforming of these brittle materials. In fact, an elaboration and characterization of PET-hemp fiber composites for thermoforming applications is a case study which seeks to fill the existing void in the applications of vegetal fibers reinforced composites, achievable in three stages:

(i) Extending the process of reinforcing thermoplastics by ligno-cellulosic fibers to the group of high temperature melting matrices;

(ii) Characterization and analysis of different formulations;

(iii) Evaluating the potential thermoformability of the resulting composites

The work presented herein makes use of standard knowledge and practice from the materials science, plastics-composite, engineering and numerical modeling.

1.5 *Thesis contributions*

Today, many fibers-reinforced thermoplastic materials have entered the foray of composite materials in aerospace, automobile, recreational and other applications. In this work, a focus is made on natural fibers-reinforced composites which have an under exploited potential with high temperature melting matrices (melting above 200°C). PET-hemp fiber composites fall under such under exploited group. The contributions of this work include the elaboration of a novel material from uncommon precursors, its characterization and its application through a process which is not necessarily compatible with its properties yet which is highly efficient and practical for general composite applications.

The elaboration and characterization of PET-hemp fiber composites for thermoforming applications is therefore innovative in many aspects. The first by addressing the challenges of melt processing high temperature melting thermoplastics with natural fibers; the second is its further application to the thermoforming process which requires large deformations of such composites which are rather known to be brittle. The knowledge derived from this work [1–3], mentioned for the first time in the scientific community, will provide scientists with a potential new research avenue in composites of high temperature melting thermoplastics.

In an industrial perspective, this work is a critical step in the development of plastic-composite related applications and recycling. Its potential impacts will range from the development of the industrial hemp production including post-harvest processing, the increase of the volume of recycled plastics and the development of a new range of natural fibers-reinforced composites applications. Indeed, according to JEC magazine [4], there was a rebound in the American composites market of approximately 15% to 201 million

pounds in 2012. This represents 35% of the global composites industry that was valued at over $100 billion and currently employs approximately 550 000 professionals worldwide [5], the largest market sector being the transportation industry. Cost to produce final assembled modules of composites in several automotive applications have proven advantageous, particularly in structural and semi-structural components when compared to other material technologies [6]. In the aircraft industry, significant portions of structural fuselage and airfoil components are nowadays made of composites, primarily due to their high strength-to-weight ratios. The new perspectives offered by the knowledge derived from this work will obviously further boost this market sector.

Table 1-2: List of peer-reviewed publications included in the PhD thesis.

Chapter in this report	Publications
CHAPTER 4 (Paper I)	Talla, A. S. F.; Mfoumou, E.; Jeson, S.; Pagé, D.; Erchiqui, F. Properties of a Novel Melt Processed PET-Hemp Composite: Influence of Additives and Fibers Concentration. *Reinf. Plast. Compos.* ***2013****, 32, 1526–1533.*
CHAPTER 5 (Paper II)	Talla, A. S. F.; Godard, F.; Erchiqui, F. Thermal Properties and Stability of PET-Hemp Fiber Composites. *The 19th International Conference On Composite Materials (ICCM'19); Montreal, Canada,* ***2013****.*
	Fotso Talla, A. S.; Erchiqui, F.; Kaddami, H.; Kocaefe, D. Investigation of the thermo-stability of poly(ethylene-terephthalate)-Hemp fiber composites: Extending natural fibers reinforcement to high temperature melting thermoplastics. *Appl. Polym. Sci.* **2015**, *132*.
CHAPTER 6 (Paper III)	Fotso Talla, A. S.; Erchiqui, F ; Godard, F.; Kocaefe, D.

	An Evaluation of the Thermal Degradation Kinetics of Novel Melt Processed PET-Hemp fiber composites *Thermal Analysis and Calorimetry (submitted, September **2015**).*
CHAPTER 7 (Paper IV)	F. Erchiqui, A.S. Fotso Talla, H. Kaddami, M. Souli Investigation of the Relaxation Properties and Potential Thermoformability of PET Reinforced with Hemp Fibers *Materials and Design (Submitted, July **2015**).*
CHAPTER 8 (Paper V)	F. Erchiqui, A.S. Fotso Talla, H. Kaddami Elaboration and Thermoformability Investigation of a Novel Composite Material of PET Reinforced with Hemp Fibers *Journal of Processing and Technology (Submitted, July **2015**).*
	Talla, A. F. S., Erchiqui, F., Kocaefe, D. and Kaddami, H., ***2014***, Effect of Hemp Fiber on PET/Hemp Composites, *J. Renew. Mater., 2(4), pp. 285–290*
	F. Erchiqui, A. Fotso Talla, D. Pagé, A. Bourihane Influence of the choice of additives in High Temperature Melting Polyesters (HTMP) reinforced with natural fibers (NF) in view of structural applications. *The 26th ASC Annual Technical Confrence / The Second Joint US-Canada Conference on Composites, September 26-28, **2011**, Montreal*
CHAPTER 4-7	Book Chapter Talla, A. F. S., Erchiqui, F.; Poly(ethylene-terephthalate) reinforced with hemp fibers: Elaboration, characterization and applications Handbook of composites from renewable materials *WILEY-Scrivener Publisher* (*Submitted, September **2015***).

1.6 *Thesis outline in the manuscript format*

This thesis is organized in seven chapters. The present chapter gives the general background of the work. It covers an introduction to the formulation and applications of composite materials reinforced with vegetal fibers, the opportunities they offer and the necessity and challenges of developing them with high temperature melting matrices like PET. It is followed by the motivation, objectives and methods of elaborating composite materials with PET reinforced with hemp fibers for thermoforming applications, followed by the thesis contribution. Chapters 4 and 5 are duplicated from two published journal articles, while chapters 6 to 8 are duplicated from three submitted journal articles. These chapters are classified following Section 3.1 of the University of Quebec in Chicoutimi's guideline for thesis preparation.

In the duplicated sections, the figures and tables are numbered according to the thesis preparation and a single compounded reference list given at the end.

A general thesis conclusions are given in Chapter 9 with the most important findings about the potential reinforcement of PET with hemp fibers for thermoforming applications as well as the recommendations for exploring new horizons with other high temperature melting thermoplastics reinforced with vegetal fibers.

Chapter 4 is based on the following article published in the Journal of Reinforced Plastics and Composites [1]

A.S. Fotso Talla, E. Mfoumou, S. Jeson, J.S.Y.D. Pagé, F. Erchiqui, Mechanical and structural properties of a novel melt processed PET-Hemp composite: Influence of additives and fibers concentration; Journal of Reinforced Plastics and Composites; ***2013****; 32 (20) 1526-1533.*

The mechanical and structural properties of a novel melt processed PET-Hemp fiber composites for engineering applications were investigated. First, four reinforcement formulations were compared with the PET modified with PCL: Hemp, Clay/Hemp, PMDA/Hemp and GMA/Hemp. Next, the effect of hemp fibers concentration was analyzed as well as the effect of heat treatment. A significant difference was observed in the mechanical and structural properties of the composites. Moreover, we observed a good fiber-matrix interface was observed without the use of a coupling agent, particularly in the absence of additives. Our data suggest that a careful trade-off exists between the additives, the hemp fiber concentration and the desired engineering application is the key requirement for the applications of high temperature melting polymers reinforced with natural fibers.

Chapter 5 is based on the following article published in the Journal of Applied Polymer Science [3]

A. S. Fotso Talla, F. Erchiqui, H. Kaddami, D. Kocaefe; Investigation of the thermo-stability of PET-Hemp fiber composites: Extending natural fiber reinforcement to high-melting thermoplastics; Journal of Applied Polymer Science; ***2015****, 132.*

The thermal stability of poly-ethylene terephthalate (PET) reinforced with 1, 5, 10, 15 and 20% (w/w) hemp fibers was investigated with the aim of extending the applications of bio-composites to high temperature melting thermoplastics. The material was injection-molded following compounding with a torque-based Rheomix at 240, 250 and 260°C. A combination of thermo-gravimetric methods at 5, 10 and 20°C.min^{-1}, Liu and Yu's collecting temperature method and the Friedman's kinetic method were used for testing and analysis. A significant thermo-stability for all formulations was observed

below 300°C, demonstrating their potential for successful melt processing. Moreover, two degradation steps were observed in the temperature ranges of 313-390°C and 390-490°C. The associated apparent activation energies within the temperature ranges above determined as 150-262 $kJmol^{-1}$ and 182-242 $kJmol^{-1}$ respectively. It was found that the thermo-stability was significantly affected by the heating rates; however, the effect of the temperature of the mixing chamber was negligible. These findings suggest that the successful melt processing of high temperature melting thermoplastics reinforced with natural fibers is possible with limited fiber thermo-degradation.

Chapter 6 is based on the following article submitted for publication in the Journal of Thermal Degradation and Stability (Journal of thermal analysis and calorimetry)

A. S. Fotso Talla, F. Erchiqui, F. Godard, D. Kocaefe; *An evaluation of the thermal degradation kinetics of novel melt processed PET-hemp fiber composites; Journal of Thermal Analysis and Calorimetry*; **2015**.

The composite materials of high temperature melting matrices reinforced with vegetal fibers are potentially attractive for a wide range of applications; however, an early fiber thermo-degradation during melt processing hinders their development. The thermo-degradation kinetics of a novel melt processed polyethylene terephthalate (PET) reinforced with hemp fibers was then investigated through an application of the international confederation for thermal analysis and calorimetry (ICTAC) recommendations for the thermo-gravimetric data. The samples consisted of five compounded and injection-molded formulations containing 1, 5, 10, 15 and 20% (w/w) hemp fibers. Compounding was done in an internal batch mixer heated at 250°C. Two consecutive degradation steps were observed between 300 and 500°C. An application of

the Starink's model yielded constant iso-conversional energies whose average values vary with the fiber concentration. The kinetic triplets of the two degradation steps were also determined by non-linear curve fitting methods, using respectively the Sestak-Berggren and the truncated Sestak-Berggren models. The resultant kinetic parameters varied with the fiber concentration and their ranges were $1,8 \leq A \leq 5$; $2,25 \leq n \leq 3,17$; $7,05 \leq m \leq 12,74$ and $-2,21 \leq p \leq -1$ for the first step and $1,76 \leq A \leq 10$; $1,37 \leq n \leq 2,49$ and $0,77 \leq m \leq 2,35$ for the second. This work further confirms the thermo-stability of PET-hemp fiber composites and provides key information for the reaction mechanism, a crucial developmental step for bio-composite materials with high temperature melting thermoplastics.

Chapter 7 is based on the following article submitted for publication in the Journal of Material Science and Design

F. Erchiqui, A.S. Fotso Talla, H. Kaddami, Mhamed Souli; Investigation of the Relaxation Properties and Potential Thermoformability of PET Reinforced with Hemp Fibers; Journal of Materials and Design; ***2015****.*

The processability of polyethylene terephthalate (PET) reinforced with 0, 1, 5, 10 and 15% (w/w) hemp fibers was experimentally and numerically investigated. A thermodynamic model expressing the external work in terms of a closed volume was considered to account for the enclosed gas volume, responsible for inflating the thermoplastic composite membrane, which significantly contributes to the strength and stiffness of the thermoplastic composite structure. The pressure load was derived from the Redlich-Kwong's real gas equation of state while the visco-elastic behavior was described by the Christensen's model. A combination of the Lagrangian formulation and the

membrane theory assumption were used in the finite element implementation. Moreover, the air flow's influence on the bubble inflation was analyzed for the investigated PET-hemp fiber composite materials. The observations of the relaxation properties are critical in determining the thermoformability of the investigated composites, choosing the optimal formulation and selecting the key processing parameters.

Chapter 8 is based on the following article submitted for publication in the Journal of Material Processing Technology

F. Erchiqui, A.S. Fotso Talla, H. Kaddami; Elaboration and Thermoformability A Numerical Investigation of the Use of Novel Melt Processed PET-Hemp Fiber Composites for Thermoforming Applications; ***2015***.

The mechanical and structural properties of five formulations of a novel melt processed poly-ethylene terephthalate (PET)-hemp fibers composite were determined, followed by a numerical investigation of their thermoformability. The composite linear visco-elastic properties were determined by small amplitude oscillatory shear tests and their visco-elastic behavior characterized by the Christensen's model. The forming pressure load required by the numerical analysis was derived from the Redlich-Kwong's real gas equation of state. The Lagrangian formulation combined with the membrane theory assumption was used in the finite element implementation. Moreover, the air flow's influence on the thickness of the thermoformed part, as well as the stress and the energy required for the process were analyzed. The observations indicated that there is a small influence of the constitutive equations of the investigated formulations on the final thickness distribution of the thermoformed part. Moreover, the time and energy required for the process showed no clear variation with the fiber load.

CHAPTER: 2

LITERATURE REVIEW

A better appreciation the topic is done with respect to the state-of-the-art of formulation and application of composite materials classified with respect to the reference processing temperature of 200°C.

2.1 *Composite materials reinforced with natural fibers: Generalities*

Composites are advanced materials made mostly of a matrix and some reinforcements; however, additives and fillers are sometimes essential elements of their formulation, depending on the targeted application [7–9]. Each component used in the composite formulation aims at achieving a specific goal. The matrices are generally responsible for the application's shape, while the reinforcements provide the required improvement of its mechanical properties. In addition to the composites' mechanical properties, an improvement of certain properties required by the applications is provided by the additives such as fire retardants [10–12] and coupling agents [13–16]. Those additives are then selected based on both the intended applications and the available matrix-reinforcements. Contrary to both the reinforcements and the additives, fillers do not provide any specific strength to the final composite material; however, they contribute to the reduction of the volume of certain key composite elements while maintaining its critical characteristics. In the light of this information, one can conclude that a filler plays a more economical rather than a technical role. In fact, they significantly increase the composite material's profitability as they lower its final cost [17–19].

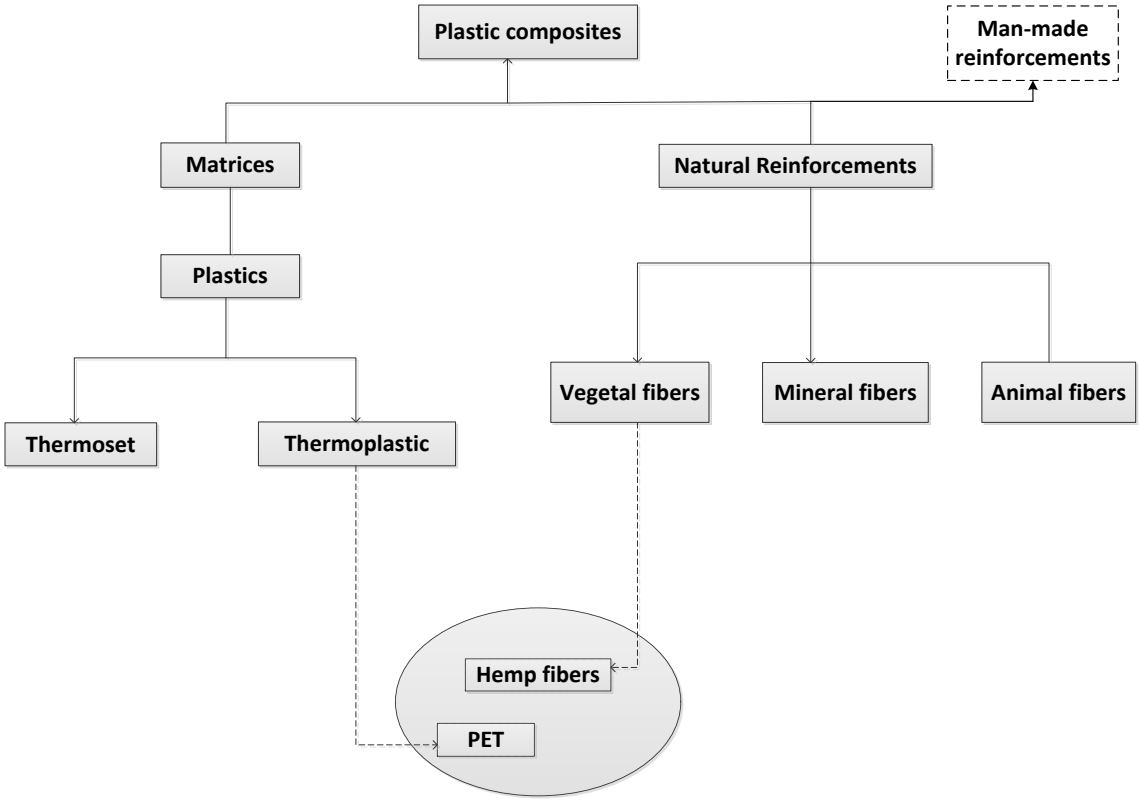

Figure 2-1: Major components of plastic composites.

The notion of composites is quite broad and unrestricted to any given industrial sector. In fact, composite materials are formulated with different kind of materials and applicable in a wide range of sectors such as the plastic industry, metallurgy and civil engineering [8,20]. In this regard, metal matrix composites and concrete matrix composites are respectively found in metallurgical and civil engineering, while thermoplastic or thermoset matrices are found in the plastic industry. In different cases, a particular composite's component can be used to achieve different objectives depending on the application. Such is the case for iron which is both used as a matrix for metal matrix composites and as a reinforcement in reinforced concrete [21–23]. This work focuses on the plastic industry where most of the reinforcements are either man-made fibers such as glass, carbon, Aramid like Kevlar or natural fibers from vegetal, animal and mineral

origins [11,24–31]. The major components of plastic composites are indicated in Figure 2-1 The most frequently used additives are either coupling agents which improve the matrix-reinforcement interface or the fire retardants. Although a significant amount of additives and fillers have been used in the plastic industry, they are not shown in Figure 2-1 in order to maintain clarity. Moreover, the remaining work is further restricted to the group of vegetal or ligno-cellulosic fiber-reinforced composites such as PET reinforced with hemp fibers.

2.1.1 The composite material's formulation with vegetal fibers

2.1.1.1 The reinforcing ability of vegetal fibers

Numerous applications of composite materials reinforced with vegetal or ligno-cellulosic fibers have been reported in the literature and newer avenues and applications are still being explored around the world through many active and intensive research programs. A wide variety of vegetal fibers have been investigated which include banana [32], hemp [33–36], flax [34,37], kenaf [17,38], jute [39], cotton [40], starch [41] and cellulose [42]. Although they stem from different sources, vegetal fibers have a common structure shown in Figure 2-2. They are made of different elements such as microfibers, microfilaments and incrusting substances which differ from each other based on their chemical compositions and their functions. In general, microfibers and microfilaments are each held together by the incrusting substances which then act as adhesives. In general, vegetal fibers are comparable to composite materials whose reinforcements are microfibers and microfilaments and which can be characterized by either their physical appearance or by their chemical structure.

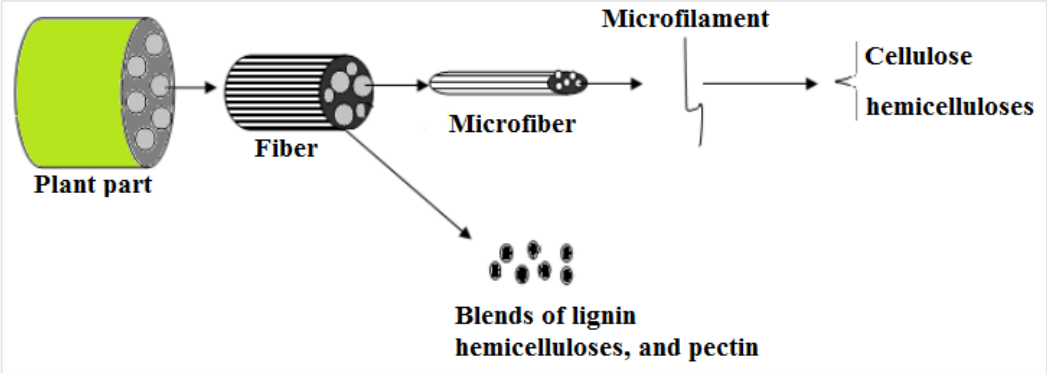

Figure 2-2: General structure of vegetal fibers.

The main components of vegetal fibers shown in Figure 2-2 can be organized under two groups of biopolymers which are cellulose and non-cellulosic materials. Cellulose, whose structure is given in Figure 2-3, is generally the most abundant element of the fibers, microfibers and microfilaments. As a biopolymer, cellulose has a repetitive unit made of two glucose molecules linked by a glycosidic bond and six hydroxyl groups which are potential sites for hydrogen bonding with polar matrices. Many properties of vegetal fibers have been reported to vary with different parameters such as the harvesting season, the geographical farming area and the post-harvest processing [17,43,44]. In this regard, naturally occurring cellulose has a degree of polymerization of 500 which is significantly lower compared to that of synthetic cellulose which can have up to 181 000 units [7,17,36,42,45,46]. Cellulose plays a major role in the mechanical properties of vegetal fibers owing to its reinforcing ability and its capacity to play a part in hydrogen bonding, which results in its potential intermolecular interactions especially with polar polymer matrices.

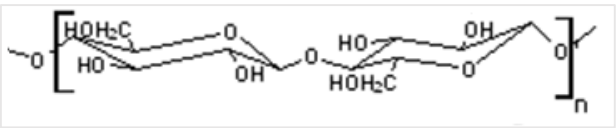

Figure 2-3: Chemical structure of cellulose, the major component of vegetal fibers.

Non-cellulosic materials of vegetal fibers, also known as incrusting substances include lignin, hemicelluloses and pectin. Contrary to cellulose, non-cellulosic do not show a regular chemical structure. Hemicelluloses for example are carbohydrate macromolecular chains containing different sugar rings, while lignin which is generally responsible for the rigidity of wood is made of poly-substituted phenolic compounds. Moreover, lignin has a much higher molecular weight than hemicelluloses. Pectins are polysaccharides linked to calcium ions. The degree of polymerization of non-cellulosic matters of vegetal fibers lies between 50 and 500 units [29,42]; moreover, they are hydro-soluble and amorphous due to their inability to show a regular repetitive pattern.

The properties of vegetal fiber-reinforced composites are directly impacted by the chemical and structural differences between cellulose and the incrusting substances. Cellulose has been shown to be an efficient reinforcement contrary to the incrusting substances which hinder an optimal fiber dispersion into the matrix [34], in addition to bearing some structural flaws and defects which eventually grow into the composite mechanical failure. Moreover, incrusting substances exhibit lower onset of thermal degradation which negatively affect natural fiber by lowering their onset of their thermal degradation (T_d) to about 190°C. Consequently, most of the actually reported vegetal fiber-reinforced composites have been formulated with lower melting thermoplastics matrices to avoid fiber thermo-degradation in the presence of high temperature melting thermoplastics as their melting points (T_m) are normally higher than 200°C.

Table 2-1: Mass composition of most common vegetal fibers [% (w/w)].

Fibers	Cellulose	Hemicelluloses	Pectin	Lignin	Wax
Jute [47]	61,0	20,4	0,2	13,0	0,5
Flax [17,47]	71,0	18,6	2,3	1-4	1,7
Hemp[47]	74,4	17,9	0,9	3,7	0,8
Ramie [47]	68,6	13,1	1,9	0,6	0,3
Sisal [17,47]	78,0	10,0	-	8,0	2,0
Coir [47]	43,0	0,3	4,0	45,0	-
Banana [48]	63-64	19	-	5	-
Pineapple [48]	81	-	-	12,7	-

The composition of some vegetal fibers reported by previous authors and summarized in Table 2-1. It shows that cellulose is the most abundant component of vegetal fibers irrespective of their origin [7,36,49]; However, contrary to man-made fibers, the properties of natural fibers vary with various parameters such as the geographical position, the harvest season and the various post-harvest treatments they have undergone. In addition to the previous properties, it is important to note that hemp fibers used in this work is highly renewable as it can be harvested up to three times a year.

There is a great similitude between vegetal fibers and composite materials, as explained in the previous sections. In fact, cellulose plays the role of reinforcement while the incrusting substances are either the matrix or the adhesives [17,29,42]. It is also possible either to decrease the mechanical strength of vegetal fibers by causing different post-harvesting defects to the fibers and microfibers or to increase it by altering their structure to lower their incrusting substances' content. Any method of complete or partial extraction of the incrusting substances would potentially improve on the reinforcing properties of vegetal fibers, especially with higher temperature melting thermoplastic materials.

2.1.1.2 The plastic matrix

The matrix, which is either a thermoplastic or a thermoset depending on its processing/synthesis method, is the second important constituent of composite materials. Thermoplastics are synthesized polymers that can be re-melted and cooled repeatedly during their life cycle. Such re-melting and cooling however have a negative impact on their mechanical properties as their chain lengths are gradually shortened by the process. There are unlimited possibilities to the applications of thermoplastics, both because they are not restricted in the plastic processing methods and because they do not have a limited shelf-life.

In the contrary, thermosets undergo polymerization during processing from their precursors and the resulting polymers cannot be re-melted after curing. This implies that the process cycle for thermosets is much longer because of the many stages involved, in addition to the limited shelf-life of their precursors. The concept of melting point is only theoretical for thermosets because of their inability for re-melting. Thermosets degrade at a given point when their temperature is increased (before the theoretical melting point). They are most suited for applications requiring a high thermal resistance; however, they are more restricted by their processing methods, processing cycles and the limited shelf-life of their precursors [21,22].

2.1.1.3 The matrix-reinforcement interface and the impact of additives

The interface between matrix and reinforcement is the connection point between the two main constituents which plays a crucial role in the composite properties. It is also

the area of stress transfer between the matrix and the reinforcement especially when the composite material is in service. In fact, its quality has an immediate effect on the mechanical, structural and rheological properties of the composite. The quality of the interface depends on many parameters like the reinforcement wetability by the matrix, the reinforcement size and the molecular interactions between the material constituents. These parameters have a major importance for vegetal fiber-reinforced composites where two alternatives exist depending on the polarity of the thermoplastic matrix. In the presence of polar matrices, the interface is reinforced by the strong chemical interactions between chemical groups. In fact, polar matrices like polyesters have the potential of forming hydrogen bonds between the hydroxyl groups of vegetal fibers and the carbonyl groups of polyesters. In the case of non-polar matrices, the interactions between chemical groups are inexistent and need to be created to improve on the matrix-reinforcement interface. In this regard, the interface between non-polar matrices reinforced with vegetal fibers is improved by the use of a coupling agent through a compatibilization process. Two main compatibilization mechanisms exist, either consisting of the modification of the main composite constituents (the matrix and the reinforcement) or the addition of a third component. The choice of the third component is crucial in the latter case. Most of the time, it is done to allow the reaction between one end of the coupling agent's chain and the matrix while the other end of the coupling agent reacts with the reinforcement. Different coupling agents have been used with vegetal fibers depending on the chemical structure of the matrix. Most of the applied coupling methods can then be classified based on their chemical reactions or their interactions [15]. Furthermore, reaction-based coupling operations can be qualified as chemical or physico-chemical, based on the nature of the modification reaction taking place in any or both of the constituents.

Three coupling mechanisms exist based on the interaction mechanisms. The most referred to, depicted in Figure 2-4, is the miscibility of the coupling agent into the matrix, the modification of the vegetal fibers and the modification of the matrix using chain extenders. Figure 2-4 is an illustration of a typical coupling mechanism based on the miscibility of the coupling agent (MA-PP) in the matrix (PP). Its shows the coupling of PP chains with vegetal fibers through MA-PP, while another end of MA-PP is miscible into the PP matrix [29,42,50]. Many coupling agents act through the same mechanism, since they both have affinities with the matrix and the reinforcement. Figure 2-4 shows how other polar components such carbonyls, hydroxides and amines grafted with polyolefin can be used as coupling agents.

The coupling mechanism based on the modification of the components is the most used for reinforcement with vegetal fibers. As explained in the previous sections, the coupling method based on vegetal fibers treatment or activation is frequently applied in the presence of polar matrices, while the coupling method based on vegetal fibers protection often applies in the presence of non-polar matrices.

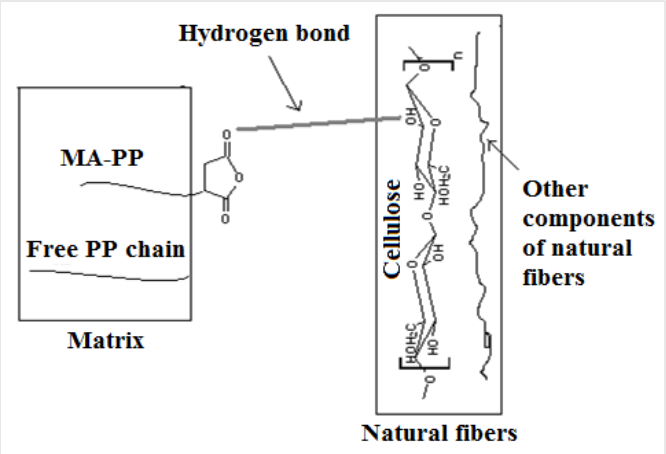

Figure 2-4: Chemical coupling between PP and vegetal fibers.

The coupling method based on vegetal fiber activation consists of an alkaline reaction to modify the structure as given in Figure 2-2 to release more hydroxide groups to chemically interact with the matrix. Some examples of these treatments are fiber activation and fiber mercerization which both include dissolving organic volatile components and hemicelluloses, releasing more cellulose chains, thus creating a potential for hydrogen bonding. In addition to activating vegetal fibers for hydrogen bonding, their chemical treatment also reduces fibers into microfibers which are much easily dispersed in the matrix [29,30,42,45,51].

The coupling agent is carefully selected when the compatibilization is based on vegetal fibers protection, so that some of its sites bind the vegetal fibers while others bind the matrix both through covalent and hydrogen bonding. It often proceeds by fiber coating with the coupling agent and the overall processes occur by physico-chemical transformations and chemical bonding. Some examples of fiber surface modifications have been reported by Pracella *et al.* [30] and Ana Espert [42] who respectively grafted glycidyl methacrylate on hemp fibers to reinforce polypropylene and esterified vegetal fibers while using butyric anhydride as a coupling agent. The chemical structure of the above mentioned coupling agents (glycidyl methacrylate, butyric anhydride) are shown in Figure 2-5 and the coupling mechanism based on vegetal fibers modification with anhydrides and epoxides for the reinforcement of polar matrices are given in Figure 2-6 and Figure 2-7.

Figure 2-5: Example of coupling agents used for vegetal fibers modification.

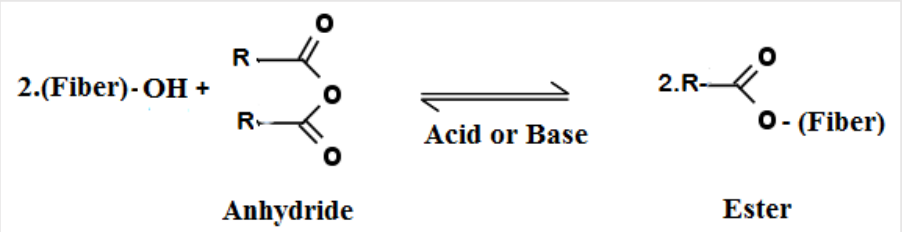

Figure 2-6: Mechanism for the modification of vegetal fibers with butyric anhydride.

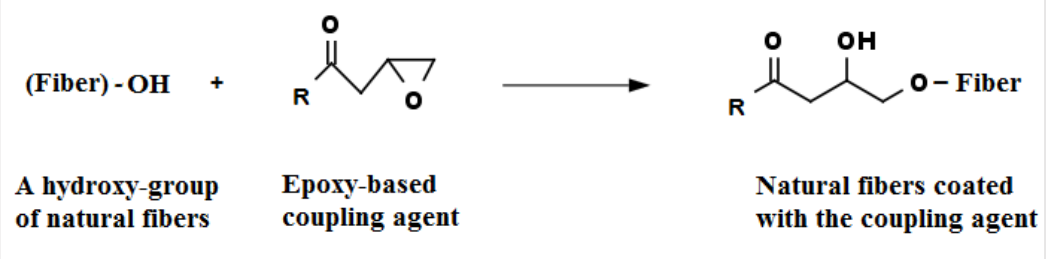

Figure 2-7: Mechanism of the modification of vegetal fibers with an epoxy-based coupling agent.

The last coupling method is similar to that presented in the previous section; however, it is based on the matrix modification by different methods such as ozonolysis [52] and chain extension [53]. Ozonolysis in one hand consists in breaking down unsaturated chemical bonds to form polar groups such as carbonyls. It is a chemical reaction which takes place in the presence of ozone. On the other hand, polymer chain extension consists in using chemical agents also known as chain extenders to primarily bind different polymeric chains; however, it often leads to the creation of secondary bonds between the matrix chain and the reinforcement molecules. This means that the use of a chain extender creates a network between matrices and reinforcements, thus improving the resulting composite material interface.

In addition to the chemical agents used for the coupling between matrices and reinforcements, other additives such as fire retardants and fillers are often used depending on the final composite material's targeted application. The use of fire retardants is justified by the flame vulnerability of both the plastic-based material and the vegetal fibers. Many fire retardants have been reported showing different formulations and different operation mechanisms including ignition reduction and deceleration of flame progression. The state of application of fire retardants shows a high prevalence of poly-brominated and phosphorous containing compounds. However, there is an intensive ongoing research focusing on developing environmental friendly fire retardants and nano-clay has been reported as a potential alternative although its dispersion into the matrix is still challenging [28,31]. In the next section, the literature search given on the actual vegetal-fiber reinforced composite applications provides a better appreciation of the interface quality.

2.1.2 The rich potential of composite materials reinforced with vegetal fibers

An appreciable number of applications of vegetal fiber-reinforced composites are found across many disciplines, such as in construction [54,55], in automobiles [49,56] and in biomedicine [57]. Although numerous construction applications are reported worldwide, one of the oldest uses can be traced back to the ancient Egypt, where mud and straw were successively used as matrix and reinforcement for the construction although they were limited to commodities like garden benches. In the case of the automobile industry, an increase in their use by 28000 tonnes has been reported by "IENICA" between 1994 and 2000 in the form of compression or injection molded epoxy, urea and

phenol formaldehydes reinforced with flax, sisal and kenaf [49,52,58]. Most of the mentioned increase is the direct consequence of the improved mechanical and structural properties of ligno-cellulosic fiber-reinforced composite reflected by the quality of the interface between the matrix and the reinforcement. In fact, ligno-cellulosic fiber-reinforced composites offer numerous important advantages such as:

- The ease of processing, especially in the presence of lower melting matrices;
- Their low cost due to both the availability and the renewability of the main components;
- Their good mechanical properties which are comparable to those of man-made fibers-reinforced composites;
- Their good acoustic and thermal insulating properties;
- The good fiber-matrix interface due to the available chemical group interactions (at times in the presence of a coupling agent);
- The high surface to volume ratio for natural fiber, thus a large area for matrix-fiber interaction;
- The low mass density of vegetal fibers which induces the processed part weight reduction by 10-30%;
- Their resistance to corrosion;
- Their good health and safety record, especially at low temperature where there is no gas and odor emission.

2.1.3 The specific case of PET reinforced with hemp fibers

Hemp (Cannabis sativa L.) is an old industrial bast plant which has been prominent over the years because of its fiber properties, such as the length, the cellulose content and the renewability. Hemp fibers can be as long as 2 to 3m which is an advantage over wood fibers which are only a few centimeters long. They can however be shortened by post harvesting operations shown in Figure 2-8 [35]. There is no serious health concern about industrial hemp fibers as they contain less than 0,3% (w/w) of delta (9) tetrahydrocannabinol (THC). Furthermore, hemp fiber is highly renewable with up to three farming cycles per year [52,59]. Hemp fibers show a good reinforcing potential especially for polar matrices through its high cellulose content (70% (w/w)). Its early high end applications include ship ropes in East Europe and China [43], as well as previously mentioned applications with low temperature melting thermoplastics.

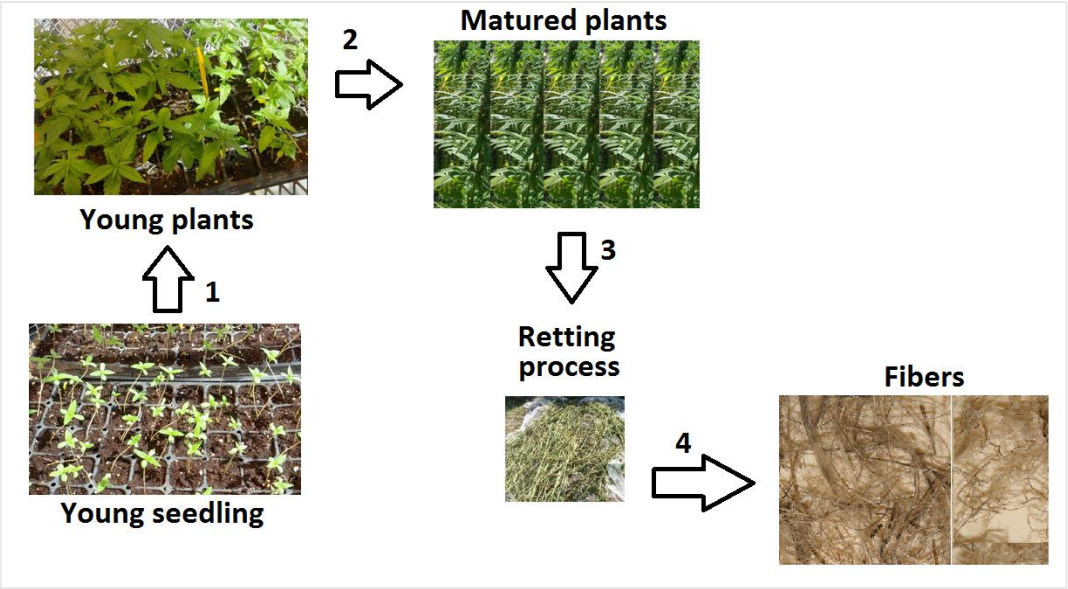

Figure 2-8: Photographs of hemp plants and hemp fibers (By courtesy of Dr Tango, Acadia University, NS, Canada)**.**

PET is a high temperature melting thermoplastic resin (T_m~250°C) which is widely used in the packaging, biomedical and textile industries. It is either synthesized by esterification in the petrochemical industry or by recycling in the textile and packaging industries [60]. Its gas barrier properties as well as its ability of being easily molded by the injection-blow process makes PET an interesting candidate for the brewing industry [60,61]. Other advantages of working with PET are based on its structure shown in Figure 2-9 and include its polar groups which provide a good interface through hydrogen bonding with polar reinforcements and the benzene ring which is responsible for the toughness of its applications. Although the largest use of PET is in the packaging and textile industries, major applications for sutures [57] are also found in the biomedical engineering. In fact, PET is both biocompatible and bio-inert.

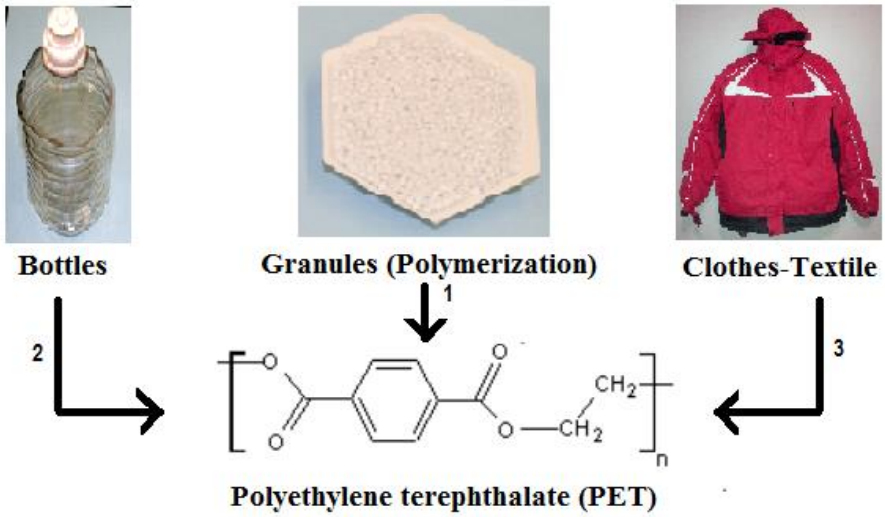

Figure 2-9: Chemical structure and a few uses of PET: Chemical synthesis (1), recycling from the packaging (2) and the textile (3) industries.

Based on the structures of PET and cellulose (most abundant component of hemp fibers), it is advantageous to reinforce PET with hemp fibers. In fact, their polarity is beneficial for an improved interface through hydrogen bonding as shown in Figure 2-10.

Furthermore, the high glass transition temperature (T_g = 60°C) of PET with respect to room temperature, is a guarantee for the solid state of the processed parts. Finally, their close densities as shown in Table 2-2, reduces the possibility of unwanted stress concentration in the parts during the cooling stage of the process.

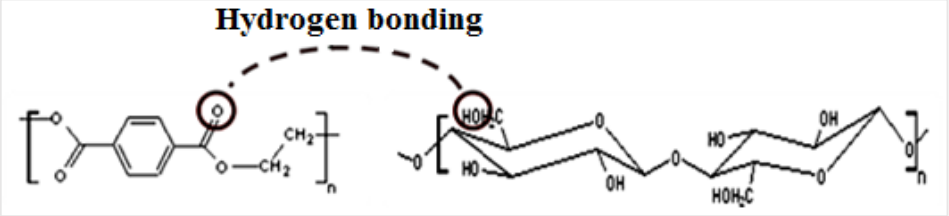

Figure 2-10: Illustration of the possible hydrogen bonding site between PET and cellulose.

A good potential for reinforcing PET with hemp fibers can then be expected, which, in the best of our knowledge has only been beneficially exploited through filament winding by Bo Madsen [62]. Since our intention is to apply such formulation through thermoforming, the following section will be devoted to such process prior to finding a proper methodology.

Table 2-2: Comparison of the mechanical properties of various materials.

Materials	Density [kgm^{-3}]	E-Tension [GPa]
Wood[63]	600	12-100/Microfilament
Steel [64]	7850	200
PET[57]	1370	3
Hemp fibers[65][66]	1480	30-60
Glass fibers[65][66]	2560	76
Carbon fibers[65][66]	1790	370

2.2 *Applications of vegetal fiber-reinforced composites*

An important volume of the applications of vegetal fiber-reinforced composites reported in the literature can either be classified based on the matrix class or based on the difference between the onset of thermal degradation of vegetal fibers (T_g = 190°C) and the melting point/processing temperature of the matrix.

In this regard, there are vegetal fiber-reinforced composites with either thermoplastic or thermoset matrices based on the matrix class. However, the previous classes can be further subdivided into vegetal fiber-reinforced composites with high temperature melting thermoplastic matrices (T_m>200°C), vegetal fiber-reinforced composites with low temperature melting thermoplastic matrices, as well as vegetal fiber-reinforced composites with thermoset matrices having either a low or a high processing temperature (the threshold being T_m=200°C). The "processing temperature" is more appropriate to the thermosets matrices as previously explained in Section 2.1.1.2. Many authors have used 200°C as the threshold temperature [8,17,19] to separate these classes.

2.2.1 Applications of thermoset matrices reinforced with vegetal fibers

Thermoset matrices are mostly processed between 100°C and 200°C. Consequently, low temperature processing thermosets reinforced with vegetal fibers is the most prevalent group of thermosets reinforced with vegetal fibers based on the definition of section 2.2. In fact, very few cases of wood plastic composites have been reported with high processing temperature by authors such as Michaud [29]. These works

describe, woven vegetal fibers impregnated within thermoset matrices such as epoxy prior to molding by classical methods like compression and pultrusion and directed to applications in the construction, automobile, recycling and commodities.

Applications of low temperature processing thermosets reinforced with vegetal fibers are mostly found in the construction industry in the form of wood fibers-reinforced composites. It is an extensively studied group of composites by authors like Michaud [29] and Singh and Gupta [39]. Their work was respectively based on medium density fiber board made of urea formaldehyde reinforced with wood chips following a polymerization process below 200°C and the production of a door-frame with jute fibers impregnated in phenolic matrices.

The automobile industry has seen a considerable amount of applications of vegetal fiber-reinforced composites with low temperature processing thermoset matrices. Many of these applications reported by Ellison *et al.* [49], include the manufacture of door liners, headliners, boot liners, parcel shelves, interior sunroof, headrest, seat backs and floor pan substrates for companies such as Audi, Ford AG, Opel and Mercedes. These applications were mostly made with matrices of epoxy and polyurethane reinforced with jute, flax and kenaf fibers. Rodriguez *et al.* [67] have reported similar applications in the automobile industry based on recycled low temperature processing thermosets reinforced with vegetal fibers by milling vinyl ester reinforced with flax fibers which was later used as reinforcements or fillers depending on the targeted application.

Commodity applications have been an important portion of low temperature processing thermosets reinforced with vegetal fiber. An example of such application was reported by Sapuan *et al.* [58], in the form of a household telephone stand processed at

room temperature by impregnating woven banana fibers in a blend of epoxy resin and the hardener.

Few works exist about low temperature processing thermosets reinforced with vegetal fibers aiming at showing the chemical interactions between esterified vegetal fibers and polyester resins. They were reported by Sebe *et al.* [68] in 2000 and Tong *et al.* [69]. Sebe *et al.* observed an absence of fiber pull-out following polyester's transfer molding with virgin hemp fibers as well as hemp fibers treated with either pyridine or esterified with methacrylate anhydride in the presence of pyridine. Tong *et al.* also reported similar observations, with unsaturated polyester reinforced with hemp fibers impregnated in epoxy resin prior to compression molding and three-hour polymerization.

2.2.2 Applications of thermoplastic matrices reinforced with vegetal fibers

A larger amount of work on thermoplastic matrices reinforced with vegetal fibers is found in literature compared to those of thermosets. They can also be divided into low and high temperature melting thermoplastics reinforced with vegetal fibers, following the definition of Section 2.2. These applications, which are found in areas such as construction, automobile, biomedicine and aerospace are also in constant growth.

2.2.2.1 Applications of low temperature melting thermoplastics reinforced with vegetal fibers

The automobile industry is actually highly impacted by thermoplastics reinforced with vegetal fibers. Almost all the applications of Section 2.2.1 concerning the

applications of thermosets reinforced with vegetal fibers found in the automobile industry have also been found with thermoplastics matrices [49]. Moreover, they have been increasing steadily since 1996 as a result of an efficient research and development sector. In fact, the European Union for the automobile industry has reported an increase of 5-10kg in utilization of vegetal fibers per car between 1994 and 2000, thus a total of 28ktons from an initial amount of zero tons [52]. Some common applications include the windshield and dashboards respectively reported by C. Holmes [52] and Rodriguez *et al.*[67].

The construction industry is also highly impacted by thermoplastics reinforced with vegetal fibers as attested by the many reported applications and R&D cases. Most of those applications are either in the form of plastic lumber or wood plastic composites. Some examples include doors and window frames, floor panels, ceiling boards, deck boards as well as other classical applications of wood in construction [54,70], generally molded by injection, compression and extrusion.

Wood plastic composites are characterized by their formulation which contains 50% (w/w) of wood products (or other vegetal fibers) and 50% (w/w) of thermoplastic matrices. They are cost effective and they generally show appreciable mechanical properties. They are either extruded into sheets intended for thermoforming or injection molded to the desired part. Some matrices frequently used in wood plastic composite formulation include PP, HDPE, PS, ABS and PVC. Some representative works of wood plastic composites in construction were reported by Michaud [29] and Clemons *et al.* [9,17] with the above mentioned matrices in areas such as floor, deck and garden bench.

Plastic lumbers constitute the main group of low temperature melting thermoplastics reinforced with vegetal fibers. They are bio-composite materials

formulated as a blend of polymeric resins mostly from recycling, reinforced with vegetal fibers. In fact, the melt blending of a mixture of recycled matrices with vegetal fibers is less challenging; however, those products are limited by the uniformity of their properties. Some examples of applications in this group are reported by Lampo *et al*. [70] and Clemons *et al*. [17] in the fields of design, construction and use of an I-beam for the construction of Wharton State Forest Bridge in cooperation with Rutgers University and McLaren Engineering. Such application had a tremendous impact on both the reduction of the processing cycle and the wasted materials. Other reported applications of plastic lumber include railway crosstie [55], marine pilings and bridge sub-structures [71]. Plastic lumber has made a significant contribution to plastic recycling and production of high end construction products.

2.2.2.2 Applications of high temperature melting thermoplastics reinforced with vegetal fibers

It was mentioned earlier that melt processing composite materials reinforced with vegetal fibers at high temperature is challenging owing to the risk of the fiber thermo-degradation. Consequently, there is just few applications of high temperature melting thermoplastics reinforced with vegetal fibers. Four major related applications have been reported in the literature respectively by Field *et al.* [72], Caulfield *et al.* [73,74], Madsen [62] and Lei and Wu [75]. In each of the cases, a specific strategy had been designed to tackle the related melt processing challenge.

In this regard, Field *et al*. had performed a cold compounding of PET and cellulose in the presence of trifluoroacetic acid (TFA) and methylene chloride. Caulfield *et al.* had

processed polyamide 6 (PA 6; T_m = 220°C) and polyamide 6, 6 (PA 6, 6; T_m = 225°C) reinforced with purified wood-pulp fibers through the "chill processing" which consisted of introducing the fibers in the matrix at a temperature above their melting point, followed by composite processing by extrusion, injection and rapid cooling. Madsen worked with PET and hemp fibers; although the raw materials are similar to ours, he avoided complete melt processing by applying a combination of PET and hemp fiber filaments winding followed by compression molding. Finally, Lei and Wu have successfully extruded wood plastic composites of HDPE-25% (w/w) PET reinforced with up to 40% (w/w) of wood flour [75]. Although all these methods were successful, they are unsuitable for scaling up to an industrial plant as they are either environmentally unfriendly or cost ineffective.

As indicated in Section 2.2, the restriction of the applications of thermoplastics reinforced with vegetal fibers to the formulations with low temperature melting matrices is due to the gap between their melting points (T_m > 200°C) and the onset of thermal degradation of vegetal fibers (T_d = 190°C). The immediate consequence of such gap is the thermal degradation of vegetal fibers during melt processing. A great potential, however, exists for composites of high temperature melting thermoplastics matrices and vegetal fibers. This potential, which is based on their chemical group synergies is even more reinforced in the presence of polyester like PET.

2.3 *Elaboration of ligno-cellulosic fiber-reinforced composites*

Two main elaboration methods of vegetal fiber-reinforced composites can be deduced from the different classes of their applications, introduced in the previous section and shown in Figure 2-11. They can be categorized as chemical or physical, depending

on the nature of the operations that they require to tackle the processing challenges and improving the matrix-reinforcement's interface.

The chemical methods of bio-composite elaborations include the addition of a coupling agent, treatment with an acid or alkaline solution, as well as an enzymatic modification of the ligno-cellulosic fibers. The coupling methods and their various mechanisms have been discussed in Section 2.1.1.3, showing that their need is mostly required in the presence of non-polar matrices in the example of polyolefins [13,14]. The acid and alkaline treatment methods are mostly applied for the activation of ligno-cellulosic fibers in order to improve the matrix-reinforcement interface [37,76–78]. An alkaline treatment disrupts the vegetal fiber structure thereby leading to the extraction of low temperature or molar mass volatile organic compounds (Low-VOC) as well as non-cellulosic matters like hemicelluloses and lignin which normally show lower thermal stability [47,76,79]. The alkaline treatment also affects the hydrophilic and hygroscopic nature of vegetal fibers, reducing it to 2-3% (w/w); the absorbed water vapor often act as a processing lubricant or a plasticizer [8]. On the other hand, acid hydrolysis had been applied to ligno-cellulosic matters at some stage of the production of nano-crystals which are excellent reinforcements for vegetal fiber-reinforced composites [36]. In conclusion, acid and alkaline treatments can differ by the structural changes on the reinforcement.

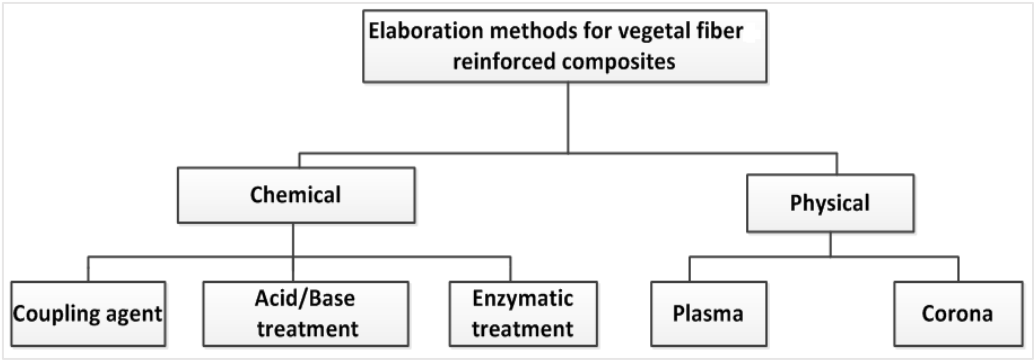

Figure 2-11: Methods of elaboration of vegetal fiber-reinforced composites.

The enzymatic treatment arose in the quest of developing bio-degradable materials from plastics based on environmental friendly processes. Similar results to those achieved by the application of alkaline solutions have been reported for most of the enzyme treatments. Such is the case for the application of Lignin peroxidases (LiP), laccases and some fungi for example reported by Pickering *et al.* [51] and by Lui *et al.* [80] for the matrix-reinforcement interface through a combination of lignin extraction and cellulose. Moreover, enzymatic treatments have been extensively applied for the formulation of bio-degradable vegetal fiber-reinforced composites [81].

There are many physical methods of fibers and matrix treatment which occur during the elaboration of vegetal fiber-reinforced composites. They bring about changes in the fiber structure as well as changes in their surface properties. The most applied methods are calendaring, stretching, thermo-treatment as well as some electric discharge methods [47] such as plasma and corona treatments. The electric discharge methods are based on ionizing an inert gas such as helium (He), oxygen (O_2), nitrogen (N_2) or air by a subjected electrical discharge, thereby producing an equal number of cations and anions which in turn modifies the surface without changing the bulk properties. These methods have been studied by many authors [79,82,83]. Although the results are dependent on various parameters such as the intensity of the electrical discharge, the time of exposure and the type of gas, the frequency of the electrical discharge is the main difference between plasma and corona. In fact, high frequency electrical discharge produced by microwave energy is related to cold plasma treatment while low frequency alternating current discharge is related to corona treatment. Moreover, the plasma method can be classified as a thermal treatment method, while coronas are non-thermal treatment methods.

Calendering, stretching and thermo-treatments are mostly applied to the compounded mix as a physical mean of elaboration and interface improvement [83–85]. During calendering, the air bubbles are extracted from the compounded mix which is shaped into fine sheets by passing through calendar rolls of about 89 $kgcm^{-1}$. The method is quite practical for mixtures that are thermo-degradable as well as blends which composition do not allow proper blending. The challenges related to calendering are the equipment costs as well as their adjustment during the process [86].

2.4 *Characterization of ligno-cellulosic fiber-reinforced composites*

The concepts of material formulation and its optimal application are interrelated, especially when dealing with composites. In fact, composite elaboration offers the means to combine the constituent properties into the targeted application design parameters. Material characterization is thus of paramount importance to any successful elaboration process and principally when specific applications are targeted.

Two main level of characterization are generally considered in the composite field; the first one focuses on the material behavior in-service, while the second one is concerned with its behavior during the forming process. Moreover, since the structures of composite materials are either heterogeneous or homogeneous at the micro and macro scales, most composite material's properties are either anisotropic or isotropic at the micro and macro viewpoints. Most of the characterization which is normally based on the investigation of various structural responses to different loading situations [82] is performed at the macro scale to provide the mean values of the investigated properties.

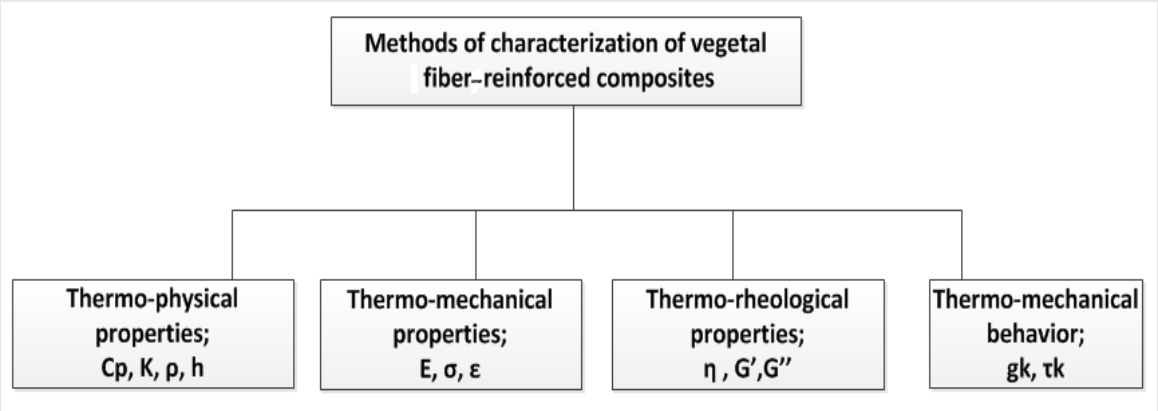

Figure 2-12: Methods of characterization of vegetal fiber-reinforced composites.

A summary of the essential parameters for a successful design and processing with vegetal fiber-reinforced composite materials is shown in Figure 2-12. Their impact is generally a function of the final application and the relevant process. Many factors associated with the equipment, the operator, the sample and the testing conditions do influence the outcome of each characterization technique; however, almost all of them are temperature dependent. Thus, this is the reason behind investigating the combined behavior of the materials such as thermo-physical, thermo-mechanical, thermo-rheological and the thermo-mechanical behavior. Some examples of such thermal association can be found in the literature concerning the impacts of the thermo-mechanical behavior on processing and recycling [8,87], the thermo-mechanical and thermo-rheological history on the in-service performance [88], the thermo-mechanical degradation on processing [89], the thermo-rheological properties on both processing and in-service performance and the thermo-physical properties on processing [90,91].

Most of the properties introduced in Figure 2-12 have been determined following the applicable standards under isothermal conditions and are more relevant to the in-service properties; however, the ideal description of the material behavior which is relevant to the forming process is done under non-isothermal testing processes. Although

the description of these properties in the following sections deals mostly with isothermal variations, the equipments used always offer provision for non-isothermal variations. The most applied testing standards are provided by organizations such as the American Society for Testing and Materials (ASTM) or the International Organization for Standardization (ISO). The instrumental methods of analysis are powerful techniques for vegetal-fiber reinforced composites analysis because of their simplicity, sensitivity, versatility and their speed of application.

Other composite material properties relevant to the design of their applications and their successful forming process are omitted in Figure 2-12. Some examples are the moisture represented by swelling coefficient and moisture diffusivity which seem significant when the diffusion rate difference between the constituents is important [82,92–94]. They also include the effect of time variation of the properties which may be necessary especially when dealing with properties like creep, strain relaxation, fatigue, durability, vibration [82].

2.5 *The thermoforming of ligno-cellulosic fiber-reinforced composites*

2.5.1 The process

Thermoforming is one of the numerous methods of plastic and composite processing. It is applied for the molding of a wide variety of products with different parameters including different size as well as a limited thickness. Thermoformed products are found in various sectors including aerospace, automobile, biomedical, food packaging and construction.

A summary of some important elements of the thermoforming process are shown in Figure 2-13. They include the molds (male and female), the plastic/composite sheet and the thermoforming equipment including its heating system. During the thermoforming process, a sheet of plastic or composite is successively subjected to various conditions. In order to mold the sheet into the desired product, a pressure drop is applied to its sides, after it has been heated until it is in its rubbery zone. The process can be further subdivided into the following steps [85,95]:

- Mold installation on the mold support;
- Plastic or composite sheet fixation on its holder;
- Plastic-composite sheet heating until the optimal thermoforming temperature;
- Part forming either by air suction or pressure drop;
- Part cooling and ejection.

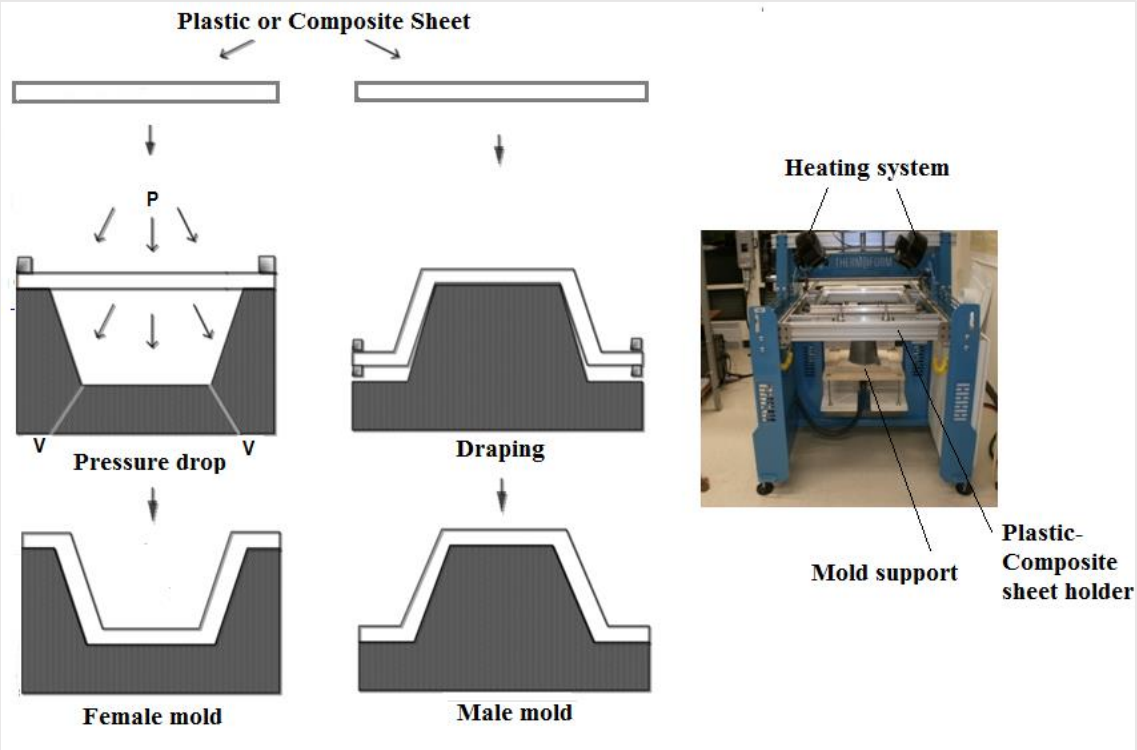

Figure 2-13: A few steps of the thermoforming process.

Since the behavior of thermoplastics and their composites is highly temperature dependent, temperature and pressure are the important thermoforming parameters. Their long entangled molecular chains normally get into motion as their temperature is increased and their nature is gradually changed from glass to rubbery and finally to viscous. Such variations of thermoplastic material properties have an impact on their thermoforming since it is characterized by large deformations within the rubbery range.

In comparison to other plastic-composite forming processes, thermoforming offers many advantages including the low cost of the equipment, the fine thickness of the parts, the ease of mold modification and the possibility of molding large parts while displaying fine details. In addition, thermoforming is well suited for prototyping in Research and Development, since the needed modifications can easily be implemented on the prototype

prior to the final industrial application. Thermoforming has been largely applied and studied in the plastic industry [96–98].

Certain plastic and composite parameters such as the degree of crystallinity, the reinforcement and the viscosity are obstacles to their thermoforming processing. In general, reinforcements drastically lower composite elongation at break and the degree of crystallinity increases during heating between the glass transition (T_g) temperature and the melting point (T_m). Finally, both low and very high viscosities are also limiting thermoforming conditions, especially in the presence of semi-crystalline resins and reinforcements.

2.5.2 Current states of the thermoforming of vegetal fiber-reinforced composites

Many authors have been interested in the thermoforming of vegetal fiber-reinforced composites; however, their works are either limited to the group of low temperature melting thermoplastics reinforced with vegetal fiber or to the aspects of modeling and simulation [38,66,85,99,100]. Thermoforming vegetal fiber-reinforced composites is challenging because the process requires large deformations even if the reinforcement with vegetal fibers reduces the elongation at break of the composites.

Although little has been done concerning the thermoforming of thermoplastic matrices reinforced with vegetal fibers, some significant literature results involving large deformations are transferrable to the thermoforming of high temperature melting thermoplastics reinforced with natural fibers. Such are the work of Erchiqui *et al.* [101,102] concerning the neural characterization of visco-elastic materials and the potential thermoforming of HDPE-reinforced with wood fibers.

CHAPTER: 3

MATERIAL AND METHODOLOGY

3.1 *Materials*

Table 3-1: Materials and suppliers.

Material	Supplier	Characteristics
PET (AA-48)	CCC-Plastics, Montreal, QC., Canada	CZ-602
PCL	Sigma-Aldrich, Oakville, ON., Canada	70,000-90,000 PU
Hemp fibers	Stemergy (London, ON.)-Lanaupôle (Joliette, QC.)	5 cm average length
NaOH	Sigma-Aldrich	99% Purity
Hydroquinone	Sigma-Aldrich, Oakville, ON., Canada	-
Triethylamine	Sigma-Aldrich, Oakville, ON., Canada	-
Clay	Southern Clay Products, Inc., Gonzales, TX, USA	Cloisite 30B
PMDA	Sigma-Aldrich, Oakville, ON., Canada	-
GMA	Sigma-Aldrich, Oakville, ON., Canada	-
H_2SO_4	Sigma-Aldrich, Oakville, ON., Canada	-

Table 3-1 gives a summary of the materials used in different stages of this work as well as their source. Moreover, clay, pyromelitic dianhydride (PMDA) and glycidyl methacrylate (GMA) were respectively used as fire retardant [31], chain extender [103,104] and fiber coating agent [75] while triethylamine, hydroquinone and sodium hydroxide were used as chemical agents in different stages of the process described in the following sections.

3.2 *Methods*

3.2.1 Methods of PET-hemp fiber composite elaboration

The successive elaboration of PET-hemp fiber composites and the thermoforming of their applications are achievable by tackling the challenges presented in Section 1.3. The methodological milestones draw inspiration from the publications of previous authors. This includes processing non-thermally degraded PET-hemp fiber composites by simultaneous hemp fibers treatment and PET modification, followed successively by the compounding of the various elements, composite processing and characterization and finally the numerical thermoforming of the optimal formulation using the determined composite parameters.

3.2.1.1 Hemp fiber treatment

Different hemp fiber treatment methods were investigated with the objective of improving their thermal stability [78] and the quality of PET-hemp fiber interface. The most common methods consist in hemp fiber activation and mercerization previously described in Section 2.1.1.3. It was also coupled with fiber coating with substances with a dual functionality as thermal protection and coupling agent [42,79].

The fibers were treated with a 5N solution of NaOH based on a variation of the methods presented by Specht [37] and Espert [42] and described in Appendix III. They were additionally protected from thermal degradation by coating with GMA following the method published by Pracella [30] in one case and coating with PCL in the presence of tetrahydrofuran (THF) in the others. The choice of the coating agents is based on comparable reactions which are suspected to take place between hemp fibers and GMA

in one case and between hemp fibers and PET in another, owing to the similarities of chemical groups involved. Some physical and morphological differences between virgin and alkaline treated hemp fibers are noticeable in Figure 3-1. In fact, treated fibers are converted into microfilaments revealing a cotton-like appearance. They are subsequently easily dispersed into the matrix and they provide a larger surface area of interactions.

Figure 3-1: Aspect variation of hemp fibers: Virgin (A) and alkaline treated (D).

3.2.1.2 Matrix modification

The processing temperature of PET was lowered following the melting point depression method reported by previous authors [105,106]. The melting point depression was achieved in a preliminary work by blending PET with polycaprolactone (PCL), a lower melting (T_m = 60°C) polyester. In the preliminary phase, compounding was done with a thermo-kinetic mixer type Gelimat shown in Figure 3-2. Batches of 250 g of materials were blended and 5% (w/w) PCL-PET was the optimal blend selected for reinforcement with hemp fibers in the presence of some additives. A grade of polycaprolactone containing 70,000 - 90,000 units was also selected to achieve the main objective while inducing only a minimal modification of the matrix structure. In fact, a network of polyester chains is created by a blend of PET and PCL.

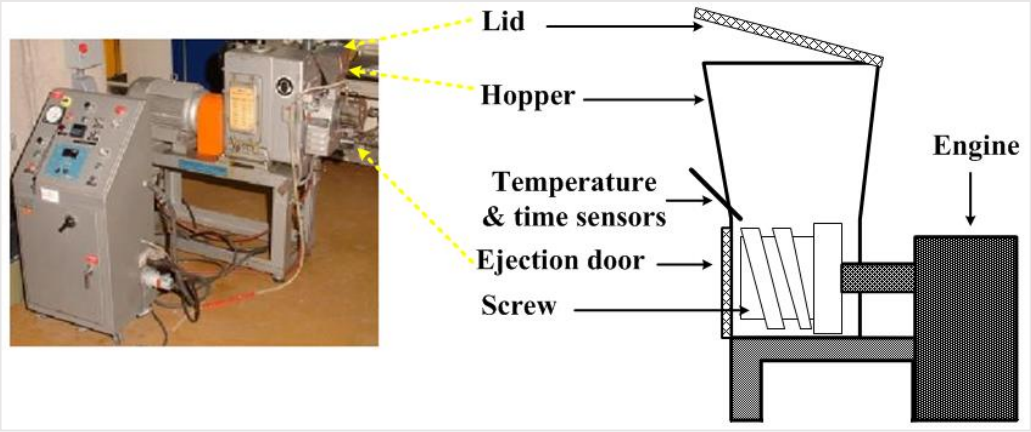

Figure 3-2: Thermo-kinetic mixer; Gelimat (Werner & Pfleiderer corp., Germany).

The thermo-kinetic mixer is an internal batch mixer in which the blend is submitted to both a high shear stress and a rotational speed of an ultra-high range (>2000 rpm). The blending operation with a thermo-kinetic batch mixer is accompanied by the conversion of the system kinetic energy into the thermal energy which eventually melts the polymeric resin. In this regard, thermo-kinetic mixers have been used by previous authors to handle complex blends in which dispersion is challenging [107–109]. The possibility for ongoing additives insertion motivated its choice. Those additives acted through a physico-chemical coupling mechanism.

3.2.1.3 PET-hemp fiber composite compounding and processing with and without additives

A stepwise process was applied by varying the composite formulation during the compounding and processing steps with the objective of determining those best suited for the thermoforming process. In this regard, two major composite groups comprising PET-

5% (w/w) PCL-5% (w/w) hemp fiber-Additives and PET-5% (w/w) PCL-hemp fiber blends, were investigated in the first and second groups respectively.

In the first step, the ability of various additives used in common applications to be effective with PET-hemp fiber composites was investigated by processing and characterizing the composite of the first group (PET, 5% (w/w) PCL, Additives).

In the second step, an analysis of the reinforcing ability of hemp fibers was done by processing and characterizing the composite of the second group while varying hemp fiber concentration between 5 and 20% (w/w).

3.2.1.4 The compounding of PET-Hemp Fiber with and without additives

The composite formulations reinforced with 5% (w/w) hemp fibers and containing different additives were compounded with the thermo-kinetic mixer described in Figure 3-2, using the procedure described in Section 3.2.1.2.

The formulations without additives were compounded with a torque based rheometer system (Haake Rheomix, polylab OS system, USA) shown in Figure 3-3 as a method for handling the important fiber volume processed. Each mixing batch contained about 300 grams of each formulation reinforced by respectively 1, 5, 10, 15 and 20% (w/w) hemp fibers and repeated three times with the Rheomix mixing chamber heated at 240, 250 and 260°C. During the process, the equipment blades were rotating at 60 rpm. The reinforcement concentration was limited to 20% (w/w) due to the equipment restriction. The torque based rheometer operates by shearing, melting and blending the materials under a combined effect of the applied torque, the heated mixing chamber and a counter-rotation of the blades.

Many previous works have reported the production of homogenous material blends using a torque based rheometer [110–115]. Amongst other advantages of this equipment, it has been reported that it can effectively handle complex blends like PET-Hemp fiber-Additives investigated in this work noting that surface to bulk ratio of hemp fibers is large.

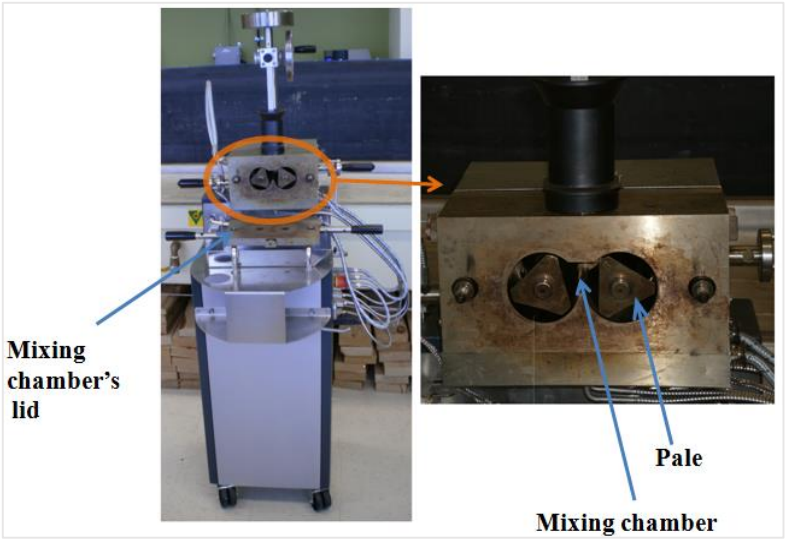

Figure 3-3: Torque based batch mixer (Rheomix, polylab OS system, USA**).**

3.2.1.5 Injection molding and thermo-compression

The investigated composite formulations were injection molded following compounding and granulation. The composite formulations with 5% (w/w) hemp fibers and different additives were injection molded at 250°C with a 15 tons injection molder model Engel 55 shown in Figure 3-4, while those without additives were processed with a Haake minijet II shown in Figure 3-5.

The mold temperature was maintained at 50°C in each case. Moreover, injection molding was preceded by pre-drying of the granulated formulations at either 80°C for 16 hours or 150°C for 4 hours. Such procedure was indispensable to avoid the thermal

degradation by reverse esterification. Injection molding was further followed by an induced crystallization of some samples by annealing at 110°C for 2 hours. The minijet replicates the operations of the classical injection molder. Other samples were also processed by thermo-compression using the 12 tons' Carver equipment shown in Figure III-6.

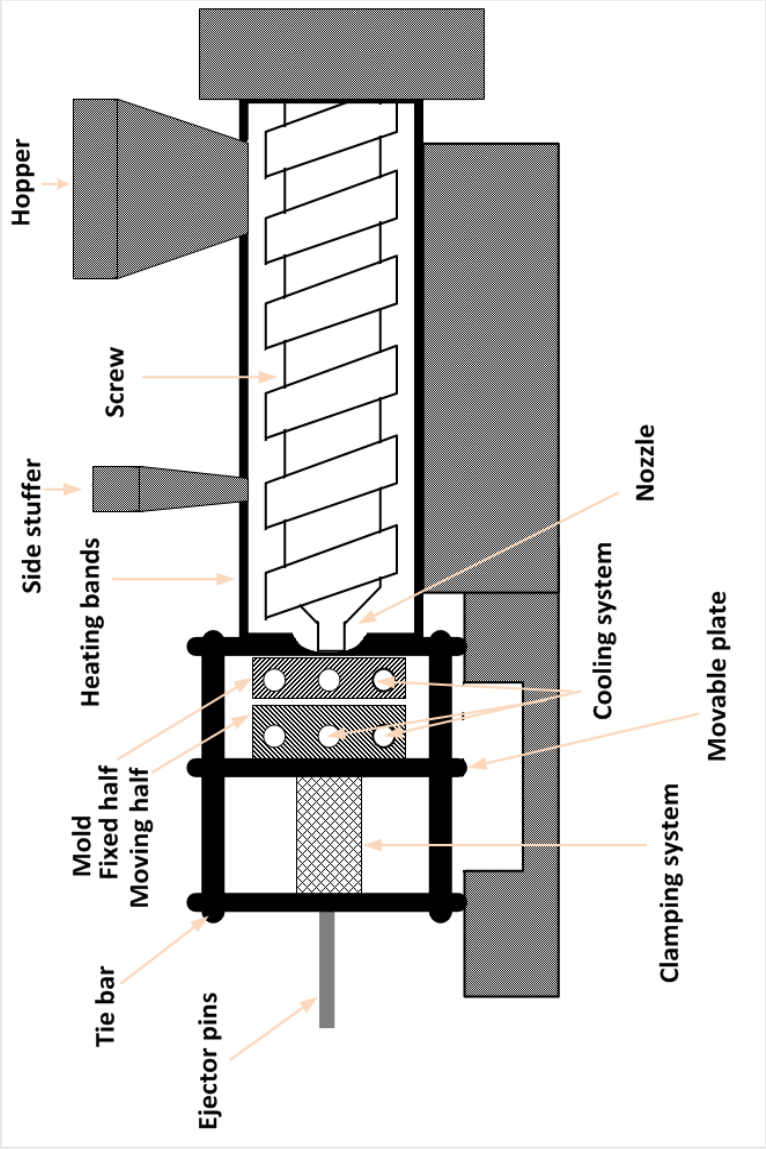

Figure 3-4: Cross section and main elements of an injection molder.

Figure 3-5: Mini injection molder, Haake Minijet II (A), its important parts, some flexural and tensional test samples (B).

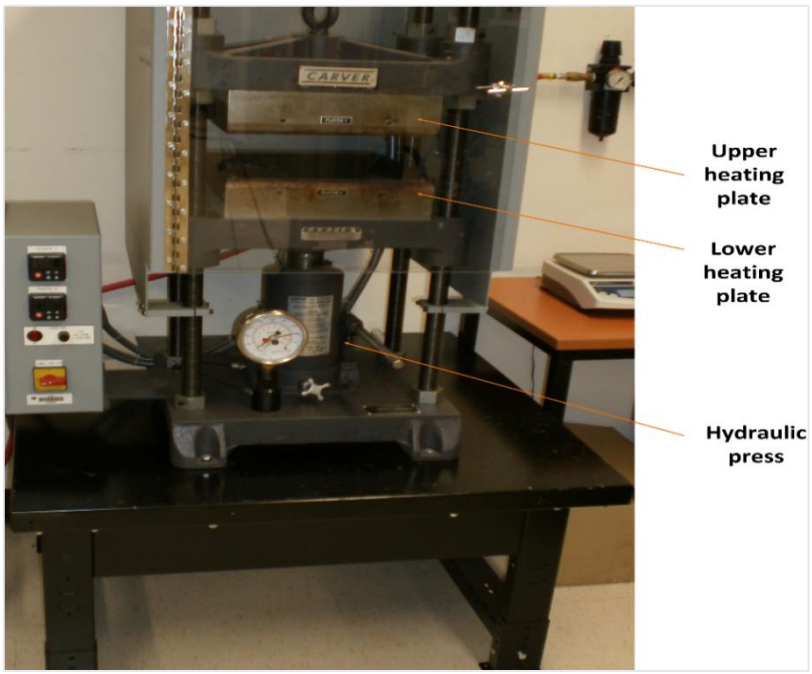

Figure 3-6: Small scale thermo-compression molding equipment (Carver**).**

3.2.2 The methods of characterization

The mechanical, structural/morphological and thermo-rheological properties of the different investigated composite formulations are three important characterization groups. They were carried out with the objective of validating their thermal stability, determining the reinforcing ability of hemp fibers and finding their thermal and rheological properties which are needed for the determination of their constitutive equations and the simulation of their thermoforming process.

3.2.2.1 The thermal properties and thermal stability of PET-hemp fiber composites

The material thermo-physical properties generally vary either with the temperature or the heat flow while its chemical identity is retained. Their importance on vegetal-fiber reinforced composites is demonstrated by the volume of related work published by various researchers [38,116,117]. These properties have an impact on both the efficiency of the process and the quality of the final product.

The initial processing challenge of PET-hemp fiber composites was tackled by investigating their thermal stability using a combined TGA and DSC system.

The characterization with TGA allows to follow the mass variation of a sample heated in a furnace under nitrogen or air atmosphere, as well as other thermally induced changes in its physical and chemical properties. The experiments are either done isothermally or at a constant heating rate. The generated data is analyzed through a method to achieve the intended objectives. The kinetics of the thermal degradation reaction of the investigated material and specific features such as the reaction's

reversibility or autocatalysis are the examples of phenomena which can be deduced from the thermo-gravimetric data. These analyses are based on established standards such as those published by the International Confederation for Thermal Analysis and Calorimetry (ICTAC) [118] for kinetic analysis, including the methods for the determination of the thermo-degradation reaction profile and its kinetic triplets. Some of the applications include the determination of the percentage of absorbed moisture [119,120] by the material and the decomposition following different pathways [121].

The thermo-gravimetric analysis is commonly used in the characterization of vegetal fiber-reinforced composites. It has been used in some works including the study of pyrolysis kinetics of both wood components and wood-polymers by Jin *et al.* [119] and the evaluation of hemp fiber-reinforced composites with either fungal or alkali-based interface modification by Pickering *et al.* [51]. However, it has not been applied to the group of high temperature melting thermoplastics reinforced with vegetal fibers which is not exploited yet.

The thermo-gravimetric analyses were carried out with a TGA/DTG (TA Instrument, Model Q50, New Castle, DE, USA), at constant nitrogen flow rate of 70 $mLmin^{-1}$ and pressure of 60 Pa. The composite samples weighing about 12mg were heated from room temperature to 600°C at a constant heating rate of 5, 10 and 20°$C.min^{-1}$ and the generated data were analyzed with respect to the compounding chamber temperature and the fiber concentration. The temperature interval of analysis was selected to include both the main thermo-degradation steps and the classical melt processing temperature of plastic and composite materials.

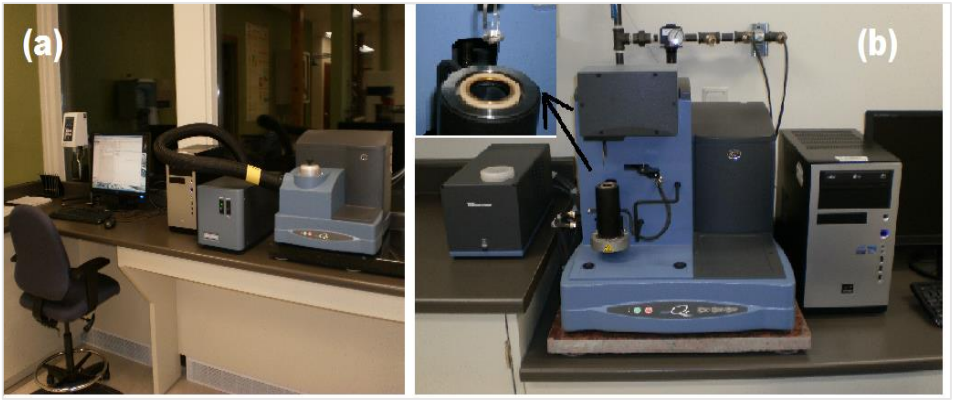

Figure 3-7: TA's thermal testing equipment: Differential scanning calorimeter (DSC) (a), thermo-gravimetric analyzer (TGA) (b).

A few parameters of the formulations were determined for comparison, including Liu and Yu's [122] collecting temperature previously used for the same type of analysis, as well as the kinetic parameters of each thermo-degradation step.

The collecting temperature (T_c), defined in Equation (1) by Liu and Yu [122], where T_i, T_p and $T_{1/2}$ are respectively the onset temperature, the maximum peak temperature and the temperature at which the half conversion of the thermo-degradation is achieved. C_i is the weight coefficient of "i" also known as the factor influencing the effect of each typical thermo-degradation temperature. The value of triplet (C_1, C_2, C_3) set suggested by Liu and Yu as (7,2,1) was adopted in this study [122].

$$T_C = \frac{C_1 T_i + C_2 T_P + C_3 T_{1/2}}{\sum C_i} \quad (1)$$

The kinetic parameters of each degradation step were determined by the Friedman's kinetic model shown in Equation (2) [122–125] where α denotes the species conversion computed using Equation (3), E_a, T, R, A and n are respectively the apparent activation energy, the absolute temperature, the universal gas constant (8,3145 $Jmol^{-1}K^{-1}$), the pre-

exponential factor and the apparent reaction order. The sample initial weight as well as the weight at time t are respectively w_0 and w_i, while the residual weight of the sample is at the end of the degradation step is w_r.

$$\frac{d\alpha}{dt} = A \cdot e^{-\frac{E_a}{RT}} (1-\alpha)^n \tag{2}$$

$$\alpha_i = \frac{w_0 - w_i}{w_0 - w_r} \tag{3}$$

Equation (4) is obtained by taking the natural logarithm of both side of Equation (2) with the implications that E_a and n can be obtained by -Ea/R and Ea/nR which are respectively the slopes of the linear plots of ln(dα/dt) versus 1/T and ln(1−α) versus (1/T) at constant heating rate.

$$\ln\left(\frac{d\alpha}{dt}\right) = \ln(A) + n \cdot \ln(1-\alpha) - \frac{E_a}{R \cdot T} \tag{4}$$

The DSC is a versatile thermal analysis technique describing a material heat capacity (Cp) variation with temperature and which applications are found across many disciplines. It is based on heating or cooling a sample in a furnace while its thermal transitions as well as their associated enthalpies are tracked with respect to time and temperature. Different types of DSC apparatus exist depending on the precision required; however, they can be classified as either heat flow (also known as power compensated) or heat flux DSC.

In a heat flow also known as a power-compensated DSC, the sample and reference pans are heated by separate heaters in separate furnaces to the same temperature. The

difference in thermal power required maintaining the same temperature by the sample and the reference is measured and plotted as a function of temperature or time.

In the case of heat flux DSC, both the sample sealed in a crucible pan and an empty reference pan are placed in the same furnace and heated through the thermoelectric disk. The heat flow (Q) is related to both the temperature difference (ΔT) between the sample and the reference and the resistance of thermo-electric disk (R) by the relationship of Equation (5).

$$Q = \Delta T / R \tag{5}$$

DSC have been applied for the study of the thermo-physical properties of different kinds of material in the example of polyolefins reinforced with natural fibers [44,126], mineral fiber-reinforced composites [127,128], animal fiber-reinforced composites [8], wood products [12,19] and bio-structural material [129].

The heat capacity of the investigated composite formulations was determined by an application of an inbuilt software with the data gathered from a multi-step DSC experiments including sample equilibration at 0°C, a 10 minutes' isotherm, a sample temperature ramp up at 20°Cmin^{-1} to a maximum temperature of 300°C, followed by another 10 minutes' isotherm and finally a temperature ramp down at 10°Cmin^{-1}. All the DSC experiments were carried out in a DSC from TA Instruments (Q20, New Castle, DE, USA) shown in Figure 3-7, while nitrogen was used as an inert gas to avoid the thermo-oxidation of the sample and for cooling purposes. Finally, sapphire was used as the reference for Cp analysis.

3.2.2.2 Mechanical properties

All the engineering structures and in-service materials from different applications are subjected to loads which are exerted in tension, compression, torsion, bending, internal pressure or in a combination of different loading modes. The thermo-mechanical properties give an indication of the behavior of the investigated material under those different loading modes, thereby serving as a mean to verify their suitability to the intended application. A number of physical parameters can be experimentally determined to mechanically characterize the behavior of plastic/composite materials. Specific tests are chosen depending on the end use and the physical state of the samples. In this regard, material characteristics such as elasticity, toughness, ductility and resilience which are required for application design and numerical simulation of its in-service behavior can be derived from experimental thermo-mechanical data.

Some basic thermo-mechanical parameters resulting from time-independent analysis include the modulus, strain, elongations and loads determined under tensile, flexural and compression mode. However, other parameters such as the loss and storage moduli result from the dynamic mechanical analysis while the creep, fatigue and stress relaxation are determined by either cyclic loading or time dependent analysis. The reproducibility of the investigated mechanical parameters is ensured by an application of the mechanical characterization techniques following the guideline of approved standards which address various testing aspects including the sample preparation, test performance and data analysis. The Zwick's mechanical testing equipment used for the tensile, flexural and compression mode is given in Figure 3-8 (a) while the one for impact testing is shown in Figure 3-8 (b). Independently of the loading mode, the mechanical test works by

clamping the sample and applying a chosen load at a given speed until either the end of the test or the point of failure is reached. The test data collected are further analyzed by either manual processing or with an inbuilt-software.

The mechanical and structural properties were necessary to evaluate the reinforcing ability of hemp fibers, leading to a guided choice of reinforcing load which combines both an ease in the processing with the best outcome. This was done through the tensile analyses which were conducted on both the Instron model 4206 and the "Zwick-Roell" at a cross head speed of 5mmmin^{-1} based on ASTM D638-08.

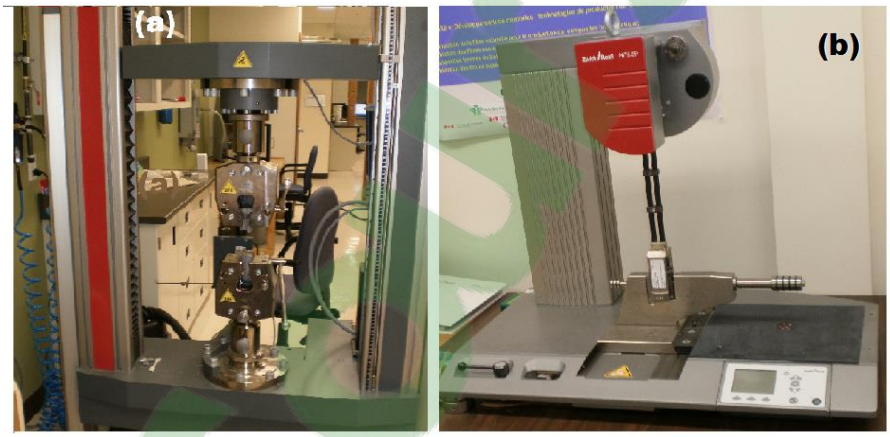

Figure 3-8: Zwick-Roell's tensile, flexural (a); and impact (b) testing equipment.

3.2.2.3 Structural properties

The structural properties of the composite material are related to its fiber-matrix interface parameters, whose effects are significant on both the composite quality and its in-service performance as previously explained in Section 2.1.1.3. Their structural characterization is then carried out with the objective of evaluating the quality of their fiber-matrix interface and in certain cases confirming the existence of some structural and

morphological features such as the composite crystalline structure, the effect of fiber dispersion into the matrix and the fibers quality for natural fiber-reinforced composites.

The methods of the fiber-matrix interface characterization found in the literature are either qualitative or quantitative. Although the qualitative methods are the most common, a review of a significant number of quantitative methods have been published by authors such as Zhandarov *et al.* [130] and Utracki *et al.* [89].

The structural effects of the additives and the reinforcing concentrations on the composites were analyzed with a Scanning Electron Microscope Hitachi (model S-3500N, Tokyo, Japan). The samples were neatly fractured using liquid nitrogen and their electrical conductivity was induced by gold coating.

Figure 3-9: Scanning Electron Microscope, Hitachi S-3500N

3.2.2.4 Thermo-rheological properties

The rheological characterization aims at predicting a material behavior based on its micro and nano-structures. In one way, the flow aspect studies the Newtonian and non-Newtonian behavior of the material based on their viscosity, shear rate, shear stress, phase

transitions as well as the complex viscosity when necessary, while the deformation aspects study the linear and non-linear stress/strain behavior. The general stress/strain behavior was introduced in the previous section. The Newtonian processes are characterized by a constant viscosity as described by Equation (6); meanwhile, the viscosity of non-Newtonian processes varies with different parameters. The first constitutive equation describing non-Newtonian processes is the power law given in Equation (7) where K is the consistency index and n_f is the flow index. The power law can take numerous forms including the Carreau-Yasuda model described by Equation (8) and the Cross model given in Equation (9) where η, η_∞, η_0, θ_C, n, a and Cc are respectively the viscosity, the infinite shear rate viscosity, the zero shear rate viscosity, the natural time, the power index and the constants. The Cross model has the added advantage of showing the variation of the viscosity with the temperature.

$$\tau = \eta \cdot \dot{\gamma} \tag{6}$$

$$\tau = K \cdot \left(\dot{\gamma}\right)^{n_f} \tag{7}$$

$$\eta = \eta_\infty + \left(\eta_0 - \eta_\infty\right)\left[1 + \left(\theta_C \cdot \dot{\gamma}\right)^a\right]^{\frac{(n-1)}{a}} \tag{8}$$

$$\eta\left(T, \dot{\gamma}\right) = \frac{\eta_0\left(T\right)}{1 + \left[C_C \cdot \eta_0\left(T\right) \cdot \dot{\gamma}\right]^{1-n}} \tag{9}$$

The complex viscosity (η^*) is another important rheological parameter of vegetal-fibers reinforced composites, which is related to the elasticity/viscosity of the material. The elasticity is described by the storage modulus (G') while the viscosity is described by the loss modulus (G''). Moreover, the complex viscosity is defined by Equation (10) where ω is the angular frequency.

$$\eta^* = \frac{\sqrt{G'^2 + G''^2}}{\omega} \tag{10}$$

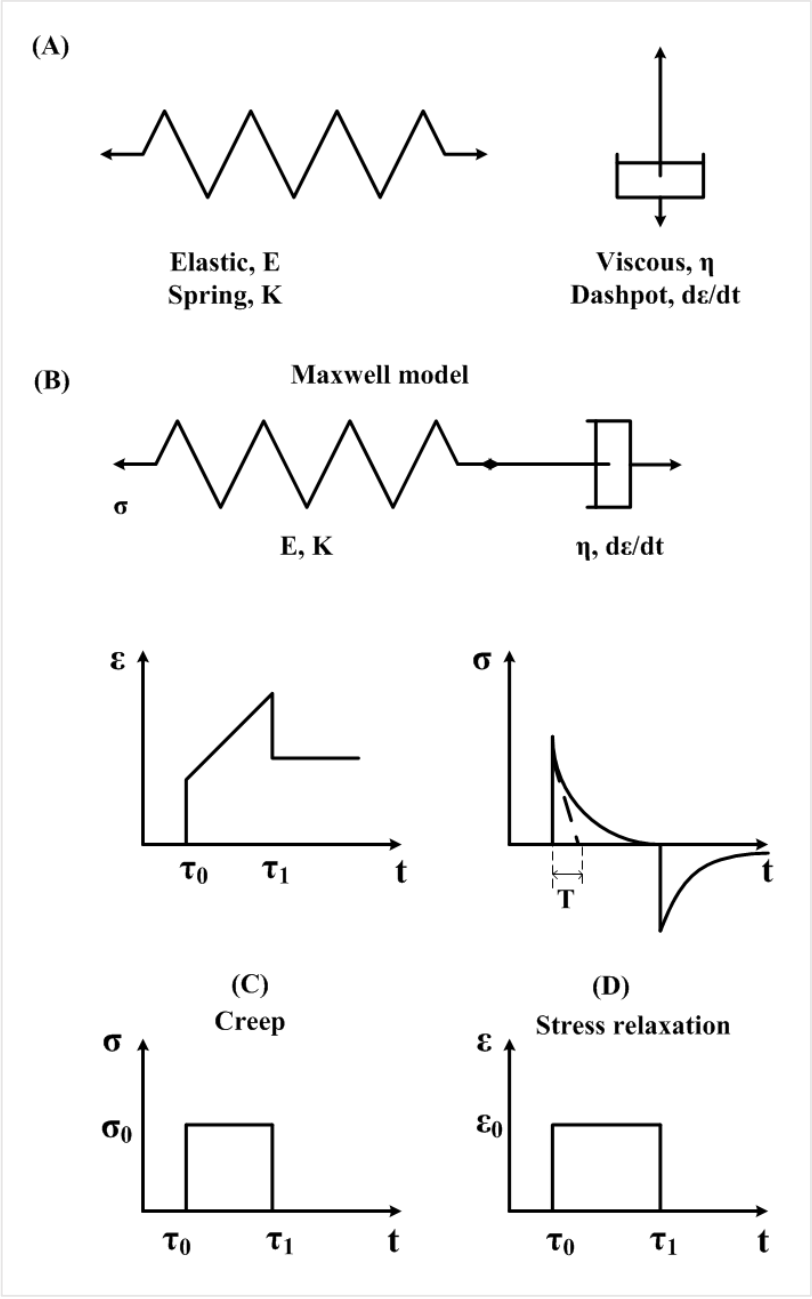

Figure 3-10: Maxwell elements (A); Maxwell model (B); Creep (C); Stress relaxation (D).

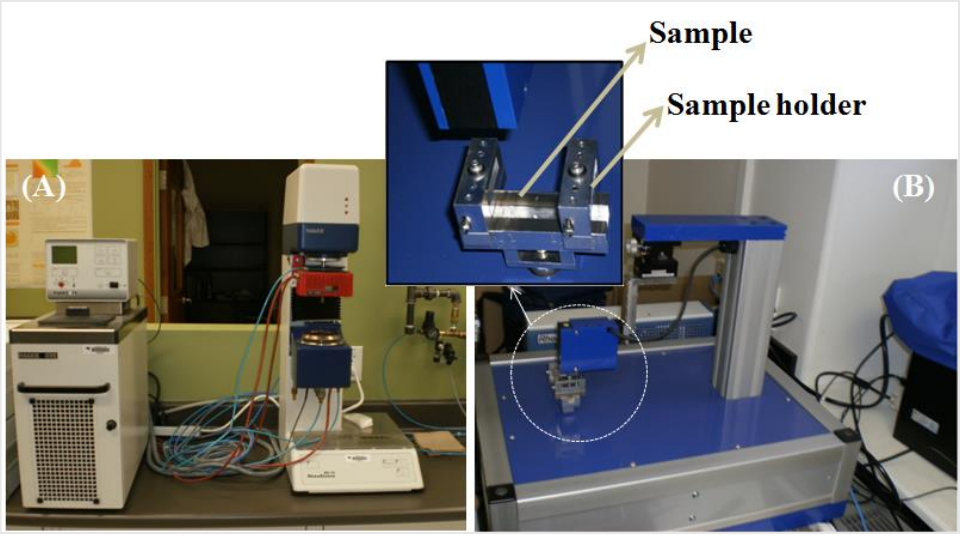

Figure 3-11: Parallel plate rheometer (A) and Rheospetris C500 (B)**.**

The thermo-rheological properties were needed to explore the thermoformability of the different composite formulations. The storage moduli, loss moduli and related parameters were first determined by low amplitude shear tests carried on flexural samples with the RheoSpectris C500 from Rheolution (Montreal, QC, Canada) shown in Figure 3-11 at room temperature and secondly applying the ThermoForm® code for the identification of the constitutive equation parameters. Three readings were performed for each sample. As alternative, we used of the internal batch mixer data using the model of Goodrich *et al.* [110] and Cheng *et al.* [131]. Some thermo-rheological parameters are shown in Figure 3-10.

3.2.3 Methods of thermoforming

Various circular PET-hemp fiber composite sheets of 15,0 cm diameter and 1,47 mm thickness as well as different formulations were numerically thermoformed following a two stage process.

In the first stage, the behavior of the heated sheets submitted to free air was followed while in the second stage both the heating and air flow were preceded by the sheet installation on a hemispherical mold.

The methodological approach was inspired by the abundant plastic and composite thermoforming literature as shown in the following sections. In addition to the classical approaches which includes the discretization and the selection of appropriate conditions, modeling and simulation were also applied to the determination of the constitutive equations describing the behavior of the investigated PET-hemp fiber composites formulations as a function of their reinforcing load.

3.2.3.1 Determination of the constitutive equations

The relationship between the constitutive equations and the investigated PET-hemp fiber composite formulations was established by a process identification technique, through which the rheological data compiled from the RheoSpectris C500 was fitted to the existing constitutive models using the ThermoForm® code. Such identification operation provided a selection method for thermoformable PET-hemp fiber composites formulations, or formulations which can successfully undergo large deformations.

3.2.3.2 Modeling and simulation assumptions

The following assumptions were made during the course of the thermoforming modeling and simulation:

- The sheets of PET-hemp fiber composites of thermoformable formulations were assumed to follow a membrane behavior due to negligible flexural effects;

- The mold was considered as solids with plane surfaces and discretized accordingly;
- The PET-hemp fiber composites /mold interface was assumed to be viscous;
- The various PET-hemp fiber composite sheets of different formulations were assumed to be incompressible, with plain stress deformations ($\sigma_{13} = \sigma_{23} = \sigma_{31} = \sigma_{32} = \sigma_{33} = 0$) and the fitted or identified constitutive equations were applied;
- The external forces exerted on different PET-hemp fiber composites were expressed in terms of the air pressure (or number of moles) which in turn was derived from the Redlich-Kwong's real gas equation of state. However, an ideal gas equation is also applicable at such low pressure.

3.2.3.3 Discretization

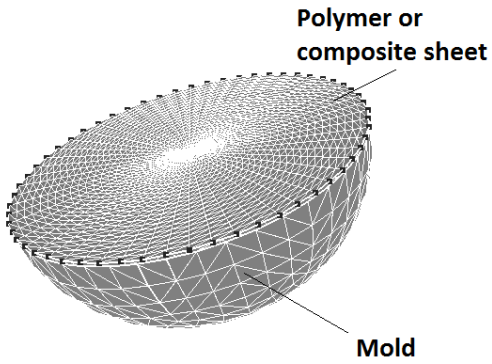

Figure 3-12: Aspect of the discretization of both circular composite sheet and the mold using triangular mesh.

The circular composite sheets, as well as a combination of the sheet and the mold were discretized in the first and the second stages respectively during the thermoforming process, as shown in Figure 3-12. The discretization was applied for both the time and space domains using the meshes of triangular type. A time discretization is required

because of the presence of the inertial force. The spatial discretization was based on the principle of virtual work.

3.2.3.4 Modeling and simulation

The free forming of the circular PET-hemp fiber composite sheets under gravity and their thermoforming with a round mold were modeled using the Lagrangian formulation and simulated using the ThermoForm® code. The operation consisted in monitoring the important processing and material parameters such as the temperature distribution during the heating and the cooling phase, the thickness distribution during the forming phase, the von Mises stress distribution as well as the variation of the heating time with the formulation.

An analogy was drawn between the polymer/composite sheets and a deformable milieu of configuration C_t occupying volume V_t with contour S_t at time "t". Consequently, the successive configurations adopted by the material during each stage of the process were monitored during the simulation process, based on the incremental method which consists of discretizing the loading and finding the successive C_t. The pressure load used in modeling was derived from the Redlich-Kwong's gas equation. The ThermoForm® code takes into consideration the non-linearity arising from the high deformations associated to the thermoforming process, as well as the material behavior and the boundary conditions.

CHAPTER: 4

THE MECHANICAL PROPERTIES OF PET-HEMP FIBER COMPOSITES

This chapter explores the method of elaboration of PET-hemp fiber composites and partially investigates their properties for an optimal choice of the thermoformable formulation as stated in objectives 1 and 2 presented in Section 1.4 and Table 1-1.

This work was funded by the FQRNT, NSERC, CTRI and the Ontario Centre for excellence.

4.1 *Introduction*

Natural fibers-reinforced composites offer many advantages for applications in various engineering fields. These advantages include their recyclability, cost-efficiency, weight reduction and non-vulnerability to corrosion. In this regard, fibers-reinforced composites have been intensively used in various applications during the past decades [8,49,57]. In these applications fiber load and fiber-matrix interface are important parameters which directly impact both the structural and the mechanical properties of the composite materials. Furthermore, the quality of the fiber-matrix interface depends on the synergy and the chemical interactions between the matrix and the reinforcement. Many studies have been conducted on the structure of natural fibers [29,36,132,133]. They all report a complex composite-like structure for natural fibers with many polymers involved. Many of the constituents of natural fibers such as cellulose, hemicellulose and lignin possess many polar groups; as a consequence, a potential synergy exists with polar matrices such as polyesters. The interface between fiber and matrix is often improved by compatibilization using specific additives, either to create or to improve existing group synergies between natural fibers and the matrix, in the absence of polar matrices [29,36,132,133].

Nowadays, most of the existing natural fibers-reinforced composites are based on polyolefins and low temperature melting thermoplastics, thus not fully using the potential of high temperature melting thermoplastic matrices. Very few works have investigated high temperature melting thermoplastics and the effects of reinforcement on their properties [62,72–74]. Caulfield *et al.* [73,74] processed polyamide 6 (PA 6) and polyamide 6,6 (PA 6,6) reinforced with purified cellulosic wood pulp-fibers by extrusion, followed by cooling. Field *et al.* [72] blended polyethylene terephthalate (PET) and cellulose using a mixture of TFA and methylene chloride. Madsen [62] processed PET fibers reinforced with hemp fibers through filament winding of both filament yarns followed by thermo-compression.

PET is an attractive polyester for many engineering applications. Its high glass transition temperature (T_g = 60°C > 25°C), coupled with additional toughness which is provided by its aromatic rings justifies its attraction for structural applications. On the other hand, both PET and cellulose which is a high constituent of natural fibers (70% (w/w)) can readily form hydrogen bonds thus rending coupling agents optional [72]. Moreover, hemp fibers and PET have similar densities and are widely available.

Hemp fibers have a composite-like structure with cellulose-rich microfibers and microfilaments bound by walls of non-cellulosic matters such as pectins, hemicellulose and lignin. Some authors have reported a hemp fiber composition with 18% (w/w) pectins, 16% (w/w) hemicellulose and 4% (w/w) lignin; however such composition depends on several factors like its origin and their harvesting season [132].

In comparison with other natural fibers, hemp fibers offer various advantages to include an appreciable environmental, economic and structural impact. The length of primary hemp fibers which is about 2m is an appreciable structural advantage over wood fibers;

however, due to post harvest processing, such advantage can only be better exploited in the woven form. In addition, there can be up to three cycles of industrial hemp fiber production per year. Hemp seeds and oil which are side products of industrial hemp fiber production are also high end raw materials for the food industry. Hemp fibers can then be used as a potential alternative to wood fibers, thus generating an appreciable environmental and economic impact.

Choosing the appropriate additive for a given application is a crucial task, as reported in the literature [8,126]. This is the case for high temperature melting polyesters because of the problem of thermal degradation of the fibers which onset is reported in various literatures around 190°C. Such thermal degradation has been linked to the thermal instability of its non-cellulosic content [8]. However, the challenge of processing high temperature melting thermoplastics with natural fibers requires a best match between the onset temperature of thermal degradation of natural fibers and the melting point of such resins (T_m > 200°C). In order to address this issue, an alkaline treatment has been applied to hemp fibers for the extraction of some of its non-cellulosic and amorphous contents [8,36,132] followed by the reinforcement of PET through melt processing in the absence of a coupling agent in the present work. The effects of the fiber concentration as well as the use of additives on the mechanical and structural properties were analyzed. This work emphasizes the potential of high temperature melting polyesters reinforced with natural fibers in engineering applications.

4.2 *Experimental studies*

4.2.1 Materials

PET grade AA-48 (Eastman, Montreal, QC, Canada), PCL (Sigma Aldrich, Oakville, ON, Canada) and hemp fibers of composite grade C40Z (Stemergy, London, ON, Canada) were used in this work. These fibers had an average length and diameter of respectively 50 mm and 20-25 µm. The following additives, Clay grade Cloisite 30B (Southern Clay Products, Inc., Gonzales, TX, USA), Pyromelitic dianhydride (PMDA) and Glycidyl methacrylate (GMA) from Sigma Aldrich (Oakville, ON, Canada) were respectively used as fire retardant, chain extender and fiber coating agent [30,31,104]. Moreover, triethylamine, hydroquinone and sodium hydroxide were used in different stages of the process as chemical reagents.

4.2.2 Fiber treatment and polymer modification

The fibers were treated for thermal stability, which is required for composite's melt processing at high temperature. This was achieved by activation through an alkaline treatment with a sodium hydroxide (NaOH) solution at a concentration of 5N. The mechanism of such treatment had been reported by different users as the extraction of some of its non-cellulosic and amorphous contents [8,36,132]. Additionally, the treated fibers were coated with GMA for further protection while increasing the networking with the polymeric chains as reported by Pracella *et al*. [30]. The reactions between GMA and hemp fibers are similar to those between PET and hemp fibers owing to the similarities in the chemical groups involved.

The composite processing temperature was lowered by compounding PET together with 5% (w/w) PCL, which is a lower melting polyester (T_m = 60°C). Such matrix modification also took advantage of the synergetic interactions with the polar groups of the natural fibers.

4.2.3 Composite preparation

The various composite formulations (matrix, reinforcement and additives) were processed through compounding followed by injection molding. The formulations were compounded with a torque-based rheometer system (Haake Rheomix, polylab OS system, USA). The compounded blends were pre-dried at 80°C for 16 hours to avoid degradation and they were injection molded at 250°C with a 15 tons Engel 55 injection molder from Engel, Austria.

The pre-drying stage was essential to avoid sample degradation due to the hygroscopic nature of both PET and hemp fibers as reported by La Mantia and Morreale [8]. In addition, PET which is synthesized through an esterification reaction between terephthalic acid and ethylene glycol, with water as a by-product, would decompose by hydrolysis in the presence of water and heat. Pre-drying is an essential part of both the PET industry as reported by Awaja *et al.* [104] and the wood plastic industry.

The mold was kept at 50°C during injection molding. Crystallization was later induced in a group of samples by annealing of the injection molded specimen at 110°C for 2 hours.

4.3 *Mechanical and structural properties*

The effects of the additives used and the reinforcing concentration on the mechanical properties of the composites were evaluated using tensile tests. The tensile tests were conducted on an Instron model 4206 at a cross head speed of 5mmmin^{-1} based on ASTM D638-08.

The structural effects of the additives and the reinforcing concentrations on the composites were analyzed with a Scanning Electron Microscope Hitachi (model S-3500N, Tokyo, Japan) on cryo-fractured and gold coated samples.

4.4 *Results and discussions*

Table 4-1: Identification of the material groups, together with the corresponding formulations and codes.

Groups	Formulations	Codes
Group 1	PET	G1-1
	PET/PCL	G1-2
Group 2	PET/PCL/HEMP	G2-1
	PET/PCL/HEMP/GMA	G2-2
	PET/PCL/HEMP/PMDA	G2-3
	PET/PCL/HEMP/CLAY	G2-4
Goup 3	PET/PCL/1HEMP	G3-1
	PET/PCL/5HEMP	G3-5
	PET/PCL/10HEMP	G3-10
	PET/PCL/15HEMP	G3-15
	PET/PCL/20HEMP	G3-20

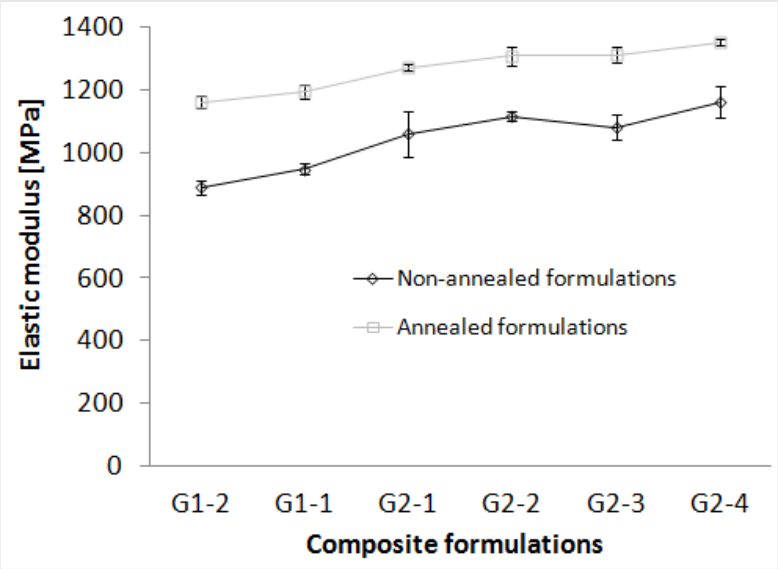

Figure 4-1: Elastic modulus for the composite formulations in Groups 1 and 2.

Table 4-1 gives the various composite formulations studied. Group 1 consists of PET (G1-1) and a blend of PET and 5% (w/w) PCL (G1-2); Group 2 (G2-1, G2-2, G2-3 and G2-4) is made of PET-PCL-5% (w/w) HEMP (G2-1) and the same formulation with the chosen additives (GMA, PMDA or Clay). Group 3 is made of PET-PCL-HEMP composites with various hemp fiber concentrations. The elastic modulus, the maximum force, the strain at break and the structure were investigated for each formulation.

Figure 4-1 shows the variation of the elastic modulus of the composite with the formulations. The different data were calculated by the inbuilt software of the Instron testing equipment. The addition of (5% (w/w)) PCL (G1-2) lowers the modulus of the non-annealed sample by 6% (w/w) with respect to virgin PET (G1-1). However, such reduction in the modulus dropped to 2,8% (w/w) for the correspondent annealed formulations with respect to annealed virgin PET. Additionally, the elastic modulus of the blends (Group 2) increases by 10 to 20% with respect to the unreinforced formulations (Group 1) and by 2 to 10% with respect to the reinforced formulation without additives

(G2-1). The melt process of the studied composites was achieved with minimal fiber degradation and little loss in elastic modulus due to the impact of 5% (w/w) PCL. This is the first investigation of melt processed PET reinforced with natural fibers to the best of our knowledge; therefore, no other data was available for comparison.

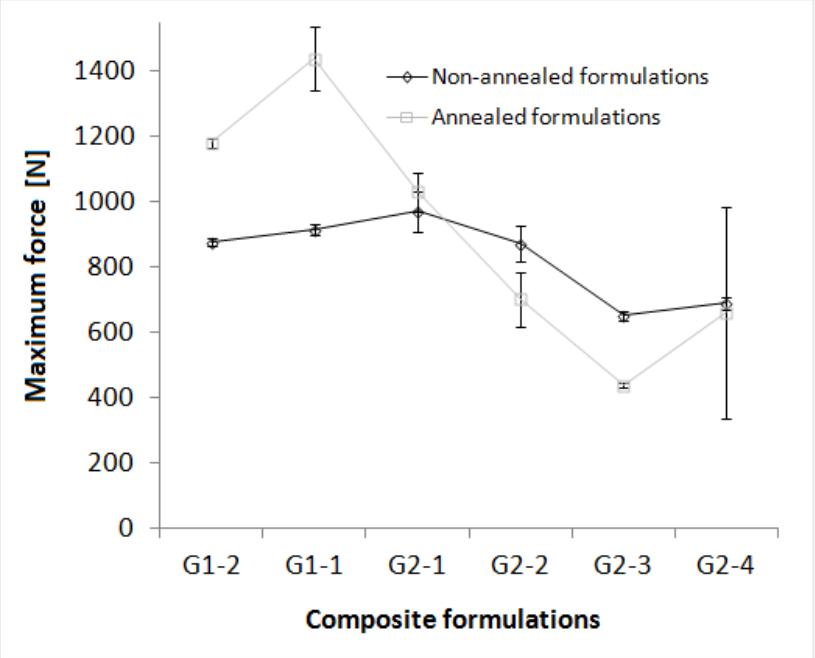

Figure 4-2: Maximum force for the composite formulations in Groups 1 and 2.

Figure 4-2 shows the variation of the maximum force of the composite with the formulations. The addition of 5% (w/w) PCL in non-annealed composite formulation lowers the maximum force by 4% with respect to virgin PET and by 1,8% for the correspondent annealed composite formulations with respect to annealed PET. Moreover, in the presence of additives, the maximum force of the annealed reinforced formulations is lower than those of the non-annealed formulations, which are in turn lower than those of the unreinforced formulations. The formulation with clay (G2-4) appeared to have the most dispersed maximum force and this behavior could be attributed to the limitations in

clay distribution in the matrix. Such limitation in clay dispersion is in agreement with observations previously reported by Qin *et al.* [31]. The highest strength is obtained for PET (G1-1) in the annealed group and for the 5% hemp fiber without additives (G2-1) for the reinforced formulations.

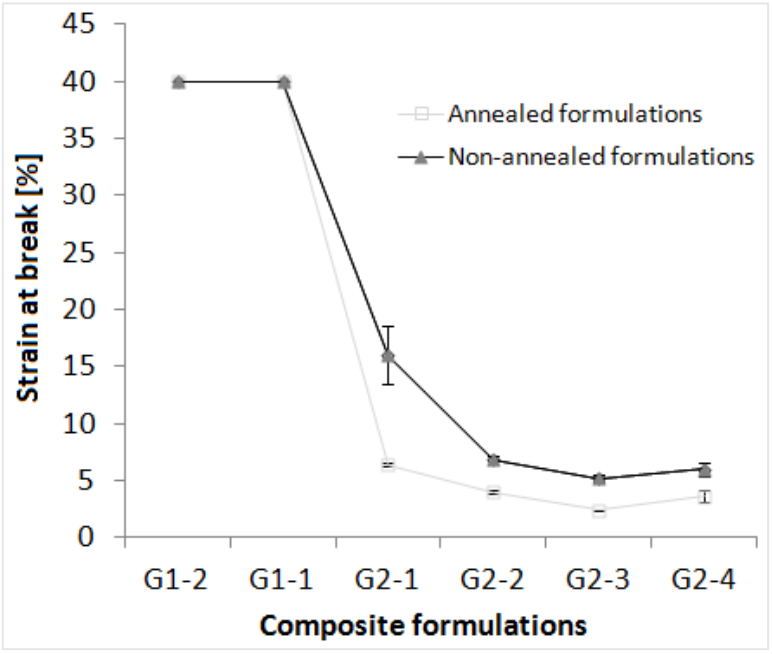

Figure 4-3: Strain at break for the composites' formulations in Groups 1 and 2.

Figure 4-3 shows that the heat treatment lowers the strain at break of the composites in Group 2, the materials become brittle compared to the unreinforced formulations (Group 1). This observation can be attributed to the nucleating ability of the additives acting as impurities [134,135] and is comparable with those of low temperature melting thermoplastics reinforced with natural fibers [8,126]. The strain at break of both PET and PET-5% (w/w) PCL were higher than 40%.

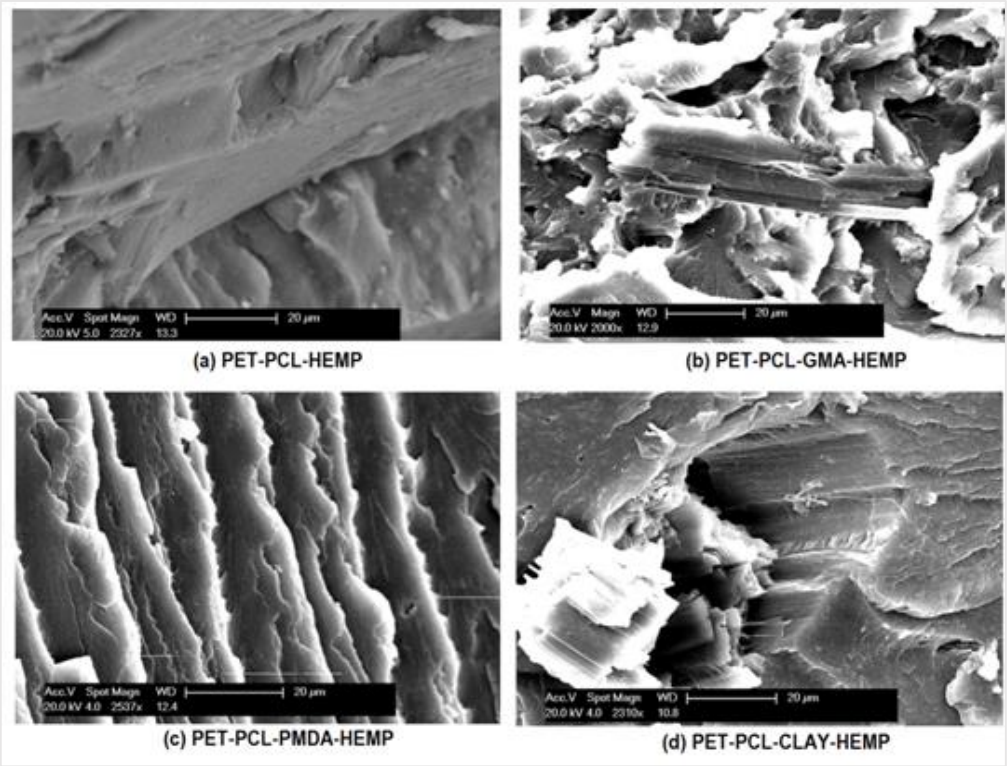

Figure 4-4: Micrographs for the composite formulations in Groups 1 and 2.

Figure 4-4 shows the micrographs of the formulations in Group 2, displaying additives and reinforcement dispersion into the matrix, the various interactions and their possible effects. A good fiber wetting is shown in almost all the micrographs (a-d), thus inducing their reinforcement capacity. This reinforcement is however followed by the brittleness and crystallization of the formulations (in Group 2) indicated by the neat fractures of Figure 4-4 (c) and Figure 4-4 (d).

The brittleness can be related to the dispersion of some additives and their ability to induce crystallization. This is the case for PMDA and Clay, which is not easily uniformly dispersed and which act as impurities or nucleation sites for crystallization. Additionally, “Fiber Pull-out” resulting from a possible PCL degradation in the presence of Clay can

result from the interactions between the various composite constituents. Therefore, these micrographs show the impact of additives on the structural property of the composites.

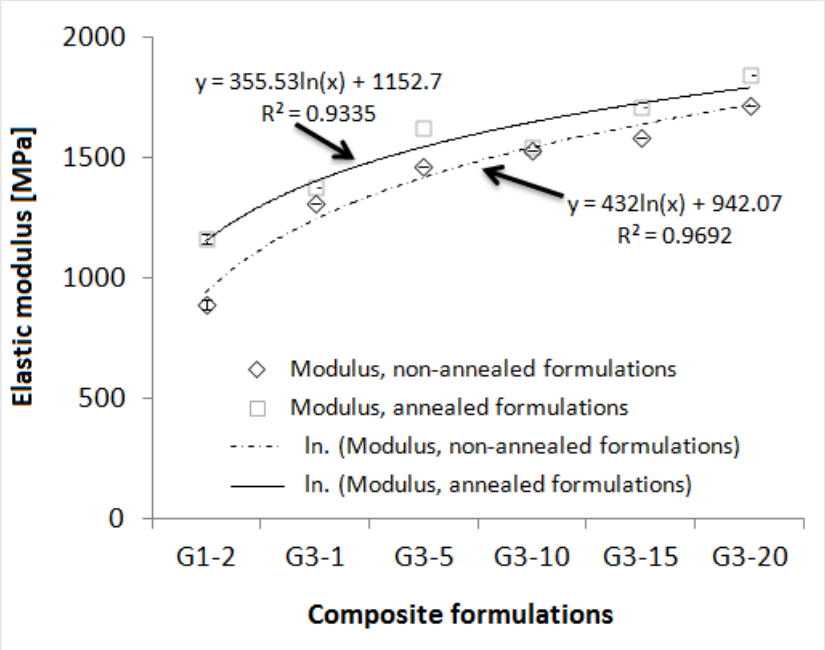

Figure 4-5: Elastic moduli for the composite formulations in Group 3.

Figure 4-5 shows that the elastic modulus in Group 3 increases logarithmically with the fibers concentration (up to 20% (w/w)), with the annealed formulations displaying the highest values. This is consistent with the work reported by Godard *et al.* [126], in which a further increase in the fiber concentration yielded a decrease in the tensional stress of the formulations without the coupling agent around 40%. The difference from the current work may be due to the fiber morphology, the fiber-fiber contact and the difference in resin density. Godard *et al.* [126] used sawdust which offers limited fiber-fiber contact as compared to the long fibers considered in this work, making it more challenging to compound PET-hemp composites with more than 20% (w/w) hemp concentration. A subsequent work will make use of the long fibers advantage over wood fibers by weaving them.

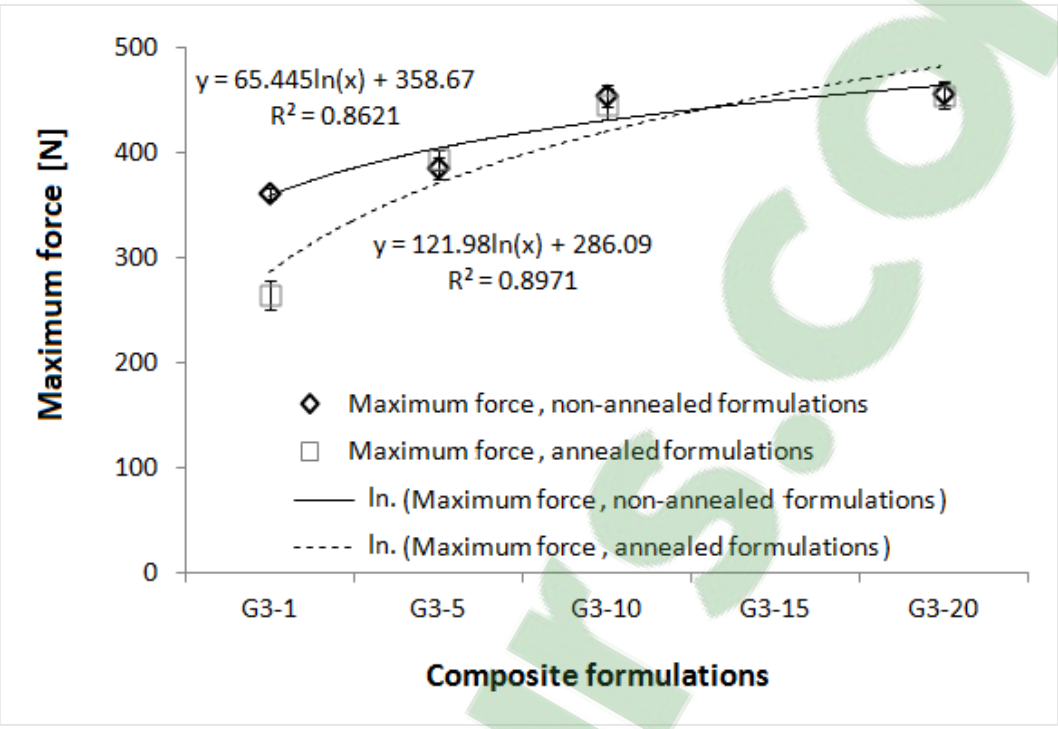

Figure 4-6: Maximum force for the composite formulations in Group 3.

Figure 4-6 shows that an increase in the maximum force of the composites in Group 3 follows the increase in the hemp concentration from 1 to 20% (w/w). Moreover, adding fibers to the resin consistently drops the strain at break from above 40 to around 5% as shown in Figure 4-7. In both cases, annealed and non-annealed formulations show the same behaviour with increasing hemp fiber concentration. The maximum force as well as the strain at break at 15% (w/w) hemp fiber concentration are not displayed here. A typical variation of hemp fiber composition with geography and season is shown by the differences between the mechanical properties of G3-5 and G2-1. In fact the fibers used in the reinforcement of group 3 and group 2 were provided by the same supplier at different harvesting season.

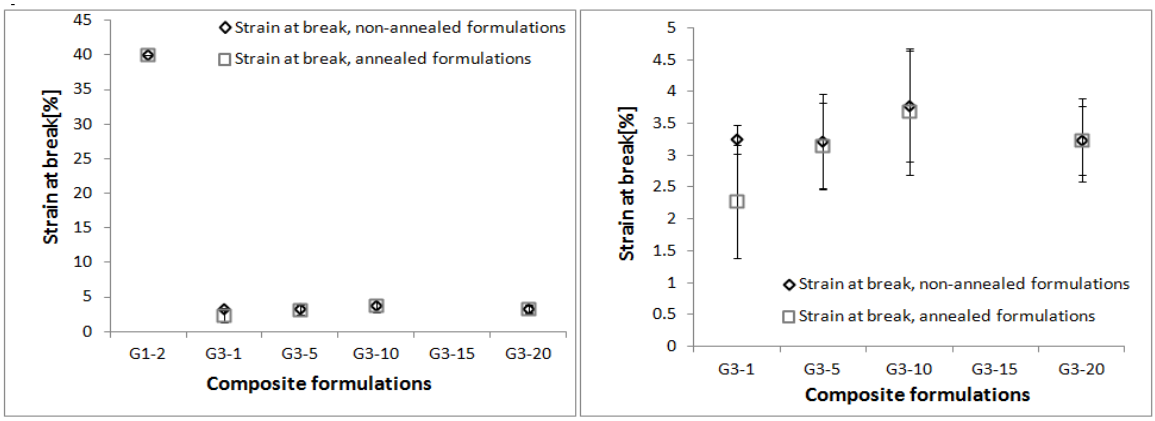

Figure 4-7: Strain at break of the composite formulations in Group 3 together with the control G1-2 (left) and without the control G1-2 (right).

The micrographs for the material formulations in Group 3 are displayed in Figure 4-8, showing the effects of heat treatment on the structural organization of the composites. Non-annealed and annealed groups all appear brittle and this is consistent with the earlier observed mechanical properties. This is due to fiber non-degradation. Moreover, we observed a good fiber-matrix bonding (without use of coupling agent). Hemp fibers can be seen in almost all formulations without any specific orientation. These observations confirm the thermal stability of the treated hemp fibers in the processing method suggested in this study. Above 10% (w/w) of hemp fibers concentration, more fiber-fiber contact can be observed. This indicates potential weak structural points.

Overall, the observed effects of the studied additives on the mechanical and structural properties of PET-hemp fiber composites are an indication of their importance for properly tuned properties. Therefore, a trade-off between the required properties, the additives and the targeted applications is necessary. Finally, the trends observed on the mechanical properties of the materials investigated are similar to those of low temperature melting thermoplastics reinforced with natural fibers [126].

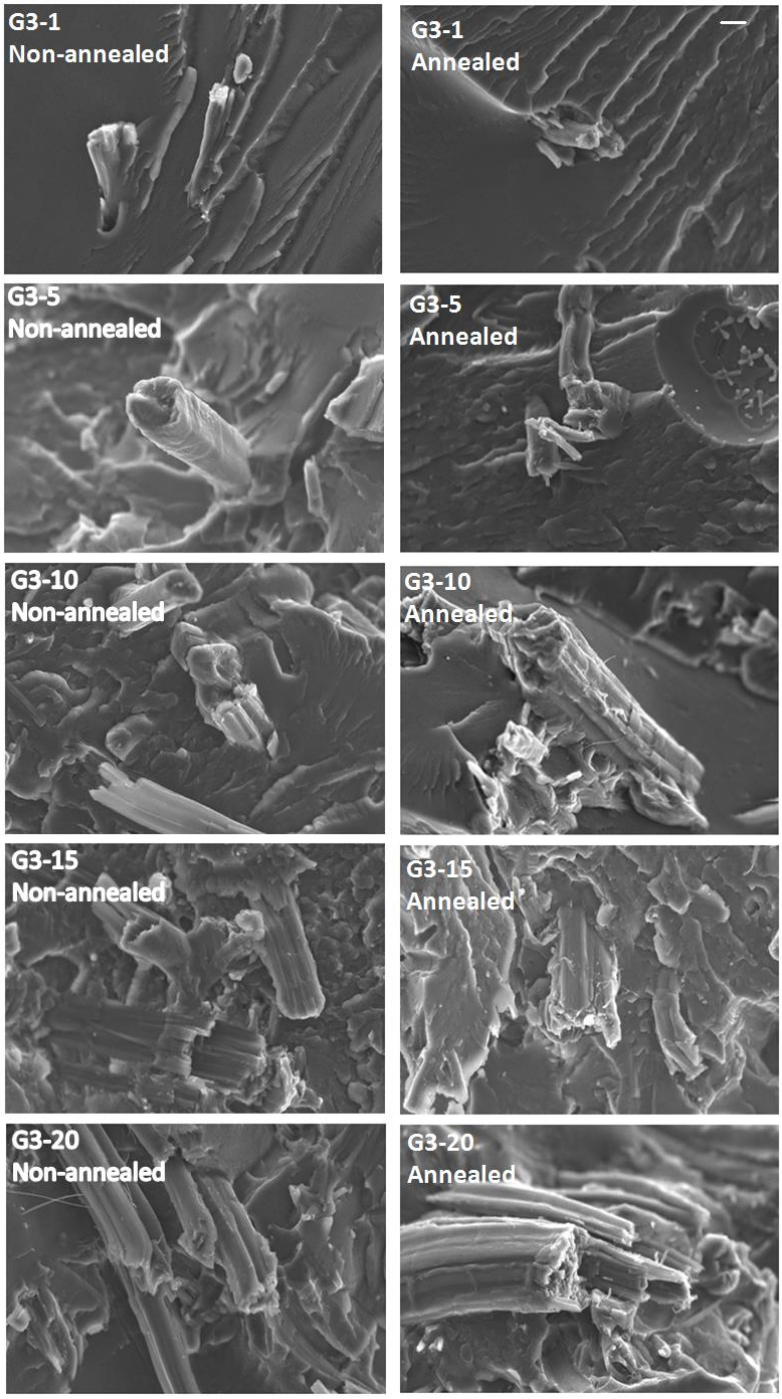

Figure 4-8: Micrographs for the composite formulations in Group 3, non-annealed (left column) and annealed (right column). Scale bar (on upper-right figure): 100µm. In both groups, hemp fiber concentration increases downwards.

4.5 *Conclusion*

Melt processed PET-hemp fiber composites were studied as an example of natural fibers reinforced high temperature melting thermoplastic. A torque-based compounding was adopted. The impact of additives (PMDA, clay and GMA) and the effect of the fiber concentration on the mechanical as well as structural properties were analyzed. Additionally, the effects of heat treatment were studied. We found that the additives increase the elastic modulus and lower the strain at break. Moreover, we observed a good fiber-matrix interface without the use of a coupling agent, in particular in the absence of additives. However, "fiber pull-out" was observed in the presence of clay. Finally, a trade-off between the mechanical and structural properties appears to be a key requirement in the related engineering applications.

CHAPTER: 5

THE THERMAL STABILITY OF PET-HEMP FIBER COMPOSITES

This chapter evaluates the resistance of the elaborated PET-hemp fiber formulations against thermal degradation as a confirmation of their possible melt and multistage processing. This work contributes to an achievement of objectives 1 and 3 of Section 1.4 and Table I-1.

The financial and logistic supports were provided by FQRNT, NSERC and the CTRI.

5.1 *Introduction*

The composites of high temperature melting thermoplastics reinforced with natural fibers are potential materials for numerous engineering applications. They are, however, still underexploited due to possibility of thermo-degradation during processing of the melt [38,73]. In fact, the melt onset of high temperature melting thermoplastics is by definition higher than 200°C, while the onset of thermal degradation of natural fibers has been reported [12,66,132] to be as low as 160-190°C. Such disparity coupled with the variation of natural fibers properties with fiber type, harvesting season and even post-harvest treatments are detrimental to processing of the molten composites as well as their optimal applications. The thermo-degradation of the non-treated natural fibers during production of their composites with high temperature melting thermoplastics is thus an immediate consequence of such temperature difference. The thermo-degradation of natural fibers has a strong effect on both composite processing and their optimal applications, because of the crystallization process. In fact, it has been reported [1,37] that both the presence of natural fibers and the application of heat treatment operations enhance the crystallization of bio-composite materials. This yields a significant increase in their

elastic moduli and a drastic reduction of their elongation-at-break. Although the former is necessary for many high end composite applications, the latter is an additional challenge to multistage processing and to large deformation-related processes such as thermoforming. Moreover, the thermo-degradation of natural fibers negatively affects every optimal application of high temperature melting thermoplastics reinforced with natural fibers since randomly degraded fibers represent bio-composite structural flaws which cannot easily be traced out. Thus, determining the bio-material life cycle is challenging [8].

Our study has shown that strategically processed PET-hemp fiber composites are thermally stable below 300°C and can thus undergo multiple stage processing. Moreover, two main thermo-degradation steps were found below 600°C. Based on the case study of PET-hemp fiber composites, this work is an assessment of the thermo-stability of high temperature melting thermoplastics reinforced with natural fibers with respect to their compounding parameters and fiber concentration. It aims at achieving an optimal use of natural fibers as reinforcement for bio-composite materials while limiting their thermo-degradation in the presence of high temperature melting thermoplastics. Consequently, this study provides a basis for an optimal formulation of bio-composite materials with high temperature melting thermoplastics, as well as safe processing conditions for natural fibers. Furthermore, the results are directly applicable to thermoforming applications as they do not require further melting.

5.2 *Materials and method*

5.2.1 Materials

PET grade AA-48 (Eastman, QC, Canada), with an intrinsic viscocity (I.V.) of 0.80±0.02 $dL.g^{-1}$ and containing less than 60% crystallinity, PCL (Sigma Aldrich, Oakville, ON, Canada) with an average molecular weight (M_n) of 70,000-80,000 units and hemp fibers of composite grade having an average length of 6 cm (Lanaupôle, Berthierville, QC, Canada) were used in this work. They were modified through selected applications to allow melt processing with limited thermo-degradation and to create an improved fiber-matrix interface.

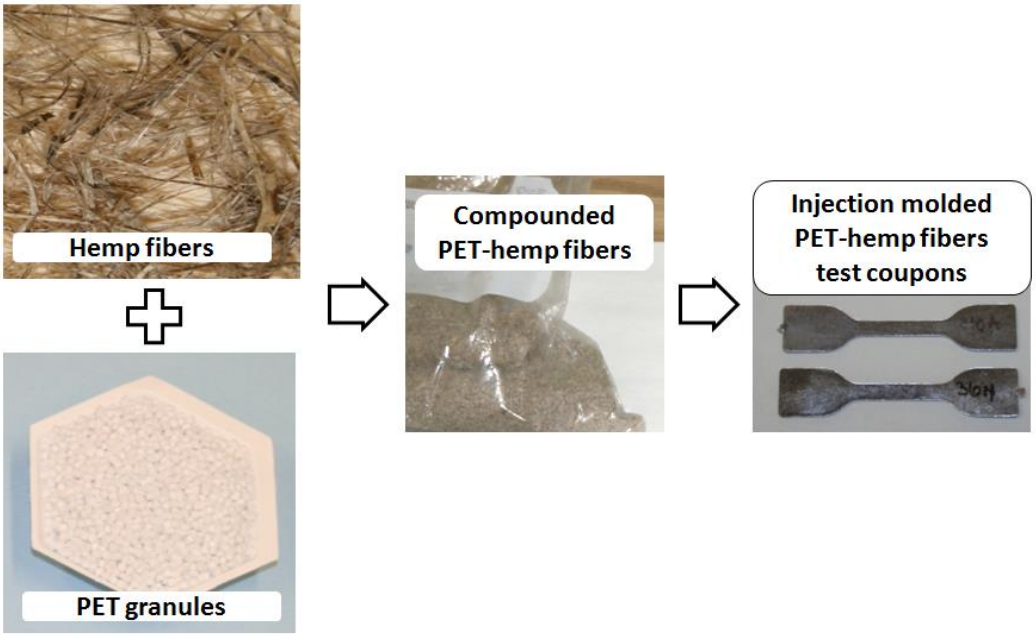

Figure 5-1: Overview of major products and semi-products involved in PET-hemp fiber composites processing.

An overview of the major products, semi-products and the steps involved in PET-hemp fiber composites processing is given in Figure 5-1. Since esterification is an alternative synthesis route for PET with water as a side product, it is degradable through reverse esterification [60,136,137] especially in the presence of water at high temperature. In the same manner, natural fibers are hydrophilic in nature and vulnerable to humidity [138]. Therefore, in order to avoid such degradation in the presence of humidity, PET and its various bio-composite formulations were pre-dried at 150°C for 4 hours prior to each processing stage.

5.2.2 Methodology

During PET-hemp fiber composite processing, the thermal stability of hemp fibers and the melt depression of PET were assured as follows. The thermal stability of hemp fibers was achieved by treatment with an alkaline solution in view of melt processing above 200°C. The treatment method is a modification of the method presented by Bledzki *et al.* [37]. The fibers were soaked in an alkaline solution and heated at 80°C for 4 hours, followed by neutralization with acetic acid and drying for 4 hours at 125°C. Based on some preliminary work, 5N was chosen as an optimal concentration for the alkaline solution.

The melting point depression of PET was achieved by blending it with 5% (w/w) PCL with the same torque-based rheomix also used for PET-PCL-Hemp fiber composites processing. Such concentration was appropriate for an efficient blending process and the blend melting point depression based on preliminary work summarized in Figure 5-3. In fact PET-PCL blends have been largely studied by many authors who reported the impact

of the blend composition on both its thermal and rheological properties [139–141]. The blends investigated by these authors showed a macromolecular behavior with the existence of different crystal populations. However, a greater impact was shown on the melting point of the blends containing less than 20% (w/w) PCL.

The composites of PET reinforced with 1, 5, 10, 15 and 20 % (w/w) alkaline treated hemp fibers were produced by compounding with 5% (w/w) PCL in a torque-based internal batch mixer (Haake Rheomix, polylab OS system, USA) at temperatures of 240, 250 and 260°C, followed by injection molding with a Haake-Minijet at 250°C.

The thermal properties of composites and those of their constituents were determined with TGA/DTG (TA Instrument, Model Q50, New Castle, DE, USA), at constant nitrogen flow rate of 70 $mLmin^{-1}$ and pressure of 60 Pa. During the first stage, the composite samples weighing about 12mg were heated from room temperature to 600°C at a constant heating rate of 5, 10 and 20°$Cmin^{-1}$. Then the thermo-gravimetric data were analyzed taking into account the temperature of the compounding chamber and the fiber concentration. The temperature interval used was selected based on the main thermo-degradation steps and the temperature range used for classical melt processing of plastic and composite materials. Finally, the study was carried out within the range of Liu and Yu's collecting temperature [122] which lies within the temperature intervals previously determined and where the Friedman's kinetic model is applicable.

The collecting temperature (T_c), defined in Equation (11) by Liu and Yu [122], was the first investigation and analysis method used to study the composite formulations during the identified thermo-degradation steps. T_i, T_p and $T_{1/2}$ are the onset, the maximum peak temperatures and the temperature at which half conversion of the thermo-

degradation is achieved, respectively. C_i is the weight coefficient of each degradation temperature considered "i" also known as the factor which influences the effect of each typical thermo-degradation point. In this paper, the triplet ($C_1, C_3\ C_2$,) suggested by Liu and Yu as (7,2,1) is adopted [122].

$$T_C = \frac{C_1 T_i + C_2 T_P + C_3 T_{½}}{\sum C_i} \tag{11}$$

The investigated PET-hemp fiber formulations were compared for the determined degradation steps. Their kinetic parameters such as the activation energies and reaction orders where determined using Friedman's kinetic model shown in Equation (12) [122–125]. α_i is the species conversion calculated at a given time from Equation (13), E_a, T, R, A and n are the apparent activation energy, the absolute temperature, the universal gas constant (8,3145 $Jmol^{-1}K^{-1}$), the pre-exponential factor and the apparent reaction order, respectively. w_0 is the initial weight of the sample, w_i is the weight of the sample at time "t" and w_r is the residual weight of the sample at the end of the degradation step.

$$\frac{d\alpha_i}{dt} = A \cdot e^{-E_a/RT}(1-\alpha_i)^n \tag{12}$$

$$\alpha_i = \frac{w_0 - w_i}{w_0 - w_r} \tag{13}$$

The formulations were assumed to follow two consecutive thermo-degradation steps until 500°C. Taking the natural logarithm of both sides of Equation (12), Equation (14) is obtained.

$$\ln\left(\frac{d\alpha}{dt}\right) = \ln(A) + n \cdot \ln(1-\alpha) - \frac{E_a}{R \cdot T} \tag{14}$$

The formulation of Equation (14) implies that the linear regressions of ln(dα/dt) versus 1/T and ln(1−α) versus (1/T) at constant heating rate yields E_a and n, from the respective slopes -E_a/R and E_a/nR. The apparent activation energies were determined and compared for the various formulations and heating rates. Finally, the onset temperature and duration of the composite thermo-degradation were compared with those of the classical melt processing cycle of thermoplastic matrices.

5.3 *Results and discussion*

5.3.1 Thermo-stability of various components and composite formulations

The thermo-stability of the composites and their constituents are given in Figure 5-2 and Figure 5-4 to Figure 5-6. All the data were analyzed with an in-built TA's universal analysis software.

Figure 5-2 shows the thermo-stabilities of various composite constituents. It indicates a good thermo-stability of the matrix blend (PCL and PET) below 400°C, as well as an appreciable stability of the alkaline-treated hemp fibers below 300°C. The residual weight of PET can be attributed to its pyrolysis which has been studied by authors like Brems *et al.* [142]; it yields benzoic acid and solid carbonaceous residues depending on the applied heating rate. These observations are in good agreement with previous works reported in the literature [138,143,144] and suggest a possible thermo-stability of the composite materials derived from their combination. Moreover, no clear difference was observed between the thermal degradation of individual polymers in the PET-PCL

blend further suggesting its macromolecular structure. These results also show the effects of the applied treatment on the hydrophilic nature of the constituents as well as the thermo-degradation of hemicelluloses and α-cellulose. In fact, hemp fibers showed about 30% weight loss following alkaline treatment, indicating a composition which is consistent with hemp fiber cellulose content reported by authors such as Bledzki *et al.* [37] and Ouajai *et al.* [132] as well as the cellulose and hemicelluloses content reported by White *et al.* [12]. The degradation peak displayed by the weight derivative of alkaline-treated hemp fibers around 350°C had previously been identified by D'Almeida *et al.* [138] as the degradation point for α-cellulose.

An onset of the thermo-degradation of alkaline-treated hemp fibers heated at 20°Cmin^{-1} was found around 275°C, a higher temperature than virgin hemp fibers. This suggests some early hemicelluloses-pectin degradation and confirms the effect of the alkaline treatment on the fibers' thermo-stability. These results are also in agreement with earlier observations made by previous authors such as Ouajai *et al.* [132] and White *et al.* [12]. A 10% (w/w) loss by depolymerization of hemicelluloses and pectin from 250 to 320°C was reported in the former, while a possibility for the pyrolysis of hemicelluloses and lignin from 225 to 450°C was mentioned by the latter. Among all the constituents, only virgin hemp fibers showed a marked weight loss at 75°C, contrary to previous works reported by D'Almeida *et al.* [138]. This suggests that virgin hemp fibers have higher vulnerability to moisture when compared to alkaline-treated fibers; however, the untreated hemp fibers were only tested up to 300°C. The thermo-stability of alkaline treated hemp fibers and those of unmodified composite constituents were previously reported by Saheb and Jog [38], McNeill *et al.* [145] and Bacaloglu *et al.* [146]. These

further highlighted their critical effects on the processing of high temperature melting thermoplastics with natural fibers and their potential engineering applications.

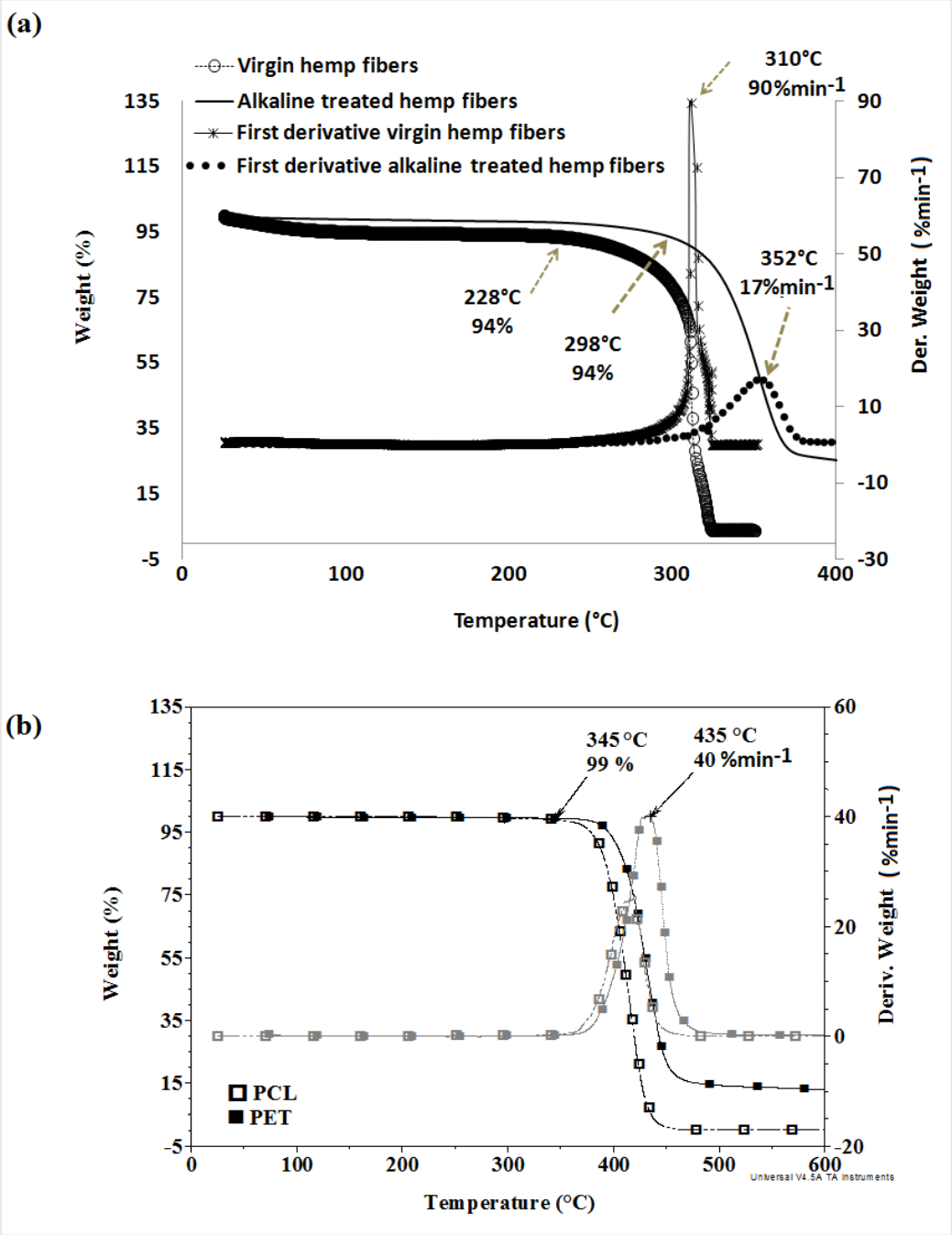

Figure 5-2: TGA and DTG thermograms of raw materials tested at 20°Cmin^{-1}: Virgin and alkaline-treated hemp fibers (a); PCL and PET (b).

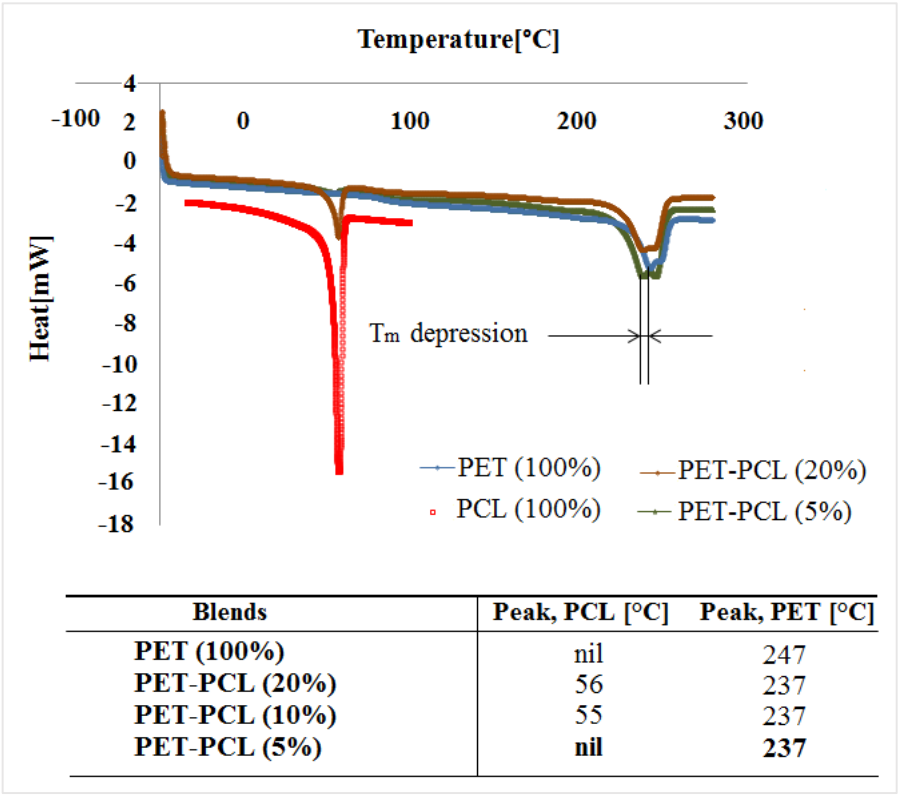

Blends	Peak, PCL [°C]	Peak, PET [°C]
PET (100%)	nil	247
PET-PCL (20%)	56	237
PET-PCL (10%)	55	237
PET-PCL (5%)	**nil**	**237**

Figure 5-3: DSC thermograms showing the melt depression of PET with 5% (w/w) PCL.

The thermo-stabilities of PET-hemp fiber composites compounded using the mixing chamber heated at 240, 250 and 260°C are given in Figure 5-4 to Figure 5-6. Many observations are similar to those reported in the previous section for the matrices and alkaline-treated hemp fibers. For temperatures below 300°C, all the composite formulations showed comparable thermo-stability to those of the isolated constituents, shown in Figure 5-2, irrespective of the compounding chamber temperature. This observation indicates a significantly low impact of the mixing chamber's temperature on the thermo-stability of the composites studied, especially below 300°C. A similar impact [136,147] is thus expected within the PET melt processing temperature range (250 to 280°C). These observations are in agreement with those previously reported by Samperi

et al. [144] suggesting the importance of processing time and additives used at the processing temperature of fiber-reinforced composites. Furthermore, the data suggests a lesser moisture absorption by the composite formulations, either due to hemp fibers alkaline treatment or a possible hydrogen bonding between the fiber hydroxyl groups and the carbonyl groups of PET. The latter hypothesis which has been verified earlier with the mechanical properties of the investigated composites [1] was also the motivation for processing without the use of coupling agents.

As it can be seen from Figure 5-2 and Figure 5-4 to Figure 5-6, the height of thermo-degradation peaks of alkaline-treated hemp fibers observed around 340°C, decreased in the composite formulations without being shifted. This indicates that the functional groups responsible for those peaks decreased as they form coupling bonds with PET. Moreover, peak intensities increased with increasing fiber concentration for all compounding temperatures. Finally, the onset of thermo-degradation of hemp fibers was found to increase in all the composite formulations with decreasing alkaline treated fiber percentage and compounding temperatures. In fact, the alkaline treated fibers' onset of thermo-degradation (~250°C) was significantly increased to 316, 301 and 295°C, for the composites compounded at 240, 250 and 260°C respectively. This highlights the importance of the compounding temperature on the thermo-stability of PET-hemp fiber composites and suggests their minimum effect in the reduction of the fibers stability. Overall, a better thermal stability of PET-hemp fiber composites can be achieved through a careful trade-off between fiber load, compounding temperature and process cycle. In all cases, two consecutive steps of thermo-degradation were observed. The first one was in the range of 313 to 390°C and the second one was in the range of 390 to 490°C,

corresponding to an overall conversion between 15 and 85% or 2 and 15% depending on the fiber concentration.

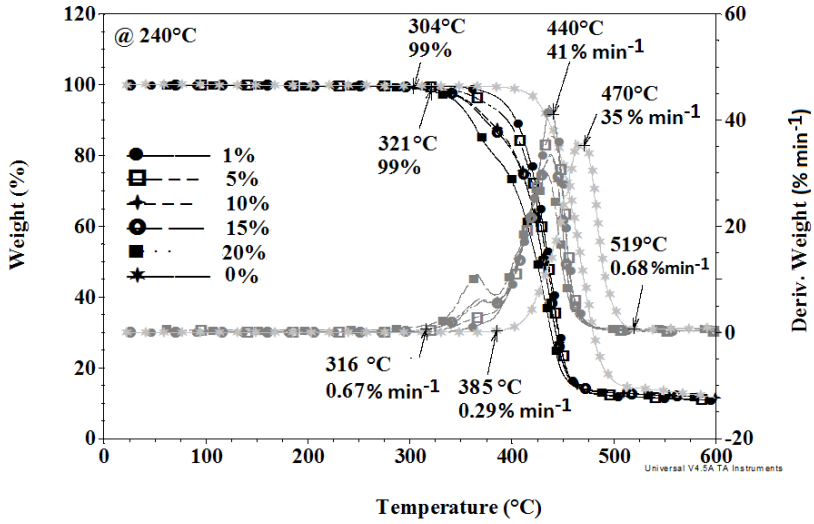

Figure 5-4: TGA and DTG thermograms for PET-PCL blend as well as PET-hemp fiber composites reinforced with 1, 5, 10, 15 and 20% (w/w) fibers compounded with the mixing chamber heated at 250°C and tested at 20°Cmin^{-1}.

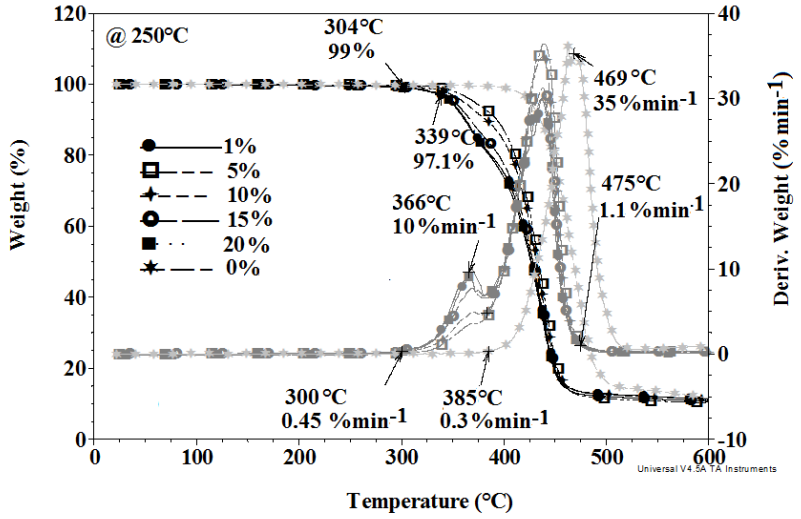

Figure 5-5: TGA and DTG thermograms for PET-PCL blend as well as PET-hemp fiber composites reinforced with 1, 5, 10, 15 and 20% (w/w) fibers compounded with the mixing chamber heated at 250°C and tested at 20°Cmin^{-1}.

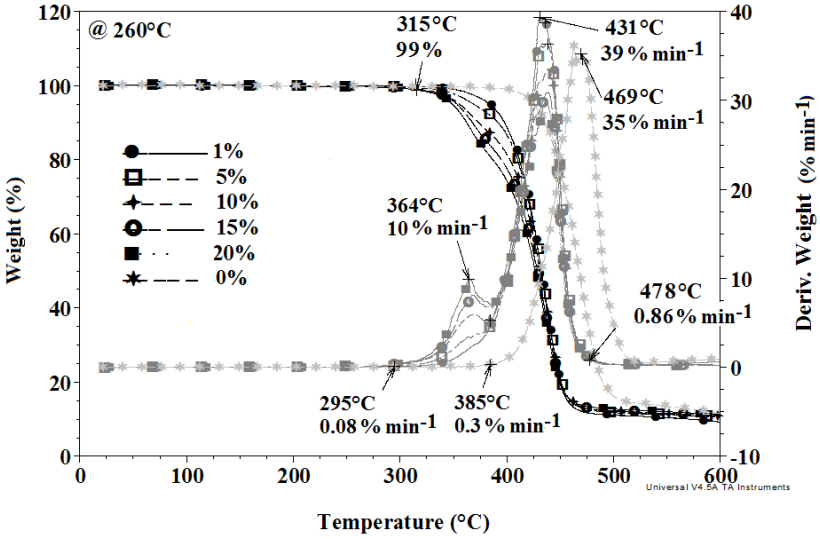

Figure 5-6: TGA and DTG thermograms for PET-PCL blend as well as PET-hemp fiber composites reinforced with 1, 5, 10, 15 and 20% (w/w) fibers compounded with a mixing chamber heated at 260°C and tested at 20°Cmin^{-1}.

5.3.2 Comparison of the thermo-degradation steps based on the collecting temperature

The variation of the collecting temperature with the fiber concentration is given in Figure 5-7. By definition, high values of the collecting temperature index are an indication of the thermo-stability of the materials investigated. The average values of the first and second collecting temperatures observed are T_{C1} = 334 ± 3°C and T_{C2} = 400 ± 2°C, respectively. These values show little variations with the fiber concentration and are significantly higher than the classical melt processing temperature of PET. In this regard, both values confirm the thermo-stability of all the composite formulations investigated in this study irrespective of their fiber concentration. A similar behavior was observed for

the formulations compounded at all the three temperatures of the mixing chamber. The composite properties obtained at different mixing temperatures were repeatable, which is a confirmation of the consistency of the formulated material using the developed processing method.

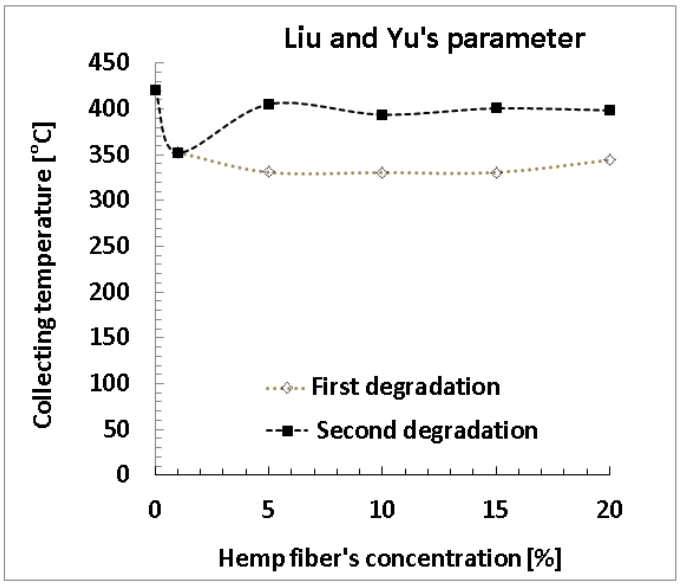

Figure 5-7: Comparative "collecting temperature" between the thermo-degradations of PET-PCL blend and the two thermo-degradations of PET reinforced with 1, 5, 10, 15 and 20% (w/w) hemp fibers.

Although the collecting temperature is a good indication of the thermo-stability of the natural fiber-reinforced composites as explained above, it cannot be adequately applied to differentiate or choose between different formulations of these composites, contrary to the thermo-stability of man-made high performance fibers reported by Liu and Yu [122]. This behavior can be related to the thermo-insulation properties of natural fibers and natural fiber-reinforced composites as earlier reported by Valorvita [148] which indicates that the thermo-degradation observed can only have significantly

negative effects on very long processes. This drawback of the collecting temperature can be solved by considering the intensities of various thermo-degradation peaks.

5.3.3 Comparison of the thermo-degradation steps based on Friedman's parameters

Different thermo-stability parameters have been considered including the onset and cycle of the various thermo-degradation processes, the variation of the apparent activation energy and the apparent reaction order with respect to time, temperature and composition. Taking advantage of the comparable effects of the mixing chamber temperature on the thermo-stability of PET-hemp fiber composites reported in the previous section, only the values of E_a and n investigated for the composite formulations compounded at 250°C are reported.

The onset of thermo-degradation of the PET-hemp fiber formulations as well as degradation cycle as a function of hemp fiber concentration at different heating rates are reported in Figure 5-8 (a) and Figure 5-8 (b), respectively. In general, the onset time of thermo-degradation measured from the beginning of the heating process is found between 22 and 60 minutes (Figure 5-8 (a)). Moreover, the onset varies inversely with the heating rate. The thermo-degradation cycle was found to vary between 5 and 32 minutes. The results show that it is somewhat dependent on the heating rate. In fact, the thermo-degradation cycle was found to be almost constant at high and medium heating rate ($20°Cmin^{-1}$ and $10°Cmin^{-1}$) for all fiber concentrations. However, it varied significantly with the fiber concentration at $5°Cmin^{-1}$ (Figure 5-8 (b)). The observed onset of thermo-degradation of the composite materials studied and their cycle are significantly higher

compared to the classical melt processing cycle (30-240s.) for composite materials [149,150]. This is another indication of the thermo-stability of PET-hemp fiber composites in this range.

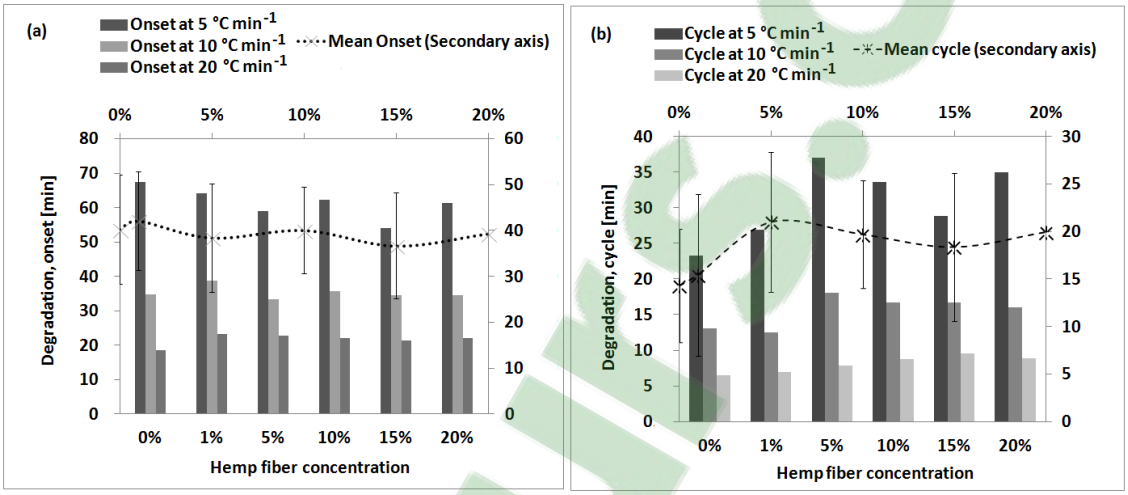

Figure 5-8: Onset (a) and cycle (b) of the thermo-degradation of PET-PCL blend and PET-hemp fiber composites at 5°Cmin^{-1}.

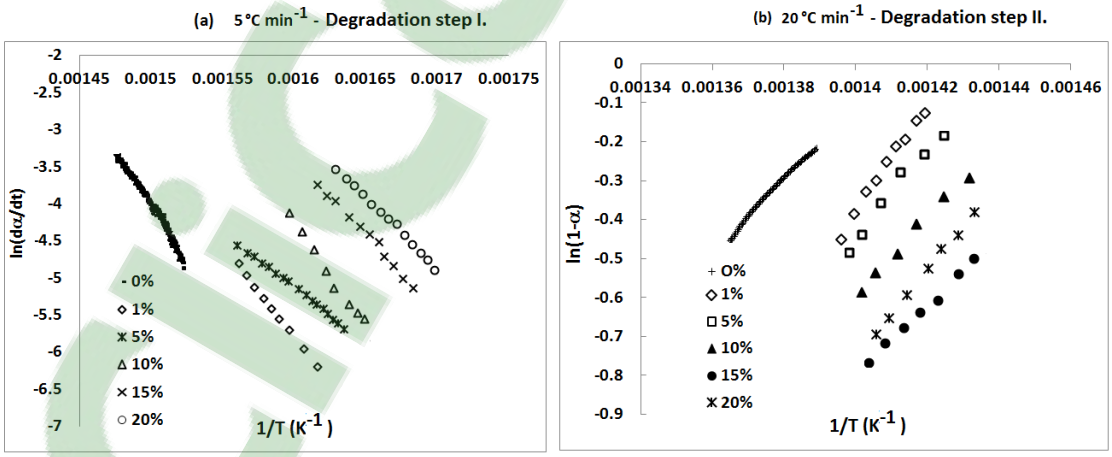

Figure 5-9: Example of Friedman's application method for PET-CL blend as well as PET-hemp fiber composites, at 5°C.min^{-1} for Ea (a) and 20°Cmin^{-1} for the reaction order (b).

Table 5-1: Apparent activation energies and reaction constants for the two steps of PET-PCL blend and PET-hemp fiber composites degradation.

Degradation step I				
	Ea [kJmol^{-1}]			
	Heating rate [°Cmin^{-1}]			
Formulation [% (w/w)]	**5**	**10**	**20**	**Mean**
0	213,3	181,0	218,3	204,2±12
1	247,0	231,3	252,3	243,5±6
5	151,6	172,0	167,0	163,5±6
10	200,3	199,4	190,6	196,8±3
15	180,00	154,03	135,26	156 ±13
20	168,11	172,82	167,7	169,53±1,6
Degradation step II				
	5	**10**	**20**	**Mean**
1	188,00	167.0	246,07	200,3±23,7
5	194,2	238,7	294,6	242.5±29,0
10	214.0	222,6	214.0	216,8±3
15	182,0	235,1	160,5	193±22,1
20	126,5	223,2	198,5	183,±29,0

Degradation step I				
	n			
	Heating rate [**°Cmin^{-1}]**			
Formulation [% (w/w)]	**5**	**10**	**20**	**Mean**
0	5,7	3,20	6,08	5,0±0.9
1	13,4	12,0	11,2	12,2±0.6
5	13,2	12,3	10,6	12,01±0.8
10	13.6	10.0	12.7	12.1±1.0
15	13.9	9.2	13.6	12.22±1.5
20	10.3	7.2	13.7	10.4±2
Degradation step II				
	5	**10**	**20**	**Mean**
1	3.08	1.95	2.05	2.36±0.36
5	5.00	3.6	4.04	4.20±0.42
10	2.2	1.9	3.2	2.4±0.40
15	4.03	2.4	2.6	3.01±0.51
20	1.6	2.9	2.15	2.2±0.40

A summary of the apparent activation energies (E_a) and the reaction order (n) for the two degradation steps of all the PET-hemp fiber formulations investigated is given in Table 5-1. All the data were derived from the Friedman's kinetic method, based on the various applicable linear regressions. These were also found to properly match with the two degradation steps earlier indicated by the DTG results below 500°C. Examples of such regression for the E_a and n are shown respectively in Figure 5-9 (a) and Figure 5-9 (b). Almost all the slopes observed were found to be related to the fiber concentration with linear regression coefficients $r^2 > 0,99$. However, a few deviations were found for the first thermo-degradation of the formulations reinforced with 1% (w/w) hemp fibers. This either indicates the minimal magnitude of the matrix-reinforcement interface in comparison to the thermo-degradation process of this formulation or simply the kind of random variations often found with composite materials processed with natural fibers.

The values of the average apparent activation energies derived from the variations of the type shown in Figure 5-9 (a), are respectively 150-262 $kJmol^{-1}$ and 182-242 $kJmol^{-1}$ for the first and second degradation steps. The magnitudes of the apparent E_a of the first and second degradation steps are comparable which suggests that the difference between the two thermo-degradation steps are due to the chemical species involved. Moreover, for the second thermo-degradation step, E_a variation with the fiber concentration is highly influenced by the heating rates, while the first shows no special variation pattern. In this regard, for all applied heating rates, the apparent activation energy of the second thermo-degradation step increases with the fiber concentration until a maximum value is reached followed by a gradual decrease. Such behavior is similar to the variation of the elastic modulus of the same formulations which had been reported in the previous work [1].

Two major observations can also be drawn from the comparison of the present data with those of previously reported works in literature. Firstly, it is observed that the first thermo-degradation step has an average E_a higher than those of pure PET, which is thermally stable between 280-320°C, reported successively by Kelsey *et al.* [151] and Coudane *et al.* [152]. Secondly, the combined first and second thermo-degradations have E_a values which are higher than pure E_a values of PET (~ 227 $KJmol^{-1}$) found in literature [41].

These observations are an indication of the thermo-stability of the PET-hemp fiber composites investigated. In fact, high E_a values are associated with the difficulties in initiating thermo-degradation reactions, as earlier suggested by Ruseckaite *et al.* [143], about the thermal stability of PET reinforced with cellulose derivatives and Girija *et al.* [41], about the thermal stability of PET-cyanocell as well as PET-cyanowood. Moreover, specific implications can also be drawn from their variations with the fiber concentration and from the magnitude of the reaction order.

Furthermore, a comparison of the variations of E_a with the fiber concentration at different heating rates (Table 5-1) shows the slightest variation at 10°$Cmin^{-1}$. This heating rate can then be considered as an optimal processing parameter to limit PET-hemp fiber thermo-degradation. This information is not available in the literature [38,57] alongside the relationship between low heating rates and longer thermo-degradation.

Still in Table 5-1, the values of the average reaction order (n) derived from Figure 5-9 (b) are between 10 and 12; and 2 and 4 for the first and second thermo-degradation steps, respectively. This implies significantly higher values for the first step of each formulation. One can only speculate that the difference is due to the high number of

species involved in the first step which at times also take part in the second thermo-degradation step. White and Dietenberger [12] have listed cellulose, lignin and aromatic chain scission as example of such species. An implication of all those species can result in an increase in the overall reaction order.

The variation of "n" affects the composites kinetic of thermal stability in two ways. These include the complexity and the slow nature of these reactions which further confirms their thermo-stability. In fact, although there is no specific meaning for high reaction order, they have been associated to complex reactions [153]. Similar reactions include the thermo-degradation reactions of PET, initiated by the instability of the vinyl end groups which act as a competing reaction was investigated by Kelsey *et al.* [151]. Such complexity has been associated with the fractional nature of "n" in the example of the pyrolysis of coal blends with corn and sugarcane residues [154]. Moreover, the first degradation steps of all formulations have higher "n" values, indicating complex reactions. Given the high error associated to the values, they are comparable to those previously published by Jandura *et al*. [155] for the thermo-degradation of cellulose fibers, partially esterified by organic acids and Tang *et al.* [124] for the thermal decomposition kinetics of thermotropic copolyesters made from trans-p-hydroxycinnamic acid and p-hydroxybenzoinc acid. Jandura *et al.* have attributed such observations to physical rather than chemical means and suggested the implication of various parameters in the thermo-degradation of the material investigated. Owing to the importance of the kinetic study on the reaction mechanism, further investigation of the kinetics of PET-hemp fiber composites thermo-degradation is ongoing.

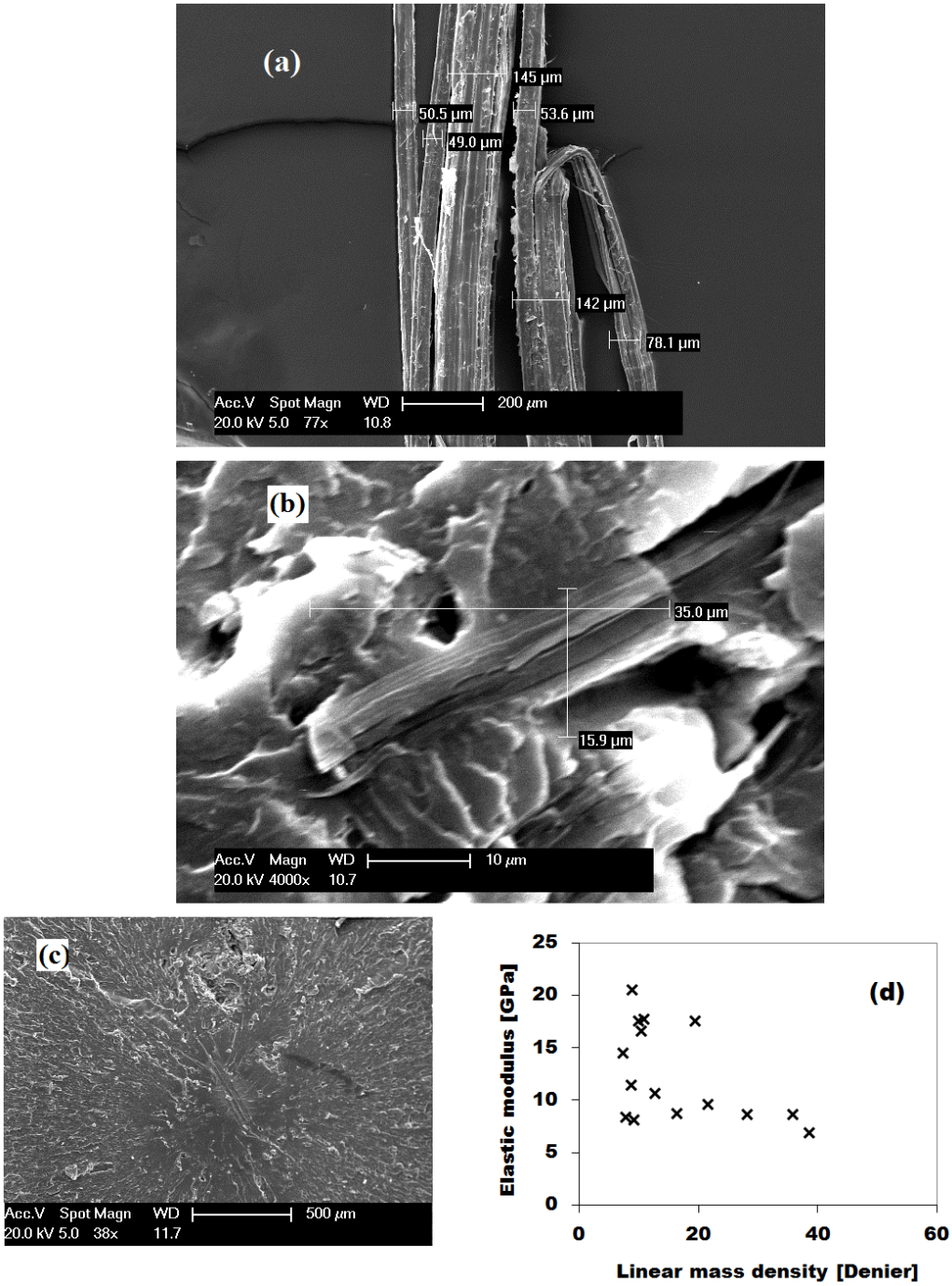

Figure 5-10: Scanning electron micrographs of virgin hemp fibers (a), PET-5% (w/w) hemp fibers (b), pattern of crystal growth around hemp fibers (c), and variation of hemp fibers' modulus with the linear density (d).

In general, the reinforcement of PET with hemp fibers induces the thermo-stability of PET-hemp fiber composites as indicated by the disappearance of all their thermo-degradation steps before 316°C, especially with respect to virgin PET, the shift in the onset of thermo-degradation of the composites, the stability of the "collecting temperature" and an increase in the apparent activation energy. Moreover, a significantly high value of the first thermo-degradation reaction order indicates empirical values related to the complexity of the reactions. Similar observations have been made for low temperature melting thermoplastics reinforced with natural fibers [156], however the melt reinforcements of high temperature melting thermoplastic with natural fibers have not been reported by any other author, to the best of our knowledge. These observations have also shown the minimal effects of the mixing chamber temperature on the thermo-degradation of the PET-hemp fiber composites investigated.

Apart from PET-PCL blend which showed an approximate single thermal degradation step in the range of our studies, all the other results are based on an assumption of the consecutive two step thermo-degradation until 500°C. Such choice is justifiable by the work of Lautenberger *et al.* [157] which showed an insignificant difference of the kinetic parameters resulting from the application of either a single or a 3-step degradation of polyester composites.

The considered thermo-stability of alkaline treated hemp fibers during melt processing with PET and PET-hemp fiber composites is further supported by Figure 5-10 where (a), (b), (c) and (d) are respectively the micrographs of virgin hemp fibers, PET-5% (w/w) alkaline treated hemp fibers used from the tensile tests, the structural pattern

around a fiber of heat treated PET-5% (w/w) hemp fiber composite and the variation of virgin hemp fiber's elastic modulus with the linear density (Denier).

Hemp fibers can clearly be seen in the composite structure, signifying their limited thermal degradation during melt processing at high temperature. Moreover, the alkaline treated and the virgin hemp fibers have significantly different sizes, the former being much smaller. This indicates the structural transformation which occurs during the alkaline treatment. In fact, Figure 5-10 (d) indicates that microfibers and microfilaments may have better reinforcing abilities as higher moduli correspond to lower deniers. Furthermore, a closer look at the hemp fibers in Figure 5-10 (c) indicates a possible crystallization following reinforcement and heat treatment. These structural observations are consistent with the same phenomenon previously reported with lower temperature melting thermoplastics by authors like Ho *et al.* [66] and Aigbodion *et al*. [156].

5.4 *Conclusion*

The thermo-stability of melt processed composites of PET reinforced with hemp fibers were investigated as an important melt and multistage processing parameter. All the formulations were processed by compounding alkaline-treated hemp fibers of different concentrations (1, 5, 10, 15 and 20% (w/w)) and modified PET at three different mixing chamber temperatures (240, 250 and 260°C).

The constituents showed a single peak of maximum degradation for variations below 600°C, while the composites showed closely related double peaks in the same temperature range. Two consecutive thermo-degradation steps were considered. A combination of TGA results analysis, Liu and Yu [122] collecting temperature and the

Friedman's kinetic method have attested their thermo-stability with respect to the fiber concentration, the individual constituents, the heating rates and the mixing chamber temperatures.

The onset of thermal degradation of alkaline treated fibers is 275°C and that of the matrix is around 400°C. However, those of the composites are above 300°C, indicating the thermo-stability in the presence of hemp fibers. Such thermo-stability was further shown by the variation of Liu and Yu's collecting temperature (330 to 400°C).

Two consecutive composite thermo-degradation steps were observed at 316 to 500°C, with apparent activation energies between 150 and 262 $kJmol^{-1}$ and between 182 and 242 $kJmol^{-1}$ for the first and second degradation steps respectively. High values of the reaction order were also observed, indicating the complexity of the reaction mechanism. The results suggest an appreciably good thermo-stability of PET-hemp fiber composites both within the classical processing cycle and the melt temperature range of natural fiber reinforced composites.

The thermo-stability of composites materials made of thermoplastics reinforced with natural fibers is significantly important with applications in the industries and academia. Its impact extends to the processing and recycling of bio-composite materials as it increases the melt processing range of thermoplastics reinforced with natural fibers. Therefore, this work provides a proof for the thermo-stability of PET-hemp fiber composites which indicates non degrading processing conditions. These results show the potential of reinforcing high temperature melting thermoplastics such as PET with natural fibers and the multistage processing for engineering applications with limited thermo-degradation. They also reveal the complexity of the thermo-degradation reactions involved. Further work on the kinetics of PET-hemp fiber composite thermo-degradation is on-going based on the ICTAC standards.

CHAPTER: 6

THE THERMAL DEGRADATION KINETICS OF PET-HEMP FIBER COMPOSITES

Along the previous chapter, this one evaluates the ability of the elaborated PET-hemp fiber formulations to resist thermal degradation. The kinetics of thermal degradation being an indication of the strength of the interactions between PET and hemp fibers, contributes in achieving the first objective of this research.

The financial and logistic supports were provided by FQRNT, NSERC and the CTRI.

6.1 *Introduction*

The low onset of thermal degradation of vegetal fibers is a limiting factor for composite processing with high temperature melting thermoplastics (T_m >200°C) [38,73]. Therefore, most applications of vegetal fiber reinforced composites are currently restricted to the formulations with lower melting thermoplastics (T_m ≤200°C). In fact, the melt onset of high temperature melting thermoplastics is by definition higher than the onset of thermal degradation of vegetal fibers, reported as low as 160 to 190°C, depending on its source and type [12,66,132]. Consequently, an important potential for applications of high temperature melting thermoplastics reinforced with vegetal fibers is unused. An investigation of PET reinforced with hemp fibers is an example of the reinforcement and valorization of high temperature melting thermoplastics with vegetal fibers.

In some previous works [1,3,158], the authors have addressed the strategy for processing PET with hemp fibers and investigating the properties of the resulting bio-composites. In those articles, both the advantages and drawbacks of the bio-composite formulations were shown, including their toughness, an improvement of their elastic

modulus with the fiber concentration, a good fiber-matrix interface and the brittleness of the resulting bio-composites. It appeared that most of the advantages of reinforcing PET with hemp fibers are related to their chemical structures and the chemical synergy between the polyester groups of PET and the hydroxyl functions of hemp fibers. Such synergy of chemical groups is mostly responsible for the quality of PET-hemp fiber interface, while the reported composite toughness is provided by PET's aromatic rings. Moreover, it has been reported that vegetal fibers has the potential of enhancing the crystallization of bio-composite materials which also implies increasing their elastic moduli and reducing their elongation at break [1,3,37].

Vegetal fiber reinforced composites with low temperature melting thermoplastics have been extensively studied [37,38,66] with the objectives of improving on the fiber-matrix interface and investigating the effects of different parameters such as the fiber type, fiber volume and additives on the resulting bio-composite properties. Such studies also include the thermal stability and the kinetics of the thermal degradation of the bio-composite materials formulated with lower temperature melting thermoplastic matrices. However, an evaluation of the kinetics of thermal degradation is essential for the development and application of high temperature melting thermoplastics reinforced with vegetal fibers as it involves an analysis of its critical processing parameters. Despite their potential importance in the fields related to the applications of plastics and composites, high temperature melting thermoplastics reinforced with vegetal fibers are poorly reported in the literature. In this regard, an investigation of the kinetics of thermal degradation of PET-hemp fiber composites is motivated by a dual objective. It provides additional information on the existing materials regarding the expansion of vegetal fiber

reinforced composite applications to the group of high temperature melting thermoplastics as shown by the previous work of the authors on the thermal stability of the investigated composite formulations [3] and the evaluation of hemp fibers' reinforcing ability [1]. It is also a preliminary step in determining the thermo-degradation mechanism for PET-hemp fiber composite.

The thermo-degradation kinetics of solid state materials is well known. It has been extensively analyzed following its first report by Kujirai and Akahira [159]. Thermo-degradation studies play a significant role in processing new materials such as PET-hemp fiber composites reported in this work. This work is both interesting for composite designers and users; moreover, it particularly impacts applications which require multistage processing.

6.2 *Experimental methods*

6.2.1 Materials

PET grade AA-48 (Eastman, QC, Canada), with an intrinsic viscosity (IV) of 0,80 ± 0,02 dLg^{-1} and containing less than 60% crystallinity; PCL (Sigma Aldrich, Oakville, ON, Canada) with an average molecular weight (M_n) of 70.000 to 90.000 units and hemp fibers of composite grade having an average length of 6 cm (Lanaupôle, Berthierville, QC, Canada) were used in this study. They were modified through selected applications to allow melt processing to be carried out with limited thermal degradation and to create an improved interface as stated in previous publications of the authors [1,3]. The kinetic parameters of their thermal degradation, especially their iso-conversional activation

energy, their reaction profile and the kinetic triplets were determined with respect to the fiber concentration.

6.2.2 The kinetic analysis theory

Various methods of kinetic analysis are described in the literature. Their classification is either based on the data collection techniques or on the mathematical approach used for the data analysis. The common data collection operations are either isothermal or non-isothermal while the most applied data analysis methods include the curve fitting, single heating rate and iso-conversions. Most data analysis methods such as those based on single heating rate and the oldest analysis methods which are solely based on curve fitting cannot provide detailed information on the reaction mechanism. Moreover, single heating rate methods are based on mathematical approximations which may yield erroneous and inconsistent results. The suitability of each data analysis method depends on both the set objectives and the available experimental data. However, the iso-conversional methods or model free analyses have been widely discussed by the International Confederation for Thermal Analysis and Calorimetry (ICTAC) as the basis for determining the reaction kinetics as they provide the variations of the activation energy with the conversion rates [118].

The thermal degradation kinetics of PET-hemp fiber composites has been described following the general expression of Equation (15) similar to the Arrhenius Equation where α_i is the materials conversion parameter defined by Equation (16). The parameters t, T, R, E and A are the time, absolute temperature, universal gas constant (8,3145 $Jmol^{-1}K^{-1}$), apparent activation energy and the pre-exponential factor, respectively.

Furthermore, w_0, w_i and w_r are the sample weight at respectively the beginning of the thermo-degradation reaction at the considered conversion time, and at the end of the degradation process, respectively. The activation energy has been described by many authors as the energy barrier required for the reaction to occur [151,154], the pre-exponential factor is associated with the frequency of the activation complex and f(α) is the reaction profile [118,151,160].

$$\frac{d\alpha}{dt} = A \cdot \exp(-E/R \cdot T) \cdot f(\alpha) \tag{15}$$

$$\alpha_i = \frac{w_0 - w_i}{w_0 - w_r} \tag{16}$$

Equation (15) is applicable to different processing conditions in the example of the single and multiple reaction steps; the different testing conditions such as the single and multiple heating rate programs as well as the integral or differential data sets. Nevertheless, the ICTAC has recommended the multiple heating rate programs for kinetic analyses. The integral and differential data are respectively derived from thermo-gravimetric analysis (TGA) and differential scanning calorimetry (DSC).

There is no analytical solution to the reaction profile of the integral methods described by Equation (17); however different approximations have been formulated by authors such as Doyle, Flynn-Wall-Ozawa and Kissinger-Akahira-Sunose [118], as well as Starink [160]. The generalized approximations are shown in Equation (18); however, the most accurate according to the ICTAC's standard is the Starink's model given by Equation (19).

$$g(\alpha) = \int_0^{\alpha} \frac{d\alpha}{f(\alpha)} = \frac{A}{\beta} \int_0^{T} \exp\left(-\frac{E}{RT}\right) dt \quad (17)$$

$$Ln\left(\frac{\beta_i}{T_{\alpha,i}^{B}}\right) = Const - C\left(\frac{E_\alpha}{R \cdot T_\alpha}\right) \quad (18)$$

while β_i is the heating rate number i

(B;C) = (0; 1,052): Doyle's method

(B;C) = (2;1): Kissinger-Akhura-Sunose's method

(B;C) = (1,92; 1,0008): Starink's method

$$Ln\left(\frac{\beta_i}{T_{\alpha,i}^{1,92}}\right) = Const - 1.008\left(\frac{E_\alpha}{R \cdot T_\alpha}\right) \quad (19)$$

6.2.3 Methodology

Five composite formulations of PET reinforced with 1, 5, 10, 15 and 20% (w/w) hemp fibers were investigated. They were processed by compounding in a torque-based batch mixer (Haake Rheomix, polylab OS system, USA) with the temperature of the mixing chamber set around PET's melting point of 250°C, followed by injection molding at 250°C with a Haake-Minijet. The investigated composite formulations were pre-dried at 150°C for 4 hours prior to each processing stage, in order to avoid moisture catalyzed degradation. In fact, the pre-drying of unreinforced PET is required to avoid the degradation by reverse esterification which occurs at high temperature in the presence of water or moisture. Such operation is essential in the presence of vegetal fibers which normally absorb moisture due to their hydrophilic nature [8,136–138].

The thermo-gravimetric data were determined at a constant nitrogen atmospheric environment of 60Pa using a Q600 DSC-TGA analyzer from TA instruments. The samples weighing about 12mg were first tested at 20°Cmin^{-1} between room temperature and 600°C. In a four stage process analysis, the ICTAC's recommendation [118] was applied to the thermo-gravimetric data.

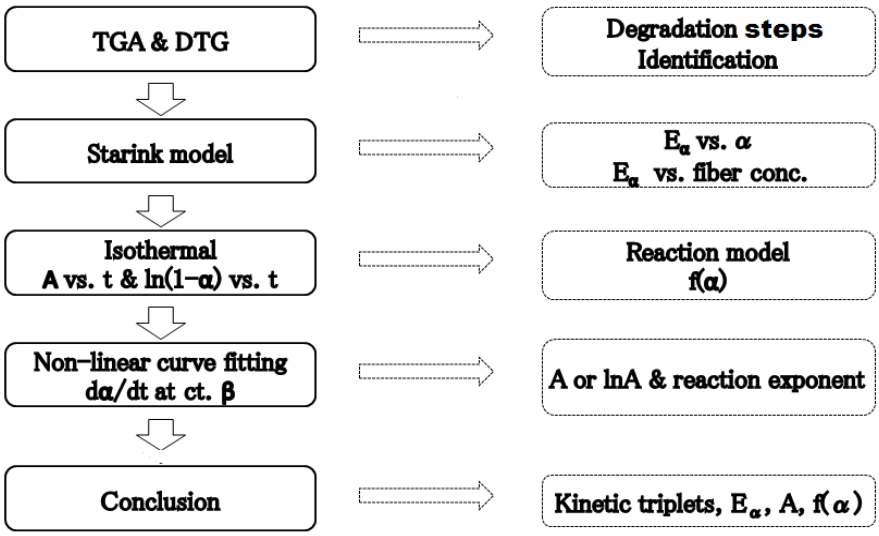

Figure 6-1: Overview of the kinetics investigation process for PET-hemp fiber composites.

The reaction profile for each thermo-degradation step was first identified through a 30minutes isothermal samples treatment at 300°C and 600°C respectively followed by the determination of their apparent activation energy from the Starink's model application to the integral iso-conversional data generated at the heating rates of 5, 10 and 20°Cmin^{-1}. A combination of the potential reaction profile equations derived from the variation of isothermal parameter variation and the previously determined apparent activation energies were further applied to a non-linear curve fitting process, both for the validation of the reaction profile and the determination of the remaining reaction kinetic parameters.

The determination of the kinetic triplets for the thermo-degradation of PET-hemp fiber composites was achieved by a combination of the non-linear curve fitting method, the initial values of the activation energy derived from the iso-conversional Starink's model and the reaction profile which can be accelerating, decelerating or sigmoidal, based on the variation of the conversion with time at constant temperature. An algorithm summarizing these operations is shown in Figure 6-1.

6.3 *Results and discussion*

6.3.1 Thermo-gravimetric analysis

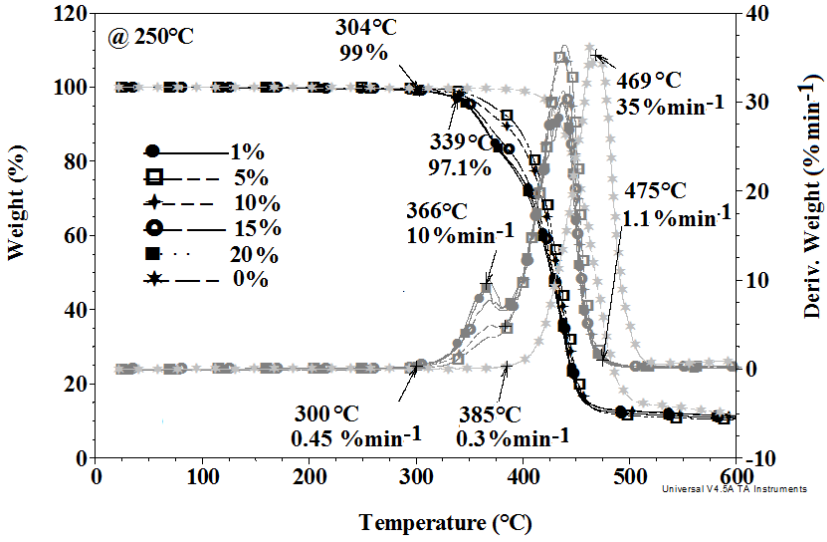

Figure 6-2: TGA and DTG thermograms for PET-hemp fiber composites compounded at 250°C and tested at 20°Cmin^{-1}.

Figure 6-2 shows the thermo-gravimetric parameters for all PET-hemp fiber composite formulations compounded in an internal batch mixer heated at 250°C and tested at 20°Cmin^{-1}. An appreciable thermal stability is shown until 300°C followed by two

consecutive thermo-degradation steps at 290 to 385°C (Step I) and 385 to 490°C (Step II), respectively.

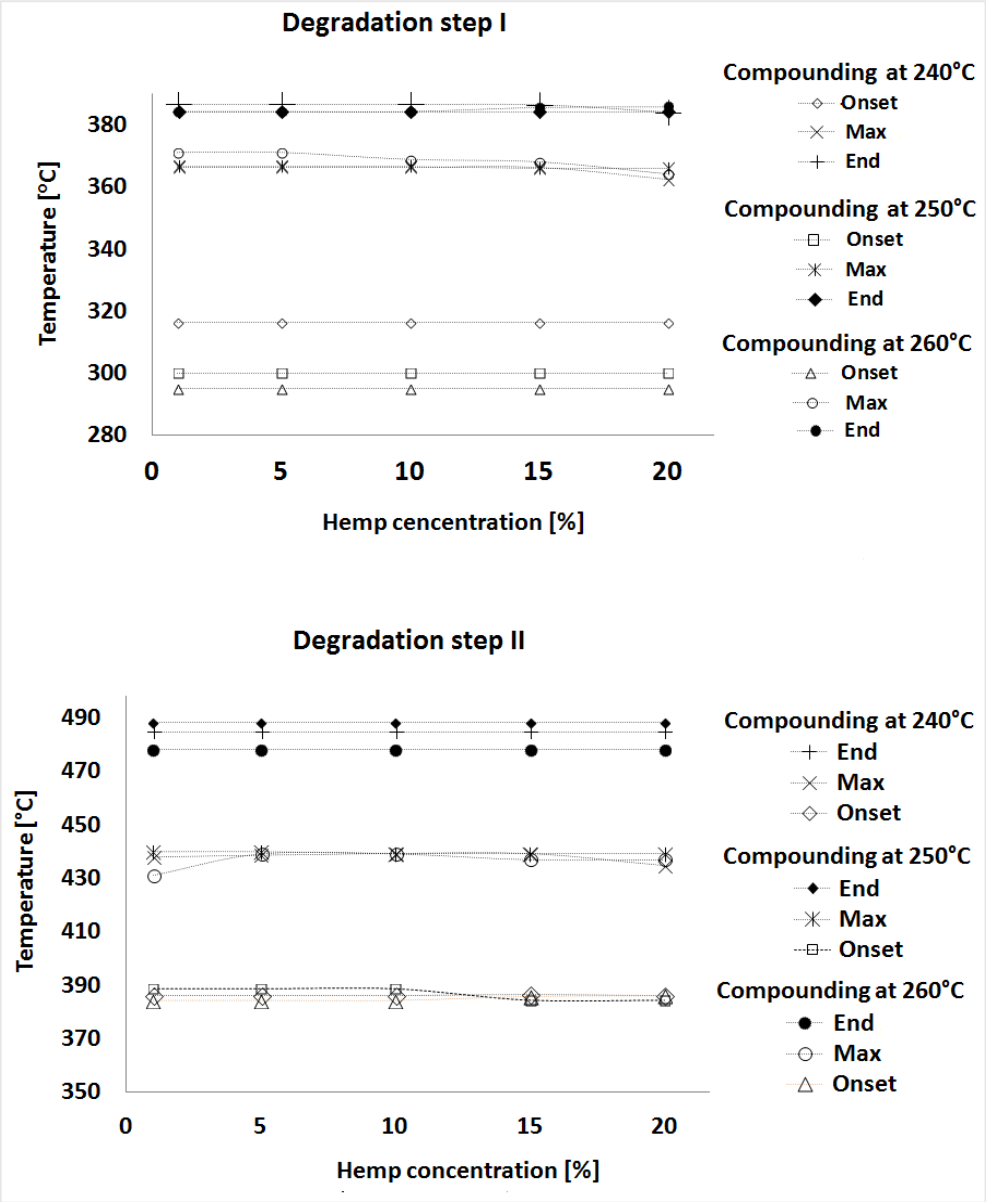

Figure 6-3: Time variations of the thermo-degradation characteristic of PET-hemp fiber composites based on TGA and DTG thermograms.

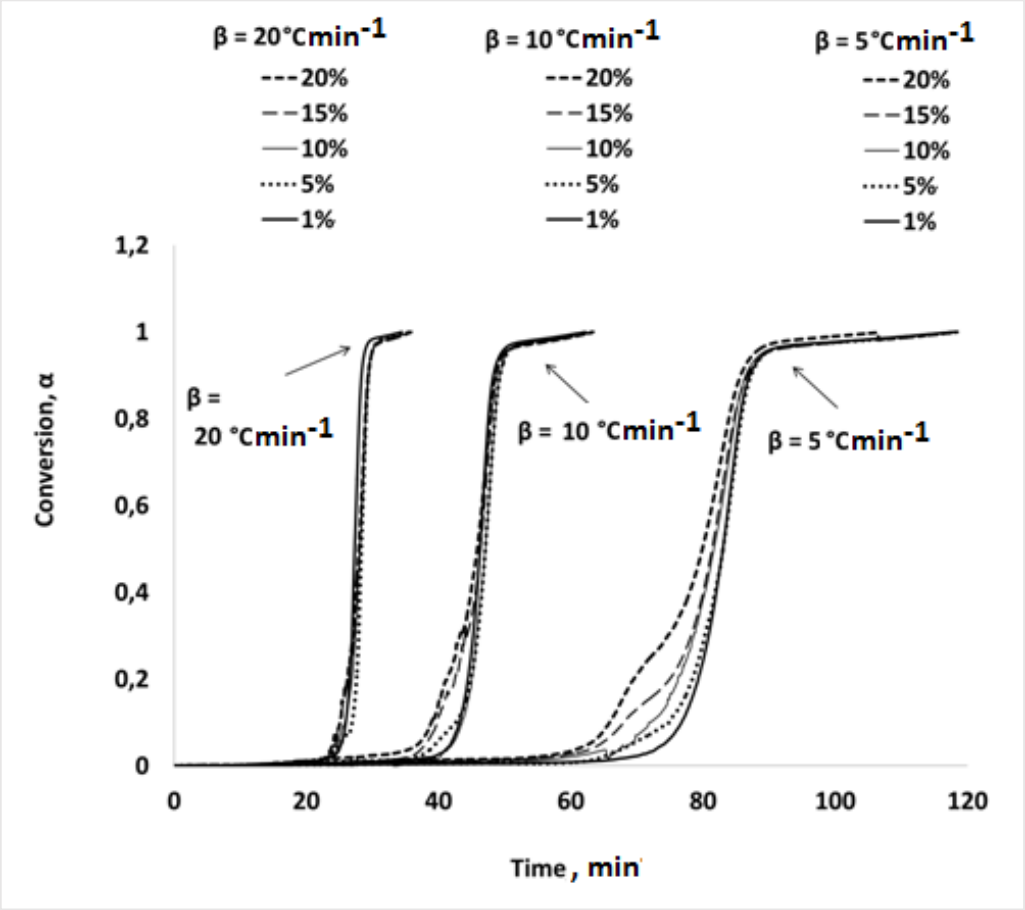

Figure 6-4: Time variations of the non-isothermal conversion of PET-hemp fiber composite formulations.

Some preliminary thermo-gravimetric studies of PET-hemp fiber formulations compounded with the mixing chamber heated at 240°C, 250°C and 260°C showed similar behavior. This is why we choose to focus only on the group compounded at 250°C in this work. However, the variations of the primary thermal degradation parameters with both the investigated hemp concentrations and the applied compounding parameters for all three temperatures are given in Figure 6-3.

A negligible variation of both degradation steps was observed with respect to the hemp concentration; however a variation with respect to the initial chamber temperature was observed respectively for the onset of degradation of step I and the end of degradation of step II. In both cases, lower thermal degradation temperature was associated to higher mixing chamber temperature as an indication for the degree of hemp fibers degradation in such cases.

Moreover, Figure 6-4 shows the variations of the composites conversion in various investigated non-isothermal conditions. Independently of the heating rates, the onset of thermal degradation of all formulations is found between 20 and 80 minutes, with the longest cycle associated with the lowest applied heating rate. Moreover, the thermal conversion of the investigated bio-composite shows a strong dependence on the fiber concentration at lower heating rates. The same parameters indicate a strong dependence of the thermal conversion of the investigated bio-composites on the fiber concentration at lower heating rates.

6.3.2 Iso-conversional activation energy

Figure 6-5 shows the variations of the iso-conversional activation energies of the composite formulations with the fiber concentration. All the values were derived from the application of both the Starink's kinetics model and the inbuilt TA software. They were found to be constant across the investigated fiber concentrations [154]. The observation, which indicates a constant reaction is also in agreement with previous studies such as the work of Aboyade *et al.* [154] concerning the kinetics of the pyrolysis of coal blends with corn and sugarcane residues.

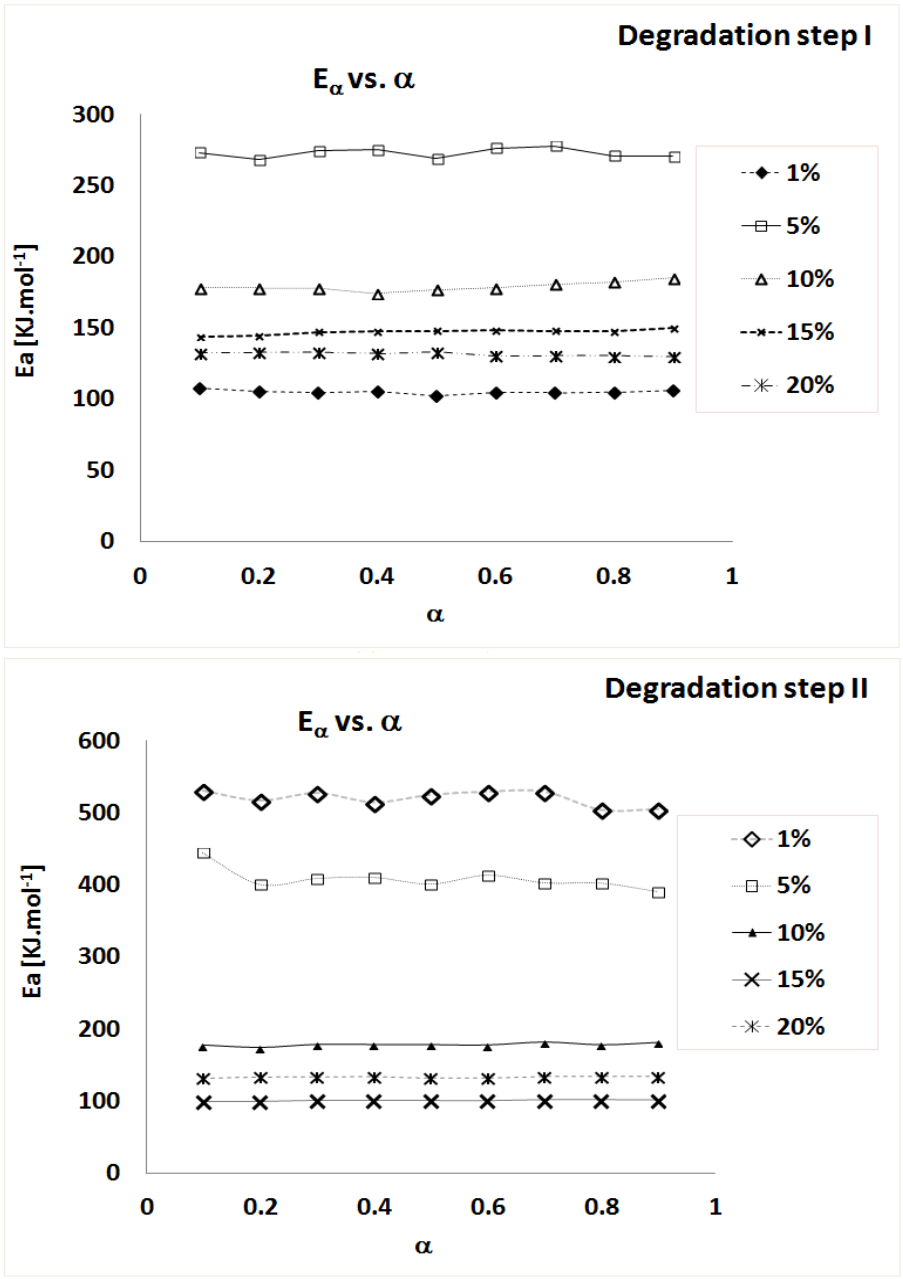

Figure 6-5: Variation of the iso-conversional energies of the two thermo-degradation steps of PET-hemp fiber composite with the fiber concentration.

Moreover, the iso-conversional values were found to decrease with the fiber concentration except for the cases of 1% (w/w) reinforcement for Step I and 20% (w/w) for Step II. These exceptions correspond to extreme composite formulations with either the least or the highest applicable hemp fibers reinforcement. In fact, 1% (w/w) hemp reinforcement is the formulation with the smallest iso-conversional energy in Step I which may be due to the smallest amount of hemp fibers, leaving most of the composite behaving like the unreinforced formulation. In the same manner, 20% (w/w) hemp fibers corresponded to a challenging process-able fiber volume, resulting in the lowest iso-conversional values for Step II. These effects of the fiber parameters on different bio-composites have been reported by Moran *et al.* [161] and Ho *et al.* [66].

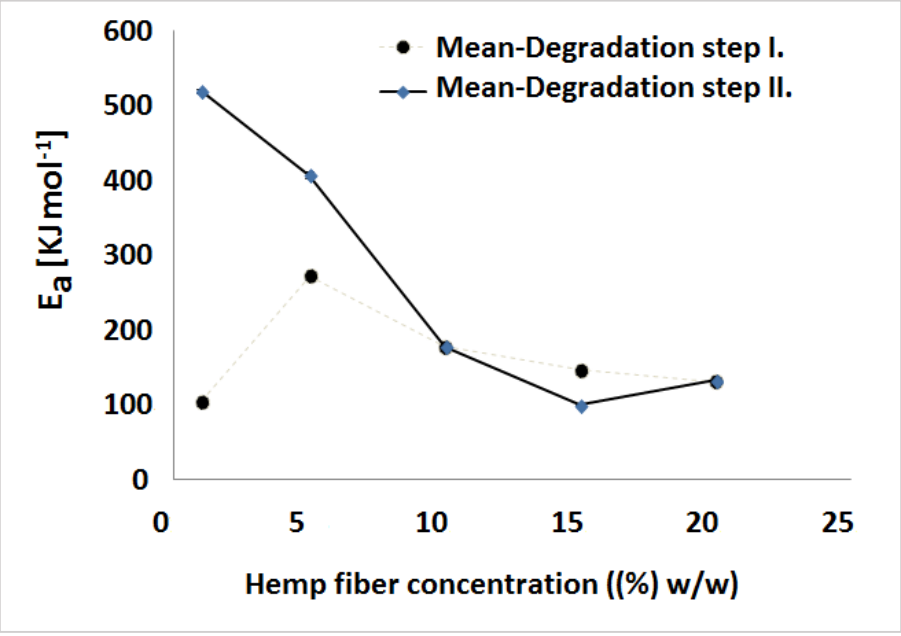

Figure 6-6: Variation of the average values of the activation energies of the two thermo-degradation steps of PET-hemp fiber composites with the fiber concentration.

The average values of the apparent activation energies of all the bio-composite formulations based on the iso-conversional energies are given in Figure 6-6 and show a variation with respect to the fiber concentration. Moreover, it yields significantly high value at low hemp fiber concentrations in Step II, followed by a reduction until a plateau is reached at high hemp fiber concentrations. Similar variations are made in Step I, with the exception of the formulation reinforced with 1% (w/w) hemp fibers, which shows a comparatively low value. As previously suggested, such behavior may result from the insignificant amount of hemp fibers in Step I and its effects on crystallization prior to Step II. Indeed, 1% (w/w) hemp fiber can simply act as an impurity in Step I, while it can cause significantly high crystallization to increase the apparent degradation energy of Step II. These observations are in agreement with those reported by Nabar *et al.* [134], who indicated the influence of both cellulose and other recycling impurities in the crystallization of PET reinforced with cellulose acetate blends. Moreover, the variations of the average activation energy of the first thermo-degradation step is comparable to the variation of the elastic moduli of the same formulations as previously reported, while the second step is comparable with the elongation at break of the non-annealed formulations [1]. Furthermore, the two thermo-degradation steps showed very close activation energies for 10% (w/w) hemp fibers reinforcement. This may either suggest some thermal degradation of the blends associated with the compounding challenges of high fibers volume or a resulting poor composite interface due to fiber-fiber contact.

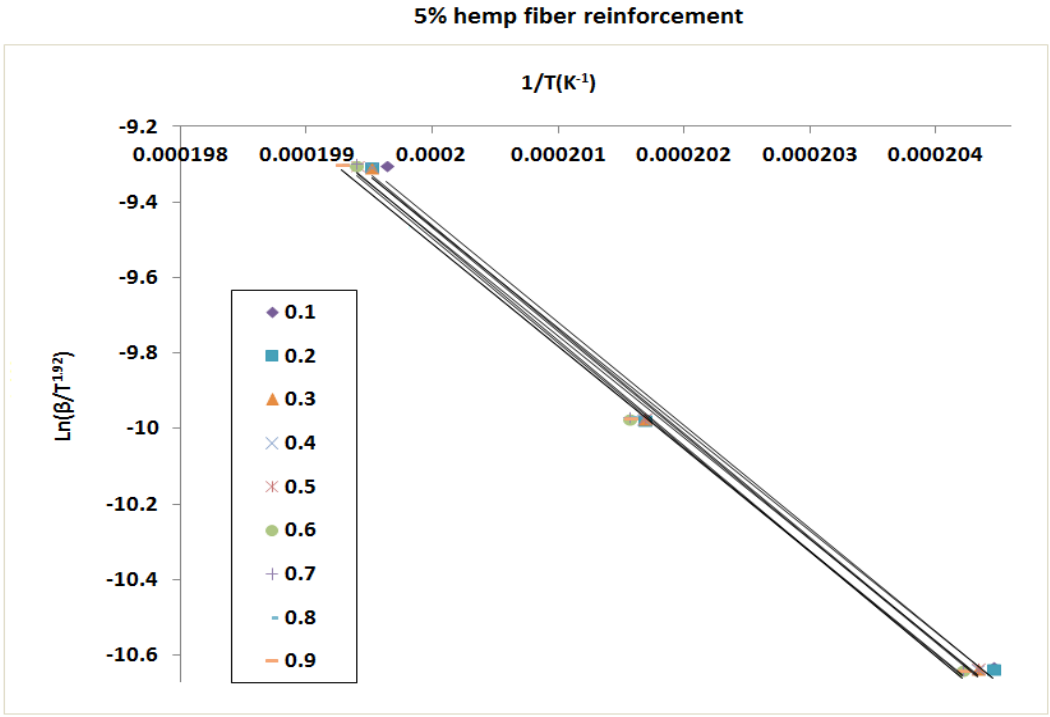

α	Linear regression, regression coefficient	α	Linear regression, regression coefficient	α	Linear regression, regression coefficient
0.1	y = -273165x + 45.189 R^2 = 0.9915	0.4	y = -274908x + 45.518 R^2 = 0.9964	0.7	y = -277742x + 46.059 R^2 = 0.9967
0.2	y = -267813x + 44.096 R^2 = 0.9946	0.5	y = -268895x + 44.29 R^2 = 0.998	0.8	y = -270841x + 44.657 R^2 = 0.9982
0.3	y = -274298x + 45.392 R^2 = 0.9966	0.6	y = -276259x + 45.756 R^2 = 0.9965	0.9	y = -270723x + 44.632 R^2 = 0.9981

Figure 6-7: Example of Starink's model application in the determination of the activation energy (Case of PET-5% (w/w) hemp composite, degradation step I).

Figure 6-7 shows the application of the Starink's model in the determination of the iso-conversional energies of PET-5% (w/w) hemp fiber composite, with high linear regression coefficients (R^2 > 0,99). The behavior of PET-5% (w/w) hemp fiber is representative for all the other investigated formulations since they showed similar

behavior. All the other cases were studied and their results were considered in computing the apparent activation energies of Figure 6-5 and Figure 6-6.

6.3.3 Determination of the reaction profile

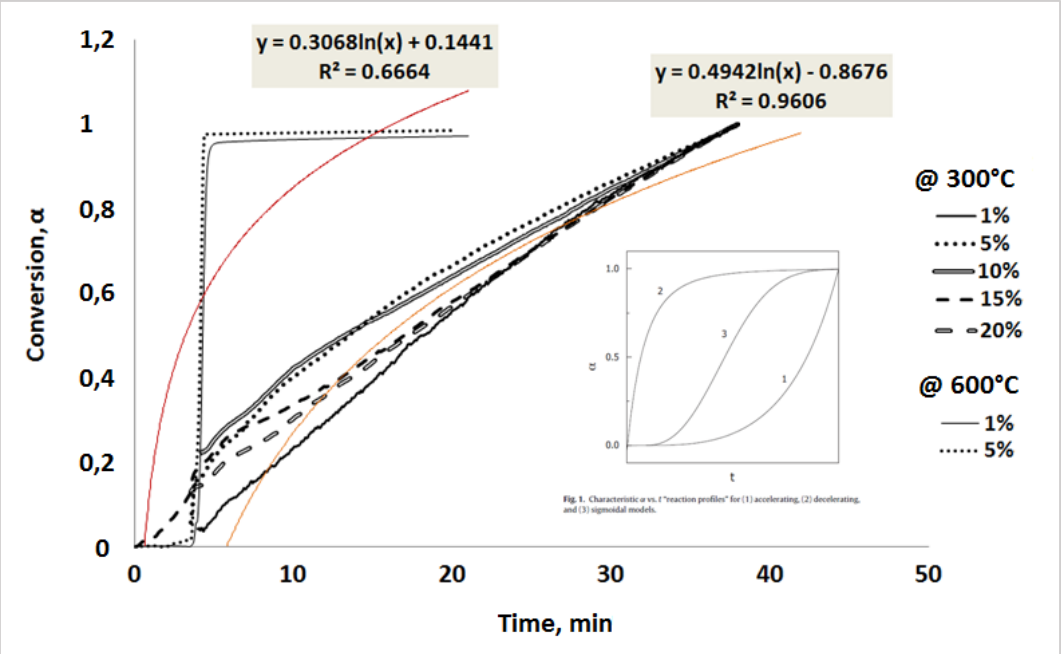

Figure 6-8: Variation of the isothermal conversion of PET-hemp fiber composites with the time, for the first stage of determining the thermal degradation's reaction profile. The internal graph shows the models endorsed by ICTAC [118].

The reaction profiles for the thermo-degradation of PET-hemp fiber composites or the mathematical expression f(α) describing the process was selected through a two-step operation based on the approved recommendations. The first step, which is summarized in Figure 6-8, describes the isothermal degradation of the composite blends with respect to both the reinforcement concentration and the heating time. There was a significant disparity between the resulting curves and the three classical types of reaction profile

published by the ICTAC (shown in miniature in Figure 6-8). This implies the inefficiency of the method for yielding an appropriate choice. The observed difference can be attributed to the multitude of species involved in the thermo-degradation mechanism. It is also in good agreement with previous observations respectively indicating the degradation of hemicelluloses in the first steps and cellulose in both steps [143]. The observed failure of the isothermal analysis to provide an appropriate reaction profile choice for the thermal degradation of PET-hemp fiber composites justifies the need for a second analytical stage which is based on the variation of ln(1-α) with the inverse of the absolute temperature.

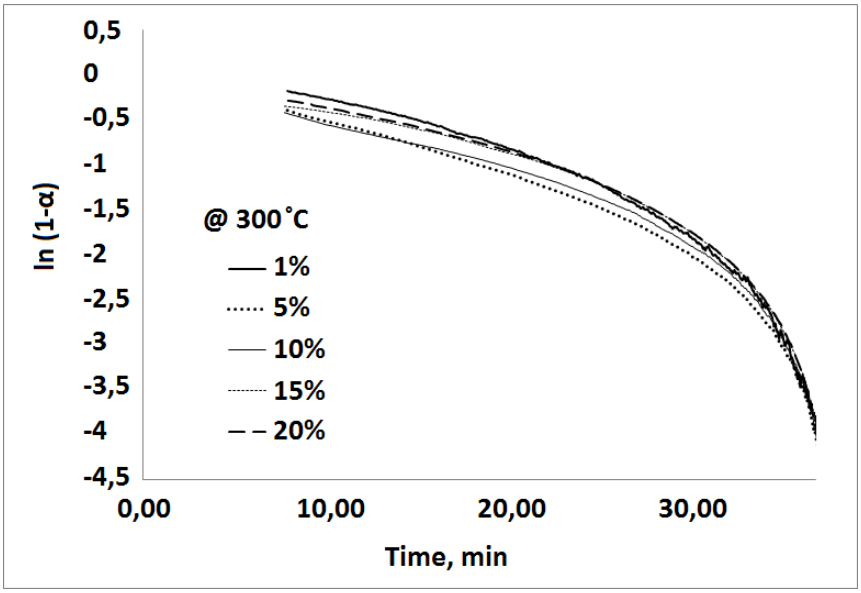

Figure 6-9: Second stage of the determination of the thermo-degradation reaction profile for PET-hemp fiber composites.

Figure 6-9 shows that the thermo-degradations of the investigated composite formulations can be described similarly through a two-stage operation involving a linear range during the first 15 minutes of the heating process, followed by a concave

downwards range. In this regard, based on different ICTAC recommendations, the two thermo-degradation steps were shown to follow different mechanisms. Furthermore, they can be viewed as first rate and contracting volume reactions, respectively. The various reaction profile parameters were determined by an application of the curve fitting method to the general contracting volume/cylinder model described in Equation (20). Moreover, the degradation steps I and II were specifically fitted by the Sestak-Berggren and the truncated Sestak-Berggren's autocatalytic models described in Equations (20), (21) and (22) respectively.

$$f(\alpha) = C\alpha^{n}(1-\alpha)^{m} \quad \text{General contracting sphere / cylinder} \tag{20}$$

$$f(\alpha) = C\alpha^{n}(1-\alpha)^{m} \quad \text{Truncated Sestak-Berggren's equation} \tag{21}$$

$$f(\alpha) = C\alpha^{n}(1-\alpha)^{m}[-\ln(1-\alpha)]^{p} \quad \text{Sestak-Berggren's equation} \tag{22}$$

The observed existence of different reaction profiles for the two degradation steps suggests their occurrence through different reaction mechanism and the involvement of different species. These observations are in agreement with the findings reported by Ruseckaite *et al.* [143], about the thermo-degradation of polycaprolactone-cellulose derivatives mixtures. However, the direct influence of cellulose on each degradation steps was not the focus of this work.

6.3.4 Determination of the reaction profile parameters

The non-linear fitting of the experimental data with the previously selected reaction profiles was done with all the investigated formulations. It further confirms a possible description of the two degradation steps by different kinetic models. These observations

show that the best fit for the first and second thermo-degradation steps are achieved using the Sestak-Berggren and the truncated Sestak-Berggren models, respectively.

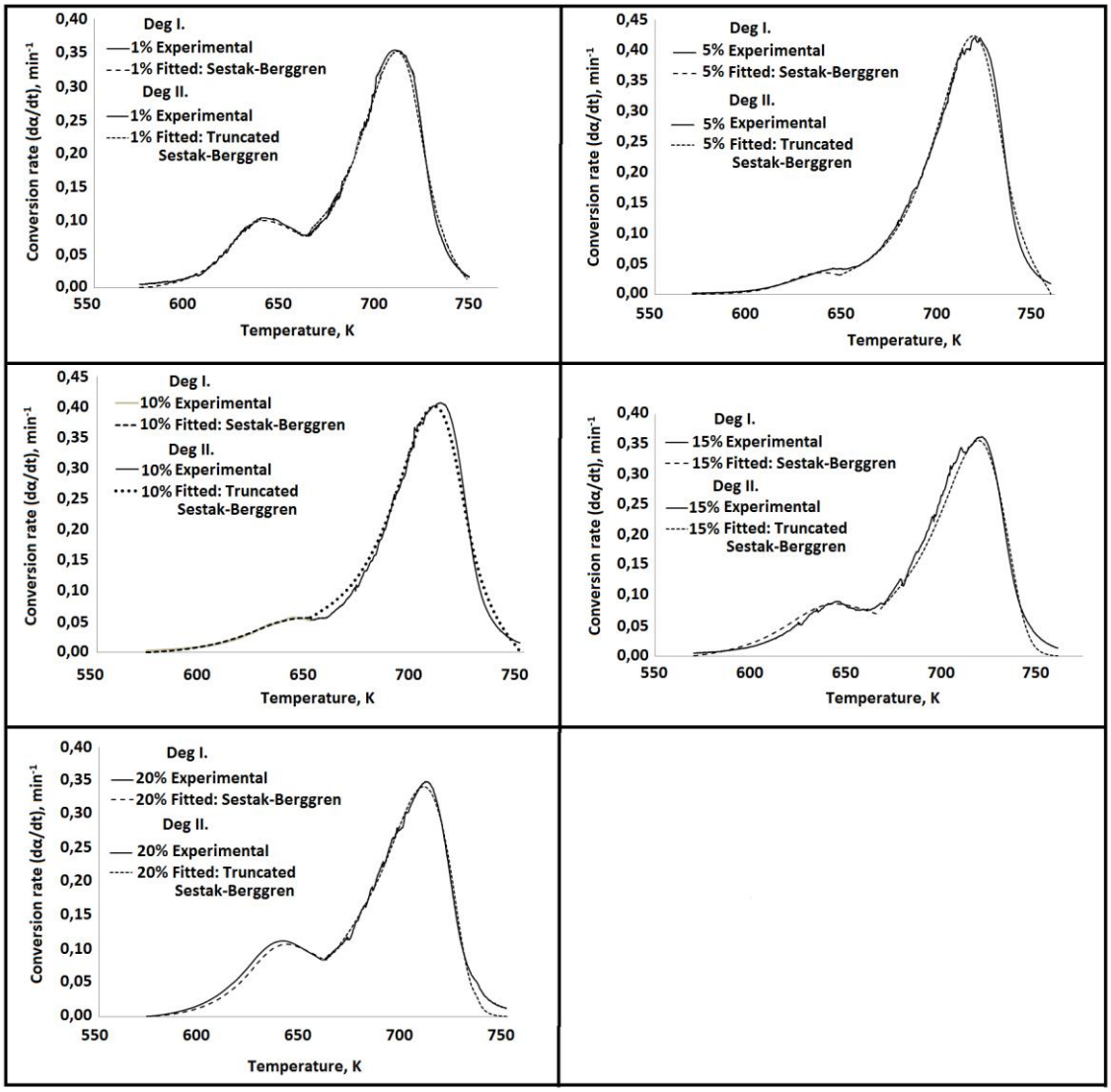

Figure 6-10: Nonlinear curve fitting for the thermo-degradation rate variations of PET-hemp fiber composite formulations.

It further implies the possible existence of different chemical species involved in each stage, which is in agreement with previous observations related to the kinetics of the thermal degradation of both cellulosic and bio-composite materials [125,132]. The

resulting curves fitting are shown in Figure 6-10 while the variations of the fitted kinetic parameters with the fiber concentration are summarized in Table 6-1 and Table 6-2 for the thermo-degradation Steps I and II, respectively.

Table 6-1: Kinetic parameters of the first thermo-degradation step of PET-hemp fiber composites based on the Sestak-Berggren's model.

Hemp load [% (w/w)]	n	m	p	A
1	3,17	7,67	-1,94	4,25
5	3,22	12,74	-2,21	1,80
10	2,89	9,55	-1,81	2,12
15	2,23	7,05	-1,11	2,49
20	2,25	8,25	-1,00	5,00

The parameters reported in Table 6-1 are quite close and show similar variations, thus the consistency of the Sestak-Berggren's model for the description of the kinetics of the first thermo-degradation of PET-hemp fiber composites. An individual analysis of each parameter indicates the general variations of the pre-exponential factor between 1,80 and 5,00. The formulations reinforced with 1 and 20 % (w/w) fiber showed some differences which can be attributed to the fiber volume and its effects on the molecular chains motion in the general system. On the one hand, a 1% (w/w) hemp fiber is negligible as earlier mentioned and may induce crystallization which in turn limits the polymeric chains motion. On the other hand, 20% (w/w) hemp fibers also limit molecular motion by the small proportion of the polymeric chains available for fiber-matrix bonding. The same effect has been observed by Mutje *et al.* [162], in the study of polypropylene (PP)-

hemp strand which demonstrated the properties of PP-15% (w/w) hemp strand to be closer to those of PP-glass fibers.

All the remaining parameters of the first degradation step were also quite close and found to vary in the ranges $2,25 \leq n \leq 3,17$; $7,05 \leq m \leq 12,74$; and $-2,21 \leq p \leq -1,00$. Other references with high temperature melting thermoplastics were not available for comparison, due to the fact that PET-hemp fiber composites are pioneer formulations of high temperature melting thermoplastics reinforced with vegetal fibers, to the best of our knowledge.

Table 6-2: Kinetic parameters of the second thermo-degradation step of PET-hemp fiber composites based on the truncated Sestak-Berggren's model.

Hemp load [% (w/w)]	A	n	m
1	2,18	2,00	0,87
5	1,82	1,37	0,77
10	1,76	1,42	0,80
15	8,39	2,24	2,28
20	10,00	2,49	2,35

An analysis of the kinetic parameters of the second thermo-degradation step reported in Table 6-2 shows that both the pre-exponential factor ($1,76 \leq A \leq 10,00$) and the first reaction exponent ($1,37 \leq n \leq 2,49$) shows an increase with the fiber concentration except for the case of 1% (w/w) fiber reinforcement. Moreover, based on the fiber concentration, the formulations can be partitioned as 1 to 10% (w/w) and 15 to 20% (w/w) which are two groups with comparable kinetic parameters. The second reaction exponent shows much closer values ($0,77 \leq m \leq 2,35$) but concurs with the two groups.

The fitting process was successful for both thermo-degradation steps, although its effectiveness differs between the two. Such behavior which is likely resulting from competing reactions during the early stage of the process have also been reported with polyolefins reinforced with vegetal fibers [125].

6.4 *Conclusion*

The kinetics of thermo-degradation of PET reinforced with 1, 5, 10, 15 and 20% (w/w) hemp fiber were investigated with the objective of expanding the utilization range of vegetal fiber reinforcements from low to high temperature melting thermoplastics as well as optimizing their applications. This investigation was based on the combination of thermo-gravimetric experiments and analysis, the Starink's iso-conversional method and nonlinear curve fitting methods. Two ranges of thermal degradations were observed from 290 to 385°C and from 385 to 490°C respectively. The first step involved the partial degradation of both the fibers and the matrix. The two thermo-degradation steps were analyzed using different non-linear curve fitting methods namely the Sestak-Berggren and the truncated Sestak-Berggren models.

The results suggest an appreciable thermal stability of PET-hemp fiber composites within the classical processing temperature range and processing cycle for vegetal fiber-reinforced composites. It supplements the authors' previous works which indicated the potential of reinforcing high temperature melting thermoplastics such as PET with vegetal fibers, based on a tradeoff among the fiber concentration, processing conditions and composite applications. This work can be applied for extending the utilization of other high temperature melting thermoplastics reinforced with vegetal fibers and their industrial applications.

CHAPTER: 7

THE DYNAMIC MECHANICAL ANALYSIS AND RELAXATION PROPERTIES OF PET-HEMP FIBER COMPOSITES

This chapter evaluates the dynamic mechanical analysis and the relaxation behavior of PET-hemp fiber composites for the choice of the optimal thermoformable formulation. It is directly related to the second and third objectives of this research.

The financial and logistic supports were provided by FQRNT, NSERC and CTRI.

7.1 *Introduction*

The thermoforming process is one of the most important plastic and composite material forming technique whose applications are found across various industries. It consists in heating up an extruded or cut sheet until it reaches a softened state, followed by its forming into the mold shape using an applied pressure, a vacuum, a moving plug or a combination of these media. The thermoforming industry is constantly innovating to manufacture more complex geometries and to process a wider list of potential materials. The material selection must be done at an early stage of the product development process, based on the cost, the properties in service and its processability. In this regard, sufficient work has not been done about the processability by thermoforming of high temperature melting thermoplastics reinforced by vegetal bast fibers. In fact, during the past decades, there has been a significant development of composite materials made up of thermoplastic matrices such as polypropylene (PP), high density polyethylene (HDPE) and nylon reinforced with fibers of vegetal origin. However, very little work was done with higher temperature melting thermoplastics such as polyethylene terephthalate (PET). Most of the current vegetal reinforcements are in the form of fibers, wood flour, or sawdust whose structures are advantageous for industrial processing methods such as extrusion and

thermoforming. Although the wood-related reinforcements can be as high as 70% by weight, the reinforcing volume of bast fibers such as hemp is limited owing to the challenges associated with their high surface to volume ratio [1]. Such limitation also affects the thermoforming of bast fibers reinforced composites. In comparison with mineral reinforcements, vegetal reinforcements are more advantageous because of their low density, their attractive low cost and their non-abrasive properties. Moreover, they are abundant, recyclable and they have a limited toxicity [77,163]. Some applications of these composite materials have recently been found in different industrial fields in the sector of the construction, aerospace, equipment and automobile.

An incompatibility exists between the hydrophilic vegetal-based reinforcements and some hydrophobic thermoplastic matrices such as polyolefins resulting in unsatisfactory mechanical properties [164–166]. This is not the case with polar matrices like PET reinforced with hemp fibers, as better interfaces result from the hydrogen bonds between the carbonyl groups of PET and the hydroxyl groups of cellulose. In fact, the previous works of the authors have shown an improvement of the mechanical and structural properties of PET-hemp fiber composites in the absence of coupling agents [1]. In the case of polyolefin matrices reinforced with vegetal fibers, such improvement of the mechanical resistance requires the creation of an improved bond between the fiber cellulose molecules and the matrix, either through a chemical modification of the components or the addition of a coupling agent aiming at connecting these components [77,166].

The final properties of the composite materials made of plastics and reinforced with vegetal fibers are a function of different parameters such as the properties of the matrix and the reinforcement, the reinforcement concentration and geometric parameters (L/D

ratio, granulometric distribution), the coupling agent concentration and the processing conditions [77,163–167]. Other crucial parameters include the blend quality, the thermal degradation of vegetal fibers and the blend's viscosity. In fact, an effective mixing process is crucial since a homogeneous blend ensures that optimal composite material properties are attained. Moreover, reinforcing high temperature melting thermoplastic matrices such as PET with vegetal fibers is rather challenging due to the fibers thermal degradation which occurs at temperatures as low as 190°C [38]. PET-hemp fiber composites were successfully processed by combining an alkaline fibers treatment to the matrix melting point depression, followed by compounding in a Torque-based Rheometer and injection molding. Additionally, it has been shown by various authors that the presence of vegetal fibers such as wood chips significantly increases the viscosity of the mixture, thereby limiting its formability with standard equipment such as the twin screw extruder [38,167].

In this work, the processability of five formulations of polyethylene terephthalate reinforced respectively with 0, 1, 5, 10 and 15% (w/w) hemp fibers was investigated experimentally and numerically. The dynamic explicit problem of inflation of a thin visco-elastic composite structure subjected to an air flow power loading was considered during the numerical analysis [168] while the virtual external work which is involved in the finite element formulation was expressed in the form of a volume integral [169]. The pressure was further derived from the Redlich-Kwong's real gas equation of state [170]. However, ideal gas equations are applicable at such low pressures. The process was numerically modeled by an application of the finite element method based on the Lagrangian formulation and by assuming both the validity of the membrane theory and the incompressibility of the composite material. The membrane structure was discretized by

plane finite elements [171] while the Christensen model and characterization technique were considered for their ability to describe free inflations [172]. The influence of the Lodge constitutive model on the thickness and the stress distribution in the free inflation of five PET-hemp fiber composite formulations was investigated.

This work is ground-breaking at various levels. It extends the applications of thermoplastics reinforced with vegetal fibers to high temperature melting matrices like PET and further investigates the conditions for processing the applications of the formulated material by thermoforming.

7.2 *Preliminary considerations*

The thermoplastic composite materials were considered above their glass transition temperature in this work. Moreover, they were assumed incompressible while following the membrane theory. They were then assumed to satisfy the conditions for a visco-elastic isotropic constitutive equation.

7.3 *Experimental and results*

7.3.1 Composites preparation for the dynamic mechanical analysis

The various PET-hemp fiber composite samples were processed by combining an alkaline treatment of the fibers and the melting point depression of the matrix, followed successively by compounding and injection molding. The virgin hemp fibers, having an average initial length of 6 cm (Lanaupôle, Berthierville, QC., Canada) were treated with

5N alkaline solution to increase their thermal stability following an alternative to the procedure of Specht *et al.* [37]. PET's melting point depression was achieved by blending it with 5% (w/w) polycaprolactone (PCL, Sigma Aldrich, Oakville, ON., Canada) following a previously published method by Papageorgiou *et al.* [105]. The compounding of alkaline-treated fibers and modified PET was done in a torque-based Rheometer (Haake Rheomix, Polylab OS system, USA) between 4 and 10 minutes with the melting chamber heated at 250°C, while injection molding was done at 250°C with a Haake Minijet.

7.3.2 Constitutive equation

The Christensen constitutive model shown in Equation (23) was applied for the behavior description of the isotropic PET-hemp fiber composite material [13]. The visco-elastic integral model is more appropriate for the description of polymers behavior at the semi-solid or molten state. Consequently, it can be used for the thermoforming of semi-solid materials. In fact, the Christensen model expresses the true matrix stress $[\sigma(t)]$ at a given time t as a function of the Lagrangian strain history $[E(\tau)]$.

$$[\sigma(t)] = p[I] + g_0\,[F].[F]^T + [F].\left(\int_0^t g_1(t-\tau)\,\frac{\partial[E(\tau)]}{\partial\tau}\,d\tau\right)[F]^T \qquad (23)$$

The parameters of Equation (23) are defined as follows: $[F]$ is the deformation gradient, p is the isostatic pressure, g_0 is the hyperelastic modulus and g_1 is the material relaxation function given by the formula of Equation (24)

$$g_1(t-\tau) = \sum_k C_k\, e^{-(t-\tau)/\tau_k} \qquad (24)$$

Moreover, the material relaxation function is a relaxation spectrum with moduli C_k and relaxation time τ_k. The temperature dependency of these models is accounted for by an application of the Williams-Landel-Ferry (WLF) function [16].

7.3.3 Characterization techniques

The PET-hemp fiber composites' material constants were identified by an application of different characterization techniques. First, the linear properties were derived from small amplitude oscillatory shear tests on solid samples [173], a technique commonly used for the determination of the storage and loss moduli with respect to the frequency as shown in Figure 7-1. Second, the discrete relaxation spectra for the five PET-hemp fiber composite formulations were determined from the dynamic data by means of a search pattern which minimizes the objective function F defined by Equation (25); where N is the number of data points $\left(G'_{i,\text{exp.}}, G''_{i,\text{exp.}}\right)$ which are available from the dynamic experiments and $\left(G'_{i,\,fit}, G''_{i,\,fit}\right)$ are their best fitted values defined by Equation (26).

$$F = \sum_{i=1}^{N}\left[\frac{G'_{i,\text{exp.}} - G'_{i,\,fit}}{G'_{i,\text{exp.}}}\right]^2 + \left[\frac{G''_{i,\text{exp.}} - G''_{i,\,fit}}{G''_{i,\text{exp.}}}\right]^2 \tag{25}$$

$$G'(\omega) = g_0 + \sum_k \frac{C_k \omega^2 \tau_k^2}{2(1+\tau_k^2\omega^2)}, \quad G''(\omega) = \sum_k \frac{C_k\, \omega\tau_{\,k}}{2(1+\tau_k^2\omega^2)}, \tag{26}$$

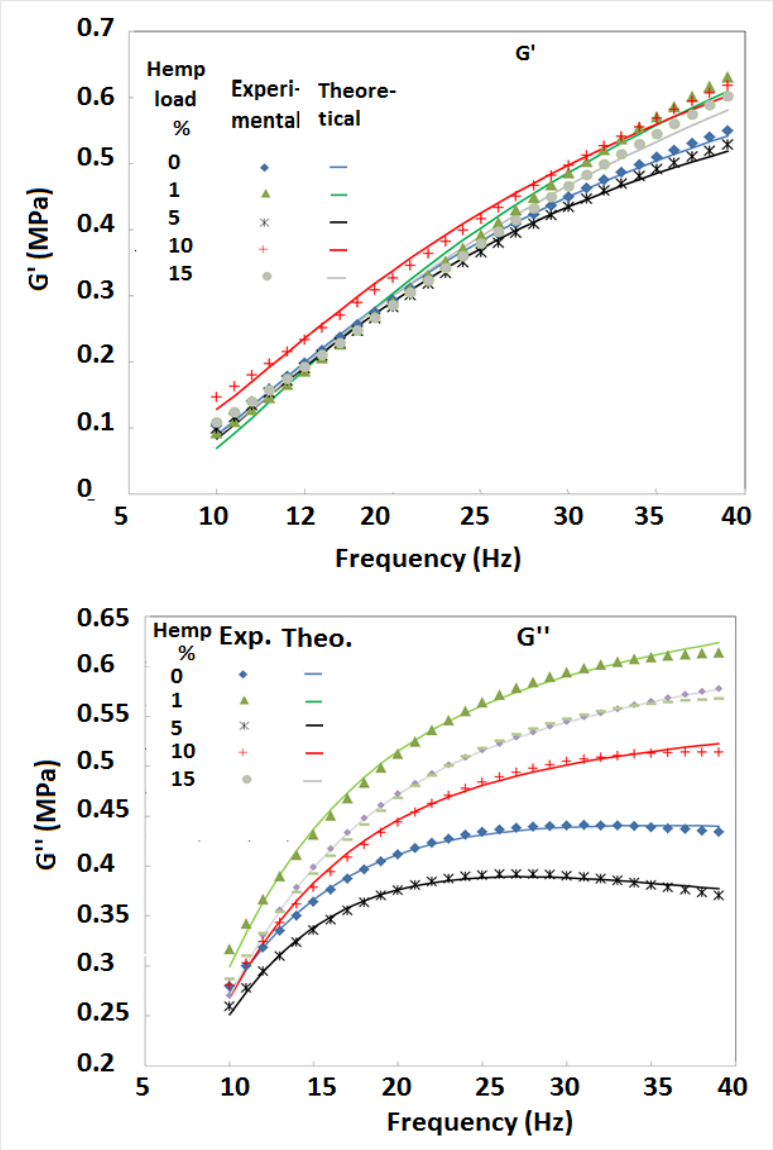

Figure 7-1: Storage and loss moduli of PET-hemp fiber composites compounded at 250°C.

One notes that all the formulations show the same shape for the variations of G' and G'' with pretty closed values at low frequencies and a huge disparity for the frequencies above 25Hz for G' and above 10Hz for G''. Moreover, the investigated formulations did not show a monotonic behavior with respect to the fiber concentration. We suspect that such behavior is linked to the volume of the fiber, the interactions

between the fibers and the matrix, the degree of mixing, and even some thermo-degradation of the fibers.

The low-frequency behavior and the high-frequency response are controlled by the long and short relaxation times respectively. This representation allows a description of the linear visco-elastic behavior over a wide range of time values by means of only a few constants.

Table 7-1: Relaxation spectrum for PET-hemp fiber composites.

Hemp fiber load [% (w/w)]	0	1	5	10	15
C_0 [MPa]	0,5	0,5	0,5	0,5	0,5
τ_k [sec]	g_k [MPa]	g_k [MPa]	g_k [MPa]	g_k [MPa]	g_k [MPa]
0,010	1,091	2,095	0,700	1,636	1,977
0,050	1,312	1,448	1,340	1,307	1,314
0,500	0,250	-0,740	0,083	-0,490	0,741
1,000	-1,348	0,465	1,199	-0,555	-0,400

The values of the relaxation strength g_k which describe the contribution to the rigidity associated with the relaxation times are listed in Table 7-1. At a constant C_0, the variations of the relaxation function with the relaxation time or the contribution to rigidity associated to the relaxation time is neither similar nor monotonic with the fiber concentration. This behavior may be caused by the same reasons suggested for the behavior of G' and G''. The highest value of g_k was found for 1% (w/w) reinforcement at 0,010 seconds while some negative values were found except for PET-5% (w/w) hemp fibers. The observed negative values have been reported to carry no special physical meaning without invalidating the fitting results.

7.3.4 Finite elements discretization

The numerical free inflation of PET-hemp fiber composite membranes by explicit dynamic finite element method was achieved following an application of both the space and time discretization. In fact, through an application of the finite element methodology, the principle of virtual work (weak form) was expressed on the un-deformed configuration for both the inertial effects and internal work followed by discretization and assembly [96]. The time discretization is justified by the presence of inertial forces. Moreover, it is achieved by using a conditionally stable centered finite difference technique [174].

A summation of all the elemental contributions reduces the inflation problem to the discrete system of Equation (27) [169]; where $\mathbf{F_{ext}}$, $\mathbf{F_{grav}}$ and $\mathbf{F_{int}}$ are the external, body and internal global nodal force vectors on the composite membranes, and **M** is the mass matrix.

$$M \cdot \ddot{u}(t) = F_{ext} + F_{grav} - F_{\text{int}} \tag{27}$$

Following the diagonalization of Equation (27), each degree of freedom of the diagonal form of the M matrix can be treated independently. Finally, an application of the centered finite difference scheme to Equation (27) yields Equation (28) where $\mathrm{M}_{\mathrm{ii}}, d$ are the diagonal components of the matrix $\mathbf{M^d}$.

$$u_i(t+\Delta t) = \frac{\Delta t^2}{M_{ii}^{d}}\left(F_{i,ext}(t) + F_{i,grav}(t) - F_{i,\text{int}}(t)\right) + 2u_i(t) - u_i(t-\Delta t) \tag{28}$$

The convergence of the explicit dynamic finite element method is controlled by the Courant-Friedrichs-Lewy criterion for nonlinear problems defined by Equation (29).

$$\Delta t \le \Delta t_{crt} = \varepsilon . \frac{l}{c} \tag{29}$$

It states that convergence occurs when the time step is smaller than the critical time steps. Other parameters of Equation (29) include **c** which ***is*** the wave speed in the medium and **l** is the element size. Consequently, **l/c** is the time needed by a wave to propagate across an element of size **l**. The proportionality constant ε depends on the applied integration scheme.

The initial conditions required for the solution of the current composite membrane free forming problem are given in Equation (30). They indicate that the displacement and velocity vectors are zero at the initial time t_0.

$$\begin{aligned} u_i(t_0) &= 0 \\ \dot{u}_i(t_0) &= 0 \end{aligned} \tag{30}$$

7.3.5 Plane-stress assumption

During the process, the heating phase precedes the inflation of the composite membranes. A successful simulation will then require an accurate evaluation of the internal forces through the computation of the relationship between the stresses and deformations for each element. Furthermore, the components of the Cauchy stress tensor satisfy the conditions expressed by Equation (31) when a plane-stress assumption is combined with the incompressibility of the composite membranes.

$$\sigma_{13} = \sigma_{23} = \sigma_{31} = \sigma_{32} = \sigma_{33} = 0 \tag{31}$$

7.3.6 Gas equation of state and pressure loading

In this work, the external forces are expressed in terms of the air flow pressure responsible for the blowing process. Such pressure is related to the internal volume of the composite membrane via the Redlich-Kwong's real gas equation of state [170] defined by Equation (32), where n(t) is the moles of gas used for the inflation of composite membrane, P(t) is the internal pressure, V(t) is the volume occupied by the membrane at time *t*, T_{gas} is the absolute temperature of the gas and $\overline{R}$ is the universal gas constant, $\overline{R} = 8{,}314 kJ kmol^{-1} K^{-1}$. Moreover, the parameters *a* and *b* are related to the critical point (P_c, T_c) of the gas through Equation (33).

$$P(t) = \frac{n(t) R T_{gas}}{V(t) - n b(t)} - \frac{n^2(t) a}{V(t)(V(t) + n(t) b)\sqrt{T_{gas}}} \tag{32}$$

$$a = 0{,}42748 \cdot \frac{\overline{R}^2 T_C^{2,5}}{P_C} \;.\; b = 0{,}08664 \cdot \frac{\overline{R} T_C}{P_C} \tag{33}$$

The following additional assumptions were made for the dynamic pressure evaluation:

- The gas temperature (T_{gas}) is constant;
- The pressure (P_0) between the sheet and the mold is constant;
- The initial volume V_0 enclosing the composite membrane at the initial time t_0 contains n_0 moles of gas;
- At a constant forming temperature, the Redlich-Kwong's equation can be reformulated as Equation (34).

$$P_0 = \frac{n_0 R T_{gas}}{V_0 - n_0 b} - \frac{n_0^2 a}{V_0 (V_0 + n_0 b)\sqrt{T_{gas}}} \tag{34}$$

- In case n(t) moles of gas produce an internal pressure p(t), the pressure difference during the forming process is computed by Equation (35) where V_0+V(t) is the volume occupied by the composite membrane at time t.

$$\begin{aligned} \Delta P(t) &= P(t) - P_0 \\ &= \left[\frac{(n(t)+n_0) R T_{gas}}{(V(t)+V_0) - (n(t)+n_0) b} - \frac{(n(t)+n_0)^2 a}{(V(t)+V_0)((V(t)+V_0) + (n(t)+n_0) b)\sqrt{T_{gas}}} \right] \\ &- \left[\frac{n_0 R T_{gas}}{V_0 - n_0 b} - \frac{n_0^2 a}{V_0 (V_0 + n_0 b)\sqrt{T_{gas}}} \right] \end{aligned} \tag{35}$$

Equation (35) gives the time variation of the pressure inside the composite membrane as a function of its internal volume based on the thermodynamic equation of state. Consequently, the external virtual work is expressed in terms of a closed volume by Equation (36) [169].

$$\delta W_{ext} == \left[\begin{array}{l} \left[\frac{(n(t)+n_0) R T_{gas}}{(V(t)+V_0) - (n(t)+n_0) b} - \frac{(n(t)+n_0)^2 a}{(V(t)+V_0)((V(t)+V_0) + (n(t)+n_0) b)\sqrt{T_{gas}}} \right] \\ - \left[\frac{n_0 R T_{gas}}{V_0 - n_0 b} - \frac{n_0^2 a}{V_0 (V_0 + n_0 b)\sqrt{T_{gas}}} \right] \end{array} \right] \delta V \tag{36}$$

Such equation which expresses the forming load as a function of the gas flow instead of the pressure is advantageous for the investigation of the load-deformation behavior without dealing with the instability associated with the classical pressure. In fact, in the case of constant pressure loading, a quasi-static and dynamic finite element computation of the pressure is divergent beyond a critical point [174,175].

7.4 *Numerical simulation of the free inflation of PET membranes reinforced with hemp fibers*

The targeted application consists of the free inflation of PET-hemp fiber composite discs of 15,0 cm diameter and an initial thickness h_0 of 1,47 mm, using the composite formulations reinforced with 0, 1, 5, 10 and 15% (w/w) hemp fibers. During the process, the ThermoForm® code was applied for the implementation of the dynamic finite element steps outlined in the previous sections. This code was developed by Erchiqui [176] for the investigation of a material stress and deformation behavior under large deformation based forming processes such as the thermoforming and the stretch-blow molding. All computations were performed on a PC in single precision.

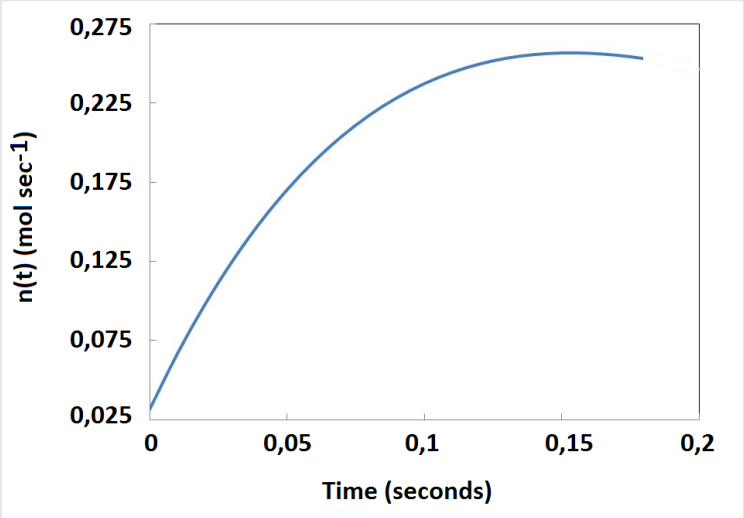

Figure 7-2: Time variations of the air flow.

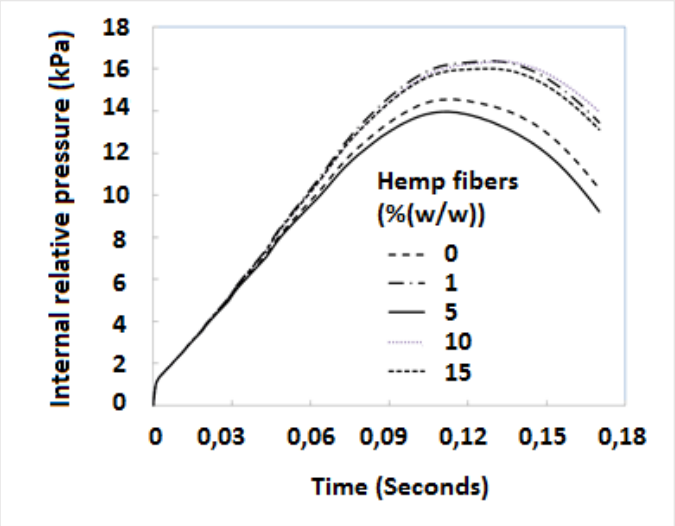

Figure 7-3: Time variations of the internal relative pressure for different PET-hemp fiber composite formulations.

The variations of the non-linear air flow responsible for the blowing process is shown in Figure 7-2. The resulting blowing cycle was found to be fixed and equal to 0,17 seconds. Figure 7-3 illustrates the time variations of the internal relative pressure of the investigated composite membrane formulations during the blowing process. The general shape of the relative pressure/time curve and the partition of the formulations into groups with comparable behavior are two important facts resulting from such variations. The variation trends are similar for all the formulations, and consists of an increase during the early part of the process until an extremum is reached around 0,12 seconds followed by a sudden decrease. Moreover, the variations are nearly linear and identical in the first stage which ends around 0,04 seconds while they are different elsewhere. Based on these observations, the investigated composite membranes can be classified into two groups of comparable behavior which are respectively reinforced with 0 and 5% (w/w) hemp fibers on one hand and 1, 10 and 15% (w/w) hemp fibers on the other.

In fact, the relative pressure generated within 0,17seconds for the composite formulations reinforced with 1 and 10% (w/w) hemp fibers which are respectively 16,370 and 16,360 kPa, are comparable to the values observed for 15% (w/w) reinforcement. In the same manner, the maximum relative pressure for virgin PET is 14,550 Pa while the minimal value which is 13,960 kPa is found in the presence of 5% (w/w) reinforcement. This implies that the behavior of the composite reinforced with 1% (w/w) hemp fibers is more elastic than visco-elastic. Such behavior indicates a composite whose thermoformability is less interesting than those reinforced by 5% (w/w) hemp fibers. Consequently, the formulations reinforced with 10 and 15% (w/w) hemp fibers are less interesting for both the thermoforming and the blow molding processes than the formulation reinforced with 5% (w/w) hemp fibers. In fact, the hardening of the composite formulation reinforced with 1, 10 and 15% (w/w) hemp fiber indicates potential membrane blowing challenges.

Figure 7-4 illustrates the time variations of the volume of the investigated composite membrane formulations during the blowing process. All the investigated formulations displayed an increase of the membrane volume with time; moreover, their variations were identical until 0.12 seconds and different elsewhere. This signifies that the observations made for the time variations of the volume are in agreement with those made for the time variations of the internal relative pressure.

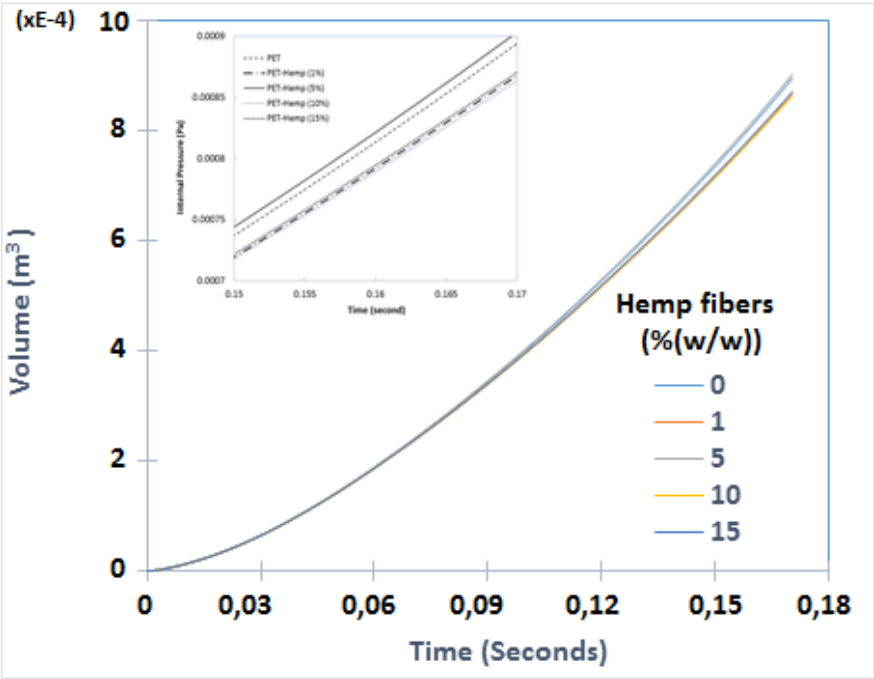

Figure 7-4: Time variations of the volume of different PET-hemp fiber composite membrane formulations.

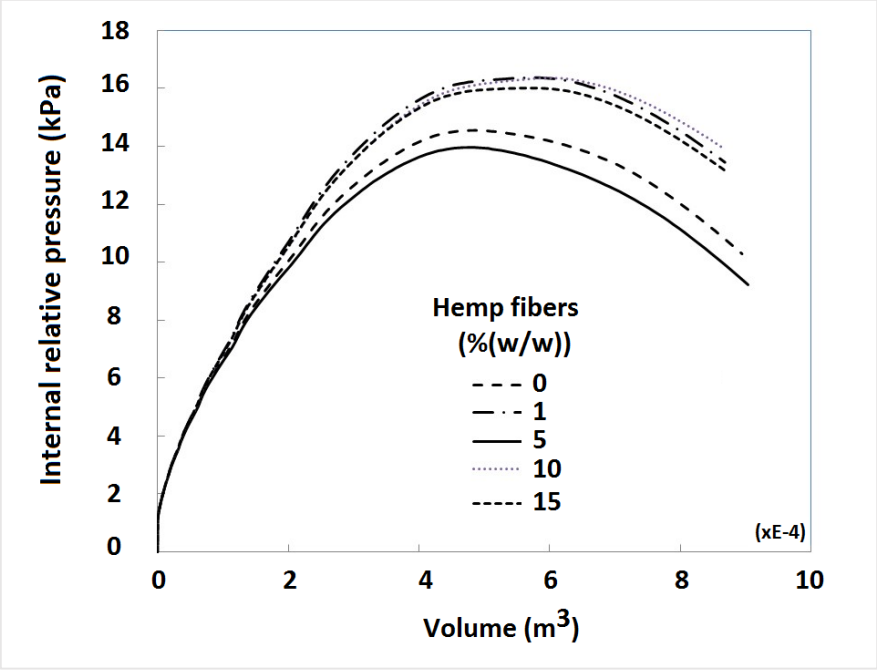

Figure 7-5: Internal relative pressure variations with the volume of different PET-hemp fiber composite membrane formulations.

The thermoformability of these composite formulations was further clarified by an analysis of the variations of their internal relative pressure with the volume at the end of the blowing cycle as shown in Figure 7-5. It shows that the evolution of the internal relative pressure is presented as a function of the blown air volume through an elimination of the time variable from the five investigated composite membrane formulations. The resulting variations are comparable to the time variations of the internal relative pressure. This implies that the variations of the internal relative pressure with the volume during the blowing phase of the composite membranes depend on the fiber concentration.

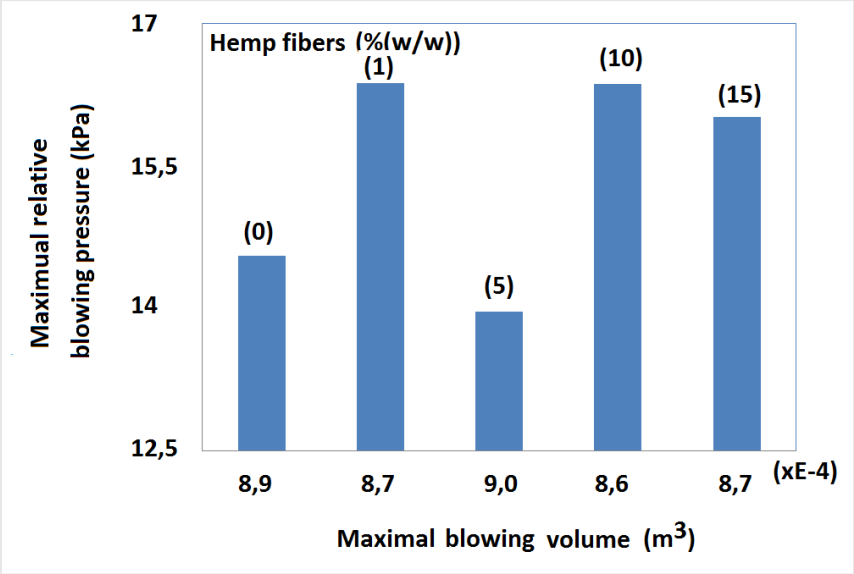

Figure 7-6: Variations of the maximal relative blowing pressure with the maximal blowing volume for different PET-hemp fiber composite formulations at t = 0.1 seconds.

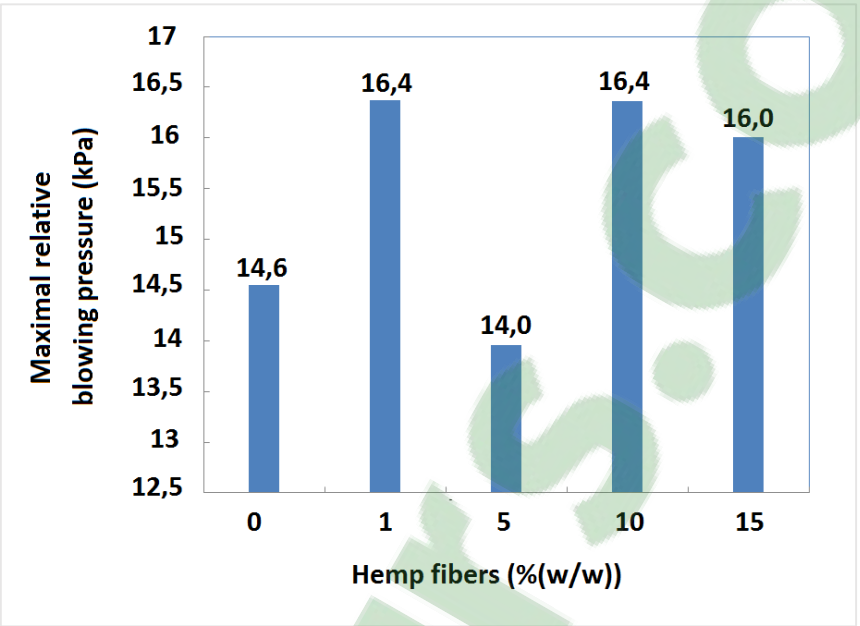

Figure 7-7: Maximal internal blowing pressure for different PET-hemp fiber composite membrane formulations at t = 0.17 seconds.

In the same manner, Figure 7-6 and Figure 7-7 show the variations of the maximal blowing pressure with the maximal blowing volume as well as the variations of the maximal blowing pressure with the fiber concentration.

In fact, the volumes and pressures generated by the five composite membrane formulations (0, 1, 5, 10 and 15% (w/w) during the blowing cycle which lasted 0.17 seconds are respectively (894 cm^3; 14,55 kPa), (868 cm^3; 16,37 kPa), (903 cm^3; 13,96 kPa), (864 cm^3; 16,36 kPa) and (870 cm^3; 16,01 kPa). These observations further indicate the advantage shown by PET-5% (w/w) hemp fiber towards the thermoforming process over the rest of the investigated PET-hemp fiber composite formulations.

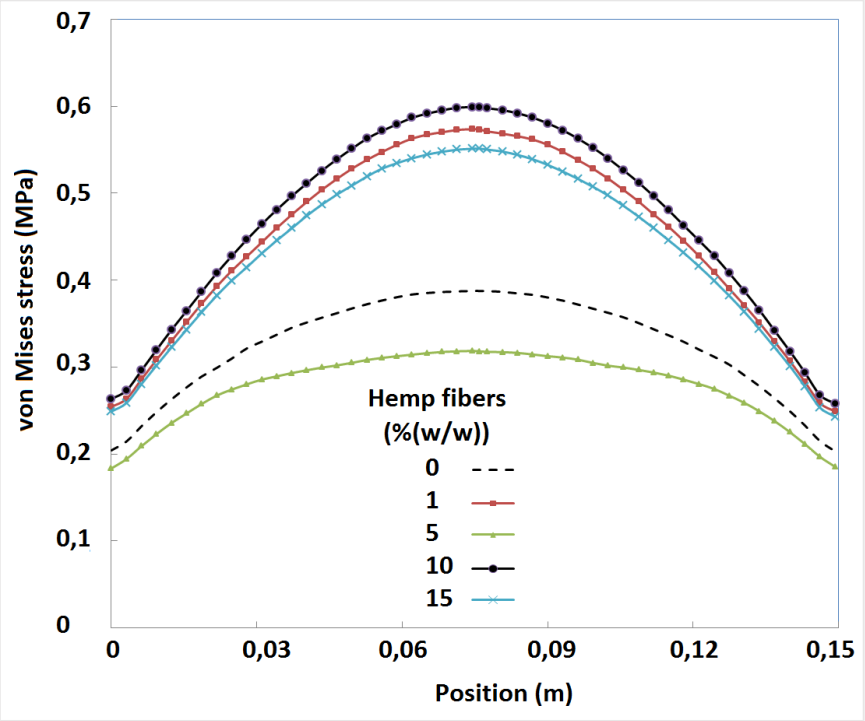

Figure 7-8: Von Mises stress variations on the XZ half-plane of symmetry of different PET-hemp fiber composite membrane formulations.

The thickness prediction is an important goal in the numerical simulation of both the blow molding and thermoforming process. However, the stress estimation is invaluable in part design. In fact, the prediction of the residual stress and the shape stability of the part are strongly related to the estimated stress. In this section, the stress prediction obtained from different investigated composites is discussed for the free membrane inflation. The localized thinning effect of the deformed membrane is generally accompanied by the increase in the Cauchy stresses or the true stresses of the material.

Figure 7-8 shows the final von Mises stress ($\sigma_{eq.}$) distribution on the XZ half-plane of symmetry of PET-hemp fiber composite membranes as a function of the fiber concentration, based on Christensen's constitutive model.

Table 7-2: The critical values of the von Mises stress and volume of different PET-hemp fiber membrane formulations.

Hemp fibers [% (w/w)]	0	1	5	10	15
σ_{eq} [MPa]	0,388	0,574	0,319	0,599	0,551
V [cm^3]	894,2	868,0	903,4	863,9	870,7

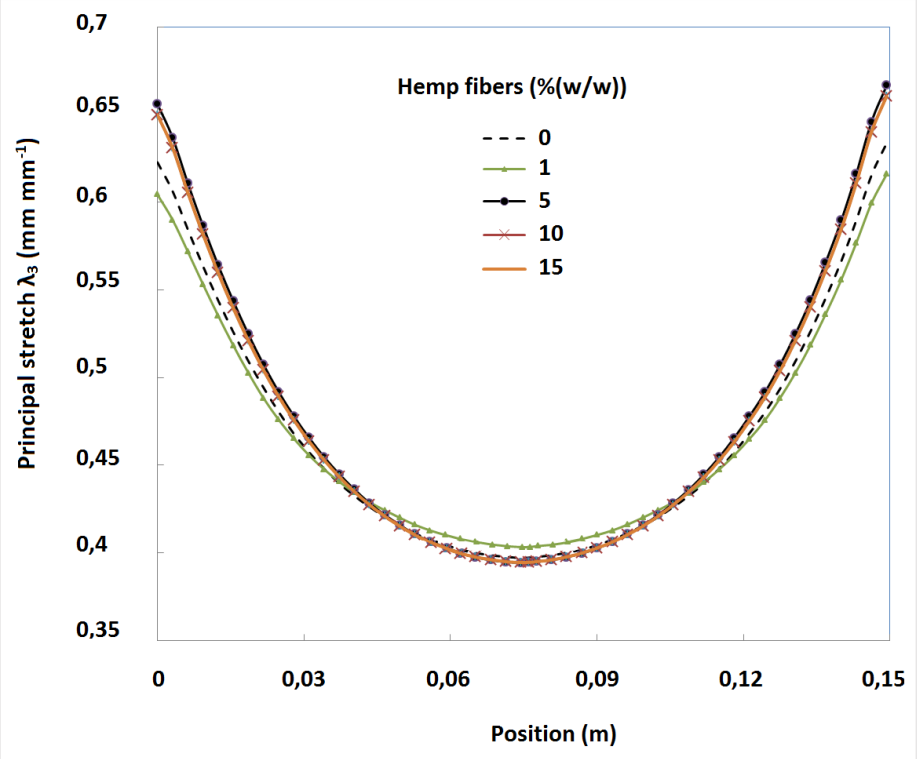

Figure 7-9: Stretch ratio on the XZ half plane of symmetry for different PET-hemp fiber composite membrane formulations.

The critical values of the von Mises stress and the corresponding inflated volumes in the central area of the membranes are presented in Table 7-2 for different formulations. The von Mises stress distribution (σ_{eq}) on the XZ half-plane exhibits a maximum of 0,599 MPa for 10% (w/w) hemp fiber reinforcement with a volume of 863,9 cm^3 and a minimum of 0,319 MPa for PET-5% (w/w) hemp fibers with a volume of 903,4 cm^3.

These values are identical in the YZ half-plane. Finally, the von Mises stress distribution and the localized thinning effect indicate that material failure due to large deformations induced by the inflation is most likely to occur in the central area of the blown membrane as shown in Figure 7-9.

Figure 7-10 and Figure 7-11 respectively present different views of the thickness and von Mises stress distributions of different PET-hemp fiber composite membrane formulations at the end of the inflation induced in the final shape using the Christensen's model. In the light of the results given above, the following remarks can be made.

The thickness distributions obtained from the investigated PET-hemp fiber composite membranes and particularly those with 1, 10 and 15% (w/w) reinforcements are similar while the stress prediction exhibits some discrepancies. The similarity of the thickness distributions is likely related to the incompressibility assumption. Such observation about the final thickness distribution in the parts which are thermoformed with isotropic and incompressible materials was previously made by DeLorenzi and Nied [177]. According to these authors, the thickness distribution is less dependent on the law describing the material behavior than the geometry imposed by the mold. Our study, concerning isotropic visco-elastic material reinforced with hemp fibers also shows that the constitutive behavior of these materials has little influence on the final thickness distribution for free membrane inflation.

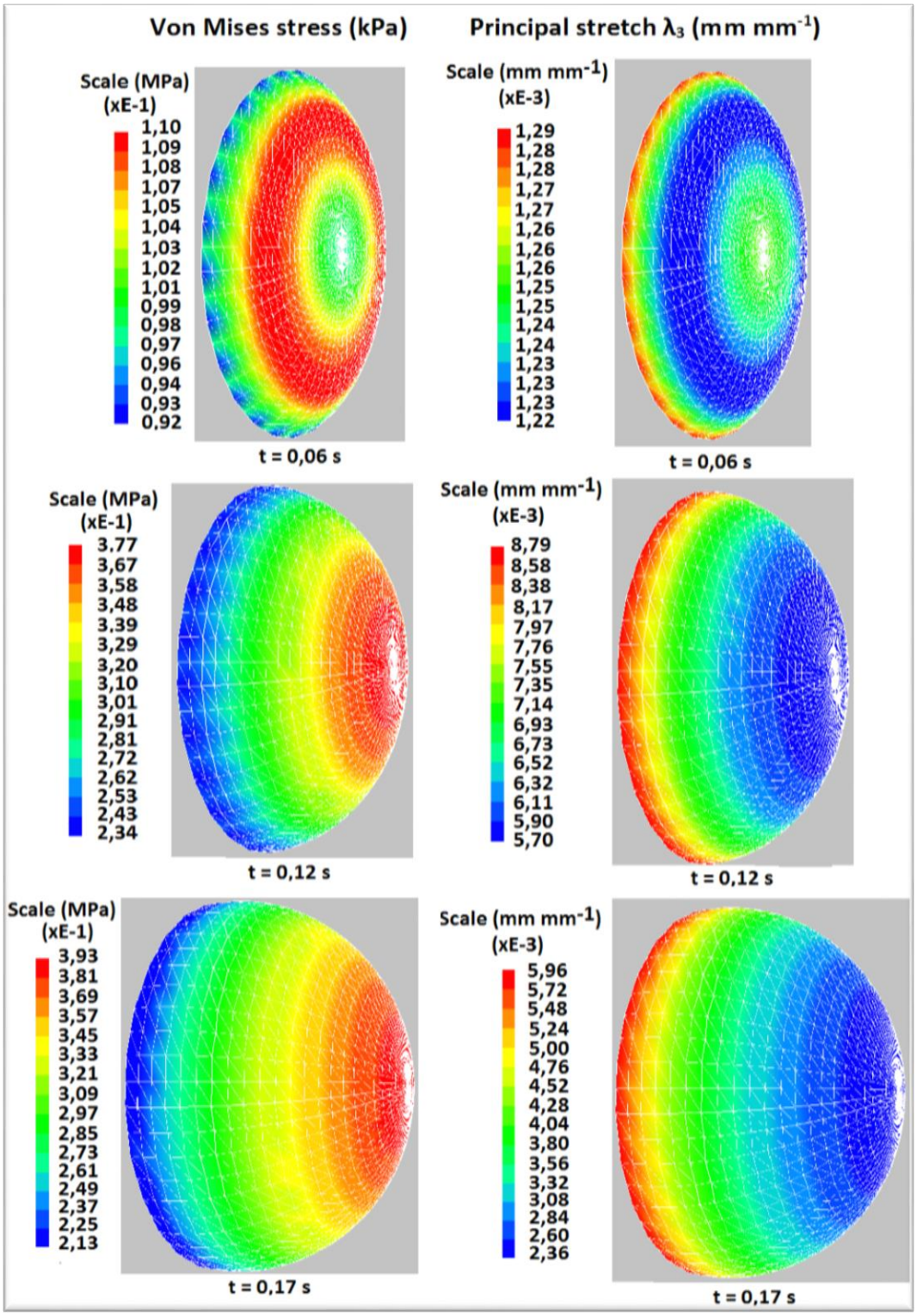

Figure 7-10: Distributions of the principal stretch and von Mises stress for PET.

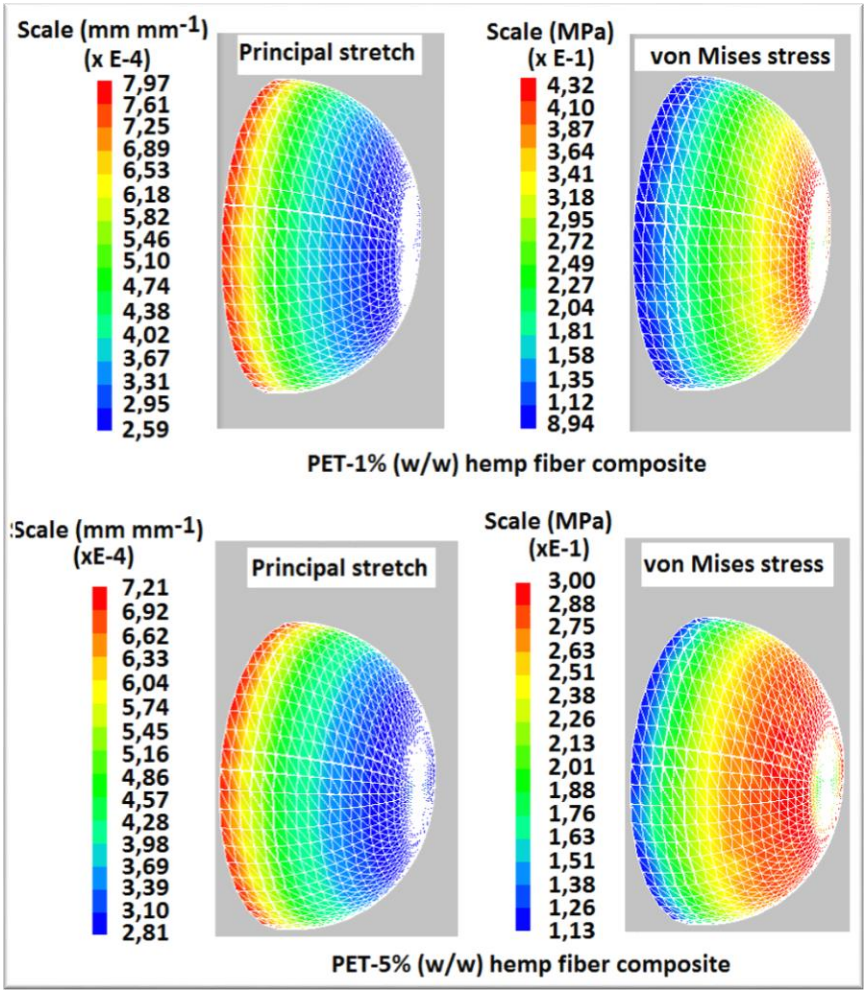

Figure 7-11: Distribution of the principal stretch and von Mises stress for PET reinforced with 1 and 5% (w/w) hemp fibers at t = 0.17 seconds.

The choice of both the experimental technique and the mathematical model to determine the material parameters associated with the constitutive models is critical for a reliable prediction of the free membrane inflation. In the example of bubble inflation technique where the air flow pressure rate is controlled while the forming pressure and the sheet height are measured, the experimental setup and the analytical model yield a predicting solution for the thickness distribution for the free membrane inflation. Thus,

the use of this technique is necessary for a better prediction and it is applicable by using a more extended control of the measurable physical variables such as temperature and relaxation.

The simple example of the free membrane inflation of PET-hemp fiber composite materials shows the advantage of using the dynamic finite elements method based on a total Lagrangian approach as well as a pressure load derived from the thermodynamic laws for the simulation of the structural behavior of composite materials.

1.1 Conclusion

The numerical free forming of PET-hemp fiber composite formulations with 0, 1, 5, 10 and 15% (w/w) reinforcement was successfully investigated with the ThermoForm® code based on a combination of key assumptions and experimental data. The visco-elastic behavior of the composite formulations was described by the Christensen model. During the finite element's implementation phase, the Lagrangian formulation was applied together with the assumption of the membrane theory. The Redlich-Kwong's real gas equation was applied for the determination of the forming load while the external work was expressed in terms of a closed volume.

An investigation of the effects showed that lower reinforcements like 1 and 5 % (w/w) show a good potential for free forming. However, an important air flow pressure would be required for the formulation reinforced with 1% (w/w) hemp fibers. The free forming of the formulations reinforced with higher fiber concentrations like 10 and 15% would also require powerful air flow pressure although their formulation may lead to the partial thermo-degradation of hemp fibers leading to relatively low mechanical

performance. Consequently, the formulations reinforced with 5% (w/w) hemp fibers combines a good performance and the opportunity for a less challenging free forming process.

CHAPTER: 8

THE NUMERICAL THERMOFORMING OF PET-HEMP FIBER COMPOSITES

This chapter studies the behavior of various PET-hemp fiber formulations towards the thermoforming process. It is related to the third objective of this research.

The logistic and financial supports were provided by FQRNT, NSERC, CTRI and the Moroccan Ministry of Higher Education, Scientific Research and Personnel training (CNRST), under the "FINCOM-CNRST" project.

8.1 *Introduction*

The thermoforming process is one of the most important plastic and composite material forming techniques, with extensive uses in various industrial and commercial applications. It consists of heating a material sheet which is either extruded or cut until its softened state and subsequently deforming it into the mold shape by an applied pressure, a vacuum, a moving plug or a combination of the three. The constant innovation of the thermoforming market results in the processing of more complex geometries and an expansion to a wider list of potential materials which selection is based on their cost, their working properties and their processability. In this regard, sufficient work has not been done to elucidate the visco-elastic behavior of thermoplastic matrices reinforced with vegetal fibers especially towards the thermoforming process. Moreover, high temperature melting thermoplastic reinforced with vegetal fibers have only recently regained researchers' attention and been developed [1,3], making them a good target for thermoforming studies.

As described below, current observations show that low and high temperature melting thermoplastics exhibit different kind of behavior with respect to the reinforcement by vegetal fibers and with respect to secondary forming processes like thermoforming.

During the past decades, a significant amount of work has been done for the development of low temperature melting thermoplastic matrices such as polypropylene (PP), high density polyethylene (HDPE) and Nylon reinforced with natural fibers such as wood flour, sawdust and bast fibers like hemp. The low processing temperature of these matrices is rather advantageous for the thermal stability of vegetal fiber and a justification of the high volume of their applications with wood-related reinforcements as high as 70% by weight [1]. Moreover, vegetal reinforcements have been reported to be more advantageous due to their low density, their attractive low cost and their non-abrasive properties. In addition, they are abundant, recyclable and they have a limited toxicity [77,163]. These composite materials have recently been found in different fields of application in the example of construction materials, the aerospace industry, as well as furniture and car parts.

There are only a few challenges in processing low temperature melting thermoplastics with vegetal fiber including the chemical incompatibility between hydrophilic fibers and hydrophobic matrices which results in disappointing mechanical properties [164–166] and the limited process-able volume of bast fibers due to their high surface to volume ratio. Many methods of tackling the chemical incompatibility challenge have been reported in the literature based on improving the bonding quality between the fiber cellulose molecules and the matrix either through a chemical modification of the components or the addition of a coupling agent to connect its components [77,166].

Contrary to the composites with low temperature melting thermoplastics, it is more challenging but advantageous to reinforce high temperature melting thermoplastics with vegetal fibers. The temperature difference between the onset of thermal degradation of vegetal fibers (T_d = 190°C) [38] and the melting point of high temperature melting thermoplastic matrices (T_m > 200°C) is the main challenge to processing such composite material without the thermo-degradation of vegetal fibers. However, polar matrices like PET offer the possibility of hydrogen bonding between the carbonyl groups of the matrix and the hydroxyl groups of cellulose. In fact, our previous works have shown an improvement of the mechanical and structural properties of PET-hemp fiber composites in the absence of coupling agents [1].

Apart from the challenges discussed in the previous sections, many other parameters influence the final properties of a composite material made of plastics and vegetal fibers. They include the reinforcing load and its geometric parameters (L/D ratio, granulometric distribution), the proportion of the coupling agent as well as the processing conditions [77,163–167], the blend quality, the thermal degradation of vegetal fibers and the blend viscosity. In fact, an effective mixing process is crucial to achieve a homogeneous blend resulting in optimal composite properties. Additionally, various authors have shown that the presence of vegetal fibers such as wood chips significantly increase the viscosity of the mixture, thereby limiting its ability to be formed with standard equipment such as the twin screw extruder [38,167] thus the necessity to investigate their behavior towards the thermoforming process.

This work investigates the elaboration and the numerical thermoformability of the novel melt processed polyethylene terephthalate (PET)-hemp fiber composites. PET-

hemp fiber composites were successfully processed by combining an alkaline fiber treatment to the melting point depression of the matrix, followed by compounding in a Torque-based Rheometer and injection molding.

The dynamic explicit problem of forming a thin visco-elastic composite structure subjected to an air flow pressure loading was used during the numerical analysis [168] while the virtual external work which is involved in the finite elements' formulation was expressed in the form of a volume integral [169]. The pressure was then derived from the Redlich-Kwong's real gas equation of state [170]. The process modeling was done by an application of the finite element method based on the Lagrangian formulation and assuming both the membrane theory and the incompressibility of the composite material. The membrane structure was discretized by plane finite elements [171] while the Christensen model and the characterization technique were considered for their ability to describe free inflations [172]. The influence of the Christensen constitutive model on the thickness and the stress distribution in the free inflation of five PET-hemp fiber composite formulations were investigated.

8.2 *Experimental*

The PET-hemp fiber composite samples were processed by combining an alkaline treatment of the fibers with the melting point depression of the PET matrix, followed successively by compounding and injection molding. Furthermore, the three groups of composite properties described below were necessary for the intended thermoformability investigation.

8.2.1 Materials

PET grade AA-48 (Eastman, Montreal, QC, Canada), polycaprolactone (PCL, Sigma Aldrich, Oakville, ON, Canada) and hemp fibers of composite grade from Lanaupôle (Berthierville, QC, Canada) were used in this work. These fibers had an average length and diameter of respectively 50 mm and 20-25 µm. The preliminary work investigated the effect of some additives such as clay grade Cloisite 30B (Southern Clay Products Inc., Gonzales, TX, USA), pyromelitic dianhydride (PMDA) and glycidyl methacrylate (GMA) from Sigma Aldrich (Oakville, ON, Canada) were respectively used as fire retardant, chain extender and fiber's coating agent [30,31,104]. Moreover, triethylamine, hydroquinone and sodium hydroxide were used in different stages of the process as chemical reagents.

8.2.2 Composite elaboration

The virgin hemp fibers were treated for an hour with 5N NaOH solution in order to increase their thermal stability based on an alternative to the procedure of K. Specht *et al.* [37]. The melting point depression of PET was achieved by blending with 5% (w/w) polycaprolactone in an internal batch mixer (Haake Rheomix, Polylab OS system, USA), based on a previously published method by Papageorgiou *et al.* [105]. The compounding process of alkaline treated fibers and modified PET was done in an internal batch mixer (Haake Rheomix, Polylab OS system, USA), with the melting chamber heated at 250°C. Furthermore, injection molding of the mechanical and the dynamic mechanical samples was done at 250°C with a Haake Minijet, with a mold heated at 50°C.

All the hygroscopic substances such as PET, the modified PET and the compounded PET-hemp formulations were pre-dried prior to compounding and injection molding to avoid sample degradation as reported by authors like La Mantia and Morreale [8] and Awaja *et al.* [104]. In fact, PET being synthesized by esterification reaction between terephthalic acid and ethylene glycol with water as a by product, would decompose when heated in the presence of water.

8.2.3 Composites characterization

The mechanical properties of the investigated composites were evaluated using tensile tests with an Instron model 4206 at a cross head speed of $5mmmin^{-1}$ based on ASTM D638-08. The data were analyzed by inbuilt software to determine the influence of both the additives used and the variation of hemp fibers concentration.

The structural properties of the investigated composites were analyzed with a Scanning Electron Microscope Hitachi (model S-3500N, Tokyo, Japan) to determine the effects of the additives and the reinforcing concentrations. The samples were cryo-fractured and gold coated prior to the analysis.

The loss and storage moduli of the investigated PET reinforced with 0, 1, 5, 10 and 15% (w/w) hemp fibers were determined by small amplitude oscillatory shear test [173] and the results applied to the finite element ThermoForm® code developed by the senior researcher for both an identification of their dynamic mechanical behavior and the determination of their relaxation properties.

8.2.4 Mechanical and structural impacts

The mechanical and structural properties of the investigated PET-hemp fiber composites indicated the same trend earlier observed by other authors about the behavior of low temperature melting thermoplastic matrices reinforced with vegetal fibers [126] and the need for a trade-off between the required properties, the additives and the targeted applications is necessary. In fact, our previous works indicated an increase of both the elastic modulus and the maximum force following an increase of the hemp concentration from 1 to 20% (w/w) and the same behavior in the presence of different additives. In the contrary, the strain at break dropped consistently from above 40 for virgin PET to around 5%. Moreover, an improved interface was observed from the micrographs of all the PET-hemp fiber formulations without additives, indicating a good fiber-matrix bonding [1]. The micrographs of all the investigated formulations confirmed the thermal stability of the treated hemp fibers in the suggested processing method and the thermal stability of those formulations were studied for further processing [1,3]. However, above 10% (w/w) of hemp fibers concentration, more fiber-fiber contact was observed indicating potential weak structural points.

8.3 *Modeling and simulation*

The behavior of PET-hemp fiber composite formulations was investigated through the numerical thermoforming of circular membranes of 15 cm diameter and an initial thickness h_0 of 1.47 mm. The processing load was expressed in terms of non-linear air flow rate as described in Figure 8-2.

8.3.1 Preliminary considerations

In this work, apart from the membrane theory and the incompressibility of the composite materials, PET-hemp fiber composite materials were considered above their glass transition temperature. Therefore, the investigated materials were assumed to satisfy a visco-elastic isotropic constitutive equation.

8.3.2 Constitutive equation

The Christensen constitutive model [13] was used to describe the behavior of PET-hemp fiber composite materials, considered isotropic. Such integral model which is more appropriate for the description of polymeric behavior in both their semi-solid or molten state can be used for the description of the thermoforming of semi-solid materials. The Christensen model describes the true matrix stress $[\sigma(t)]$ at time t as a function of the Lagrangian strain history $[E(\tau)]$ as shown in Equation (37) where $[F]$ is the deformations gradient, p is the isostatic pressure, g_0 is the hyper elastic modulus and g_1 is the material relaxation function described by Equation (38).

$$[\sigma(t)] = p[I] + g_0\,[F].[F]^T + [F].\left(\int_0^t g_1(t-\tau)\,\frac{\partial[E(\tau)]}{\partial\tau}\,d\tau\right)[F]^T \qquad (37)$$

$$g_1(t-\tau) = \sum_k C_k\, e^{-(t-\tau)/\tau_k} \qquad (38)$$

The relaxation function of the material is a relaxation spectrum with moduli C_k and relaxation time τ_k. The dependency of these models on temperature is accounted for by using the WLF function [16].

8.3.3 Characterization techniques

Different characterization techniques were used to identify the material properties of PET-(0, 1, 5, 10 and 15% (w/w)) hemp fiber composites needed for the simulation process. The linear properties were obtained from small amplitude oscillatory shear tests [173] known for the determination of the storage and loss moduli as a function of the frequency as shown in Figure 8-1. Moreover, their relaxation spectra were determined by optimizing the dynamic data and minimizing the objective function F defined by Equation (39), where N is the number of data points $\left(G'_{i,\text{exp.}}, G''_{i,\text{exp.}}\right)$ available from the dynamic experiments and $\left(G'_{i,\,fit}, G''_{i,\,fit}\right)$ are the best fit values based on Equation (40).

$$F = \sum_{i=1}^{N} \left[\frac{G'_{i,\text{exp}} - G'_{i,\,fit}}{G'_{i,\text{exp}}} \right]^2 + \left[\frac{G''_{i,\text{exp}} - G''_{i,\,fit}}{G''_{i,\text{exp}}} \right]^2 \tag{39}$$

$$G'(\omega) = g_0 + \sum_k \frac{C_k \omega^2 \tau_k^2}{2(1 + \tau_k^2 \omega^2)}, \quad G''(\omega) = \sum_k \frac{C_k \omega \tau_k}{2(1 + \tau_k^2 \omega^2)}, \tag{40}$$

Taking advantage of the fact that low-frequency behavior is dominated by the long relaxation times, just as high-frequency response is controlled by the short relaxation times, the linear visco-elastic behavior of the composite material is described over a wide range of time values with just a few constants.

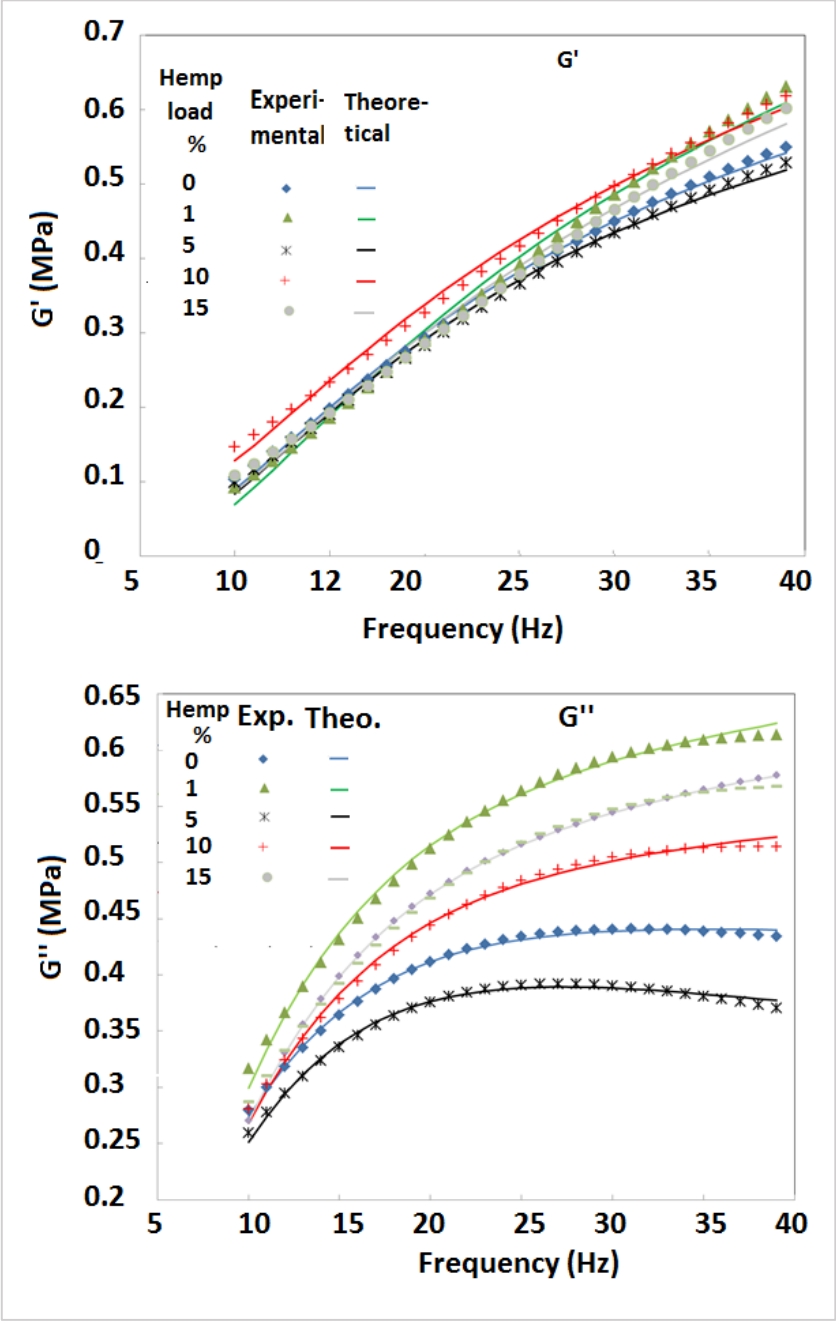

Figure 8-1: Storage and loss moduli of PET-hemp fiber composites compounded with the mixing chamber heated at 250°C.

Figure 8-1 shows that the Christensen model adequately describes the behavior of the investigated PET-hemp fiber composites while fitting the experimental data and the theoretical model. The associated relaxation strengths g_k are given in Table 8-1. This behavior slightly differs from the observations made by Erchiqui *et al*. [102] about the formulations of HDPE reinforced with 0, 20, 30, 40, 50 and 60% (w/w) wood flours. In fact, an application of the same fitting method in the latter case resulted in the description of the composite behavior by the Lodge model. Furthermore, the variations of different parameters related to the numerical thermoforming of PET-hemp fiber composites are analyzed in the following sections.

Table 8-1: Relaxation Spectrum of PET-hemp fiber composites compounded with a mixing chamber heated at 250°C.

Hemp fiber load [% (w/w)]	**0**	**1**	**5**	**10**	**15**
C_0 [MPa]	**0,5**	**0,5**	**0,5**	**0,5**	**0,5**
τ_k [sec]	**g_k [MPa]**	**g_k [MPa]**	**g_k [MPa]**	**g_k [MPa]**	**g [MPa]**
0,010	1,091	2,095	0,700	1,636	1,977
0,050	1,312	1,448	1,340	1,307	1,314
0,500	0,250	-0,740	0,083	-0,490	0,741
1,000	-1,348	0,465	1,199	-0,555	-0,400

8.3.4 Finite element discretization

The thermoforming of PET-hemp fiber composite membranes was achieved by applying the space and time discretization to the explicit dynamic finite element method [96]. The principle of virtual work was thus applied on the un-deformed configuration for both the inertial effects and internal work. The time discretization was required to handle the inertial forces while avoiding their associated instability. It was achieved by the use of a conditionally stable centered finite difference technique [174]. The thermoforming problem was then reduced to the discrete system of Equation (41) [169]. $\mathbf{F_{ext}}$, $\mathbf{F_{grav}}$ and $\mathbf{F_{int}}$ are respectively the external, body and internal global nodal force vectors experienced by the composite membranes, and **M** is the mass matrix.

A diagonalization of Equation (41) yields Equation (42) in which the **M** matrix is transformed into a diagonal form and each degree of freedom independently controlled. $\mathbf{M_{ii}^d}$ are the diagonal components of the matrix $\mathbf{M^d}$.

$$M \cdot \ddot{u}(t) = F_{ext} + F_{grav} - F_{\text{int}} \tag{41}$$

$$u_i(t+\Delta t) = \frac{\Delta t^2}{M_{ii}^{d}}\left(F_{i,ext}(t) + F_{i,grav}(t) - F_{i,\text{int}}(t)\right) + 2u_i(t) - u_i(t-\Delta t) \tag{42}$$

The Courant-Friedrichs-Lewy criterion of Equation (43) was applied to the thermoforming of PET-hemp fiber composites as the common convergence criterion applied to explicit dynamic finite element method for nonlinear problems. The parameters *C* and *l* denote respectively the wave speed in the medium and the element size; thus the

ratio *l/c* is the time needed for a wave propagation across an element of size l and ε is a proportionality constant related to the applied integration scheme.

$$\Delta t \le \Delta t_{crt} = \varepsilon . \frac{l}{c} \tag{43}$$

The initial conditions given in Equation (44) stipulate that the displacement and velocity vectors are assumed to be zero at the beginning of the thermoforming process.

$$\begin{aligned} u_i(t_0) &= 0 \\ \dot{u}_i(t_0) &= 0 \end{aligned} \tag{44}$$

8.3.5 Plane-stress assumption

An accurate evaluation of the internal forces is necessary for the numerical thermoforming of PET-hemp fiber composite membranes. However, such process requires a computation of the stress deformation relationship for each element under a plane-stress and an incompressibility assumption. Consequently, the components of the Cauchy stress tensor satisfy the conditions of Equation (45).

$$\sigma_{13} = \sigma_{23} = \sigma_{31} = \sigma_{32} = \sigma_{33} = 0 \tag{45}$$

8.3.6 Gas equation of state and pressure loading

The forming forces were expressed in terms of the air flow on the composite membranes during the simulation process. Additional assumptions needed for the calculation of the dynamic pressure process are listed below.

- The gas temperature (T_{gas}) is constant;

- The pressure (P_0) between the composite membrane and the mold is constant;
- The initial volume (V_0) enclosing the composite membrane at the initial time (t_0) and containing (n_0) moles of gas is evaluated by formulating the external virtual work and pressure as a function of both a closed volume and the Redlich-Kwong's equation of state [169,170] following the relationships expressed in Equations (46) and (47); n(t), P(t) and V(t) are respectively the moles of air, the internal relative pressure and the volume occupied by the composite membranes at time t. The parameters a and b are determined from the critical pressure (P_c) and critical temperature (T_c) of the gas used for the blowing process as shown in Equation (48).

$$\boldsymbol{\delta W^{ext.}} = \left[\frac{\left(n(t)+n_0\right)RT_{gas}}{\left(V(t)+V_0\right)-\left(n(t)+n_0\right)b} - \frac{\left(n(t)+n_0\right)^2 a}{\left(V(t)+V_0\right)\left(\left(V(t)+V_0\right)+\left(n(t)+n_0\right)b\right)\sqrt{T_{gas}}} \right] \text{ and} \quad (46)$$
$$- \left[\frac{n_0 RT_{gas}}{V_0 - n_0 b} - \frac{n_0^2 a}{V_0\left(V_0+n_0 b\right)\sqrt{T_{gas}}} \right] \boldsymbol{\delta V}$$

$$\Delta P(t) = P(t) - P_0 = \left[\frac{\left(n(t)+n_0\right)RT_{gas}}{\left(V(t)+V_0\right)-\left(n(t)+n_0\right)b} - \frac{\left(n(t)+n_0\right)^2 a}{\left(V(t)+V_0\right)\left(\left(V(t)+V_0\right)+\left(n(t)+n_0\right)b\right)\sqrt{T_{gas}}} \right] \quad (47)$$
$$- \left[\frac{n_0 RT_{gas}}{V_0 - n_0 b} - \frac{n_0^2 a}{V_0\left(V_0+n_0 b\right)\sqrt{T_{gas}}} \right]$$

$$a = 0{,}42748 \cdot \frac{\overline{R}^2 T_C^{2,5}}{P_C} \qquad b = 0{,}08664 \cdot \frac{\overline{R} T_C}{P_C} \quad (48)$$

Equation (47) is also the time variations of the pressure inside the composite membrane following the variations of their internal volume. Such expression of the load in term of gas flow formulated based on the thermodynamic equation of state is an advantageous way to deal with the load-deformation while avoiding the instabilities associated with the

classical pressure loading. In the contrary, the use of a constant pressure as a loading force instead of the gas flow velocity in the applied quasi-static and dynamic finite element formulations yields a divergence of pressure values computation beyond a given critical point [174,175].

8.3.7 Energy and power

The energy required for the thermoforming process is equivalent to the mechanical work done by the external forces on the composite membranes during the forming stage. Its compact form is shown in Equation (49) where $\{\mathbf{F_{ext}}\}$ is the global nodal external force vector and $\{u^n\}^T$ is the associated global nodal displacement vector. The power associated with the global nodal external force vector is the energy per unit time transferred to the composite membrane during the forming stage as shown in Equation (50).

$$W^{ext} = \{u^n\}^T \cdot \{F_{ext}\} \tag{49}$$

$$P^{ext} = \frac{W^{ext}}{t_{for\,ming}} \tag{50}$$

The energy and power associated with the forming phase of the material significantly impact its part manufacturing cost and its industrial feasibility. This is the reason why they were evaluated for the potential thermoforming of the investigated PET-hemp fiber composite formulations.

8.4 *Results and Discussion*

Many thermoforming parameters were analyzed after the ThermoForm® code was used to implement the dynamic finite element method outlined in the previous sections [178]. They include the variations of the stress and deformations of the composite membranes during the process as well as the variations of the associated energy.

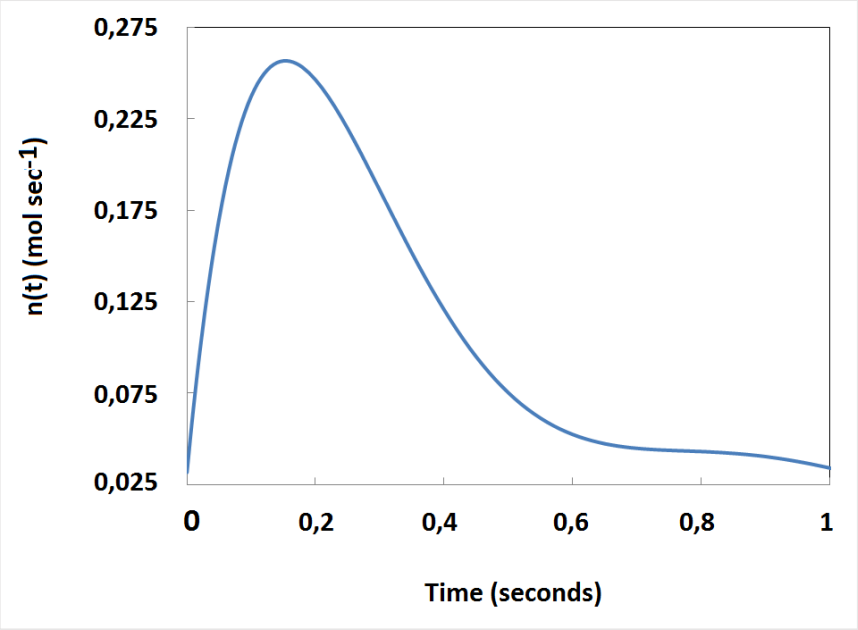

Figure 8-2: Variation of the air flow as a function of time.

An expression of the processing load was done in terms of non-linear air flow rate. Its variations shown in Figure 8-2 indicate a maximum value of 0,250 moles per seconds at 0,2 seconds. The mold geometry and the composite membranes were discretized using triangular membrane elements as shown in Figure 8-3. The discretized mold consisted of 629 elements and 338 nodes; while the discretized composite membranes consisted of 2784 elements, 1422 nodes and fixed sides. The method was repeated for PET-hemp fiber composite formulations containing 0, 1, 5, 10 and 15% (w/w) reinforcements.

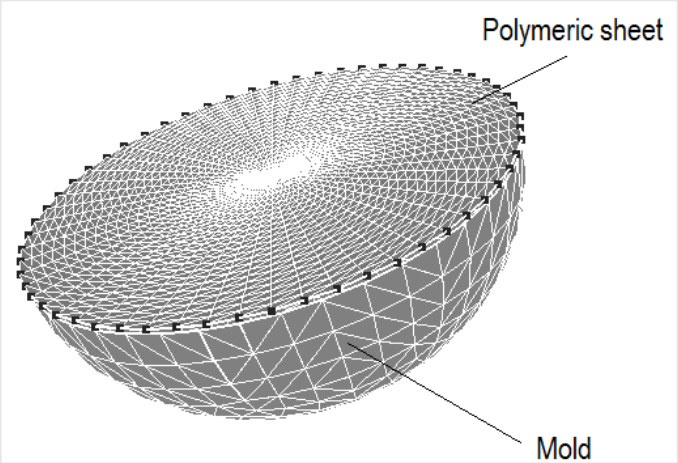

Figure 8-3: Aspect of the discretized mold as well as a discretized circular composite membrane using triangular membrane elements.

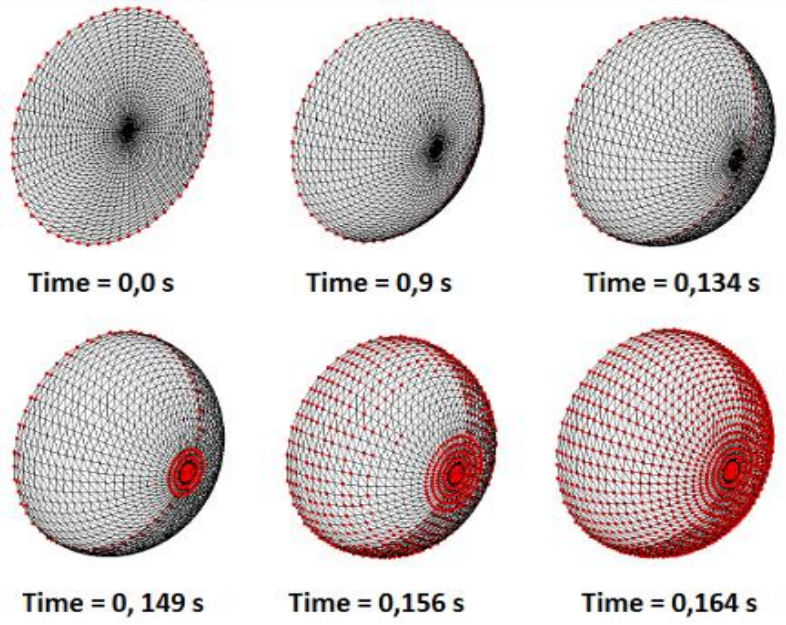

Figure 8-4: Sheet deformation-contact during forming on the mold.

The deformations of PET-hemp fiber composite membranes at selected stages of their forming process and their contact with the mold are shown in Figure 8-4. The red nodes indicate the contact points between the membrane and the mold. A progression of the contact points from the clamping section to the base of the mold is observed at respectively 0,0; 0,90; 0,134; 0,149; 0,156 and 0,164 seconds. Moreover, 0,164 seconds represents the end of the process, while most of the deformation happened during the last two tracking times.

The behavior of the investigated materials throughout the forming process is further described by the variations of the principal extension and the von Mises stress in the parts molded with representative composite formulations reinforced with 1 and 5% (w/w) hemp fibers as illustrated in Figure 8-5 and Figure 8-6.

The principal extension is found to decrease from the clamping point to the base of the mold. A similar behavior was previously observed by Szvegda [85] who associated it to additional stress from the clamping forces. Moreover, it varies from 2,59E-4 to 7,97E-4 $mmmm^{-1}$ and from 2,81E-4 to 7,21E-4 $mmmm^{-1}$ in the presence of 1 and 5% (w/w) hemp fibers respectively. Contrary to the principal extension, the von Mises stress increases from the clamping point to the base of the mold, varying from 8,94E-2 to 4,32E-1 and from 1,13E-4 to 3E-1 in the presence of 1 and 5% (w/w) hemp fibers respectively.

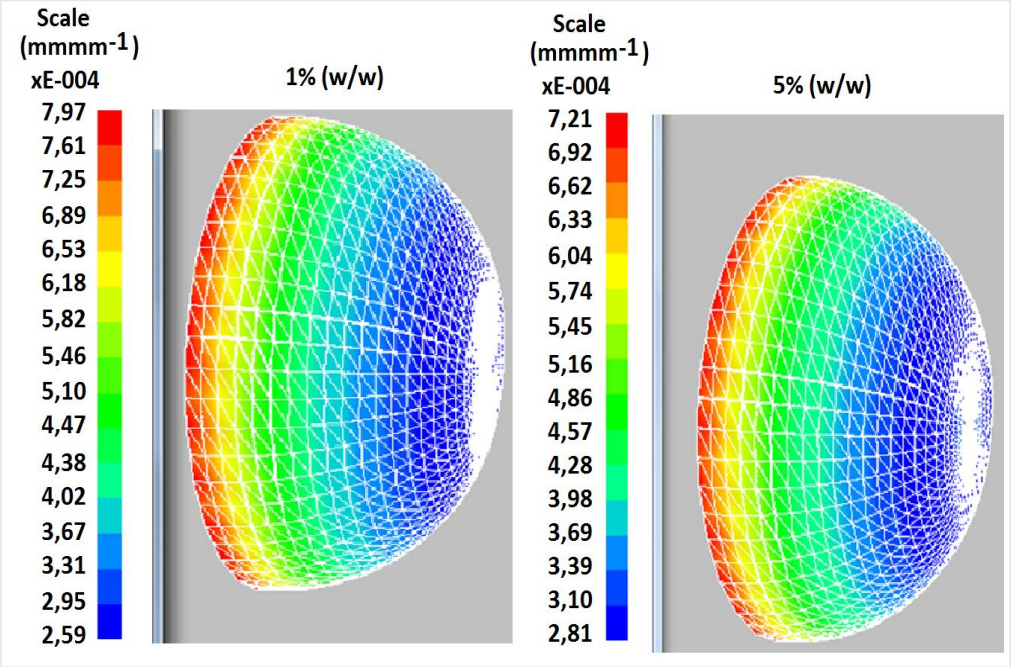

Figure 8-5: Distribution of the final extension (λ_3) in the parts thermoformed with PET-hemp fiber composite formulations with 1 and 5% (w/w) reinforcements.

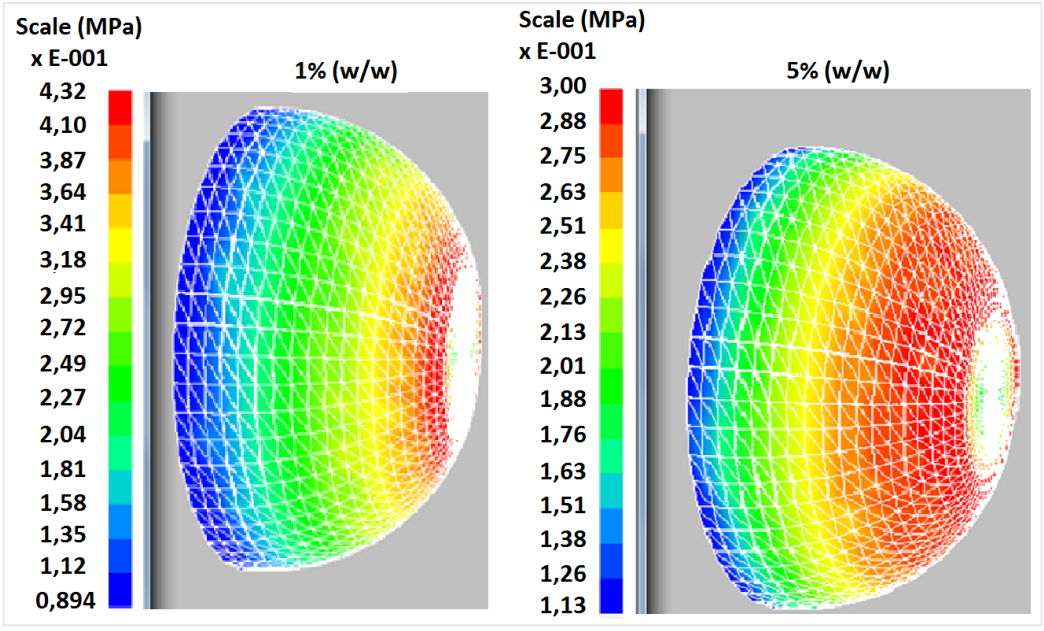

Figure 8-6: Distribution of the final von Mises stress in the parts thermoformed with PET-hemp fiber composite formulations with 1 and 5% (w/w) reinforcements.

Figure 8-7 and Figure 8-8 give the time variations of respectively the internal relative pressure and the volume of thermoformed parts with the five investigated PET-hemp fiber composite formulations. Moreover, the variations of the internal relative pressure with the forming volume is given in Figure 8-9 following an elimination of the time variable from the expressions of both the pressure and the volume. The time variations of the volume were nearly identical for all the composite formulations. In the contrary, the variations of the internal relative pressure consisted of an increase until a short plateau is reached, followed by a sudden increase at the end of the process. The material formulations can be further partitioned into two groups with identical internal relative pressure based on their reinforcement concentration. The first group is reinforced with 0 and 5% (w/w) hemp fibers, while the second is reinforced with 1, 10 and 15% (w/w) hemp fibers. An identical partition is shown by the variations of the internal relative pressure with the volume.

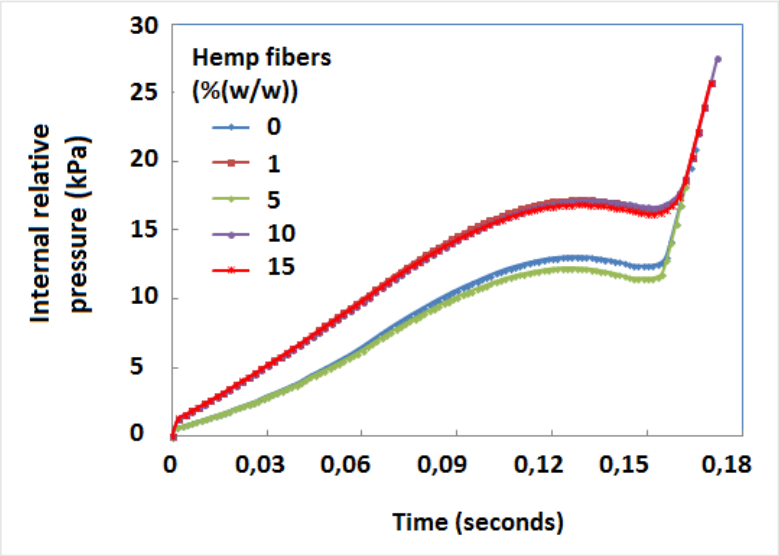

Figure 8-7: Time variations of the internal relative pressure for different PET-hemp fiber composite formulations.

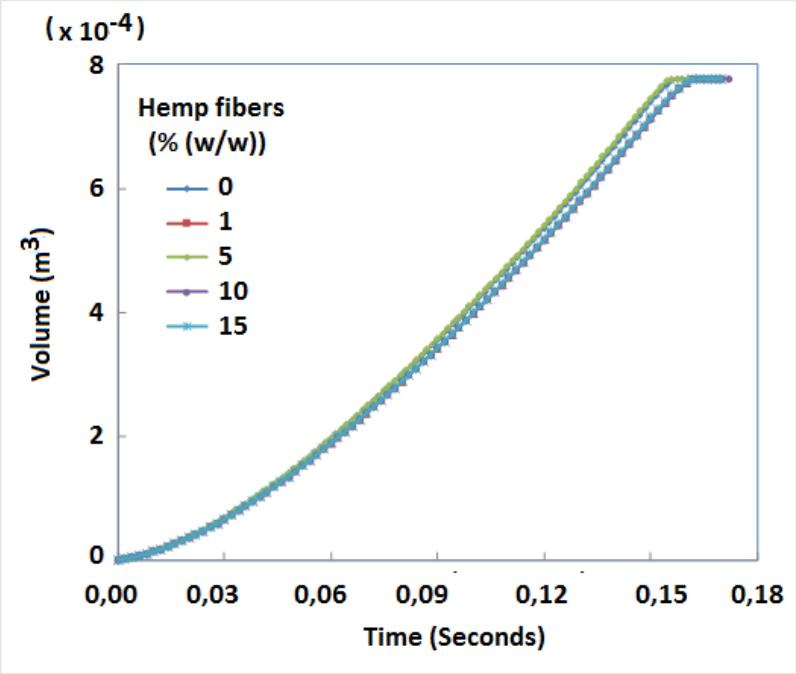

Figure 8-8: Time variations of the volume for different PET-hemp fiber composite formulations.

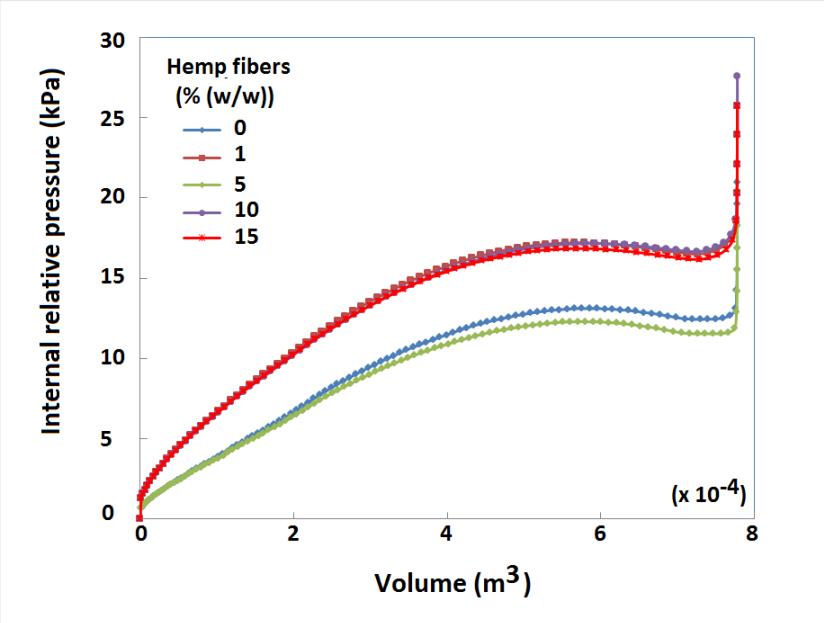

Figure 8-9: Internal relative pressure variations with the volume for different PET-hemp fiber composite formulations.

The observed behavior can be linked to different parameters such as the effect of 5% (w/w) PCL, an impact of the important volume to weight ratio of the fibers as well as their general structure. In the contrary of man-made fibers, natural fiber properties vary with different conditions and consequently hardly follow a specific trend as earlier reported in the literature [62]. The relative good performance of PET-1% (w/w) hemp fiber composites with respect to other formulations is probably caused by a combination of the high number of carbonyl groups deriving from both PET and PCL molecules, and the limited possibilities of weakened structure from fiber-fiber contacts. In fact, such high number of carbonyl groups contributes to an increase of the interaction sites with 1% (w/w) hemp fibers which is too low a concentration to favor fiber-fiber contact. In the contrary, higher reinforcement concentrations like 10 and 15% (w/w) increase the possibilities of fiber-fiber contact which yield weak points of the composite structure; moreover, they increase the possibilities for some thermo-degradation of the fibers due to the challenges associated with processing their large volumes with comparatively lower matrix volumes especially with laboratory scale equipment. Consequently, the formulations reinforced with 10 and 15% (w/w) hemp fibers showed identical behavior. This is an indication that the best formulations based on these parameters are associated with lower fiber reinforcements.

Figure 8-10 shows the variations of the maximum pressure induced in the thermoformed part at the end of the cycle with the fiber concentration. All the values are higher than 18kPa and they are reached after a period that varies with the fiber concentration. It appears that a high fiber concentration yields challenging processes due to the hardening of the composite membranes. The formulations reinforced with 1, 10 and 15 % (w/w) hemp fibers showed the maximum forming pressures higher than 25kPa indicating

more difficult and expensive forming processes than the formulations reinforced with 0 and 5% hemp fibers. This further implies that lower reinforcement concentrations are more interesting for the thermoforming process while PET-5% (w/w) hemp fiber is optimal.

Some important parameters for the simulation of the blow molding, the thermoforming processes as well as the process of parts design are the thickness prediction and the stress estimates on the half planes of symmetry. Those parameters are discussed in the following sections. In fact, the residual stress which occurs during the forming process and the shape stability predictions are strongly related to the estimated stress. In the same manner, the localized thinning effects of the deformed membranes are generally accompanied by an increase in the true stress of the material.

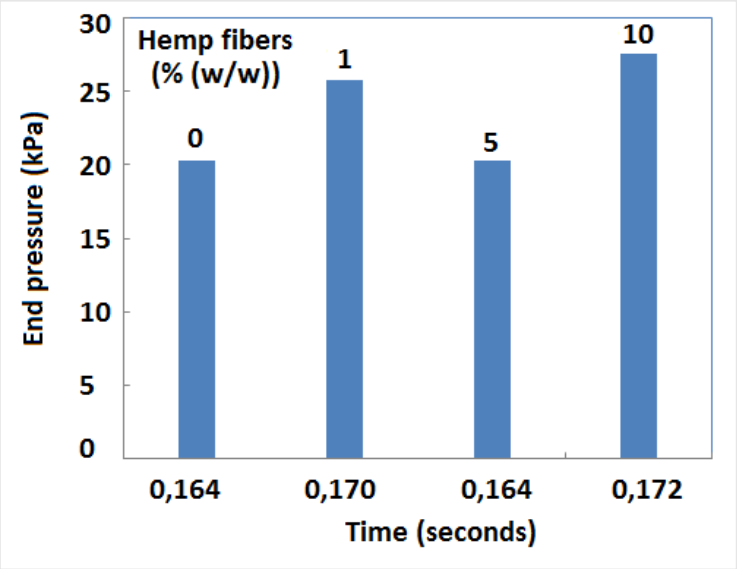

Figure 8-10: Maximal internal relative pressure variations with PET-hemp fiber formulations at the end of the forming process.

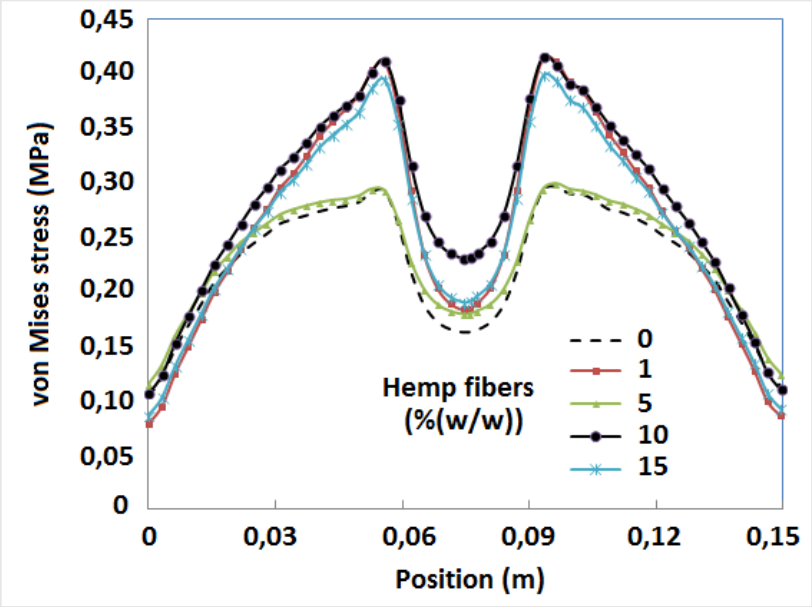

Figure 8-11: Von Mises stress distributions on the half-plane of symmetry XZ of different PET-hemp fiber composite formulations.

The distributions of the final von Mises stress ($\sigma_{eq.}$) on the XZ half plane of symmetry of PET-hemp fiber composite membranes also known as the median line of the structure is given in Figure 8-11. Such distribution deriving from the Christensen's constitutive model is similar for all the composite formulations. Moreover, it shows a maximum of about 0,411 MPa in the presence of 10% (w/w) hemp fibers and a minimum of about 0,292 MPa for virgin PET. A trend similar to the observations made in the previous sections about the time variations of the internal relative pressure is also observed except at the center of the hemisphere.

Moreover, the critical values of the von Mises stress in the final shape of the thermoformed parts with different composite formulations are presented in Table 8-2. A similar variation was observed for all the formulations with the symmetry at the center of the mold.

All these observations imply that the composite formulations can also be grouped in two groups reinforced with 0 and 5% (w/w) hemp fibers on one hand, and 1, 10 and 15% (w/w) hemp fibers on the other hand. They confirm the fact that higher reinforcement concentrations are less interesting for the thermoforming process as they require powerful air flow pressure during the forming process.

Table 8-2: The critical values of the von Mises stress for PET-hemp fiber composite parts.

Hemp fiber load [% (w/w)]	**0**	**1**	**5**	**10**	**15**
σ_{eq} (MPa)	0,292	0,410	0,294	0,412	0,394

The thickness distributions in the final shape of the thermoformed part for each PET-hemp fiber composite formulation is given in Figure 8-12. It shows similar variations for all the formulations, with a maximum of about 0,7 mmmm^{-1} close to the clamping points, and a minimum of about 0,43 mmmm^{-1} at 1,5 cm of the membrane center. The observed similarities of the thickness distributions agree with previous reports by DeLorenzi and Nied [177] relating the thickness behavior to the incompressibility of isotropic materials. Indeed, these authors have reported that thickness distribution is less dependent on the material behavior than it is on the mold geometry. Finally, the von Mises stress distribution and the localized thinning effect indicate that large deformations induced by inflation are most likely to cause material failure at about 2,0 cm of the membrane center as shown in Figure 8-12.

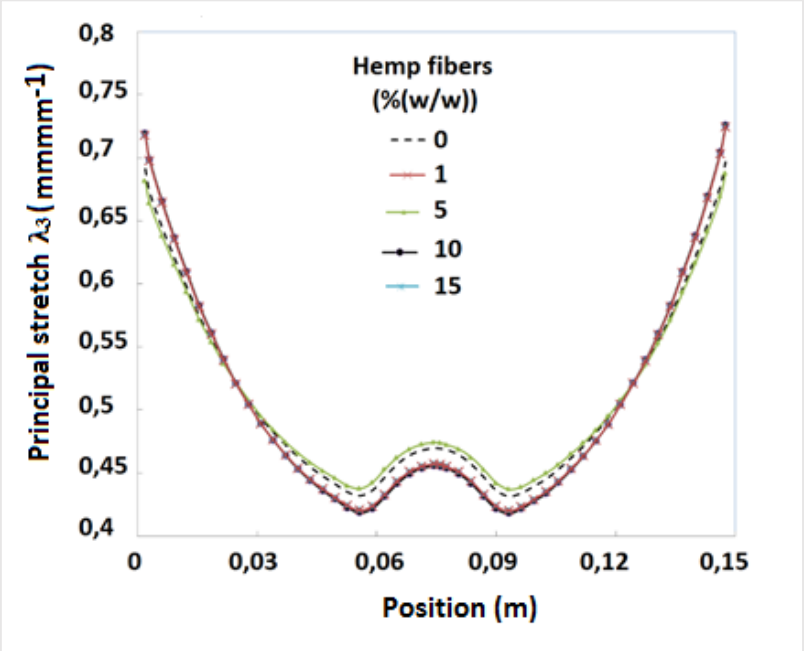

Figure 8-12: Principal stretch on the half-plane of symmetry XZ of PET-hemp fiber composites.

Furthermore, Figure 8-13 gives an illustration of the main extensions (λ_1, λ_2 and λ_3), on the XZ half plane of symmetry in the membrane for the composite formulations reinforced with respectively 0 and 10 % hemp fibers. The variations observed in the two cases are similar and the values are close. In the same manner, the principal extension of all the composite formulations show an identical critical value of 0,4 mmmm^{-1}.

Table 8-3: The critical values of the principal extension for PET-hemp fiber composites.

Hemp fiber load [% (w/w)]	**0**	**1**	**5**	**10**	**15**
λ_3 [mmmm^{-1}]	0,432	0,420	0,437	0,418	0,420

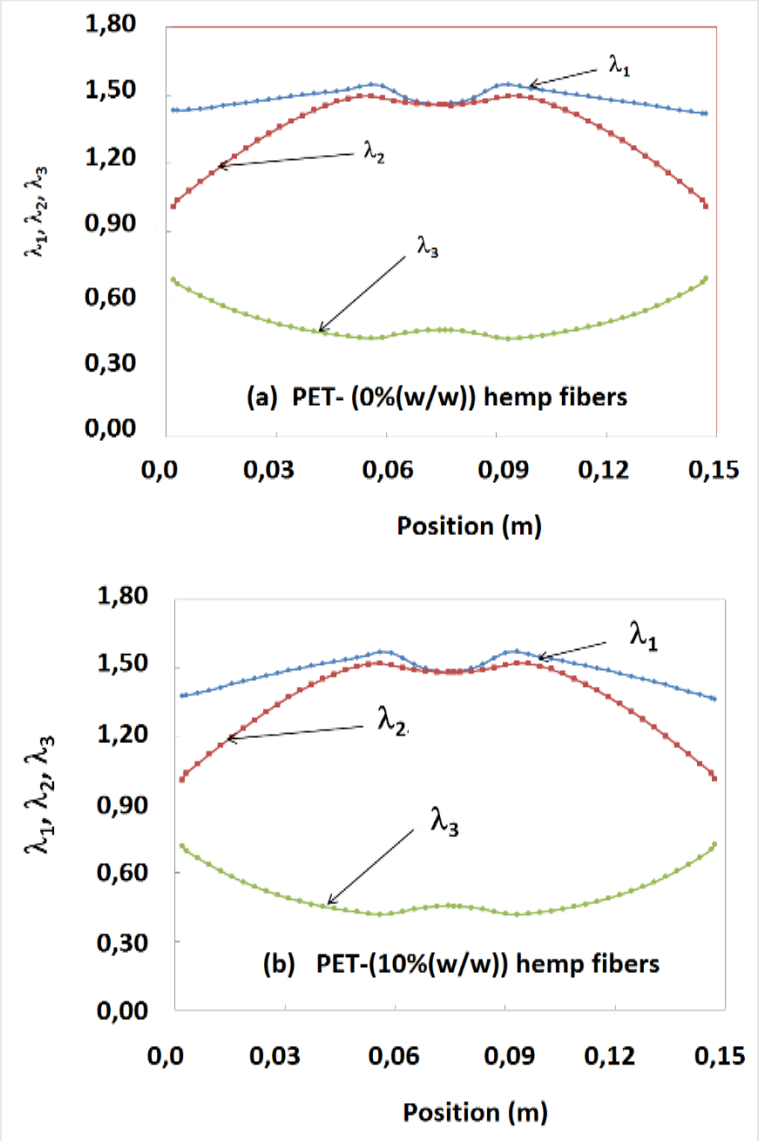

Figure 8-13: Stretch ratio on the half-plane of symmetry XZ of two composite membranes: PET-0% (w/w) hemp fibers (a) and PET-10% (w/w) hemp fibers (b).

Figure 8-14 gives the time variations of the work required for molding the needed parts with the investigated PET-hemp fiber composite formulations. It varies with the fiber concentration, however the two groups of formulation earlier mentioned can be observed based on this parameter. Moreover, these observations fully agree with those

previously made with other parameters and the previous explanations are applicable. In comparison with the energy required for the thermoforming of virgin PET, 1,380 times more energy is required for the composite reinforced with 10% (w/w) hemp fibers. In the same manner, the ratios of energy required for the molding of other formulations are 1,394 for 1% (w/w) fibers, 0,944 for 5%(w/w) fibers and 1,367 for 15% (w/w) fibers.

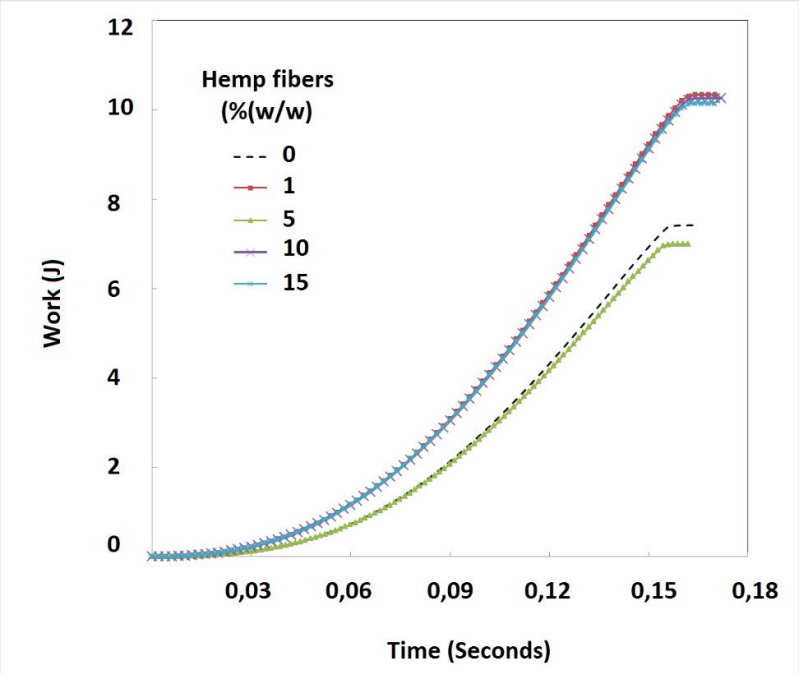

Figure 8-14: Time variations of the molding work for different PET-hemp fiber composites.

Figure 8-15 shows the power required for the thermoforming of composite parts with the investigated PET-hemp fiber formulations. Its variations are comparable to those of other parameters such as the internal relative pressure and the work required for the thermoforming process. Its values are respectively 44,95; 60,82; 43,21; 59,65 and 59,65 Watt for the composites reinforced with 0, 1, 5, 10 and 15% (w/w) hemp fibers. Similarly, to previous observations, an analysis of investigated composite formulations based on the

required power shows that they can be partitioned into the previously mentioned two groups which are (0, 5% (w/w)) on hand and (1, 10, 15% (w/w)) on the other.

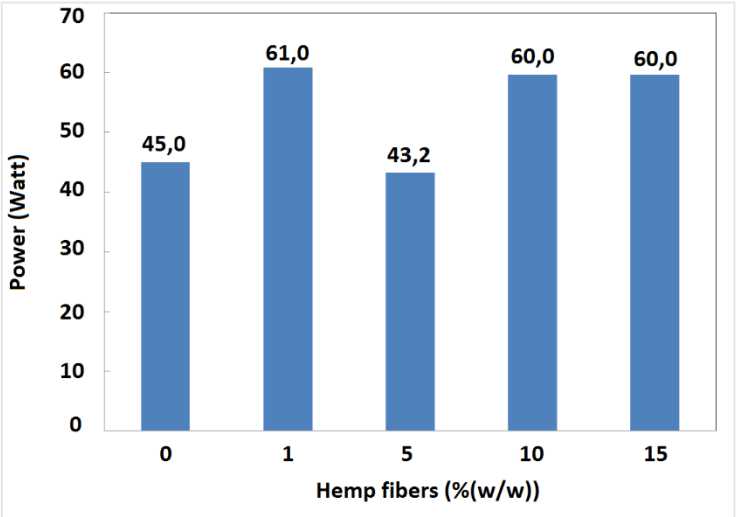

Figure 8-15: Variations of the forming power at the end of the process with the fiber concentration for different PET-hemp fiber formulations.

These observations have a significant impact on the choice of PET-hemp fiber composite formulations which are suitable for the thermoforming process based on their performance, the quality of the final product and the cost of the process.

In a cost-benefit perspective, the thermoforming cycle which is a pertinent industrial parameter also shows non-monotonic variations with the fiber concentration. In fact, the parts forming cycle with the composite containing 1 and 5% (w/w) fibers are respectively 0,170 and 0,162 seconds. Consequently, a consideration of both the forming energy and the process cycle indicate that the profitability of the thermoforming process depends on the fiber concentration.

Such simple investigation of the suitability of newly formulated PET-hemp fiber composites for the thermoforming process shows the advantage of applying the dynamic

finite element method based on both a total Lagrangian approach and the air flow loading derived from thermodynamic theories. An analysis of different molding parameters suggests that more work must be done in order to optimize both the composite formulation and the thermoforming process. This includes for example taking into consideration the energy dissipated by frictional contact between the mold and the composite membranes, and using data from industrial scale equipment.

Our future work will focus on refining the methodology for processing such high temperature melting thermoplastics reinforced with vegetal fibers while using numerical tools to facilitate their applications through the thermoforming process. Furthermore, we intend to validate the suitability of the formulations reinforced with low fiber concentrations (1 and 5% (w/w)) for the thermoforming process in an industrial environment.

8.5 *Conclusion*

The mechanical and structural properties of novel melt processed PET-hemp fiber composite formulations were investigated, followed by a numerical investigation of their suitability for the thermoforming process. The variations of the process parameters such as the air flow and the associated energy with the fiber concentration, as well as the variations of the material parameters such as the thickness, the stress, internal relative pressure and stretch with the fiber concentration were analyzed for the formulations reinforced with 0, 1, 5, 10 and 15% (w/w) hemp fibers.

Our study showed that the constitutive behavior of such composite formulations has little influence on the final thickness distribution in the thermoformed part. Moreover, important parameters such as the process cycle and the energy required for the

thermoforming process as well as the stress and stretch distribution do not show monotonic variations with the fiber concentration. However, the investigated composite formulations can be partitioned into two groups with respect to both their behavior and the fiber concentration. The composites of the first group are reinforced with 0 and 5% (w/w) fibers, while those of the second are reinforced with 1, 10 and 15% (w/w) hemp fibers.

Consequently, the formulations with low fiber concentrations such as 0, 1 and 5% (w/w) are the most suitable for the thermoforming process. A better valorization of the formulations with higher reinforcements would either require a combination of woven fibers and resin transfer molding, or the use of elastomers to tackle the challenges related to their brittle nature.

CHAPTER: 9

GENERAL CONCLUSIONS AND PERSPECTIVES

Vegetal fiber-reinforced composites are widely used in various applications. However, there still exists an under exploited potential with high temperature melting matrices (melting point higher than 200°C). PET-hemp fiber composites fall under such under exploited group. In this regard, the elaboration and characterization of PET-hemp fiber composites for thermoforming applications is innovative in many aspects, such as:

- Solving the challenges of melt processing high temperature melting thermoplastics with vegetal fibers;
- The thermoforming of vegetal fiber-reinforced composites which are brittle materials while the process requires large deformations.

This work is therefore a critical step in the development of the plastics industry. It is also expected to greatly impact the country's recycling and agricultural sectors. Such potential impacts will range from the development of the industrial hemp production including post-harvest processing, an increase of the volume of recycled plastics and the development of a new range of vegetal fiber-reinforced composites applications. The following conclusions have been drawn from various steps of this research.

The mechanical properties of PET-hemp fiber composites showed similar variations with those of other natural fiber reinforced composite materials reported in the literature.

- In the presence of the applicable additives, the elastic modulus of PET-5% (w/w) PCL-5% (w/w)-Additives (PMDA, GMA and clay) increased by 10 to 20% with respect to the unreinforced formulation and 2 to 10% with respect to the reinforced formulation without additives. However, all the formulations were significantly

brittle and their strain at break decreased from over 40 to about 4%. Their maximum force was also lowered by up to 4% with respect to virgin PET.

- In the absence of additives, the elastic modulus and the maximum force of PET-5% (w/w) PCL-5% (w/w) - (1, 5, 10, 15 and 20% (w/w)) hemp fibers increased logarithmically with the fiber concentration, while the strain at break dropped below 5%. An improved interface quality without additives is an indication of the possible hydrogen bonding between the carbonyl groups of PET and the hydroxyl groups of hemp fibers. The remaining investigation was then performed without additives.

All the composite formulations proved to be thermally stable until 315°C as an indication of their ability to undergo multistage processing. Two thermo-degradation ranges were observed from 290 to 385°C and from 385 to 490°C respectively. They were respectively described by the Sestak-Berggren and the truncated Sestak-Berggren models. Similar observations were made for the formulations compounded with the mixing chamber heated at 240, 250 and 250°C. Consequently, the numerical thermoforming process was restricted to the group compounded at 250°C.

The rheological properties fitted with the ThermoForm® code indicated the suitability of the Christensen model to describe the visco-elastic behavior of the investigated composite formulations. The numerical variations of various forming parameters indicated a partition of the formulations into two groups reinforced by 0, 1 and 5% (w/w) for the first, and 10 and 15% (w/w) for the second. The first group was better suited for both the free forming and the thermoforming process. However, a more powerful air flow pressure is needed for forming of PET -1% (w/w) hemp, leaving PET-

5% (w/w) hemp as the best thermoformable alternative with respect to the process cost and in-service performance. The second group showed a relatively poor performance which can be attributed to the fiber's partial thermo-degradation resulting from processing larger fiber volume with respect to the limited available matrix.

Although PET-hemp fiber composites have been successfully formulated and their behavior towards the thermoforming process numerically investigated, a fine tuning of the processing conditions will be the object of future work alongside the valorization of higher fiber loads through targeted applications requiring woven reinforcements.

In the same manner, a profitable use of PET-hemp fiber composites requires further investigations to relate the fibers post-harvest processing to the mechanical properties of PET-hemp fiber composites, study the effect of the compounding temperature to the thermal degradation of PET-hemp fiber blends and to monitor the composite aging process, especially relative to in-service composite parts.

REFERENCES

[1] Fotso Talla, A. S., Mfoumou, E., Jeson, S., Pagé, D., and Erchiqui, F., 2013, "Properties of a novel melt processed PET-Hemp composite: Influence of additives and fibers concentration," Reinf. Plast. Compos., **32**(20), pp. 1526–1533.

[2] Fotso Talla, A. S., Godard, F., and Erchiqui, F., 2013, "Thermal properties and stability of PET-Hemp fibers composites," The 19th International Conference On Composite Materials (ICCM'19), Montreal, Canada.

[3] Fotso Talla, A. S., Erchiqui, F., Kaddami, H., and Kocaefe, D., 2015, "Investigation of the thermostability of poly(ethylene terephthalate)-hemp fiber composites: Extending natural fiber reinforcement to high-melting thermoplastics," J. Appl. Polym. Sci., **132**(37).

[4] 2013, "The global composite market: A bright future," JEC Compos. Mag., **78**, pp. 16–19.

[5] Mutel, F., 2012, "A vribrant North American composites industry," JEC Compos. Mag., p. 3.

[6] 2011, "Advanced glass-mat thermoplastic composite applications for the automobile industry," Quadr. Plast. AG [Online]. Available: www.quadrantcomposites.com.

[7] Clegg, A. A., and Collyer, D. W., 1986, Mechanical properties of reinforced thermoplastics, Elsevier.

[8] La Mantia, F. P., and Morreale, M., 2011, "Green composites: A brief review," Compos. Part A Appl. Sci. Manuf., **42**(6), pp. 579–588.

[9] Clemons, C., 2002, "wood-plastic composites in the United States. The interfacing of two industries," For. Prod., **52**(6).

[10] Laachachi, A., Cochez, M., Leroy, E., Ferriol, M., and Lopez-cuesta, J. M., 2007, "Fire retardant systems in poly (methyl methacrylate): Interactions between metal oxide nanoparticles and phosphinates," **92**, pp. 61–69.

[11] Weil, E. D., and Levchik, S. V., 2004, "Commercial flame retardancy of thermoplastic polyesters-a review," Fire Sci., **22**(4), pp. 339–350.

[12] White, R. H., and Dietenberger, M. A., 2001, "Wood Products : Thermal Degradation and Fire," Sci. Technol., **48**, pp. 9712–9716.

[13] Pasquini, D., Teixeira, E. D. M., Curvelo, A. A. D. S., Belgacem, M. N., and Dufresne, A., 2007, "Surface esterification of cellulose fibres: Processing and characterisation of low-density polyethylene/cellulose fibres composites," Compos. Sci. Technol.

[14] Gironès, J., Méndez, J. A., Boufi, S., Vilaseca, F., and Mutje, P., 2007, "Effect of Silane Coupling Agents on the Properties of Pine Fibers/Polypropylene Composites," Appl. Polym Sci., **103**, pp. 3706–3717.

[15] Samios, C. K., and Kalfoglou, N. K., 1999, "Compatibilization of poly (ethylene terephthalate)/polyamide-6 alloys: Mechanical, thermal and morphological characterization," Polymer (Guildf)., **40**, pp. 4811–4819.

[16] Guduri, B. R., and Luyt, A. S., 2006, "Effect of Ethylene Glycidyl Methacrylate Compatibilizer on the Structure and Mechanical Properties of Clay Nanocomposites Modified with Ethylene Vinyl Acetate Copolymer."

[17] Clemons, C. M., and Caulfield, D. F., 2005, "Natural Fibers," Functional Fillers for Plastics, U.) Xanthos, M. (Otto H. York Department of Chemical Engineering and Polymer Processing Institute; NJ Institute of Technology, Suite 3901, Newark, NJ 07102, ed., WIley-VCH Verlag GmbH & KGaA, Newark, NJ 07102, pp. 195–206.

[18] Maldas, D., Kokta, B. V, Raj, R. G., and Sean, S. T., 1988, "Use of Wood Fibres as Reinforcing Fillers for Polystyrene," **104**, pp. 235–244.

[19] Lu, J. Z., Wu, Q., and Negulescu, I. I., 2004, "Wood-fiber/high-density-polyethylene composites: Compounding process," J. Appl. Polym. Sci., **93**(6), pp. 2570–2578.

[20] Lutch, R. H., 2009, "Capacity optimization of a prestressed concrete railroad tie," Michigan Technological University.

[21] Mccrum, N. G., Buckley, C. P., and Bucknall, C. B., 2005, Principles of Polymer Engineering, Oxford Science.

[22] Maurice Reyne, 1998, Technologie des composites, Hermes Sciences, Paris.

[23] Trotignon, J. P., Piperaud, J., Verdu, M., and Dobraczynski, A., 1993, Précis des matières plastiques, Nathan scolaire (Jan. 15 1993).

[24] Sain, M., Park, S. H., Suhara, F., and Law, S., 2004, "Flame retardant and mechanical properties of natural fibre – PP composites containing magnesium hydroxide," **83**, pp. 363–367.

[25] Lewin, M., 2005, "Unsolved problems and unanswered questions in flame retardance of polymers," Polym. Degrad. Stab., **88**, pp. 13–19.

[26] Si, M., Zaitsev, V., Goldman, M., Frenkel, A., Peiffer, D. G., Weil, E., Sokolov, J. C., and Rafailovich, M. H., 2007, "Self-extinguishing polymer/organoclay nanocomposites," Polym. Degrad. Stab., **92**, pp. 86–93.

[27] Huang, L., Gerber, M., Lu, J., and Tonelli, A. E., 2001, "Formation of a Flame retardant-cyclodextrin inclusion compound and its application as a Flame retardant for poly (ethylene terephthalate)," Polym. Degrad. Stab., **71**, pp. 279–284.

[28] Han, G., Feng, L. X., and Hughes, "Polybrominated styrene polymers, a platform for growth in flame retardant polyamide and polyester resins," 2nd China Exhibit on Engineering Plastics.

[29] Michaud, F., 2003, "Rhéologie des panneaux composites bois/thermoplastiques sous chargement thermomécanique: Aptitude au thermoformage," Université Laval, Canada et Université de Bordeau I, France.

[30] Pracella, M., Chionna, D., Anguillesi, I., Kulinski, Z., and Piorkowska, E., 2006, "Functionalization, compatibilization and properties of polypropylene composites with hemp fibres.," Compos Sci Technol, **66**, pp. 2218–2230.

[31] Qin, H., Zhang, S., Hu, G., and Yang, M., 2005, "Flame retardant mechanism of polymer/clay nanocomposites based on polypropylene," Polymer (Guildf)., **46**, pp. 8386–8395.

[32] Sapuan, S. M., Leenie, A., Harimi, M., and Beng, Y. K., 2006, "Mechanical properties of woven banana fibre reinforced epoxy composites," Mater. Des., **27**, pp. 689–693.

[33] Cochran, M. J., Windham, T. E., and Moore, B., 2000, Feasibility of industrial Hemp production in Arkansas.

[34] Cierpucha, W., Kozłowski, R., Mańkowski, J., Waśko, J., and Mańkowski, T., 2004, "Applicability of Flax and Hemp as Raw Materials for Production of Cotton-like Fibres and Blended Yarns in Poland," Fibres Text. East. Eur., **12**(3), pp. 13–18.

[35] Chen, Y., Gratton, J. L., and Liu, J., 2004, "Power Requirements of Hemp Cutting and Conditioning," **87**(4), pp. 417–424.

[36] Wang, B., Sain, M., and Oksman, K., 2007, "Study of Structural Morphology of Hemp Fiber from the Micro to the Nanoscale," Appl Compos Mater, **14**, pp. 89–103.

[37] Bledzki, A. K., Fink, H.-P., and Specht, K., 2004, "Unidirectional hemp and flax EP- and PP-composites: Influence of defined fiber treatments," J. Appl. Polym. Sci., **93**(5), pp. 2150–2156.

[38] Saheb, D. N., and Jog, J. P., 1999, "Natural fiber polymer composites: A review," Adv. Polym. Technol., **18**(4), pp. 351–363.

[39] Singh, B., and Gupta, M., 2005, "Performance of pultruded jute fibre reinforced phenolic composites as building materials for door frame," Polym. Environ., **13**(2), pp. 127–137.

[40] Zohdy, M. ., Sahar, S. ., Hassan, M. ., Khalil, E. ., El-Hossamy, M., and El-Naggar, a. ., 1999, "Thermal behaviour stability of polyester and cotton/polyester graft copolymers obtained by direct radiation grafting of individual and mixed vinyl monomers," Polym. Degrad. Stab., **63**(2), pp. 187–193.

[41] Girija, B. G., Sailaja, R. R. N., and Madras, G., 2005, "Thermal degradation and mechanical properties of PET blends," Polym. Degrad. Stab., **90**(1), pp. 147–153.

[42] Espert, A., 2005, "Strategies for improving mechanical properties of PP/Cellulose composites," KTH (Royal Institute of Technology), 100-44 Stockholm.

[43] Thygesen, A., 2006, "Properties of hemp fibre polymer composites -An optimisation of fibre properties using novel defibration methods and fibre characterisation," Roskilde university, Denmark.

[44] Thamae, T. M., 2008, "Developing and Characterizing New Materials Based on

Natural Fibres and Waste Plastic," Queens University, Kingston, ON., Canada.

[45] Hägglund, E., 1951, Chemistry of Wood, Academic Press Inc., London, UK.

[46] Jolan, A. H., and Prud'homme, R. E., 1978, "Studies of polymer-cellulose blends prepared from solution," Appl. Polym Sci., **22**, pp. 2533–2542.

[47] Bledzki, A. K., Reihmane, S., and Gassan, J., 1996, "Properties and modification methods for vegetable fibers for natural fiber composites," J. Appl. Polym. Sci., **59**(8), pp. 1329–1336.

[48] Idicula, M., Boudenne, A., Umadevi, L., Ibos, L., Candau, Y., and Thomas, S., 2006, "Thermophysical properties of natural fibre reinforced polyester composites," Compos. Sci. Technol., **66**(15), pp. 2719–2725.

[49] G. C. Ellison, McNaught, R., and Eddleston, E. P., 2000, The use of natural fibres in nonwoven structures for applications as automotive component substrates, London, UK.

[50] Hu, R., and Lim, J.-K. K., 2007, "Fabrication and mechanical properties of completely biodegradable hemp fiber reinforced polylactic acid composites," Compos. Mater., **41**(13), pp. 1655–1669.

[51] Pickering, K. L., Li, Y., Farrell, R. L., and Lay, M., 2007, "Interfacial Modification of Hemp Fiber Reinforced Composites Using Fungal and Alkali Treatment," Biobased Mater. Bioenergy, **1**(1), pp. 109–117.

[52] Holmes, C. A., 2000, Fibre Crops (ENICA European Summary Report 2000-2005, QLK5-CT-2000-00111), York, UK.

[53] Zhang, Y., Guo, W., Zhang, H., and Wu, C., 2009, "Influence of chain extension on the compatibilization and properties of recycled poly(ethylene terephthalate)/linear low density polyethylene blends," Polym. Degrad. Stab., **94**(7), pp. 1135–1141.

[54] Wyk, L. V., 2007, "The application of natural fibre composites in construction: A research case study," 6th International conference on composite science and technology, Durban, South Africa, p. 7.

[55] Nosker, T., Renfree, R., Lynch, J., Lutz, M., Gillespie, B., Ness, K. E. Van, and Lampo, R., 1994, A Performance-Based Approach to the Development of a Recycled Plastic / Composite Crosstie, Norfolk Southern.

[56] Sapuan, S. M., Imihezri, S. S. S., Sulaiman, S., Hamdan, M., and Zainudin, E. S., 2007, "Comparison of simulated and actual product of polymer composite automobile clutch pedal," Int. J. Mech. Mater. Eng., **2**(1), pp. 29–39.

[57] Cheung, H., Ho, M., Lau, K., Cardona, F., and Hui, D., 2009, "Natural fibre-reinforced composites for bioengineering and environmental engineering applications," Compos. Part B, **40**(7), pp. 655–663.

[58] Sapuan, S. M., 2005, "Materials & Design Design and fabrication of natural woven fabric reinforced epoxy composite for household telephone stand," Mater. Des., **26**, pp. 65–71.

[59] West, D., 2002, “The Hawaii Industrial Hemp Project,” J. Ind. Hemp (Cannabis sativa L .), **7**(2), pp. 83–86.

[60] Mantia, F. P. La, and Vinci, M., 1994, “Recycling poly (ethylene terephthalate),” Polym. Degrad. Stab., **45**, pp. 121–125.

[61] Nikles, D. E., and Farahat, M. S., 2005, “New Motivation for the Depolymerization Products Derived from Poly (Ethylene Terephthalate) (PET) Waste : a Review,” Macromol. Mater. Eng., **290**, pp. 13–30.

[62] Madsen, B., 2004, “Properties of Plant Fibre Yarn Polymer Composites: An Experimental Study,” Technical University of Denmark.

[63] Cai, Z., and Robert, J. R., 2010, “Mechanical Properties of Wood-Based Composite Materials,” Wood handbook : wood as an engineering material: chapter 12. Centennial ed. General technical report FPL ; GTR-190, U.S. Dept. of Agriculture, Forest Service, Forest Products Laboratory, Madison, WI, pp. 12.1–12.12.

[64] Brockenbrough, R. L., 1994, “Properties of structural steels and effects of steelmaking and fabrication,” Structural Steel Designer’s Handbook, R.L. Brockenbrough, and F.S. Merritt, eds., McGraw-Hill, Inc., pp. 1.1–1.35.

[65] Indian Building Materials & Technology Promotion Council, 1990, Local vegetable fibres & industrial and mineral wastes for composite materials, New Delhi.

[66] Ho, M., Wang, H., Lee, J., Ho, C., Lau, K., Leng, J., and Hui, D., 2012, “Critical factors on manufacturing processes of natural fibre composites,” Compos. Part B, **8**(8), pp. 3549–3562.

[67] Rodriguez, E., Alvarez, V. A., Moran, J., Moreno, S., Petrucci, R., Kenny, J. M., and Vazquez, A., 2006, “Mechanical Properties Evaluation of a Recycled Flax-reinforced Vinyl-Ester,” J. Compos. Mater., **40**(3).

[68] Sèbe, G., Cetin, N. S., Hill, C. A. S., and Hughes, M., 2000, “RTM Hemp Fibre-Reinforced Polyester Composites,” Appl. Compos. Mater., **7**, pp. 341–349.

[69] Tong, Y., and Xu, L., 2006, “Hemp Fiber Reinforced Unsaturated Polyester Composites,” Adv. Mater. Res., **11**(12), pp. 521–524.

[70] Lampo, G. R. A. corps of E., and Thomas J. Nosker(US Army corps of Engineer), 1997, Development and testing of plastic lumber materials for construction applications.

[71] Lampo, R. G., Sweeney, S. C., Hock, V. F., Chiarito, V. P., Diaz-alvarez, H., and Nosker, T. J., 2009, “Thermplastic composites as degradation-resistant material systems for timber bridge designs,” 2009 DoD Corrosion Conference, pp. 1–12.

[72] Field, N. D., and Chien, M., 1985, “Poly (ethylene Terephthalate)/Cellulose Blends,” Polym. Sci., **30**, pp. 2105–2113.

[73] Caulfield, D. F., Jacobson, R. E., Sears, K. D., and Underwood, J. H., 2001, “Woodpulp fibres as reinforcements for high-melting engineering thermoplastics

for ‘under-the-hood’ automotive applications,” 17th annual meeting Polymer Processing Society, The Polymer Processing Society, Montreal, Canada, p. 10.

[74] Caulfield, D. F., Jacobson, R. E., Sears, K. D., and Underwood, J. H., 2001, “Fiber reinforced engineering plastics,” 2nd International Conference on Advanced Engineering Wood Composites, O. University of Maine, ed., Maine, Orono ME 04469-5793.

[75] Lei, Y., and Wu, Q., 2010, “Wood plastic composites based on microfibrillar blends of high density polyethylene/poly(ethylene terephthalate).,” Bioresour. Technol., **101**(10), pp. 3665–71.

[76] Jiang, A., Xi, J., and Wu, H., 2012, “Effect of surface treatment on the morphology of sisal fibers in sisal/polylactic acid composites,” J. Reinf. Plast. Compos., **31**(9), pp. 621–630.

[77] Herrera-Franco, P. J., and Valadez-González, A., 2005, “A study of the mechanical properties of short natural-fiber reinforced composites,” Compos. Part B Eng., **36**(8), pp. 597–608.

[78] Islam, M. S., Pickering, K. L., and Foreman, N. J., 2010, “Influence of alkali treatment on the interfacial and physico-mechanical properties of industrial hemp fibre reinforced polylactic acid composites,” Compos. Part A, **41**(5), pp. 596–603.

[79] Kalia, S., Kaith, B. S., and Kaur, I., 2009, “Pretreatments of Natural Fibers and their Application as Reinforcing Material in Polymer Composites — A Review,” Polym. Eng. Sci., **49**, pp. 1253–1272.

[80] Liu, C. F., Xu, F., Sun, J. X., Ren, J. L., Curling, S., Sun, R. C., Fowler, P., and Baird, M. S., 2006, “Physicochemical characterization of cellulose from perennial ryegrass leaves (Lolium perenne),” Carbohydr. Res., **341**, pp. 2677–2687.

[81] Zhu, J., Zhu, H., Njuguna, J., and Abhyankar, H., 2013, “Recent development of flax fibres and their reinforced composites based on different polymeric matrices,” Materials (Basel)., **6**(11), pp. 5171–5198.

[82] US Department of Defense, 2002, Composite Materials Handbook Volume 3. Polymer Matrix Composites-Materials Usage, Design, And Analysis, Department of Defense.

[83] Mukhopadhyay, S., and Fangueiro, R., 2009, “Physical Modification of Natural Fibers and Thermoplastic Films for Composites -- A Review,” J. Thermoplast. Compos. Mater., **22**(2), pp. 135–162.

[84] Vasudeo, Y. B., and Rangaprasad, R., 2008, “The fast growing ‘wood plastic composites’- wpc,” THE Extruder Times, **April-June**(06), pp. 1–12.

[85] Szegda, D., 2009, “Experimental Investigation and Computational Modelling of the Thermoforming Process of Thermoplastic Starch,” Brunel University.

[86] Vlachopoulos, J., and E, M., 1989, “Fluid flow and heat transfer in calendering,” Transport phenomena in polymeric systems, E.H. Chichester, ed., pp. 78–104.

[87] Deepa, B., Pothan, L. A., Mavelil-sam, R., and Thomas, S., 2011, “Structure ,

properties and recyclability of natural fibre reinforced polymer composites," Recent Developments in Polymer Recycling, A. Fainleib, and O. Grigoryeva, eds., Kerala, India, pp. 101–120.

[88] Aho, J., 2011, "Rheological Characterization of Polymer Melts in Shear and Extension : Measurement Reliability and Data for Practical Processing," Tampere University of Technology.

[89] Utracki, L. A., and Shi, G. Z.-H., 2003, "Compounding polymer blends," Polymer Blends Handbook, L.A. Utracki, ed., Kluwer Academic Publishers, Netherlands, pp. 577–651.

[90] Lim, K. Y., Kim, B. C., and Yoon, K. J., 2002, "Structural and Physical Properties of Biodegradable Copolyesters from Poly (ethylene terephthalate) and Polycaprolactone Blends."

[91] Siengchin, S., "Nano-Scale Reinforcing and Toughening Thermoplastics : Processing , Structure and Mechanical Properties," **6**.

[92] Dhakal, H. N., Zhang, Z. Y., and Richardson, M. O. W., 2007, "Effect of water absorption on the mechanical properties of hemp fibre reinforced unsaturated polyester composites," Compos. Sci. Technol., **67**(7-8), pp. 1674–1683.

[93] Najafi, S. K., Kiaeifar, A., Tajvidi, M., and Hamidinia, E., 2008, "Hygroscopic thickness swelling rate of composites from sawdust and recycled plastics," pp. 161–168.

[94] Masoodi, R., and Pillai, K. M., "Modeling the Processing of Natural Fiber Composites Made Using Liquid Composite Molding," Handbook of Bioplastics & Biocomposites Applications, S. Pilla, ed., Scrivener Publishing LLC, Milwauke, pp. 43–74.

[95] Brian Sabart, and Gangel, J., 2009, "Thermoforming," Fortus 3D Prod. Syst., pp. 1–6.

[96] Erchiqui, F., A.Gakwaya, Rachik, M., Gakwaya, A., and Rachik, M., 2005, "A dynamic finite element analysis of nonlinear isotropic hyperelastic and viscoelastic materials for thermoforming applications," Polym. Eng. Sci., **45**, pp. pp.125–134.

[97] Erchiqui, F., and Souli, M., 2009, "Numerical Investigation of the Gas Flow Temperature on the Thermoforming and Blow-Molding Processes," J. Reinf. Plast. Compos., **28**, pp. 1823–1840.

[98] Lampo, R., 2005, "Applications and Opportunities for Rigid Plastic Packaging Containers," CIWMB Conference: Increasing plastic container recycling in California, CIWMB & Integrated waste management board, Sacramento, California, p. 50.

[99] Ghomari, T., 2007, "Contribution à la modélisation 3D volumique de la mise en forme des corps plastiques creux," Université de Reims Champagne-Ardenne.

[100] General Electric Co. USA, 2012, Lexan® Processing Guide.

[101] Erchiqui, F., Ozdemir, Z., Souli, M., Ezzaidi, H., and Dituba-Ngoma, G., 2011,

"Neural networks approach for characterisation of viscoelastic polymers," Can. J. Chem. Eng., **89**(5), pp. 1303–1310.

[102] Erchiqui, F., Godard, F., Koubba, A., Vincent, M., and Kaddami, H., 2008, "Investigation of Relaxation Properties and Potentiality of the Thermoformability of HDPE Charged by Wood Flours," J. Reinf. Plast. Compos., **28**(10), pp. 1153–1168.

[103] Incarnato, L., Scarfato, P., Di Maio, L., and Acierno, D., 2000, "Structure and rheology recycled PET modified by reactive extrusion," Polymer (Guildf)., **41**, pp. 6825–6831.

[104] Awaja, F., Daver, F., and Kosior, E., 2004, "Recycled Poly(ethylene terephthalate) Chain Extension by a Reactive Extrusion Process," Polym Eng Sci, **44**(8), pp. 1579–1587.

[105] Papageorgiou, G. Z., Achilias, D. S., and Karayannidis, G. P., 2004, "Melting point depression and cocrystallization behavior of poly (ethylene-co-butylene 2 , 6-naphthalate) copolymers," Polym. Int., **1367**(December 2003), pp. 1360–1367.

[106] Karayannidis, G. P., Papachristos, N., Bikiaris, D. N., and Papageorgiou, G. Z., 2003, "Synthesis , crystallization and tensile properties of poly (ethylene terephthalate-co-2 , 6-naphthalate) s with low naphthalate units content," Polymer (Guildf)., **44**, pp. 7801–7808.

[107] Wayne Machine & Die Company, The Draiswerke Gelimat, Thermo Electron Co, Berstorff, Temarex, B & P Process Equipment, Leistritz Extrusionstechnik GmbH, Noris Plastic GmbH, Coperion Group, Steer Engineering P Ltd, NFM Welding Engineers, and Entek Extruders, 2005, "Extruders for compounding," Plast. Addit. Compd., **7**(1), pp. 20–25.

[108] Gopakumar, T. G., and Pagé, J. S. Y. D., 2005, "Compounding of Nanocomposites by Thermo-kinetic Mixing," Appl. Polym. Sci., **96**, pp. 1557–1563.

[109] Pagé, J. S. Y. D., and Gopakumar, T. G., 2006, "Properties and Crystalliation of Maleated Polypropylene/Graphite Flake Nanocomposites," Polymer (Guildf)., **38**, pp. 920–929.

[110] Goodrich, J. E., and Porter, R. S., 1967, "A Rheological interpretation of torque-rheometer data," Polym. Eng. Sci., **7**(1), p. 45.

[111] Bousmina, M., Ait-Kadi, A., and Faisant, J. B., 1999, "Determination of shear rate and viscosity from batch mixer data," Rheology, **43**, p. 415.

[112] Blyber, L. L., Daane, J. H., and L. L. Blyler, J., 1967, "An analysis of brabender torque rheometer data," Polym. Eng. Sci., **7**(3), p. 178.

[113] Adragna, L., Couenne, F., Cassagnau, P., and Jallut, C., 2007, "Modeling of the Complex Mixing Process in Internal Mixers," Ind. Eng. Chem. Res., **46**, pp. 7328–7339.

[114] Shih, C.-K., 1995, "Mixing and morphological transformations in the compounding process for polymer blends: The phase inversion mechanism," Polym. Eng. Sci., **35**(21), pp. 1688–1694.

[115] Nassehi, V., Ghoreishy, M. H. R., Road, A., and Le, L., 2001, "Modeling of Mixing in Internal Mixers with Long Blade Tips," Adv. Polym. Technol., **20**(2), pp. 132–145.

[116] Tazi, M., Erchiqui, F., Godard, F., Kaddami, H., and Ajji, A., 2014, "Characterization of rheological and thermophysical properties of HDPE-wood composite," J. Appl. Polym. Sci., **131**(13), pp. 1–11.

[117] Li, X., Tabil, L. G., Oguocha, I. N., and Panigrahi, S., 2008, "Thermal diffusivity, thermal conductivity, and specific heat of flax fiber–HDPE biocomposites at processing temperatures," Compos. Sci. Technol., **68**(7-8), pp. 1753–1758.

[118] Vyazovkin, S., Burnham, A. K., Criado, J. M., Pérez-Maqueda, L. A., Popescu, C., and Sbirrazzuoli, N., 2011, "ICTAC Kinetics Committee recommendations for performing kinetic computations on thermal analysis data," Thermochim. Acta, **520**(1-2), pp. 1–19.

[119] Jin, W., Singh, K., and Zondlo, J., 2013, "Pyrolysis Kinetics of Physical Components of Wood and Wood-Polymers Using Isoconversion Method," Agriculture, **3**(1), pp. 12–32.

[120] Shin, S. M., and Kim, S. H., 2009, "Thermal Decomposition Behavior and Durability Evaluation of Thermotropic Liquid Crystalline Polymers," **17**(3), pp. 149–155.

[121] Lu, Z., Yang, L., and Guo, Y., 2006, "Thermal behavior and decomposition kinetics of six electrolyte salts by thermal analysis," **156**(800), pp. 555–559.

[122] Liu, X., and Yu, W., 2006, "Evaluating the thermal stability of high performance fibers by TGA," J. Appl. Polym. Sci., **99**(3), pp. 937–944.

[123] Gornall, T., 2011, "Catalytic Degradation of Waste Polymers," University of Central Lancashire.

[124] Tang, W., Li, X., and Yan, D., 2003, "Thermal Decomposition Kinetics of Thermotropic Copolyesters Made from trans-p-Hydroxycinnamic Acid and p-Hydroxybenzoic Acid," Appl. Polym Sci., **91**, pp. 445–454.

[125] Pielichowski, K., and Njuguna, J., 2005, Thermal degradation of polymeric materials, Rapra Technology Limited, Shawbury, Shrewsbury, Shropshire, SY4 4NR, United Kingdom.

[126] Godard, F., Vincent, M., Agassant, J.-F., and Vergnes, B., 2008, "Étude du comportement rhéologique et des propriétés mécaniques de composites sciures de bois-polyéthylène haute densité," Rhéologie, **13**, pp. 9–21.

[127] Carolin, A., 2003, "Carbon Fibre Reinforced Polymers for Strengthening of Structural Elements," Lulea University of Technology.

[128] Sengupta, R., Chakraborty, S., Bandyopadhyay, S., Dasgupta, S., Mukhopadhyay, R., Auddy, K., and Deuri, a S., 2007, "A Short Review on Rubber/Clay Nanocomposites With Emphasis on Mechanical Properties," Polym Eng SciEngineering, **47**, pp. 21–25.

[129] Ralph, S. (International T. E. C., 2012, "The Eleventh International Tissue Elasticity Conference," The Eleventh International Tissue Elasticity Conference, ITEC, ed., ITEC, Deauville, Normandy, France, pp. 1–126.

[130] Zhandarov, S., and Mäder, E., 2005, "Characterization of fiber/matrix interface strength: applicability of different tests, approaches and parameters," Compos. Sci. Technol., **65**(1), pp. 149–160.

[131] Cheng, B., Zhou, C., Yu, W., and Sun, X., 2001, "Evaluation of rheological parameters of polymer melts in torque rheometers," Polym. Test., **20**, pp. 811–818.

[132] Ouajai, S., and Shanks, R. A., 2005, "Composition, structure and thermal degradation of hemp cellulose after chemical treatments," Polym Degrad Stab, **89**, pp. 327–335.

[133] Rowell, R. M., 2005, "Thermal properties," Handbook of wood chemistry, R.M. Rowell, ed., CRC Press.

[134] Nabar, Y. U., Gupta, A., and Narayan, R., 2005, "Isothermal Crystallization Kinetics of Poly (Ethylene Terephthalate) – Cellulose Acetate Blends," Polym. Bull., **53**, pp. 117–125.

[135] Costache, M. C., Heidecker, M. J., Manias, E., and Wilkie, C. A., 2006, "Preparation and characterization of poly (ethylene terephthalate)/clay nanocomposites by melt blending using thermally stable surfactants," Polym. Adv. Tchnol., **20**(August), pp. 764–771.

[136] Assadi, R., Colin, X., and Verdu, J., 2004, "Irreversible structural changes during PET recycling by extrusion," Polymer (Guildf)., **45**, pp. 4403–4412.

[137] Liu, Y., Wang, M., and Pan, Z., 2012, "Catalytic depolymerization of polyethylene terephthalate in hot compressed water," J. Supercrit. Fluids, **62**, pp. 226–231.

[138] D'Almeida, J. R. M., Aquino, R. C. M. P., and Monteiro, S. N., 2006, "Tensile mechanical properties , morphological aspects and chemical characterization of piassava (Attalea funifera) fibers," Compos. Part A Appl. Sci. Manuf., **37**, pp. 1473–1479.

[139] Zhang, Z., Luo, X.-L., Lu, Y., and Ma, D., 2000, "Transesterification of Poly(ethylene terephthalate) with Poly(caprolactone)," Chinese J. Polyemer Sci. Sci., **18**(5), pp. 405–412.

[140] Lim, K. Y., Kim, B. C., and Yoon, K. J., 2002, "The Effect of Molecular Weight of Polycaprolactone on the Ester Interchange Reactions during Melt Blending with Poly (ethylene terephthalate).," Polym. J., **34**(5), pp. 313–319.

[141] Chiellini, E., Corti, A., Giovannini, A., Narducci, P., Paparella, A. M., and Solaro, R., 1996, "Evaluation of biodegradability of poly (Caprolactone)/ poly (ethylene Terephthalate) blends," J. Environ. Polym. Degrad., **4**(1), pp. 37–50.

[142] Brems, A., Baeyens, J., Vandecasteele, C., and Dewil, R., 2011, "Polymeric cracking of waste polyethylene terephthalate to chemicals and energy.," J. Air Waste Manag. Assoc., **61**(7), pp. 721–731.

[143] Ruseckaite, R. A., and Jiménez, A., 2003, "Thermal degradation of mixtures of polycaprolactone with cellulose derivatives," Polym. Degrad. Stab., **81**(2), pp. 353–358.

[144] Samperi, F., Puglisi, C., Alicata, R., and Montaudo, G., 2004, "Thermal degradation of poly (ethylene terephthalate) at the processing temperature," Polym. Degrad. Stab., **83**, pp. 3–10.

[145] McNeill, I. C., Ahmed, S., Memetea, L., Mohammed, M. H., Zaikov, G. E., and Polishchuk, A. Y., 1996, "Thermal degradation behaviour of some alternating copolymers," Polym. Degrad. Stab., **52**(2), pp. 171–181.

[146] Bacaloglu, R., Kleinlauth, P., Frenkel, P., and Reed, P., 2004, "Thermal Stabilization of PVC-Wood Composites," ANTEC 2004, Society of Plastics Engineers, pp. 3931–3935.

[147] Polymers, D. E., 1995, Molding guide, Rynite PET, Chestnut Run Plaza 713, P.O Box 80713, Wilmington, DE 19880-0713.

[148] Valovirta, I., and Vinha, J., 2002, "Hemp as insulation material in wooden houses," Building Physics 2002-6th Nordic Symposium, Norwegian University of Science and Technology, Trondheim, pp. 469–475.

[149] Mazumdar, S. K., 2002, Composites manufacturing. Materials, product, and process engineering, CRC Press LLC, Boca Raton, FL 33487-2742.

[150] Vlachopoulos, J., and Strutt, D., 2003, "An Overview: Polymer Processing," Mater. Sci. Technol., **19**(9), pp. 1161–1169.

[151] Kelsey, D. R., Kiibler, K. S., and Tutunjian, P. N., 2005, "Thermal stability of poly(trimethylene terephthalate)," Polymer (Guildf)., **46**, pp. 8937–8946.

[152] Coudane, V. F., and M., J. V., 1994, "Thermal degradation of poly(ethylene terephthalate) and the estimation of volatile degradation products," Polym Degrad Stab, **43**, pp. 431–440.

[153] Mansour, S. A., Al-kotb, M. S., and Kotkata, M. F., 2014, "Model-free transformation kinetics for ZnS quantum dots synthesized via colloidal reaction," Phys. B Phys. Condens. Matter, **433**, pp. 127–132.

[154] Aboyade, A. O., Görgens, J. F., Carrier, M., Meyer, E. L., and Knoetze, J. H., 2013, "Thermogravimetric study of the pyrolysis characteristics and kinetics of coal blends with corn and sugarcane residues," Fuel Process. Technol., **106**, pp. 310–320.

[155] Jandura, P., Riedl, B., and Kokta, B. V, 2000, "Thermal degradation behavior of cellulose fibers partially esterified with some long chain organic acids," Polym Degrad Stab, **70**, pp. 387–394.

[156] Aigbodion, V. S., Hassan, S. B., and Atuanya, C. U., 2012, "Kinetics of Isothermal Degradation studies by Thermogravimetric Data : Effect of orange peels ash on thermal properties of High density polyethylene," Mater. Environ. Sci., **3**(6), pp. 1027–1036.

[157] Lautenberger, C., Kim, E., Dembsey, N., and Fernandez-Pello, a., 2008, "The Role of Decomposition Kinetics in Pyrolysis Modeling - Application to a Fire Retardant Polyester Composite," Fire Saf. Sci., **9**, pp. 1201–1212.

[158] Fotso Talla, A. S., Erchiqui, F., Kocaefe, D., and Kaddami, H., 2014, "Effect of Hemp Fiber on PET/Hemp Composites," J. Renew. Mater., **2**(4), pp. 285–290.

[159] Kujirai, T., and Akahira, T., 1925, "Effect of Temperature on the Deterioration of Fibrous Insulating materials," Sci. Pap. Inst. Phys. Chem. Res., **2**(21), pp. 223–252.

[160] Starink, M. J., 1996, "A new method for the derivation of activation energies from experiments performed at constant heating rate," Thermochim. Acta, **288**, pp. 97–104.

[161] Morán, J., Alvarez, V., Petrucci, R., Kenny, J., and Vazquez, a., 2007, "Mechanical properties of polypropylene composites based on natural fibers subjected to multiple extrusion cycles," J. Appl. Polym. Sci., **103**(1), pp. 228–237.

[162] Mutje, P., Gironès, J., Lòpez, A., Llop, M. F., and Vilaseca, F., 2006, "Hemp Strands: PP Composites by Injection Molding: Effect of Low Cost Physico-chemical Treatments," J. Reinf. Plast. Compos., **25**(3), pp. 313–327.

[163] Bengtsson, M., Gatenholm, P., and Oksman, K., 2005, "The effect of crosslinking on the properties of polyethylene/wood flour composites," Compos. Sci. Technol., **65**(10), pp. 1468–1479.

[164] Balasuriya, P. ., Ye, L., and Mai, Y.-W., 2001, "Mechanical properties of wood flake–polyethylene composites. Part I: effects of processing methods and matrix melt flow behaviour," Compos. Part A Appl. Sci. Manuf., **32**(5), pp. 619–629.

[165] Kumar, R. P., Amma, M. L. G., and Thomas, S., 1995, "Short sisal fiber reinforced styrene-butadiene rubber," J. Appl. Polym. Sci., **58**, pp. pp.597–612.

[166] Lu, M., 1997, "Wood Fiber Reinforced Polypropylene Composites," Louisiana State University.

[167] Bledski, A. K., Letman, M., Viksne, A., and Rence., L., 2005, "A comparaison of compounding processes and wood type for wood fibre-PP composites," Compos. Part A Appl. Sci. Manuf., **36**, pp. pp. 789–797.

[168] Erchiqui, F., A.Gakwaya, and Rachik, M., 2005, "A dynamic finite element analysis of nonlinear isotropic hyperelastic and viscoelastic materials for thermoforming applications," Polym. Eng. Sci., **45**, pp. pp.125–134.

[169] Erchiqui, F., 2006, "A new hybrid approach using the explicit dynamic finite element method and thermodynamic law for the analysis of the thermoforming and blow molding processes for polymer materials," Polym. Eng. Sci., **46**(11), pp. 1554–1564.

[170] Redlich, O., and Kwong, J. N. S., 1949, "On the thermodynamics of solutions; an equation of state; fugacities of gaseous solutions.," Chem. Rev., **44**(1), pp. 233–244.

[171] Zienkiewicz, O. C., and Taylor., R. L., 1994, The Finite Element Method Vol. 1, McGraw-Hill Book Company Europe.

[172] Lodge, A. S., 1964, Elastic liquids: an introductory vector treatment of finite - strain polymer rheology, Academic Press, London & New York.

[173] Papanastasiou, A. C., Scriven, L. E., and C. W. Macosko, 1983, "An integral constitutive equation for mixed flows: Viscoelastic characterization.," J. Rheol. (N. Y. N. Y)., **27**(4), p. 387.

[174] Subbaraj, K., and Dokainish, M. A., 1989, "A survey of direct time-integration methods in computational structural dynamics—II. Implicit methods," Comput. Struct., **32**(6), pp. 1387–1401.

[175] Verron, E., Marckmann, G., and Peseux, B., 2001, "Dynamic inflation of non-linear elastic and viscoelastic rubber-like membranes," Int. J. Numer. Methods Eng., **50**(5), pp. 1233–1251.

[176] Derdouri, A., Erchiqui, F., Bendada, A., Verron, E., and Peseux, B., 2000, "Viscoelastic behavior of polymer membranes under inflation," Proc. Int. Congr. Rheol. 13th, Cambridge, United Kingdom, Aug. 20-25, 2000, **3**, pp. 394–396.

[177] DeLorenzi, H. G., and Nied., H. F., 1991, "Finite Element Simulation of Thermoforming and Blow Molding," Progress in polymer processing, A.I. Isayev, ed., Carl Hanser Verlag, Munich, Germany, pp. 117–171.

[178] Erchiqui, F., 2005, "Thermodynamic approach of inflation process of K-BKZ polymer sheet with respect to thermoforming," Polym. Eng. Sci., **45**(10), pp. 1319–1335.

[179] Ramesh Chandra Mohapatra, Antaryami Mishra, and Bibhuti Bhushan Choudhury, 2014, "Investigations on Thermal Conductivity of Palm Fibre Reinforced Polyester Composites," IOSR J. Mech. Civ. Eng., **11**(1), pp. 48–52.

[180] Behzad, T., and Sain, M., 2007, "Measurement and prediction of thermal conductivity for hemp fiber reinforced composites," Polym. Eng. Sci., **47**(7), pp. 977–983.

[181] Loveday, M. S., and Skelton, R. P., 1920, "High Temperature Mechanical Testing : a Review and Future Directions," pp. 1–6.

[182] Marsh, G., 2003, "Next step for automotive materials," Mater. Today, **6**(4), pp. 36–43.

[183] Franck, A. (TA/Instruments), 2004, Understanding Rheology of Thermoplastic Polymers.

[184] Cullen, P. J., O'donnell, C. P., and Houska, M., 2003, "Rotational rheometry using complex geometries: A review.," J. Texture Stud., **34**(2003), pp. 1–20.

[185] Dealy, J. M., 2010, "Weissenberg and Deborah Numbers-Their definition and Use," Rheol. Bull., **79**(2), pp. 14–18.

[186] Moore, W. R., Epstein, J. A., Brown, A. M., and Tidswell, B. M., 1957, "Cellulose Derivative-Solvent Interaction," Polym. Sci., **XXIII**, pp. 23–46.

[187] Hatzikiriakos, S. G., Heffner, G., Vlassopoulos, D., and Christodoulou, K., 1997, "Rheological characterization of polyethylene terephthalate resins using a multimode Phan-Tien-Tanner constitutive relation," Rheol. Acta, **36**(5), pp. 568–578.

[188] Forsythe, J. S., Cheah, K., Nisbet, D. R., Gupta, R. K., Lau, A., Donovan, A. R., Shea, M. S. O., and Moad, G., 2006, "Rheological Properties of High Melt Strength Poly (ethylene terephthalate) Formed by Reactive Extrusion," J Polym Sci, **100**, pp. 3646–3652.

[189] Hall, T. J., Milkowski, A., Garra, B., Carson, P., Palmeri, M., Nightingale, K., Lynch, T., Alturki, A., Andre, M., Audiere, S., Bamber, J., Barr, R., Bercoff, J., Bercoff, J., Bernal, M., Brum, J., Cohen-Bacrie, C., Couade, M., Daniels, A., DeWall, R., Dillman, J., Ehman, R., Franchi-Abella, S., Fromageau, J., Gennisson, J.-L., Henry, J. P., Ivancevich, N., Kalin, J., Kohn, S., Kugel, J., Liu, N., Loupas, T., Mazernik, J., McAleavey, S., Miette, V., Metz, S., Morel, B., Nelson, T., Nordberg, E., Oudry, J., Padwal, M., Rouze, N., Samir, A., Sandrin, L., Schaccitti, J., Schmitt, C., Shamdasani, V., Switalski, P., Wang, M., and Wear, K., 2013, "RSNA/QIBA: Shear wave speed as a biomarker for liver fibrosis staging," 2013 IEEE Int. Ultrason. Symp., pp. 397–400.

[190] Abdoos H, Khorsand, H., and Yousefi, A., 2014, "Torque rheometry and rheological analysis of powder – polymer mixture for aluminum powder injection molding," Iran. Polym. J., **23**(10), pp. 745–755.

[191] Pastorini, M. T., and Nunes, R. C. R., 2012, "Rheological characterization of ABS , PC , and their blends through the interpretation of torque rheometer data," Polym. Plast. Technol. Eng., **41**(1), pp. 161–169.

[192] Mallette, J. G., and Soberanis, R. R., 1998, "Evaluation of Rheological Properties of Non-Newtonian Fluids in Internal Mixers : An Alternative Method Based on the Power Law Model," Polym. Eng. Sci., **38**(9), pp. 1436–1442.

[193] Intawong, N., and Sombatsompop, N., 2004, "A Parallel Coextrusion Technique for Simultaneous Measurements of Radial Die Swell and Velocity Profiles of a Polymer Melt in a Capillary Rheometer," Polym. Eng. Sci., **44**(10), pp. 1960–1969.

[194] Franck, A., Künze, W., and Dallas, G., 2004, "The Combined use of Thermal Analysis and Rheology in Monitoring and Characterizing Changing Processes in materials," Am. Lab., **36**(January), pp. 2–4.

[195] Ferry, J. D., 1980, Viscoelastic properties of polymers, John Wiley & Sons, Incorporated, New York-Chichester-Brisbane-Toronto-Singapore.

[196] Dufresne, A., 2010, "Processing of polymer nanocomposites reinforced with polysaccharide nanocrystals.," Molecules, **15**(6), pp. 4111–28.

[197] Pietak, A., Korte, S., Tan, E., Downard, A., and Staiger, M. P., 2007, "Atomic force microscopy characterization of the surface wettability of natural fibres," Appl. Surf. Sci., **253**, pp. 3627–3635.

[198] Panthapulakkal, S., and Sain, M., 2007, "Studies on the Water Absorption Properties of Short Hemp--Glass Fiber Hybrid Polypropylene Composites," J. Compos. Mater., **41**(15), pp. 1871–1883.

[199] Sockalingam, S., and Nilakantan, G., 2012, "Fiber-matrix interface characterization through the microbond test: A review," Int. J. Aeronaut. Sp. Sci., **13**(3), pp. 282–295.

[200] Bathe, K.-J., Ramm, E., and Wilson, E. L., 1975, "Finite element formulations for large deformation dynamic analysis," Int. J. Numer. Methods Eng., **9**, pp. 353–386.

[201] Shabana, A. A., 2008, Computational Continuum Mechanics, Cambridge Books Online.

[202] Garcia, M. J. R., Ruiz, O. E. S., Lopez, C., Gonzalez, L. Y. S., Botero, M. G., and Betancur, M., 2005, Hyperelastic Material Modeling, Medellin, Colombia.

[203] A. M. Korsunsky, 2001, "Elastic Behavior of Materials: Continuum Aspects," Encyclopedia of Materials: Science and technology, Elsevier Science Ltd, Oxford, pp. 2398–2404.

[204] Erchiqui, F., and Kandil, N., 2006, "Neuronal Networks Approach for Characterization of Softened Polymers," J. Reinf. Plast. Compos., **25**(5), pp. 463–473.

[205] Kouba, K., Bartos, O., and Vlachopoulos, J., 1992, "Computer simulation of thermoforming in complex shapes," Polym. Eng. Sci., **32**(10), pp. 699–704.

[206] Honig, E. P., Wierenga, P. E., and Linden, J. H. M. Van der, 1987, "Theory of elastic behavior of composite materials," Appl. Phys., **65**(5), pp. 1610–1612.

[207] Albouy, W., 2014, "De la contribution de la visco-élasto-plasticité au comportement en fatigue de composites à matrice thermoplastique et thermodurcissable," Normandie Université-INSA Rouen.

[208] T. Matsuda (University of Tsukuba, J., and N. Ohno (Nagoya University, J., 2010, "Predicting the elastic-viscoplastic and creep behaviour of polymer matrix composites using the homogenization theory," Creep and Fatigue in Polymer Matrix Composites, Rui Miranda Guedes, ed., Woodhead Publishing, Cambridge, pp. 113–146.

[209] Drozdov, A. D., 2000, "Viscoelastoplasticity of amorphous glassy polymers," Eur. Polym. J., **36**(10), pp. 2063–2074.

[210] Drozdov, A. D., 2000, "Modeling the viscoelastoplastic response of amorphous glassy polymers," **41**(10), p. 19.

[211] Bles, G., Nowacki, W. K., and Tourabi, A., 2009, "Experimental study of the cyclic visco-elasto-plastic behaviour of a polyamide fibre strap," Int. J. Solids Struct., **46**(13), pp. 2693–2705.

[212] Deseri, L., and Mares, R., 2000, "Class of viscoelastoplastic constitutive models based on the maximum dissipation principle," Mech. Mater., **32**(7), pp. 389–403.

[213] Chunyu, Z., 2007, "Characterization of the Mechanical properties of visco-elastic and visco-elastic-plastic materials by nanoindentation tests," National University of Singapore.

[214] Han, W., and Reddy, B. D., 2013, Plasticity: Mathematical theory and numerical analysis, Springer-Verlag, New York.

[215] Rao, S. S., 2009, Engineering optimization, John Wiley & Sons, Incorporated, New Jersey.

[216] Müller, T. G., and Timmer, J., 2004, "Parameter Identification Techniques for Partial Differential Equations," Int. J. Bifurc. Chaos, **14**(06), pp. 2053–2060.

[217] Harth, T., and Lehn, J., 2003, "Identification of Material Parameters for Inelastic Constitutive Models: Design of Experiments," GAMM-Mitt, **30**(2), pp. 409–429.

[218] Cooreman, S., Lecompte, D., Sol, H., Vantomme, J., and Debruyne, D., 2007, "Elasto-plastic material parameter identification by inverse methods: Calculation of the sensitivity matrix," Int. J. Solids Struct., **44**(13), pp. 4329–4341.

[219] Furukawa, T., Sugata, T., Yoshimura, S., and Hoffman, M., 2002, "An automated system for simulation and parameter identification of inelastic constitutive models," Comput. Methods Appl. Mech. Eng., **191**(21-22), pp. 2235–2260.

[220] Westerberg, A. W., and Director, S. W., 1978, "A modified least squares algorithm for solving sparse n × n sets of nonlinear equations," Comput. Chem. Eng., **2**(2-3), pp. 77–81.

[221] Huang, H.-X., and Liao, C.-M., 2002, "Prediction of parison swell in plastics extrusion blow molding using a neural network method," Polym. Test., **21**, pp. 745–749.

[222] Klötzer, D., Ullner, C., Tyulyukovskiy, E., and Huber, N., 2006, "Identification of viscoplastic material parameters from spherical indentation data: Part II. Experimental validation of the method," J. Mater. Res., **21**(03), pp. 677–684.

[223] Biagiotti, J., Fiori, S., Torre, L., Lòpez-Manchado, M. A., and Kenny, J. M., 2004, "Mechanical properties of polypropylene matrix composites reinforced with natural fibers: A statistical approach," Polym. Compos., **25**(1), pp. 26–36.

[224] 2000, Scientific discovery through advanced computing, Washington, DC 20585.

[225] Mitsoulis, E., 2010, "Computational Polymer Processing," Modeling and simulation in polymers, P.D. Gujrati, and A.I. Leonov, eds., WILEY-VCH, Weinheim, pp. 127–195.

[226] Paper, C., Nguyen, H., Sup, T., Deshaies, M., and Pham, X.-T., 2015, "Simulation-Assisted mold design for forming of thermoplastic PPS/Carbon fiber composites," CASI-GARDN AERO conference, Montreal, Canada, pp. 19–21.

[227] Azoti, W. L., Koutsawa, Y., Tchalla, A., Makradi, A., and Belouettar, S., 2015, "Micromechanics-based multi-site modeling of elastoplastic behavior of composite materials," Int. J. Solids Struct., **59**(May 2015), pp. 198–207.

[228] Fish, J., 2011, Multiscale modeling and simulation of composite materials and

structures, Springer Netherlands, Dordrecht.

[229] Tosun, I., 2007, Modeling in Transport Phenomena: A Conceptual Approach, Elsevier Science & Technology Books, Amsterdam, Netherlands.

[230] Huang, H.-X., 2005, "Neural Modeling of Parison Extrusion in Extrusion Blow Molding," J. Reinf. Plast. Compos., **24**(10), pp. 1025–1034.

[231] Adeodu, A. O., Osita, A. C. O., and Oluwole, L., 2014, "Modeling of Microwave Curing of Unsaturated Polyester Based Composite Materials as Production Process Guide," J. Adv. Eng. Technol., **1**(1).

[232] Chaparro, B. M., Thuillier, S., Menezes, L. F., Manach, P. Y., and Fernandes, J. V., 2008, "Material parameters identification: Gradient-based, genetic and hybrid optimization algorithms," Comput. Mater. Sci., **44**(2), pp. 339–346.

[233] Kurtaran, H., and Erzurumlu, T., 2006, "Efficient warpage optimization of thin shell plastic parts using response surface methodology and genetic algorithm," Int J. Adv. Manuf. Technol., **27**, pp. 468–472.

[234] Luduena, L. N., Kenny, J. M., Vazquez, A., and Alvarez, V. A. ., 2014, "Effect of extrusion conditions and post-extrusion techniques on the morphology and thermal/mechanical properties of polycaprolactone/clay nanocomposites," J. Compos. Mater., **48**(17), pp. 2059–2070.

[235] Cardozo, D., 2008, "Three Models of the 3D Filling Simulation for Injection Molding: A Brief Review," J. Reinf. Plast. Compos., **27**(18), pp. 1963–1974.

[236] Erchiqui, F., 2008, "Numerical Investigation of Gas Equations of State of the Isotropic Viscoelastic Polymer Membrane in Free and Confined Inflation," J. Reinf. Plast. Compos., **27**(5), pp. 487–505.

[237] Hsiao, S., 1997, "Numerical Analysis and Optimal Design of Composite Thermoforming Process," University of Michigan.

[238] Ashter, S. A., 2014, "Modeling of thermoforming-A literature review," Thermoforming of single and multilayer laminates, Elsevier, pp. 261–271.

[239] Gilormini, P., Chevalier, L., and Régnier, G., 2010, "Thermoforming of a PMMA transparency near glass transition temperature," Polym. Eng. Sci., **50**(10), pp. 2004–2012.

[240] Novotný, P., Sáha, P., and Kouba, K., 1999, "Fitting of K-BKZ Model Parameters for the Simulation of Thermoforming," Int. Polym. Process., **14**(3), pp. 291–295.

[241] Smith, A., Chen, Z., Lee, J. Y., Lee, M. G., and Wagoner, R. H., 2014, "Effective method for fitting complex constitutive equations," Int. J. Plast., **58**(July), pp. 100–119.

[242] Rachik, M., and Roelandt, M., Algorithmes pour la simulation de la mise en forme des polymères (Application au thermoformage), Compiègne.

[243] Erchiqui, F., Imad, A., Mouloudi, A., and Hasnaoui, F. S., 2010, "Caractérisation viscoélastique du comportement d'une membrane thermoplastique et modélisation numérique de thermoformage," Can. J. Chem. Eng., **88**(1), pp. 116–125.

[244] Shrivastava, S., and Tang, J., 1993, “Large deformation finite element analysis of non-linear viscoelastic membranes with reference to thermoforming,” J. Strain Anal., **28**(1), pp. 31–51.

[245] Rauwendaal, C., “New directions for extrusion : compounding with single screw extruders,” Plast. Addit. Compd., **4**(6), pp. 24–27.

[246] Drobny, J. G., 2014, Handbook of thermoplastic elastomers, Elsevier Science & Technology Books, San Diego, USA.

[247] Gough, A., Christie, R., Farrell, G., Gaffney, B., McAneney, M., Mccann, B., and McNally, G., 2006, A Competitiveness Analysis of the Polymer and Plastics Industry on the Island of Ireland.

[248] Saadat, A., Nazockdast, H., Sepehr, F., and Mehranpour, M., 2010, “Linear and Nonlinear Melt Rheology and Extrudate Swell of Acrylonitrile-Butadiene-Styrene and Nanocomposite,” Polym Eng Sci, **50**, pp. 2340–2349.

[249] Sun, Z.-Y., Han, H.-S., and Dai, G.-C., 2009, “Mechanical Properties of Injection-molded Natural Fiber-reinforced Polypropylene Composites: Formulation and Compounding Processes,” J. Reinf. Plast. Compos., **29**(5), pp. 637–650.

[250] Pritchard, G., 2004, “Two technologies merge : wood plastic composites Geoff Pritchard describes how wood and resin are being,” Plast. Addit. Compd., (August), pp. 18–21.

[251] Michael S., F., 1999, “Compounding and Processing Additives for Woodfiber-Plastic Composites,” Quality Additives for Performance : (5th International Conference on Woodfiber-Plastic Composites), Madison, WI.

[252] Bos, H., 2004, “The Potential of Flax Fibres as Reinforcement for Composite Materials,” University Press Facility, Eindhoven, the Netherlands.

[253] Carlborn, K., and Matuana, L. M., 2006, “Influence of Processing Conditions and Material Compositions on the Performance of Formaldehyde-Free Wood-Based Composites,” Polym. Compos., **27**, pp. 599–607.

[254] Bosze, E. J., Alawar, a., Bertschger, O., Tsai, Y. I., and Nutt, S. R., 2006, “High-temperature strength and storage modulus in unidirectional hybrid composites,” Compos. Sci. Technol., **66**, pp. 1963–1969.

[255] Borzenski, F. J., 2010, Theories and Practices in Rubber Mixing Technology.

[256] Meijer, E. E. H., and Jawsen, J. M. H., 1992, Mixing and Compounding - Theory and Practice, Eindhoven.

APPENDICES

I. Composite characterization

I.1. Thermo-physical properties

The thermo-physical properties of a vegetal fiber-reinforced composite include its thermal conductivity (K) which is its ability to conduct heat, its thermal diffusivity (λ) or its rate of heat transfer under transient conditions, its heat capacity (Cp) which is the amount of heat capable of raising its temperature by one degree, as well as its phase transitions, its radiation properties and its viscosity. The heat conductivity, heat capacity, and thermal conductivity are related by Equation (51) where ρ is the material density.

$$\lambda = \frac{K}{\rho \cdot C_P} \tag{51}$$

Many authors have studied the variation of the thermal conductivity, the heat capacity and the thermal diffusivity of vegetal fiber-reinforced composites using different experimental setups. They have found a decrease of these parameters with an increase in fiber load, coupled with a negligible variation with the temperature. Moreover, they described these thermo-physical properties with known mathematical models [117,179,180], indicating the possibility of their numerical characterization based on individual constituents. The mathematical models used in describing the thermal conductivity of vegetal fiber-reinforced composites are generally based on both the fiber content and the fiber orientation, resulting to the parallel, series and random orientations. The parallel, series, as well as Maxwell and Russell models are respectively given by Equations (52)-(55); where K_f, K_m and v_F are the thermal conductivity of the fiber, thermal conductivity of the matrix and the fiber's volumetric ratio.

$$K_C = v_f \cdot K_f + (1 - v_f) \cdot K_m \tag{52}$$

$$\frac{1}{K_C} = \frac{v_f}{K_f} + \frac{(1 - v_f)}{K_m} \tag{53}$$

$$K_C = K_m \left[\frac{K_f + 2 \cdot K_m + 2 \cdot v_f \cdot (K_f - K_m)}{K_f + 2 \cdot K_m - v_f \cdot (K_f - K_m)} \right] \tag{54}$$

$$K_C = K_m \left[\frac{{v_f}^{2/3} + \frac{K_m}{K_f} \cdot (1 - {v_f}^{2/3})}{{v_f}^{2/3} - v_f + \frac{K_m}{K_f} \cdot \left(1 + v_f - {v_f}^{2/3}\right)} \right] \tag{55}$$

Moreover, the fiber volumetric ratio is given by Equation (56) as a function of the fiber density (ρ_f), the matrix density (ρ_m), the fiber weight ratio (w_f) and the matrix weight ratio (w_m).

$$v_f = \frac{\omega_f \cdot \rho_m}{\omega_f \cdot \rho_m + \omega_m \cdot \rho_f} \tag{56}$$

Bhezad *et al.* [180] have indicated that Maxwell's model works best with lower fiber concentration while Russell's model is most appropriate for fiber concentrations higher than 30% (w/w). Moreover, they have described the in plane heat conductivity of acrylic resin reinforced by hemp fibers with the model described by Equation (57).

$$K_C = 0{,}72 v_f + 0{,}40 \tag{57}$$

Based on the previous relationship, one can determine the thermal conduction and the thermal diffusivity of a composite material by measuring its heat capacity and knowing its constituents' densities and volumetric fractions. The heat capacities and the phase

transitions are generally determined from different equipment in the example of the TA's differential scanning calorimeter (DSC) and thermo-gravimetric analyzer (TGA) shown respectively in Figure 3-7 (a) and (b).

An application of the TGA technique yields close and complementary parameters to those resulting from DSC studies. The generated data from both thermo-physical analysis techniques presented above is often treated by inbuilt software for the determination of the thermo-physical properties as well as the parameters associated with the different thermal transitions of the studied material.

I.2. Thermo-mechanical properties

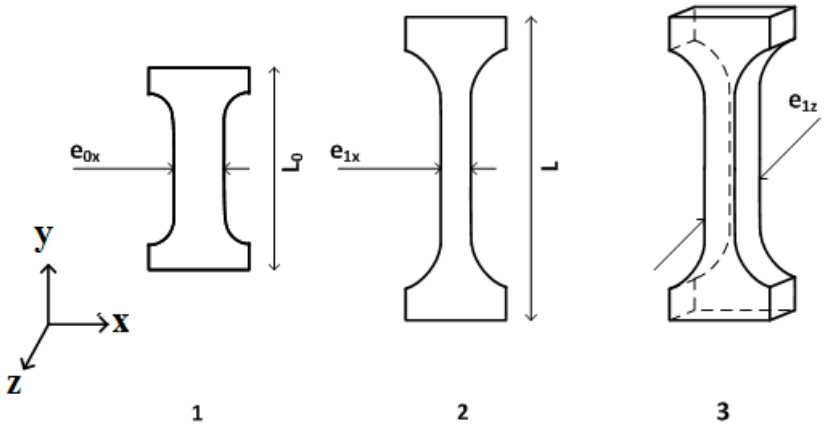

APP- 1: Directional options for mechanical testing.

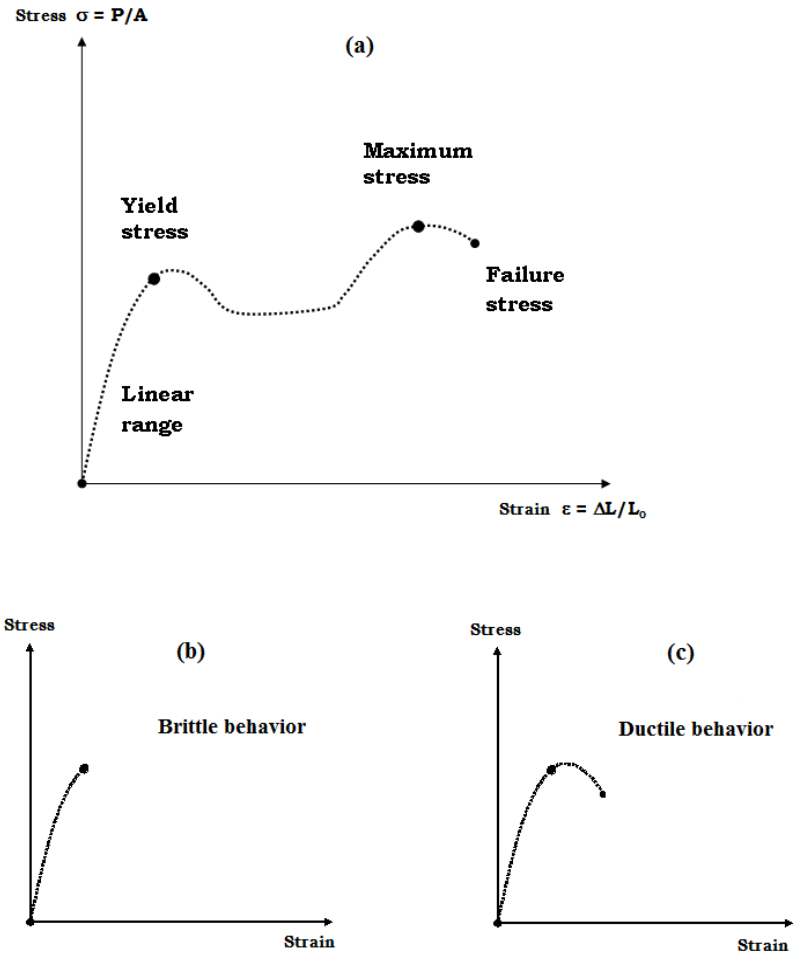

APP- 2: Parameters identification on s stress/strain curve (a). Materials behavior on the stress/strain curve: brittleness (b); ductility (c).

Under the tensional loading mode, the stress and strain are defined by Equation (58) and Equation (59), where ΔL_x, L_{0X}, ε_X, ε_Y, ν, σ_X, E, are respectively the elongation, the initial length, the strain in the X-direction, the strain in the Y-direction, the poisson's ratio, the stress in the X-direction and the modulus of elasticity. Such relationships which focus solely on the initial sample dimensions are the engineering stress and strain. The Poisson ratio measures the sample contraction in the direction perpendicular to the one in which it is subjected to a tensional load.

$$\varepsilon_x = \frac{\Delta L_X}{L_{0X}}$$
$$\varepsilon_Y = -\upsilon \cdot \varepsilon_X \quad (58)$$

$$\varepsilon_x = \frac{\sigma_X}{E} \quad (59)$$

The stress/strain behavior of a thermoplastic or thermoplastic based composite material is temperature dependent as its state changes from glassy to viscous above its glass transition temperature. The stress application in one direction usually affects the material properties in all the others. Consequently, the elastic (E), shear (G) and bulk (K) moduli are three types of modulus involved in their mechanical characterization. They are related by Equation (60) for isotropic materials, while the relationship between shear and stress moduli is given by Equation (61).

$$E = \frac{9GK}{3K + G} \quad (60)$$

$$E = 2G(1 + \nu) \quad (61)$$

When a composite material is tested following a uniaxial process, its reaction proceeds by either isotrain or isostress conditions, corresponding to either its upper or its lower bounds. The mechanical behavior of composite materials is also influenced by the reinforcement load, size and orientation, as well as other parameters which have been included in the development of two major groups of empirical and semi-empirical equations describing the mechanical properties of composite materials. The first group concerns fiber-reinforced composites while the second group is made of particle-reinforced composites.

The mechanical properties of the fibers-reinforced composites are based on the rule of mixture of Equation (62) and Equation (63) and for evaluating the material parameters for cases of iso-strain and iso-stress conditions respectively. The parameters σ_C, σ_M and σ_F are the stresses of respectively the composite, matrix and fiber; while $\varepsilon_{C,}$ $\varepsilon_{M \text{ and }} \varepsilon_F$ are the strains of respectively the composite, matrix and fiber. Moreover, φ_F is the fiber orientation coefficient and v_F is the fiber's volumetric fraction.

$$\begin{aligned} \varepsilon_M &= \varepsilon_F = \varepsilon_C \\ E_C &= \varphi_F \cdot E_F \cdot v_F + (1 - v_F) \cdot E_M \\ \sigma_C &= \varphi_F \cdot \sigma_F \cdot v_F + (1 - v_F) \cdot \sigma_M \end{aligned} \tag{62}$$

$$\begin{aligned} \frac{1}{E_C} &= \frac{\varphi_F v_F}{E_F} + \frac{(1 - v_F)}{E_M} \\ \frac{1}{\sigma_C} &= \frac{\varphi_F v_F}{\sigma_F} + \frac{(1 - v_F)}{\sigma_M} \end{aligned} \tag{63}$$

In the same manner, the mechanical properties of particle-reinforced composites are given by a series of semi-empirical equations in the example of the Einstein equation of Equation (64) applicable in the presence of very low particle volume fraction and good polymer-particle interface; the Halpin-Tsai Equation of Equation (65) which is more realistic than the Einstein's equation and Nielsen's equation given by Equation (66), which also considers the particle packing efficiency (ϕ_P).

$$\frac{E_C}{E_M} = 1 + 2.5\phi_P \tag{64}$$

$$\frac{E_C}{E_M} = \frac{1 + A_1 B_1 \phi_P}{1 - B_1 \phi_P} \tag{65}$$

$$\frac{E_C}{E_M} = \frac{1 + A_1 B_1 \phi_P}{1 - \psi B_1 \phi_P}; \psi = 1 + \left[\frac{1 - \phi_{P\max}}{\phi_{P\max}^2} \right] \phi_P \quad (66)$$

Although the rule of mixture and the other semi-empirical equations are key elements for the elaboration of a composite with specific modulus, their application is not adequate for the composite stress characterization since they are impacted by complex phenomenon such as stress concentration, environmental stress cracking, interfacial adhesion and particles/fibers distribution.

It appears that most of the thermo-mechanical testing reported in the literature has been carried out relative to a given axis, while the parameters in the others are derived from previously established relationships. Although such method provides a quick method of preliminary investigation, multi-axial testing appears as an efficient means of new material characterization, which is often supplemented by numerical identification methods. Multi-axial testing optionally takes place along the three directions shown in Figure: APP- 1. The first option considers only the parameters from the direction of stress application; the second option computes the parameters in the axis perpendicular to the direction of stress application by combining the stress/strain results and the previously reported expressions; finally, the third option considers testing in more than one direction which gives the stress/strain distribution in all directions shown as described in Appendix I.2.

The thermo-mechanical properties are impacted by parameters such as the heating conditions [181], the loading conditions, the moisture content [92], the load cell and the

cross head speed [63] which are reported by previous authors in the field of vegetal fiber-reinforced composites.

Some use of the thermo-mechanical properties of vegetal fiber-reinforced composites in their application have been reported in the household, construction and automotive industries by respectively Sapuan *et al.* [32], Lampo *et al.* [70] and George Marsh [182]. Sapuan *et al.* have reported the effect of the mechanical properties of epoxy reinforced with banana fibers for the design and manufacture of a household telephone stand; Lampo *et al.* studied the applicability of plastic lumber in construction; Marsh *et al.* has reported the different applications of vegetal fiber-reinforced composites such as PP-flax in different areas of the automotive industry.

I.3. Thermo-rheological properties

Rheology is the science that describes the flow and deformation pattern of different simple and complex material systems such as molten plastics, slurries, plastic based composites, as well as the processed pharmaceutical and food substances. The rheological pattern exhibited by a material is a means to select its optimal processing conditions as well as improving its best product quality. Rheology is particularly important in the plastic industry since much of its processing takes place in the melt or semi-melt phase. However, the rheological parameters can also be determined in the solid phase. In fact, the rheological parameters are mostly indirectly computed and serve for comparison purposes. This means that the characterization in the melt is meant for decision making about processing, while characterization in the solid phase is directed to the final product quality [183]. During a plastic based composite processing, the importance of the

rheological properties is also felt before and after the mixing process and during the setting step. Moreover, the use of additives which significantly impact the flow pattern, the product quality and the processing conditions is common leading to the high volume of R&D work in the plastic industry, especially concerning process design and optimization. Rheological testing is also necessary for the evaluation of the molecular structure of the processed material, especially the quality of the interface between fiber and matrix.

The equipment used for the rheological characterization are classifiable based on different criteria. Most of the test conducted in the melt phase is carried on with the first group of equipment whose operation is either rotational or tubular. It includes the parallel plate, concentric cylinder, mixer and cone and plates which are rotational, as well as the glass capillary, the high pressure and the pipe based rheometers which are tubular. The second group of equipment operates in a non-destructive manner based on solid samples. It includes the dynamic mechanical analyzers (DMA) and the RheoSpectris which finds more applications in bio-medicine. The parallel plate rheometer and the RheoSpectris both shown in the photograph of Figure 3-11 are examples of equipment used in the rheological characterization. In general, viscometers measure the viscosity of fluids over a limited range of shear rates, while rheometers measure both the viscosity of fluids over a wide range of shear rate and the visco-elasticity of fluids, semi-solids and solids [184–186].

Different methods of rheological characterization are found in the literature based on the system investigated. Hatzikiriakos *et al* have studied the rheology of PET with a combination of the parallel plate, a capillary rheometer and a constitutive model [187]. In

the same manners, Forsythe *et al.* have studied the rheological behavior of reactive extrusion of PET using in-line measurements with a parallel plate rheometer [188]. Other types have been developed to serve different purposes in the example of the RheoSpectris [129,189] which is based on vibrational waves, the torque based internal rheometer [110,112,190,191] and the differential rheometer [111,192].

In general, an effective description of the material under study often requires a combination of many rheological methods of analysis [193–195]. Additional constraints may however require a partial rheological description followed by numerical parameters identification. These numerical methods are also often used in the analyses of rheological data in the absence of in-built software. Some numerical methods of analysis and identification which are commonly applied in the description of the material behavior are developed in Section I.5.

I.4. Fiber-reinforcement interface

The qualitative methods of fiber-matrix interface characterization are concerned with both its global aspect and its fiber dimensions. Some examples of qualitative fiber-matrix interface characterization exist in the literature in the example of the scanning electron microscope (SEM), X-ray photoelectron spectroscopy (XPS), transmission electron microscopy (TEM) and the atomic force microscopy (AFM). They are generally chosen depending on the composite structure studied (laminates, homogeneous, or heterogeneous) as well as the details required. An example of the scanning electron microscope is shown in Figure 3-9. It operates by firing an electron beam which interacts with the sample surface to produce an image with possible bear 3-D features. Although

the sample preparation for a SEM analysis is relatively easy, sputter coaters are indispensable to induce the electrical conductivity of organic sample through either gold or carbon coating. SEM, TEM and AFM work in a closely similar manner, however TEM requires thinner samples across which the electron beam is fired. In the same manner, an AFM requires the flow of an electrical current through the sample. Moreover, its operation consists in the sample surface scanning with a cantilever beam leading to its deflection as a function of the intensity of the atomic interactions between the sample surface and the cantilever beam. XPS is another surface analysis technique which operation consists in irradiating the sample surface with low energy X-rays, leading to the excitation the atoms at the surface and the extraction of photoelectrons whose binding energy is lower than the X-ray. Many examples of the qualitative methods of fiber-matrix interface analysis have been reported by Mayu *et al.* [26] and [196] for TEM, Pietak *et al.*[197] for the AFM, Panthapulakkal *et al.* [198] for SEM and Dufresne *et al.* [196] for XPS.

The quantitative methods of fiber-matrix interface characterization are based on micromechanical testing followed by an evaluation of some significant interfacial parameters such as the local interfacial shear strength, the critical energy release rate and the adhesional pressure. Two groups of quantitative fiber-matrix interface characterization have been reported in the literature by authors like Zhandarov *et al.* [130] and Sockalingam *et al.* [199]. In the first group, the load is directly applied on the fiber during the micromechanical testing. Such is the case for the single fiber pull-out and its three variations which are the microbond, the three-fiber and the pull-out tests. The second group of micromechanical tests also known as fragmentation tests is performed

by applying the load directly on the matrix, either in the tensional mode for the Broutman test or in flexion. The reliability and compatibility of the data generated by the micromechanical tests are not universally established since the ability of the test set-up to faithfully reproduce the fiber behavior in a composite environment is still questionable. However, they have led to the development of some comparative models which facilitate the appreciation and comparison of fiber-matrix interfaces. Those models are respectively based on the stress and energy-controlled fiber debonding, as well as the adhesion pressure and the kink-force. Many examples of quantitative methods of fiber-matrix interface are reported by Zhandarov *et al.* [130] and Utracki *et al.* [89].

I.5. Description of the thermo-rheological behavior of ligno-cellulosic fiber-reinforced composites

The previous sections have shown some degrees of interdependence of the mechanical and rheological properties of plastic/composite materials, as well as the impact of parameters such as viscosity, elasticity and temperature variation on their behavior. A similar observation has been made on the effects of kinematics, equilibrium and other material laws on their final deformation. A unifying material behavior expression is thus crucial for accurate applications and suitable designs. Such expressions have been developed in the mathematical form known as constitutive equations [200] which are relationships describing bodies deformation under applied forces. It is done based on empirical relations and experimental data depicting various effects such as the stress/strain relationships, the displacement/deformations, the thermal effects and the strain history. The constitutive equations are either defined based on the actual state of

the body deformation and the expression of the stress under which it is submitted or by the type of deformation involved in its mechanical properties [201].

A material deformation is either large or small and its behavior is elastic, hyper elastic, visco-elastic or of the Cauchy elastic type. A small deformation usually refers to the strain in the linear range, which consists of the case where the geometrical deformation is neglected while other cases are considered as large deformation [200]. All the constitutive equations applied to other plastic/composite materials are also efficient in describing the behavior of vegetal fiber-reinforced composites as shown in the following sections.

I.5.1. The elastic behavior

The study of elasticity aims at defining the relationships between the stress and strain of a material when it is submitted to certain forces. An elastic behavior is characterized by the deformation reversibility under small strains. The elastic theory can be applied on a structure following its subdivision into infinitesimal elements where the theory applies. The total deformation, elastic force and potential energy are additive over those infinitesimal elements. The behavior of an elastic material is generally defined by Hooke's law and refers to cases of small strains [202] or to the cases where the measured strain is function of the applied forces. Elasticity is typically a linear theory, meaning that its constitutive equations are linear in the limits of elasticity. Different forms of the constitutive equations describing the elastic behavior of a materials are found in the literature (tensor, matrix, simple), based on the Hooke's law.

Hooke's law can be used to determine the stress at any point of the structure where the strain is known. It is an empirical expression built on the assumptions that a plane section perpendicular to the bar remains plane after the deformation, the structure dimensions are unchanged during the deformations which is assumed small and the overall deformation is additive over all the elements of the structure.

Given the strain energy density tensor of Equation (67), the generalized Hooke's law [203] is given in Equation (68), where Cijkl are the components of the fourth-order stiffness tensor of the material.

$$\hat{\psi}(\varepsilon) = \frac{1}{2} \cdot C_{ijkl} \varepsilon_{ij} \varepsilon_{kl} \tag{67}$$

$$\sigma_{ij} = \frac{\partial \hat{\psi}}{\partial \varepsilon} = C_{ijkl} \varepsilon_{kl} \tag{68}$$

In case of isotropic and homogeneous materials, the components of the fourth-order stiffness tensor are given by Equation (69) and the constitutive equations by Equation (70), where δ_{ij} ($\delta_{ii} = 1$ and $\delta_{ij} = 0$ if $i \neq j$) and (λ,μ) are respectively the Kronecker delta function and Lame's constants Equation (71).

$$C_{ijkl} = \lambda \delta_{ij} \delta_{kl} + \mu \left(\delta_{ik} \delta_{jl} + \delta_{il} \delta_{jk} \right) \tag{69}$$

$$\varepsilon_{ij} = \frac{1}{E} \left[(1+\nu) \sigma_{ij} - \nu \sigma_{kk} \delta_{ij} \right] \tag{70}$$

$$G = \mu; \quad E = \frac{\mu(3\lambda + 2\mu)}{\lambda + \mu}; \quad \nu = \frac{\lambda}{2(\lambda + \mu)}; \quad \lambda = \frac{\nu E}{(\lambda + 1)(1 - 2\nu)} \tag{71}$$

Many cases of the application of Hooke's law especially in describing the mechanical behavior of vegetal-fibers reinforced composites are found in the literature, in the example of Thamae [44] who applied it in studying the mechanical behavior of

Agave Americana and Agave Americana-PP. In general, the elastic moduli of plastic/composite materials by tensile testing are determined based on the application of Hooke's law as reported in Section I.2. Moreover, the constitutive equations are adaptable to include the thermal and hydrothermal effects on elasticity whenever necessary [203].

I.5.2. The hyper-elastic behavior

A hyper-elastic material is one that behaves elastically (exhibiting reversible deformations) when submitted to large strains. Hyper-elasticity is thus a material behavior which consists in undergoing large elastic strain under small solicitations while withholding its original properties. The behaviors of hyper-elastic materials are non-linear as their deformations are not proportional to the applied forces; however, isotropic materials with linear large deformations are defined as Neo-Hookean. Hyper-elastic behavior is generally described by constitutive equations in which the stress is function of the stored energy function and the work is independent of the pathway. The oldest applied hyper-elastic model was formulated by Mooney-Rivlin in 1948 [175,204]; however, the Ogden's model published in 1972 [204,205] is another applied hyper-elastic model.

Hyper-elastic models are applicable to large deformation analysis of incompressible materials, non-linear material behavior, as well as large shaped materials where stress solely depends on the deformations in its actual configuration. Consequently, the stress can be derived from the strain energy of deformation per unit volume (W) with respect to the stress reference. The stress energy density of isotropic materials is given by Equation

(72), where I_i are the invariants of the stress tensor and C are the components of the Cauchy-Green stress tensor.

$$W = f(I_1, I_2, I_3) \tag{72}$$

$$I_i = f(C) \Rightarrow \begin{cases} I_1 = tr(C) \\ I_2 = \frac{1}{2}\left[tr(C)^2 - tr(C^2)\right] \\ I_3 = \det(C) \end{cases} \tag{73}$$

An application of the Lagrangian formulation yields the Piola-Kirchoff stress of Equation (74) and the constitutive equation of Equation (75) where C^{-1} is the inverse of tensor C and δ_{ij} is the Kronecker delta function.

$$S_{ij} = \frac{\partial W}{\partial E_{ij}} \tag{74}$$

$$\text{Given } E = \tfrac{1}{2}\left[C - I\right],\ S_{ij} = 2\left[\frac{\partial W}{\partial I_1}\delta_{ij} + \frac{\partial W}{\partial I_2}\left(I_1\delta_{ij} - C_{ij}\right) + \frac{\partial W}{\partial I_3} I_3 C_{ij}^{-1}\right] \tag{75}$$

In the case of incompressible materials, the deformation does not happen through I_3, thus the constitutive equation becomes Equation (76) where p is an unknown derived from the equilibrium and boundary conditions.

$$S_{ij} = 2\left[\frac{\partial W}{\partial I_1} I + \frac{\partial W}{\partial I_2}\left(I_1 I - C\right)\right] - pC^{-1} \tag{76}$$

The constitutive equations of hyper-elastic materials can also be expressed by the principal elongation (λ_1, λ_2, λ_3) as follows.

$$W = f\left(I_1, I_2, I_3\right) = f\left(\lambda_1, \lambda_2, \lambda_3\right) \Rightarrow \begin{cases} I_1 = \lambda_1^2 + \lambda_2^2 + \lambda_3^2 \\ I_2 = \lambda_2^2\lambda_3^2 + \lambda_1^2\lambda_3^2 + \lambda_2^2\lambda_1^2 \\ I_3 = \lambda_1^2\lambda_2^2\lambda_3^2 \end{cases} \tag{77}$$

A few examples of hyperelastic models are given by Equations (78)-(80) based on Equations (72)-(77). Equation (78) shows the Mooney-Rivlin equation, which describe the strain energy function by the power series of first (I_1-3) and (I_2-3); Equation (79) shows the Neo-Hookean model which describes the strain energy function by power series of (I_1-3); Equation (80) shows the Ogden model which describes the strain energy function with the principal stretches where μ_r and α_r are the material constants determined by experimental analysis.

I.5.3. The visco-elastic behavior

Visco-elasticity depicts a material behavior which combines both a viscous and an elastic component while undergoing deformation. This means that under an applied force, visco-elastic materials will both deform reversibly and undergo some degree of flow. Elastic materials deform reversibly, while viscous ones show time dependent irreversible deformations which are either linear or non-linear. Such behavior which is highly time and temperature dependent is mostly found in plastic/composite based materials. It is mathematically expressed by constitutive linear and non-linear models whose equations are also based on differential, integral or molecular models.

$$W(I_1, I_2) = \sum_{ij=0}^{\infty} C_{ij} (I_1 - 3)^i (I_2 - 3)^j \tag{78}$$

$$W(I_1) = C_{10}(I_1 - 3) \tag{79}$$

$$W(\lambda_1, \lambda_2, \lambda_3) = \sum_{ij=0}^{\infty} \frac{\mu_r}{\alpha_r} \left(\lambda_1^{\alpha_r} + \lambda_2^{\alpha_r} + \lambda_3^{\alpha_r} - 3 \right) \tag{80}$$

The integral forms such as the most popular proposed by Kaye/Bernstein/Kearsley/Zapas (K-BKZ) are theoretical while the differential forms in the example of thoses proposed by Oldroyd-B in 1980 and Phan-Thien/Tanner in 1990 [187] are related to the rheological properties of the material. K-BKZ model shown in Equation (81) uses many parameters where τ is the stress tensor, λ_k are the relaxation times, G_k are the relaxation moduli, N are the number of relaxation modes, θ is a material constant, C_t is the Cauchy-Green tensor, I_C^{-1} and II_C^{-1} are the first and second invariants, H is the strain memory function. Moreover, H has been defined by Papanastasiou by Equation (82). Finally, the associated loss and storage moduli are given in Equation (83), where ω is the frequency.

$$\tau = \frac{1}{1-\theta}\int_{-\infty}^{t}\sum_{k=1}^{N}\frac{G_k}{\lambda_k}\exp\left(-\frac{t-t'}{\lambda_k}\right)H\left(I_{C^{-1}}, II_{C^{-1}}\right)\left[C_t^{-1}(t)+\theta C_t(t')\right]dt' \tag{81}$$

$$H\left(I_{C^{-1}}, II_{C^{-1}}\right)=\frac{\alpha}{(\alpha-3)+\beta I_{C^{-1}}+(1-\beta)II_{C^{-1}}} \tag{82}$$

$$G'(\omega)=\sum_{k=1}^{N}G_k\frac{(\omega\lambda_k)^2}{1+(\omega\lambda_k)^2};G''(\omega)=\sum_{k=1}^{N}G_k\frac{(\omega\lambda_k)}{1+(\omega\lambda_k)^2} \tag{83}$$

The model proposed by Maxwell is based on a combination of a spring and a dash pot representing respectively the elastic and the viscous components as shown in Figure 3-10 is finally one of the most applied linear molecular visco-elastic models.

Maxwell model has been used in describing the time dependent stress/strain relationships such as the creep and the stress relaxation illustrated in Figure 3-10. Creep represents an increase of the strain at constant stress, while stress relaxation represents a decrease of stress at constant strain. The constitutive models for Maxwell, creep and stress

relaxations are given respectively by Equation (84), Equation (85) and Equation (86). Maxwell equations are adequate for qualitative and conceptual analyses but rather poor in the quantitative description of a material behavior.

$$\dot{\varepsilon}(t)=\frac{\dot{\sigma}(t)}{E}+\frac{\sigma(t)}{\eta}\Rightarrow\varepsilon(t)=\frac{\sigma(t)}{E}+\frac{1}{\eta}\int_{\tau_0}^{t}\sigma(\tau)d\tau \tag{84}$$

$$D(t-\tau)=\frac{1}{E}+\frac{t-\tau}{\eta}\qquad t\geq\tau \tag{85}$$

$$\sigma(t)=E\int_{\tau_0}^{t}e^{-\frac{E}{\eta}(t-\tau)}\dot{\varepsilon}(t)d\tau \tag{86}$$

Other visco-elastic models proposed by authors like Christensen *et al.* [206], Lodge *et al*., Kevin-Voigt are commonly used applied in the characterization and modeling of vegetal-fibers reinforced composites.

Most of the models above are linear, however a multitude non-linear visco-elastic models have been proposed based on single and multiple integral.

I.5.4. Visco-elastoplastic behavior

The visco-elasticity of polymeric/composite materials described in the previous section properly applies to less than 2% (w/w) deformations; however, visco-elastic models fail to adequately characterize of the load/deformation phenomenon above this range, due to the importance of the visco-plastic component which relates to the time dependent irreversible deformation. A combination of both the visco-elastic (time dependent reversible) and visco-plastic (time dependent irreversible) models is necessary for a better representation of the load/deformation of polymeric/composite materials in

such range. Visco-elastoplasticity has been studied by many authors and based on the review given by Albouy [207] as well as the for the study of its contribution to the fatigue of thermoplastic and thermoset materials.

Visco-elastoplasticity is a complex material behavior which involves viscous, elastic and plastic characteristics under deformation. It results from the gradual transition from the elastic to the plastic zone and the irreversible deformation of polymeric/composite materials from the yield point as they stop being strictly solid/glassy. In this regard, the constitutive equations for the visco-elastoplasticity basically relate the micro-structure of the material under characterization and its mechanical properties [208]. The formulation of those constitutive equations is complex due to the number of terms involved; however, two main approaches exist, based on either the associated physical processes or the phenomena involved.

The approach based on physical processes in the example of those related to the transition and the dislocation state theories are mostly adequate for the visco-elastoplastic description of other materials and inapplicable for the description of polymer/composites materials for which the mechanism of those processes are not well understood. They are therefore described based on the phenomena involved.

The approach based on the phenomena involved considers a unifying approach applying the stress or strain decomposition, followed by an application of the classical theories associated to the description of each term of the decomposed expressions. Irrespective of the applied methods, some examples of the formulation of the constitutive equation for visco-elastoplastic materials are given by Drozdov [209,210], Bles *et al.* [211], Deseri [212] and Chunyu [213].

An application of the strain decomposition to the formulation of the visco-elastoplastic material behavior is described by strain history at each point as shown by Equation (87), where ε^e, ε^p, ε^{ve} and ε^{vp} are the elastic, plastic, visco-elastic and visco-plastic components of the total strain.

$$\varepsilon = \varepsilon^e + \varepsilon^P + \varepsilon^{ve} + \varepsilon^{vp} \tag{87}$$

Such method was applied by Drozdov [209,210] for the description of amorphous glassy polymers which he considered as a cooperatively relaxing regions (CRR) with total relaxation occurring in the liquid state.

The mechanical energy density is given by Equation (88) for uniaxial testing, its sum over the relaxing region is given by Equation (89) while neglecting the energy of interaction and the stress/strain relationship is given by Equation (90) where c is the rigidity of the relaxing region, τ is the time, ω is the depth of potential energy where CRR is trapped, $E_0(T) = \rho c(T) X_0$ is the initial Young modulus and $X(t, \tau, \omega)$ is the concentration of the CRR per unit mass at time t.

$$\phi(t,\tau) = \frac{1}{2} c \varepsilon^2(t,\tau) \tag{88}$$

$$\phi(t) = \frac{1}{2} c \left[\varepsilon^2(t,0) \int_0^\infty X(t,0,\omega) d\omega + \int_0^t \varepsilon^2(t,\tau) d\tau \int_0^\infty \frac{\partial X}{\partial \tau}(t,\tau,\omega) d\omega \right] \tag{89}$$

$$\sigma(t) = \rho \frac{\partial \phi(t)}{\partial \varepsilon(t)} \tag{90}$$

$$\sigma(t) = E_0(T) \left[\begin{array}{l} (\varepsilon(t) - \varepsilon(\tau)) \int_0^\infty X(t,0,\omega) d\omega + \\ \int_0^t \left((\varepsilon(t) - \varepsilon(\tau)) - (\varepsilon^{vp}(t) - \varepsilon^{vp}(\tau)) \right) d\tau \int_0^\infty \frac{\partial X}{\partial \tau}(t,\tau,\omega) d\omega \end{array} \right]$$

The decomposition of stress components approach has been reported by Bles *et al.* [211], for the characterization of cyclic visco-elastoplastic behavior of PA 66 straps. Other meaningful work include the formulation of the constitutive equations for visco-elastoplastic materials through an application of the inelastic dissipation principle by Deseri *et al.* [212], as well as the application of the indentation technique to an array of visco-elastic and visco-elastoplastic materials by Chunyu [213]. An indentation test consists in pressing a nano-indenter into a sample while measuring the variation of the applied load and indenter depth and inversely retrieving the material properties. The work of Chunyu showed the challenges of formulating the constitutive equations for visco-elastoplastic material with a large number of parameters and the advantage of choosing the strain over the stress decomposition technique.

I.6. Identification techniques for ligno-cellulosic fiber-reinforced composites

During the past decades, there has been a surge of mathematical and numerical methods in material characterization, where they are either applied to accurately solve the constitutive equations derived from different models [195,214] or to select the best fitting model from the pool of alternatives.

The parameter identification techniques are some of those numerical methods which have mostly been based on optimization processes which consist in finding the best results under given conditions, while minimizing the needed resources [215]. Two major steps are thus involved prior to the parameters identification; they include the formulation of the constitutive equations which was subject of the previous section and the

experimental analysis. Different methods of optimization have been applied for different kinds of problems. Moreover, the technique undergoes important development based on the evolution of computational capacities. In the case of material characterization, parameters identification has been used in providing a solution to the constitutional equations which describe its spacio-temporal variations [216–218]. Parameters identification significantly reduces the amount of experimentation by optimizing available experimental data for an effective description of the material behavior.

Their applications have been mostly found in the description of the kinetics of thermal degradation of vegetal-fibers reinforced composites [118,156] which is also a key element in the description of the thermo-degradation mechanism, the rheological behaviors, the time-temperature superposition, the yield stress as well as the fracture mechanics. Parameters identification techniques represent a good potential for the characterization of newly elaborated materials [94,218].

Although numerous strategies have been presented to solve the constitutive equations, they are generally based on either the classical mathematical methods or the modern techniques [219]. In this regard, the least squares method which is based on classical approaches and the neural network method which is one of the modern optimization techniques are further developed below.

I.6.1. The Least Squares method

The least squares (LS) technique is one of the classical methods of parameters identification which consists in the error minimization between the model to be fitted and the experimental data. The least squares method, which is also the most popular

regression method is thus a non-linear optimization process where the objective functions to be minimized is the sum of the squares of the errors (also called residues) between the fitted model and the experimental data points. In order word, it is a non-linear identification technique with a least squares objective function.

Let $X = \{x_1, x_2, ...x_n\}^T$ be the vector of i data parameters; $g(X)$ the vector of the model's predicted data points; and Y the vector of the experimental data points.

The residual at each i is defined by Equation (91) and the least squares method identifies the parameters which minimize the function defined by Equation (92).

$$r_i(X) = Y_i - g_i(X) \tag{91}$$

$$\sqrt{\sum_i (r_i(X))^2} = \sqrt{\sum_i (Y_i - g_i(X))^2} \tag{92}$$

Since this method uses all the spatial and temporal data, its challenges often results from some cases of noisy experimental data. Moreover, it faces the challenges which are common to other classical methods in that it does not have the ability to deal with real life systems which combine continuous and discrete variables [215,220]. The least squares methods have been applied in the characterization of polymers and vegetal-fibers reinforced composites by authors such as Baojioa *et al.* [131], Moore *et al.* [186] and Erchiqui *et al.* [101]. Such method was applied by Moore *et al.*, for the rheological characterization of the interactions between cellulose derivative and solvents; while it was applied by Baojia *et al.*, for fitting the rheological power law with mixing data of HDPE, PS and PMMA from a torque rheometer. Erchiqui *et al.* applied the neural network method whose training step is based on the least squares approach for the study of visco-elastic polymers.

I.6.2. Neural network method

The artificial neural network (ANN) is one of the modern methods of optimization which makes an efficient use of the actual high computing capacity. It proceeds by modelling the problem as a network of parallel layers of neurons which mimics the behavior of a biological system and which is trained to solve problems with a high degree of efficiency [215]. The main elements of a problem structure based on the ANN are shown in Figure: APP- 3 with three layers of 4 neurons each. During the process, each neuron accepts inputs from others and computes the output which is propagated through the output layer. The mid layers are often hidden. Some important elements include the connectivity between the networks, the weight and function associated to each neuron.

The initial part of the process consists in the training which is done by choosing different neural combinations from the input layer, providing the values of the output neurons and applying the least squares regression method to find the error between the actual and predicted output values. Based on the results of the LS method, the neuron associated weights are adjusted, thereby providing the relationship between the inputs and outputs neurons which is further applied to solve the initial problem.

Let x_i be the input of neuron i and w_i the weight associated to it. The training process is formulated by Equation (93).

$$\sum_{i=1}^{N+1} w_i x_i = W^T X \tag{93}$$

The ANN is a robust, flexible and easily learnt numerical method which is applicable in solving structural and mechanical problems as shown demonstrated by the works on polymers processing by Huang *et al.* [221], Erchiqui *et al.* [101,204], and Klotzer *et al.* [222] as well as the work on natural fibers-reinforced composites by Biagiotti *et al.* [223]. In fact, the method was applied by Huang *et al.* for the determination of the parison swell during plastic processing, while Erchiqui *et al.* have successfully applied it for the characterization of softened and visco-elastic polymers. A case of characterization of vegetal-fibers reinforced composites through artificial neural network was reported by Biagiotti *et al.* concerning PP.

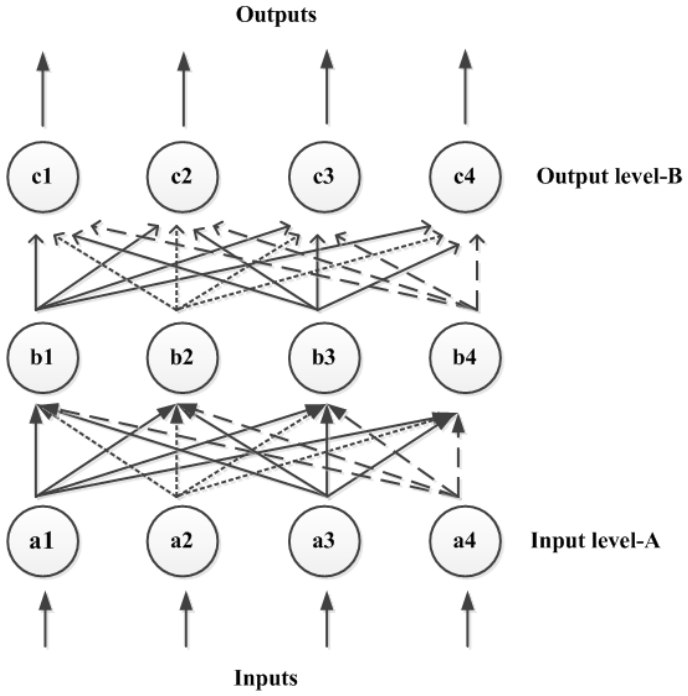

APP- 3: Illustration of a problem structure based on the artificial neural network.

I.7. Process modeling and simulation

I.7.1. General trends

The modeling and simulation of ligno-cellulosic materials processing emanate from the general advances made during the past decades in computer programming, followed by the applications of digital computing resources in solving industrial processing problems [224,225] especially those from the plastic/composite. Their applications in different areas of the plastics/composites industry involves for example mold design [226], compounding [89,115], strength of fiber-matrix interface [227], material characterization [157,228,229], behavior of different material parameters during melt processing and during the thermoforming process [225,230,231] and determination of the most favorable processing conditions to circumvent parts defects [232–234]. Consequently, the literature abounds with numerous examples of applications of modeling and simulation in different plastics/composites processes. The introduction of applications of computing resources in industrial processing around 1980-1990, paved the way for both the development of various commercial software dealing with various aspects of plastic/composites processing and the development of the identification methods to improve the efficiency of product characterization during processing.

Much commercial software has thus been developed to deal with aspects of the process such as compounding and optimization. In the case of the compounding process, the heat transfer studies have been reported by both Nassehi *et al.* [115] and Bai *et al.* in a batch mixer, while the mixing of the components has been studied by Adragna *et al.* [113] using commercial finite elements analysis (FEA) codes such as polyflow from

ANSYS and Matlab. Different aspects of process optimization [94] have been reported in the example of 3-D mold filling during injection molding studied and reported by Cardozo [235], the parison modeling during extrusion blow molding by Huang *and Liu* [221] and the investigation of the relaxation of HDPE-wood fibers and the thermoformability of HDPE by Erchiqui *et al.* [102,236]. Modeling and simulation in the plastics/composites processes also plays a key role in the parameters identification which involves the generation of the constitutive equations with a significantly reduced amount of experimental data. Some examples have been reported by Harth *and Lehn* [217], Coorman *et al.* [218] and Erchiqui *et al.* [101].

I.7.2. The thermoforming process modeling and simulation

The radiative/conductive heat transfers which take place during both the reheating and the cooling/solidification steps as well as the structural deformations which take place during the forming step are the two major physical phenomena implicated in the thermoforming process. Consequently, thermoforming problems involve both the equilibrium and momentum equations and their variations are both spatial and temporal [85,95,225,237]. Modeling and simulation is essential in reducing the process set-up time. Moreover, an optimal thickness distribution in the final part is another rationale for process modeling and simulation [238]. The most common modeling and simulation methods for the thermoforming process which are based on membrane approximations which are described in the following sections alongside the needed approximations.

I.7.3. Modeling of the thermoforming process

The multiplicity of parameters and steps involved in the formulation of the thermoforming process has resulted in an active R&D sector and a publication of numerous numerical methods dealing with modeling the thermoforming of plastic/composite materials. The relevance of the thermoforming modeling lies in the fact that apart from its classical parameters, it has to accurately take into consideration most special material structure such as the composite laminates, the heating method such as the infrared heating system and the processing methods such as the draping and the plug assisted thermoforming process. Most of actual reported methods are based on the constitutive equations describing the behavior of such materials, the process mass and heat balance, the type of the applied heating system and the applicable numerical approximation

The constitutive equations which have been used to model the thermoforming of plastic/composite materials are mostly hyperelastic and visco-elastic owing to the examples found reported in the literature. In this regard, the hyperelastic constitutive equations of Mooney-Rivlin shown in Equation (78), has been applied by Gilormini *et al.* [239] for the thermoforming of PMMA near its glass transition temperature; and the Ogden's equation shown in Equation (80) has been applied by Kouba *et al.* [205] for the thermoforming of complex shapes. In the same manners, the K-BKZ model shown in Equation (81) has been applied by Novotný *et al.* [240] and Erchiqui *et al.* [178]. Finally, the Lodge model has been applied by Erchiqui *et al.* [102] for the numerical

thermoforming of HDPE-wood flours are examples of the visco-elastic constitutive models used.

There are three modeling techniques of the thermoforming process based on the mass balance. They include the simple mass balance, finite element analysis with membrane approximation and finite element analysis without membrane approximation [225]. The simple mass balance approach only considers the geometries of both the extruded sheet and the final part while the two remaining approaches consider the geometry and the material behavior including those in the biaxial extensional mode [204] and the strain hardening [241].

The simple mass balance method is thus the least accurate while the finite element analysis (FEA) method without the membrane approximation is mostly relevant to the thermoforming of multilayered sheets. Consequently, FEA with membrane approximations remains the most applied method of numerical modeling and simulation of thermoforming applications.

I.7.4. Assumptions for the FEA with membrane approximations

The following approximations are critical for the modeling and simulation of thermoforming processes, especially with respect to the analysis with membrane approximations [85,169,237].

- The flexural effects are negligible;
- The problem is highly non-linear due to large deformations, structural/fluid interactions, the processing time;

- The fluid/structure at the boundary is viscous.

I.7.5. FEA with membrane approximations

It generally consists in finding the thickness and temperature distribution of the sheet under thermoforming, by fitting its C_i configurations at time t_i and volume V_i, or by finding the net residual surface force R(u) given by Equation (94), where F_{ext} and F_{int} are respectively the external and internal forces as indicated by Rachik [242] in his work concerning the development of simulation algorithm for the thermoforming process and other references in it.

$$R(u) = \sum_i F_{ext}(u) - \sum_i F_{\text{int}}(u) \tag{94}$$

Three numerical approaches to solve the equations describing the thermoforming process are found in the literature namely the Newton-Raphson, the dynamic explicit and the higher order explicit methods [242].

The Newton-Raphson method is an iterative operation consisting in the discretization of the total load into different increments and solving for the configuration C_i associated with each step. An expansion of the residue around u_i is given by Equation (95), where u_{i+1} is the configuration displacement, Δu_i is the displacement increment and the convergence of u_i series corresponds to the simulation solution.

$$\begin{aligned} u_{i+1} &= u_i + \Delta u_i \\ R(u_{i+1}) &= R(u_i) + \frac{\partial R(u_i)}{\partial u_i}\Delta u_i \end{aligned} \tag{95}$$

The Newton-Raphson method faces convergence issues and consequently yields less accurate results than the dynamic explicit and the higher order explicit methods described below. The dynamic explicit methods take into consideration inertia thus Equation (94) is reformulated as Equation (96), where [M] is the mass matrix and (ü) is the acceleration vector. Equation (96) can be solved by discretizing (ü) by a central finite difference method. The solution process is often long and higher order explicit methods have been developed.

$$R(u) = \sum_i F_{ext}(u) - \sum_i F_{\text{int}}(u) - [M](\ddot{u}) \tag{96}$$

The development of higher order explicit methods is based on the assumption that the value of the residual forces is zero at each time. Furthermore, it is done by taking the time derivative of the equilibrium Equation (94), followed by an integration of the expression based on the 4^{th} and 6^{th} order Runge-Kutta equations for example or other higher methods.

A few examples of FEA applications with membrane approximation have been reported by Kouba *et al.* [205] who modeled the thermoforming of complex geometries based on the application of Ogden's material model, an adaptative mesh refinement and the standard Newton-Raphson method. Novotny *et al.* [240] who described an application of the K-BKZ model based on an application of a standard iterative finite element method on various materials to show that the final thickness distribution and shape of a thermoformed part is highly influenced by the material behavior. Erchiqui *et al.* [243] who applied the Lodge and Mooney-Rivlin's model to the thermoforming of circular ABS membrane based on a dynamic finite element method and Shrivastava *et al.* [244] who used a variation of the Newton-Raphson method to model the thermoforming of plastic

based materials using a membrane approximation method coupled with the Christensen's material behavior.

II. Processing techniques for ligno-cellulosic fiber

A summary of the processing techniques applicable to vegetal fiber-reinforced composite is given in Figure: APP- 4. Although various methods of classification are applicable, the most relevant to the targeted thermoforming applications is based on the type of deformation required by the process. In this regards, thermoforming and all the blow molding processes require large deformations, whereas injection, extrusion and thermo-compression require only moderate deformations. The strain which the material undergo during the forming process is the defining parameters, thus values below 20% refer to small deformations and those at least equal to 20% correspond to large deformations. Each process is further described in the following section with a prime consideration for the thermoforming which is the end process in this work.

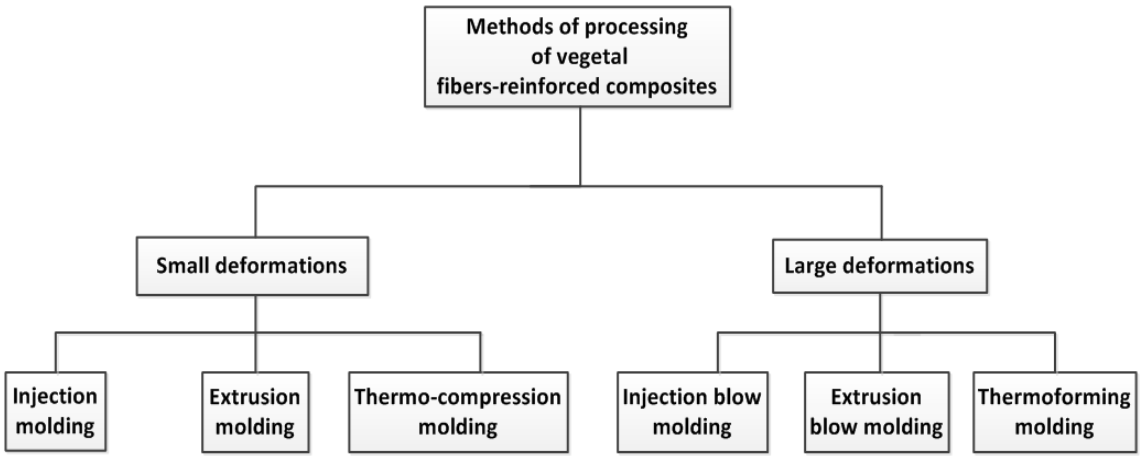

APP- 4: Methods of processing vegetal fiber-reinforced composites.

II.1. Extrusion

Extrusion is an important process in plastic industry with regard to the volume of its activities and the researchers' dedication to improve on it [245]. It is a continuous blending and forming process which is based on small deformations, as well as the material shearing along the screw system until the die where forming and cooling starts, followed by hauled-off. Extrusion represents the second most frequent processing technique in the plastic industry (15% (w/w)) [246,247].

There exist many variations of extruders whose main parts like the heating system, the transducer, the side-stuffer(s), the different temperature zones, the die, the screw line(s) and the haul-off system are shown in Figure: APP- 5(A) while an aspect of the extruder is shown in Figure: APP- 5(B). The continuous nature of the process and the limited loss of material are major advantages of the extrusion-based compounding over torque-based equipment, especially in the industrial field. Extrusion is however limited

in the details of parts processing making it less advantageous than injection molding it such cases.

The side stuffer(s) are key elements in the extrusion of vegetal-fibers reinforced composites as it plays an important role in avoiding the thermal degradation of vegetal fibers. In fact, most of the recent processing milestones in the development of vegetal fiber-reinforced composites are based on both the side stuffer(s) and the temperature variation along the screw line. It has been improved over the years to include an online drying system for the fibers [104,107,245].

Consequently, highly specialized extrusion lines have been developed for compounding vegetal fiber-reinforced composites, wood fibers-reinforced composites and composites with various additives which find applications in both the R&D [103,104,248] and the industrial sector. Extrusion blow molding is another variation of extrusion used in plastic processing.

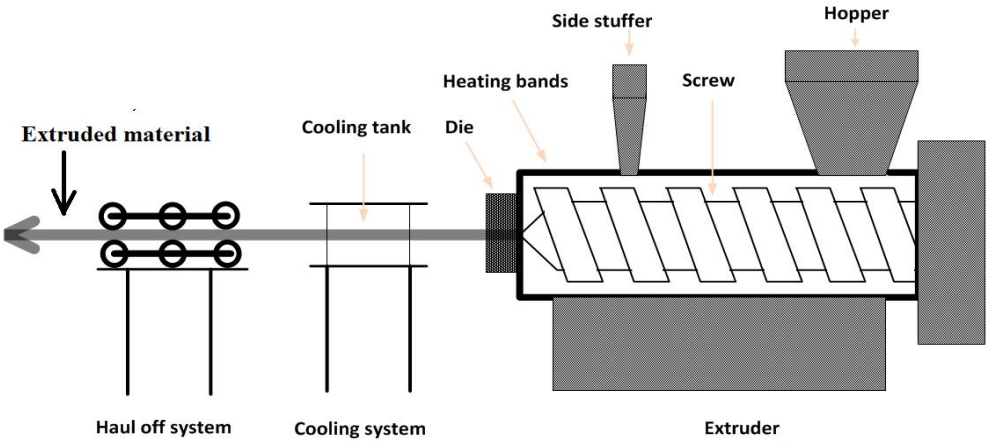

(B)

APP- 5: Extruder: Cross section and main elements (A); Photograph (B).

II.2. Injection molding

Injection molding is an important cost effective process which is applied in the plastic and composite industry for the mass production of complex parts. In fact, according to the society of plastics engineers (SPE), in 2005, injection molding was the fourth largest industry in the USA. It accounted for about 33% (w/w) of all the processed polymeric materials [235]. Moreover, it represents close to 50% of the applied molding techniques which globally delivers about 30% (w/w) of the manufactured volume [235,246,247,249]. It is technically based on the same process like extrusion molding. As indicated in Figure: APP- 5, the haul-off system is replaced by a well-developed two or multi-parts closed mold equipped with ejection and cooling systems. During the forming process, the sheared material is transferred into the mold where it is cooled, followed by the retraction of the moving parts and the ejection of parts. This implies that injection molding is not appropriate for the manufacture of long profiled parts with a constant cross section such as tubes and sheets.

Although large scale injection molders are widely used in laboratories and industries, mini piston injection molders such as the Haake Minijet II (Thermo scientific, Karlsruhe, Germany) shown in Figure 3-5 are prevalent in R&D institutions. It replicates all its operations of a conventional screw-equipped injection molding however, their mold and screw systems are quite different. Small quantities of materials are needed for the operation of a piston injection molder which can also process complex and highly viscous blends due to its 1200 bar injection pressure. The Minijet seems cost competitive in comparison to conventional injection molding equipments; however, its effectiveness

depends on the pre-compounding of the blends which justifies its operation alongside blending equipments.

Many authors have reported major applications of both screw equipped injection molders for the elaboration of wood-plastic composites [14,182,250,251], natural fiber-reinforced composites [66,162] and piston-equipped injection molder for the laboratory elaboration of both wood and short vegetal fiber-reinforced composites.

II.3. Thermo-compression

Thermo-compression is the third most frequent and the oldest process in the plastics/composites molding industry [150,247]. It is based on temperature and pressure variations especially applicable for the production of laminated structures.

The heating plates and the hydraulic system are major parts of a thermo-compressor as shown by the 12 tons thermo-compressor from Carver in Figure 3-6. The process consists in the following four successive steps: heating the plates to the required temperature, loading the mold filled with the material blend between the heated plates, pressure application until melting or curing is completed, and unloading and cooling of the parts.

Various authors have used thermo-compression at various stages of their work [61–63]. They also include Bo Madsen who worked with PET-hemp filaments [40].

II.4. Other processing techniques

Many other processing methods for plastics/vegetal fiber-reinforced composites exist. They are processes like resin transfer molding [94,246], rotational molding [150], calendering [150] and pultrusion [39,254] which in most cases are the variations of the

processes described in the previous sections. Resin transfer molding consist in melting the polymer matrix prior to its pressure transferred into the mold. It is particularly suitable for the encapsulation of metal parts and for the production of composites with woven reinforcements; however, it is time consuming due to the handwork involved. Rotational molding consists in loading powdered polymer into the mold following by melting under the effect of a heating rotational oven. Rotational molding is suitable for the production of tanks. Calendering and pultrusion are variations of the compression and extrusion process respectively. Calendering is a continuous process of sheet production by pressing the molted material under calendar rolls. Pultrusion is an efficient technique of processing profiled shapes with composites of fiber-reinforced thermosetting resins consisting in successively pulling the reinforcement through the liquid resin and through the heated die.

II.5. The compounding process

Compounding is a key step of vegetal-fibers reinforced composite processing which intention is the creation of fiber-matrix-additives interfaces even though they are not necessarily of the best quality at this processing stage. The compounding process also plays an important role in the dispersion of different additives and reinforcements into the matrix, however, it does not completely solve the issue related to their homogeneity. The common compounding methods are based on extrusion, thermo-kinetic mixing and torque based mixing.

An example of a thermo-kinetic batch mixer is shown in Figure 3-2 together with a description of the other compounding methods; the figures depicting the extrusion and

the torque-based batch mixers are respectively found in Figure: APP- 5 and Figure 3-3 of the main text.

II.5.1. Extrusion molding

The extrusion molding process has been presented in the main text as a part processing method; it is also a key compounding process applicable in different industries. It is a continuous process based on material shearing along the screw system until the die where the product is cooled and hauled-off. Some important features of the extrusion molding equipments are the screws, the heating system and the transducer. As a compounding method, the die is circular and the compounded material is further hauled-off and cut into granules Extrusion is more advantageous than torque-based mixing at the industrial scale, as its continuous operation significantly reduces time and income losses. In addition, extrusion molding manufacturers have developed specific features like the side-stuffer and the different temperatures zones along the screw line, which are highly suitable in handling natural fibers-reinforced composites without fibers degradation. Due to these features, extrusion has become a major compounding method for natural fibers-reinforced composites, wood plastic composites, plastic lumber and other composites formulations. Over the years, it has also been improved to include an online drying system [104,107,245].

II.5.2. Comparative parameters [255,256]

APP-T- 1: Comparison of the compounding methods

Parameters	Method		
	Extrusion	Torque-Based	Kinetic-batch mixer
Critical parameters	• Number of screws • Number of venting units or side stuffers • Screw rotational speed	• Batch weight/Fill factor • Rotational speed • Mixer temperature • Feed material properties • Applied pressure • Mixing procedure	• Batch weight/Fill factor • Rotational speed • Feed material properties • Mixing procedure
Advantages	• High outputs • Energy efficient • Easily optimized • Easily automated • Uniform product shear • Uniform product heat history • Variable number of screws • Ability to insert additives at different moments along the screw line	• Accepts different feed forms • Varying output range • Varying range of shear applicable • Possible automation • Highly efficient for short product runs • Long life expectancy • Possible to change the mixing chamber temperature during the process	• Accept different feed forms • Varying output range • Varying range of shear applicable • Possible automation • Highly efficient for short product runs • Ultra-high speed • Long life expectancy • Existence of different types of screw system • Efficient for highly loaded batches and difficult blends • No additional heat required
Drawbacks	• Requires free flowing feed • Requires sophisticated weight / feed systems • Inefficient for short runs • Capital intensive	• Varying power demand • Variable product properties by batch • Variable post compounding product heat history • Capital intensive	• Varying power demand • Product properties variation by batch • Variable post compounding product heat history • Capital intensive

	• May require post compounding forming	• Labor intensive • Post compounding forming required	• Labor intensive • Post compounding forming required

III. Vegetal fibers treatment modification

Specht's method [37] consists in fiber modification through the following steps:

- Soaking hemp fibers for an hour in an 18% (w/w) NaOH solution
- Successively washing the soaked hemp fibers with hot water, acetic acid and cold water
- Drying at 80°C for 24 hours.

Espert's method [42] consists in the butyration of the mercerized vegetal fibers, applied for the compatibilization of polyolefins reinforced with vegetal fibers. It proceeds successively by:

- Soaking the fibers in a 4.5 N NaOH for an hour
- Draining and washing them in water
- Soaking the alkaline treated fibers in butyric acid and 3-4 drops of sulfuric acid for an hour
- Filtering and soaking the fibers in butyric anhydride with 2 drops of sulfuric acid for 5 minutes
- Washing and drying at 80°C for 24 hours.

IV. Preliminary considerations for the numerical thermoforming process

V.1. Kinematics

Continuum mechanics studies the behavior of materials that fills space and behaves like a continuum. Its knowledge is essential for applications in the plastic/composite industry where stress/strain behavior has a major importance.

Normally, a body experiences displacement and deformation when submitted to some external forces.

There is no displacement of particles and points in a solid body; however, it is not the case for a deformation where displacement of particles results in change in size or shape.

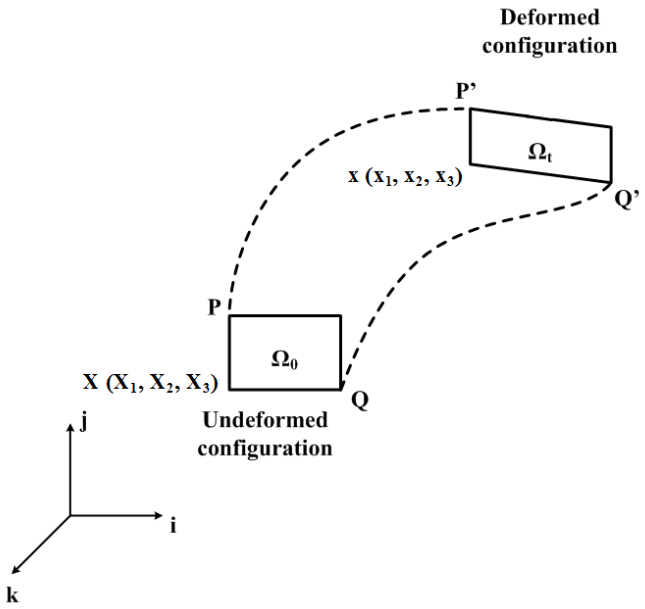

APP- 7: References for the body deformations.

The force/deformation is described by linear and non-linear stress/strain relationships either following the finite or the infinite strain theory. Two important formulations are applied to deformation problems namely the Lagrangian method which is based on a fixed reference coordinate in the initial material configuration and the Eulerian method which is based on the moving reference coordinate. The Lagrangian and Eulerian methods find applications in respectively the solid and fluid mechanics fields.

In the description of the body deformation shown in Figure: APP- 6, one considers the configuration Ω_0 at the initial time with surface Γ_0 and Ω_t at time t with surface Γ_t.

V.1.1. The lagrangian formulation: Displacement and strain

IV.1.1.1. Displacement vector

The motion is mapped by the position of points and particles with respect to the reference in the un-deformed configuration. The position and velocity are given in Equation (97).

$$\begin{aligned} x &= f(X,t) \\ V(X,t) &= \frac{\partial x}{\partial t} = \frac{\partial f(X,t)}{\partial t} \end{aligned} \tag{97}$$

The displacement or deformation vector is PP' so that.

$$\begin{aligned} PP' &= x - X \\ u(X) &= x(X) - X \end{aligned} \tag{98}$$

IV.1.1.2. Strain tensor

If point P is closer to Q, their coordinates are determined as P (X_1, X2, X3) and Q (X1+dX_1, X_2+dX_2, X_3+dX_3). In the same manner, P' and Q' are determined as P'(x_1, x2, x3) and Q'(x1+dx_1, x_2+dx_2, x_3+dx_3).

The square of length PQ and P'Q' are defined by Equation (99), the deformation gradient tensor A by Equation (100) and finally the Lagrangian or Green's stress tensor E by Equation (102).

$$\begin{aligned} PQ^2 &= |dX|^2 = (dX_1)^2 + (dX_2)^2 + (dX_3)^2 \\ P'Q'^2 &= |dx|^2 = (dx_1)^2 + (dx_2)^2 + (dx_3)^2 \end{aligned} \tag{99}$$

$$A = \frac{dx}{dX} = \begin{bmatrix} \frac{\partial x_1}{\partial X_1} & \frac{\partial x_1}{\partial X_2} & \frac{\partial x_1}{\partial X_3} \\ \frac{\partial x_2}{\partial X_1} & \frac{\partial x_2}{\partial X_2} & \frac{\partial x_2}{\partial X_3} \\ \frac{\partial x_3}{\partial X_1} & \frac{\partial x_3}{\partial X_2} & \frac{\partial x_3}{\partial X_3} \end{bmatrix} \tag{100}$$

$$\Rightarrow |dx|^2 - |dX|^2 = (dx)^T dx - (dX)^T dX = (dX)^T \left[A^T A - I\right](dX) \tag{101}$$

$$E = \frac{1}{2}\left(A^T A - I\right) \tag{102}$$

The definition of the Lagrangian strain tensor implies that the material is un-deformed if A^TA-I = 0.

A combination of the deformation tensor A and the displacement vector u gives Equation (103) which is the true displacement gradient. The relationship between the Lagrangian strain tensor and the displacement vector is given by Equation (104).

$$\nabla U = \begin{bmatrix} \frac{\partial x_1}{\partial X_1} - 1 & \frac{\partial x_1}{\partial X_2} & \frac{\partial x_1}{\partial X_3} \\ \frac{\partial x_2}{\partial X_1} & \frac{\partial x_2}{\partial X_2} - 1 & \frac{\partial x_2}{\partial X_3} \\ \frac{\partial x_3}{\partial X_1} & \frac{\partial x_3}{\partial X_2} & \frac{\partial x_3}{\partial X_3} - 1 \end{bmatrix} = A - I \tag{103}$$

$$E_{ij} = \frac{1}{2}\left[\frac{\partial U_i}{\partial X_j} + \frac{\partial U_j}{\partial X_i} + \frac{\partial U_k}{\partial X_i}\frac{\partial U_k}{\partial X_j} \right] \tag{104}$$

The last term of Equation (104) is similar to D_R and D_L which are respectively the right and left Cauchy-Green expressions defined in Equation (105) and used in the expression of the invariant as shown in Equation (106).

$$D_R = A^T A = \left[\frac{\partial x_k}{\partial X_i}\frac{\partial x_k}{\partial X_j} \right] \tag{105}$$
$$D_L = AA^T = \left[\frac{\partial x_i}{\partial X_k}\frac{\partial x_j}{\partial X_k} \right]$$

$$\begin{cases} I_1 = tr(D_R) = \lambda_1^2 + \lambda_2^2 + \lambda_3^2 \\ I_2 = \frac{1}{2}\left[tr\left(D_R^2\right) - tr\left(D_R\right)^2 \right] = \lambda_1^2\lambda_2^2 + \lambda_2^2\lambda_3^2 + \lambda_1^2\lambda_3^2 \\ I_3 = \det\left(D_R\right) = \lambda_1^2\lambda_2^2\lambda_3^2 \end{cases} \tag{106}$$

In **the infinite strain theory**, also known as small deformation theory, small displacement theory or small displacement-gradient theory, the components of the first derivatives are too small; consequently, higher terms of partial derivative are negligible, thus the strain tensor is defined by Equation (107). There is no difference between the Eulerian and the Lagrangian formulations in such case.

$$\varepsilon_{ij} = \frac{1}{2}\left[\frac{\partial U_i}{\partial x_j} + \frac{\partial U_j}{\partial x_i} \right] \tag{107}$$

IV.1.1.3. Stress tensor

Stress is defined as the force exerted over a unit surface area as shown in Equation (108).

$$\sigma = \frac{dF}{d\Gamma} = \lim_{\Delta T \to 0} \frac{\Delta F}{\Delta \Gamma} \tag{108}$$

The stress tensor is defined by Equation (109); moreover, σ_{ij} defines the stress exerted on surface (i) in (j) the direction. The stress tensor contains both normal and shear components.

$$\sigma_{tensor} = \begin{bmatrix} \sigma_{xx} & \sigma_{xy} & \sigma_{xz} \\ \sigma_{yx} & \sigma_{yy} & \sigma_{yz} \\ \sigma_{zx} & \sigma_{zy} & \sigma_{zz} \end{bmatrix} \tag{109}$$

The stress tensor is also called the Cauchy stress or the true stress. However, two classes of stress tensors exist in the Lagrangian formulation, based on the position of the exerted force and surface area with respect to the configuration. They are the first and second Piola-Kirchhoff stress tensor.

First Piola-Kirchhoff stress tensor (P):

It relates the force in the present material configuration to the surface area in the initial configuration. It is also known as the Lagrangian, the nominal and the engineering stress tensor. It is mathematically described by Equation (110) and it is the most applied formulation in the laboratory.

$$P = |A| \sigma A^{-T} \tag{110}$$

Second Piola-Kirchhoff stress tensor (S):

It relates the force and surface area which are both from the initial material configuration. It is the weighted Cauchy stress tensor also known as Kirchhoff stress tensor described by Equation (111).

$$S = |A| A^{-1} \sigma A^{-T} \tag{111}$$

The second Piola-Kirchhoff stress tensor is more suitable than the first as it is symmetrical. Moreover, the two are related by Equation (112).

$$S = A^{-1} P \tag{112}$$

IV.1.1.4. Equation of motion

The integral and differential approaches are the two methods of formulation of the equation of motion; they both consider the body and the surface forces acting on the continuum in motion. The gravitational and electromagnetic forces are examples of body forces acting on the material, whereas aerodynamic and stresses are examples of surface forces. The total forces acting on such body is thus a sum of all those acting on both its body and its surfaces as shown by Equation (113).

$$F = \oint_{\Gamma} \sigma d\Gamma + \int_{\Omega} f d\Omega$$
$$f = \begin{pmatrix} f_x & f_y & f_z \end{pmatrix}^T \quad (113)$$

IV.1.1.5. Equation of continuity

Consider the particles of the analyzed body found in the domain Ω_t at time t. Its mass is defined by Equation (114) and its equation of continuity is given by Equation (115) by differentiating both side of Equation (114) with respect to time.

$$m((t) = \int_{\Omega} \rho(x, y, z, t) dxdydz \quad (114)$$

$$\frac{dm(t)}{dt} = 0 \Rightarrow \frac{\partial \rho}{\partial t} + \frac{\partial \rho v_x}{\partial x} + \frac{\partial \rho v_y}{\partial y} + \frac{\partial \rho v_z}{\partial z} = \frac{\partial \rho}{\partial t} + \nabla(\rho v) = 0 \quad (115)$$

V.1.2. The Eulerian formulation

This approach is based on the moving reference as previously mentioned. The various relevant equations are shown in the following sections.

IV.1.2.1. Displacement and strain

The motion is mapped by the position of points and particles with respect to the deformed configuration. The position and velocity are given in Equation (116). The displacement vector is given by Equation (117).

$$X = f^{-1}(x,t)$$
$$V(x,t) = \frac{\partial f^{-1}(x,t)}{\partial t} \quad (116)$$

$$u(x) = x - X(x) \tag{117}$$

IV.1.2.2. Strain tensor

The deformation gradient tensor A is defined by Equation (118), the true displacement gradient by Equation (119) and finally the Eulerian stress tensor (e) by Equation (120).

$$A = \frac{dX}{dx} = \begin{bmatrix} \frac{\partial X_1}{\partial x_1} & \frac{\partial X_1}{\partial x_2} & \frac{\partial X_1}{\partial x_3} \\ \frac{\partial X_2}{\partial x_1} & \frac{\partial X_2}{\partial x_2} & \frac{\partial X_2}{\partial x_3} \\ \frac{\partial X_3}{\partial x_1} & \frac{\partial X_3}{\partial x_2} & \frac{\partial X_3}{\partial x_3} \end{bmatrix} \tag{118}$$

$$\nabla u = \begin{bmatrix} 1 - \frac{\partial X_1}{\partial x_1} & -\frac{\partial X_1}{\partial x_2} & -\frac{\partial X_1}{\partial x_3} \\ -\frac{\partial X_2}{\partial x_1} & 1 - \frac{\partial X_2}{\partial x_2} & -\frac{\partial X_2}{\partial x_3} \\ -\frac{\partial X_3}{\partial x_1} & -\frac{\partial X_3}{\partial x_2} & 1 - \frac{\partial X_3}{\partial x_3} \end{bmatrix} \tag{119}$$

$$e = \frac{1}{2}\left[I - \left(A^{-1}\right)^{-T} A^{-1} \right] \tag{120}$$

The definition of the Eulerian strain tensor implies that the material is un-deformed if I-$(A^{-1})^{T}A^{-1}$= 0. The relationship between the Eulerian strain tensor and the displacement vector is given by Equation (121).

$$e_{ij} = \frac{1}{2}\left[\frac{\partial u_i}{\partial x_j} + \frac{\partial u_j}{\partial x_i} + \frac{\partial u_k}{\partial x_i}\frac{\partial u_k}{\partial x_j} \right] \tag{121}$$

IV.1.2.3. Stress tensor

The Cauchy stress tensor of Equation (109) is applicable to the Eulerian formulation, while the first and second Piola-Kirchhoff equations are applicable in the Lagrangian formulation.

IV.1.2.4. Equation of motion

The same equation is applicable for the Eulerian and Lagrangian formulations.

IV.1.2.5. Equation of continuity

The same equation is applicable for the Eulerian and Lagrangian formulations.